The University of Jordan

Authorization Form

I, **Basel Nabil Abdel-Raziq**, authorize the University of Jordan to supply copies of my Thesis to libraries or establishments or individuals on request, according to the University of Jordan regulations.

Signature:

Date: 17/8/2011

الجامعة الأردنيـــــة
كلية الدراسات العليا

التاريــخ: 17 / 8 / 2011

نموذج رقم (18)
اقرار والتزام بالمعايير الأخلاقية والأمانة العلمية وقوانين الجامعة الأردنية وأنظمتها وتعليماتها لطلبة الماجستير

أنا الطالب: باسل نبيل عبد الكريم عبد الرازق الرقم الجامعي: (8070473)

التخصص: الهندسة الكيميائية الكلية: الهندسة والتكنولوجيا

عنوان الرسالة :

Thermodynamics of Supercritical Fluid Extraction of Solid Solutes Using the Weighting Matrix Approach

أعلن بأنني قد التزمت بقوانين الجامعة الأردنية وأنظمتها وتعليماتها وقراراتها السارية المفعول المتعلقة باعداد رسائل الماجستير عندما قمت شخصيا" باعداد رسالتي وذلك بما ينسجم مع الأمانة العلمية وكافة المعايير الأخلاقية المتعارف عليها في كتابة الرسائل العلمية. كما أنني أعلن بأن رسالتي هذه غير منقولة أو مستلة من رسائل أو كتب أو أبحاث أو أي منشورات علمية تم نشرها أو تخزينها في أي وسيلة اعلامية، وتأسيسا" على ما تقدم فانني أتحمل المسؤولية بأنواعها كافة فيما لو تبين غير ذلك بما فيه حق مجلس العمداء في الجامعة الأردنية بالغاء قرار منحي الدرجة العلمية التي حصلت عليها وسحب شهادة التخرج مني بعد صدورها دون أن يكون لي أي حق في التظلم أو الاعتراض أو الطعن بأي صورة كانت في القرار الصادر عن مجلس العمداء بهذا الصدد.

توقيع الطالب: باسل نبيل عبد الرازق .... التاريخ: 17 / 8 / 2011

THERMODYNAMICS OF SUPERCRITICAL FLUID EXTRACTION OF SOLID SOLUTES USING THE WEIGHTING MATRIX APPROACH

By
Basel Nabil Abdel-Karim Abdel-Raziq

Supervisor
Dr. Ahmed H. Tobgy

Co-Supervisor
Dr. Ali Kh. Al-Matar

This Thesis was Submitted in Partial Fulfillment of the Requirements for the Master's Degree of Science in Chemical Engineering

Faculty of Graduate Studies
The University of Jordan

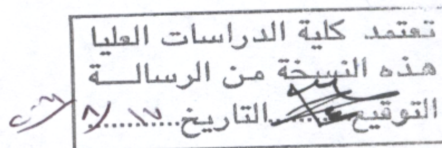

August, 2011

Committee Decision

This thesis (Thermodynamics of Supercritical Fluid Extraction of Solid Solutes Using the Weighting Matrix Approach) was successfully defended and approved on August 11, 2011.

Examination Committee	**Signature**
Dr. Ahmed H. Tobgy, (Supervisor) Associate Professor of Chemical Reaction Engineering and Simulation	
Dr. Ali Kh. Al-Matar, (Co-Supervisor) Assistant Professor of Thermodynamics and Molecular Simulation	
Dr. Khaled M. Al-Rawajfeh, (Member) Associate Professor of Chemical Engineering	
Dr. Ahmad M. Abu Yaghi, (Member) Associate Professor of Chemical Engineering	
Dr. Zaid A. Al-Anbar, (Member) Associate Professor of Molecular Simulation, Al-Balqa Applied University	

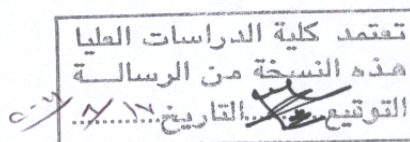

DEDICATION

To the only two persons in this world

who wish that I be better than them,

My Parents…

To my brother, sisters and relatives …

To my friends and colleagues who supported and helped me …

I dedicate this work with love and respect …

Basel …

ACKNOWLEDGMENT

Words are not enough to thank my parents who supported me and worked hard to make me what I am now, who taught me that hard work, seriousness and honesty are the basis for a good work and the way to success.

I would like to express my grateful thanks, deep appreciation and sincere gratitude to my advisors, Dr. Ahmed Tobgy and Dr. Ali Al-Matar, for their endless and generous support, patience, and supervision of my work. I really appreciate their assistance and it is an honor to me to have them as my supervisors.

Sincere thanks and appreciations are also extended to the Chemical Engineering Department staff and to the examination committee members. I was fortunate enough to have teachers and professors who did their best to be role models for their students. My gratitude and respect go to all my teachers from elementary school until my graduate studies.

Special thanks to all friends and colleagues who have contributed with helpful discussion and comments during the evolution of this work.

Table of Contents

Subject	**Page**

Subject	**Page**

List of Tables

List of Figures

List of Abbreviations and Symbols

Abbreviations

AARD	Average Absolute Relative Deviations
CAS	Chemical Abstracts Service
CP	Critical Point
EOS	Equations of State
LB	Lorentz-Berthelot Combining Rules
MADAR-1	MADAR–1 Combining Rules which are Based on the Molecularly Proposed Rules by Al-Matar and Rockstraw
MH3	Mohamed and Holder mixing rule with three adjustable parameters
PR-EOS	Peng-Robinson Equation of State
RMSD	Root Mean Square Deviations
SCF	Supercritical Fluid
SFE	Supercritical Fluid Extraction
TP	Triple Point
vdW	Van der Waals
vdW1	van der Waals one-fluid mixing rules with one adjustable binary parameter
vdW2	van der Waals one-fluid mixing rules with two adjustable binary parameters
WH	The WHAK Combining Rules which are Based on the Molecularly Proposed Rules by Waldman and Hagler and Developed for Cubic EOS by Al-Matar
WMA	Weighting Matrix Approach

Variables

a	Attraction Energy Parameter
A	Individual Species Attraction Energy Parameter

B	Individual Species Reduced Volume Parameter
b	Covolume Parameter
D	Diffusion Coefficient
$f_{i,s}$	Fugacity of Pure Solid at Temperature T
$f_{\mathrm{i,SCF}}$	Fugacity of the Solid in the SCF at the System Temperature and Pressure
k_{ij}	Attraction Energy Binary Interaction Parameter
l_{ij}	Covolume Binary Interaction Parameter
n	Number of Data Points
N	Number of Species
P	Pressure
P_{c}	Critical Pressure
$P_{\mathrm{s}}^{\mathrm{sat}}$	Sublimation Pressure of the Pure Solid at the System Temperature
R	Ideal Gas Constant
T	Temperature
T_{ambient}	Ambient Temperature
T_{c}	Critical Temperature
v	Specific Volume
V	Volume
v_{s}	Molar Volume of the Pure Solid
w	Weighting Matrix
$w_{ij,a}$	Weighting Matrix for Energy Parameter
$w_{ij,b}$	Weighting Matrix for Covolume Parameter
x	Mole Fraction in the Solid Phase
$\mathbf{x}$	Vector of Mole Fractions in the Solid Phase
$\mathbf{y}$	Vector of Mole Fractions in the SCF Phase

$y_{s,SCF}$	Mole Fraction of the Solid in SCF Phase
Z	Compressibility Factor for the SCF Phase

Greek Symbols

ϕ_s	Fugacity Coefficient of Pure Solid at Temperature *T*
$\phi_{s,SCF}$	Fugacity Coefficient of the Solid in the SCF at the System Temperature and Pressure
η	Kinematic Viscosity
λ	Thermal Conductivity
μ	Dynamic Viscosity
ρ	Density
σ	Surface Tension
ω	Pitzer's Acentric Factor

THERMODYNAMICS OF SUPERCRITICAL FLUID EXTRACTION OF SOLID SOLUTES USING THE WEIGHTING MATRIX APPROACH

By
Basel Nabil Abdel-Karim Abdel-Raziq

Supervisor
Dr. Ahmed H. Tobgy

Co-Supervisor
Dr. Ali Kh. Al-Matar

ABSTRACT

The matter of concern in this research is the prediction of the solubility of large size non-volatile organic solids in the supercritical phase. Equations of state (EOS) are considered as an important tool for the correlation and prediction of thermodynamic properties and phase behavior of pure substances and mixtures. Thus, they are widely used in the design, simulation and optimization of chemical processes such as supercritical fluid extraction (SFE). Cubic equations of state in combination with mixing rules are routinely used in the chemical and petrochemical industries to calculate thermophysical properties and phase equilibria. One of the most widely used EOS in SFE calculations is the Peng-Robinson EOS (PR-EOS). Several mixing rules have been proposed to extend the capabilities of cubic EOS and make them more useful for the modeling of complex mixtures. However, due to shortcomings of the mixing rules and/or the equation of state, binary interaction parameters have been introduced in order to improve the accuracy of models.

In this research, the weighting matrix approach (WMA) is used as an alternative to the binary interaction parameters approach. It can be shown that many of the combining rules in the literature may be reduced to the WMA proposed form with proper choice of the weighting matrix coefficients.

The solubilities of Aspirin, C.I. Disperse Red 1, C.I. Disperse Red 13, Naphthalene, Xanthene and Xanthone in supercritical CO_2 have been calculated at various temperature and pressure ranges using the PR-EOS with two modeling approaches; binary interaction parameters approach using Lorentz-Berthelot (LB), Waldman-Hagler (WH), and MADAR-1 combining rules as well as the Weighting Matrix Approach (WMA), very good agreement between modeling approaches' calculations and experimentally measured solubility was observed. Calculating the solubility of the solid solutes that were studied in this research in supercritical CO_2 was accomplished using `MatLab`© codes in combination with `Microsoft Excel`© software.

The optimum values of the energy and covolume binary interaction parameters and weighting matrix approach coefficients for Aspirin, C.I. Disperse Red 1, C.I. Disperse Red 13, Naphthalene, Xanthene and Xanthone were obtained by minimizing the average absolute relative deviations (AARD) between the experimental solubility and predicted solubility. Both modeling approaches were compared together with the purely predictive approach using the (AARD) in the mole fractions of the solid solutes in the supercritical fluid phase, and both of them provide better estimates compared to the purely predictive approach.

The binary interaction parameters and the weighting matrix approach coefficients for Aspirin, C.I. Disperse Red 1 and 13, Naphthalene, Xanthene and Xanthone respectively were fitted as linear functions of temperature, the dependence of the binary interaction parameters and the weighting matrix coefficients on temperature was compared for all systems. It was found that the binary interaction parameters are more dependent on temperature than the weighting matrix approach coefficients.

1. Introduction

Supercritical Fluid Extraction (SFE) is the process of separating the solute(s) from the mixture using a supercritical fluid as the extracting solvent. The state of a substance is called supercritical fluid (SCF) when both the temperature and pressure exceed the critical point values as schematically described in a *P-T* phase diagram shown in Figure 1.1, the substance is considered to be in the supercritical region where the maximum solvent capacity and the largest variations in solvent properties can be achieved with small changes in temperature and pressure (Mukhopadhyay, 2000).

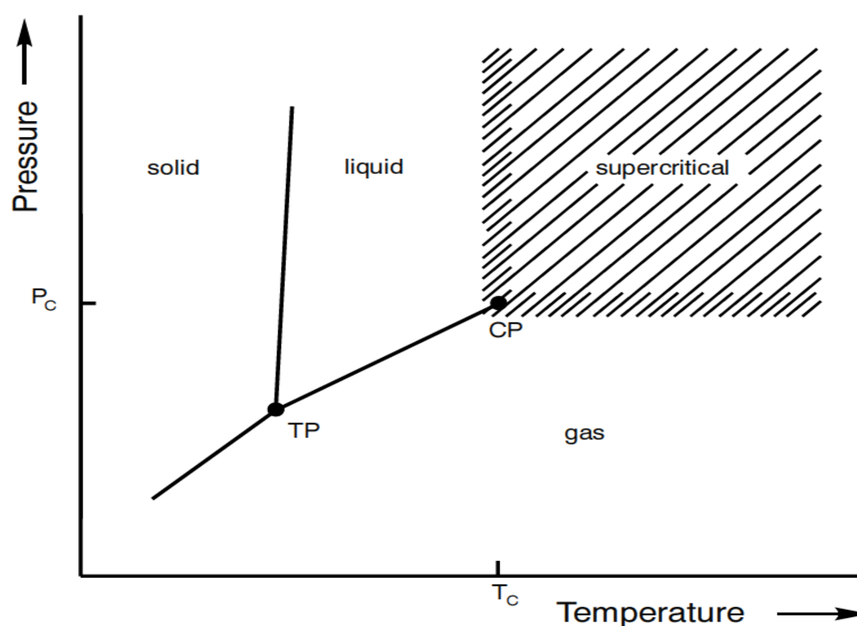

Figure 1.1: Pressure-temperature diagram for a pure component (Mukhopadhyay, 2000).

The physical properties of SCF's are in-between those of a gaseous and liquid states. Typical values of different physical properties for each fluid state are listed in Table 1.1.

Density and viscosity of SCF's are lower than those of liquids; however, diffusivities are higher. Thermal conductivities are relatively high in the supercritical state

and have very large values near the critical point (CP) because, in principle, the heat capacity of a fluid tends to infinity at the CP. Interfacial tension is close to zero in the critical region. In general, the physical properties in the critical region enhance mass and heat transfer processes (Martinez, 2008).

Table 1.1: Comparison of the physical properties of gas, liquid, and SCF's (Martinez, 2008)

Physical Property	Gas ($T_{ambient}$)	SCF (T_c,P_c)	Liquid ($T_{ambient}$)
Density ρ (kg.m^{-3})	0.6 – 2.0	200 – 500	600 – 1000
Dynamic Viscosity μ (10^{-3} Pa.s)	0.01 – 0.3	0.01 – 0.03	0.2 – 3.0
Kinematic Viscosity η (10^{6} m^{2}.s^{-1})	5 – 500	0.05 – 0.1	0.1 – 5.0
Thermal Conductivity λ (W/m.K)	0.01 – 0.025	Maximum	0.1 – 0.2
Diffusion Coefficient D (10^{6} m^{2}.s^{-1})	10 – 40	0.07	0.0002 – 0.002
Surface Tension σ (dyne/cm^{2})	—	—	20 – 40

The main advantages of using supercritical fluids for extraction is that most of SCF's are clean, safe, inexpensive, nonflammable, nontoxic, nonpolluting, more environmentally friendly than organic solvents, facilitates rapid mass transfer and faster completion of extraction than conventional liquid solvents, and offers very attractive extraction characteristics, owing to its favorable diffusivity, viscosity, surface tension and other physical properties (Mukhopadhyay, 2000).

One of the most widely used SCF's is carbon dioxide (CO_2). Carbon Dioxide is an inert, inexpensive, easily available, odorless, tasteless, environment-friendly compared to organic solvents such as CFC's, and generally regarded as safe solvent, and it also has a relatively low critical pressure (74 bar) and critical temperature (31°C). Further, in SFE processes with CO_2, there is no solvent residue in the extract, since it is a gas in the ambient

condition. Also, the energy required for attaining supercritical state of CO_2 is often less than the energy associated with distillation of conventional organic solvent (Mukhopadhyay, 2000). Consequently, it is one of the most commonly used solvents for supercritical fluid extraction. However, Carbon dioxide has the limitation that it is not a particularly good solvent for polar organic compounds, owing to its lack of polarity and lack of capacity for specific solvent-solute interactions (Huang *et al*., 2004).

Supercritical Fluid Extraction technique can be applied to a solid, liquid, or viscous mixture. It can be used as a sample preparation step for analytical purposes, or on a larger scale to either strip unwanted material from a product, e.g., decaffeination or collecting a desired product e.g., essential oils. SFE technique is also being commercialized in the polymers, pharmaceuticals, speciality lubricants, and fine chemicals industries. Supercritical fluids could be utilized in vast fields and applications in addition to SFE such as Dry Cleaning, Supercritical fluid chromatography (SCFC), Supercritical Drying, Biodiesel Production and Refrigeration. Supercritical Dyeing in Carbon Dioxide is also a new approach in textile industry, in order to reduce or eliminate effluent wastewater (Shinoda and Tamura, 2003).

In the determination of solubility of various solutes in any SFE process, thermodynamic constraints are usually described by Equations of State (EOS). EOS are important tool for the correlation and prediction of thermodynamic properties and phase behavior of pure substances and mixtures. Thus, they are widely used in the design, simulation and optimization of chemical processes. Cubic EOS in combination with mixing rules are routinely used in the chemical and petrochemical industries to calculate thermophysical properties and phase equilibria (Escobedo-Alvarado *et al.*, 2001) and

(Orbey and Sandler, 1998). One of the most widely used EOS in SFE calculations is the Peng-Robinson EOS (PR-EOS) which can be expressed as follows (Sandler, 2006):

$$P = \frac{RT}{v-b} - \frac{a(T)}{v(v+b)+b(v-b)} \tag{1.1}$$

Due to the presence of a mixture of components in the supercritical phase, mixing rules for the parameters of PR-EOS should be introduced. Consequently, the mixing rules for *a* and *b* parameters can be written as:

$$a = \sum_{i=1}^{N}\sum_{j=1}^{N} x_i x_j a_{ij}(1-k_{ij}) \tag{1.2}$$

$$b = \sum_{i=1}^{N}\sum_{j=1}^{N} x_i x_j b_{ij}(1-l_{ij}) \tag{1.3}$$

The unlike terms (a_{ij}) and (b_{ij}) [where ($i \neq j$)] are obtained from the combining rules, and the k_{ij} (k_{ij} = 0 for like terms) and l_{ij} (l_{ij} = 0 for like terms) are binary interaction parameters obtained by fitting to experimental solubility data.

Usually, van der Waals one-fluid mixing rules with one or two adjustable parameters are used for solubility calculations. The shortcoming of the van der Waals one-fluid mixing rules is that they are only applicable to mixtures which exhibit relatively moderate solution nonidealities. The van der Waals one-fluid mixing rule with a single binary parameter can't describe highly nonideal mixtures (Škerget *et al*., 2002).

Further problems, which persist in modelling phase equilibria in SCF mixtures with the use of cubic equations of state, where systems are highly nonideal due to high pressures involved, are (Škerget *et al*., 2002):

(a) The interaction parameters are often found to be temperature dependent;

(b) Reliable values of the physical parameters needed are not always available;

(c) The equation does not fit the data equally well at all temperatures and pressures, and especially in the vicinity of critical point.

Several mixing rules have been proposed to extend the capabilities of cubic EOS and make them more useful for the modeling of complex mixtures. The different approaches presented in the literature include the use of multiple interaction parameters in the quadratic mixing rules, the introduction of the local-composition concept, the connection between excess Gibbs free energy models and EOS, and the use of nonquadratic mixing rules (Valderrama, 2003).

Binary interaction parameters are usually obtained via regression analysis of experimental data. There are few attempts to correlate these parameters with certain properties or pure-component properties. Nevertheless, none of the proposed approaches appear to provide a reliable method for the estimation of the interaction parameters, so the problems have not been completely solved yet (Al-Matar and Sweis, 2010).

In this research, the weighting matrix approach (WMA) which was proposed by (Al-Matar and Sweis, 2010) will be used as an alternative to the traditional form of the binary interaction parameters. The binary interaction parameters can be replaced by a weighting matrix such that (Al-Matar, 2002), (Al-Matar and Rockstraw, 2004) and (Al-Matar and Sweis, 2010):

$$a_{ij} = \sum_{i=1}^{2}\sum_{j=1}^{2} w_{ij,a}\left(a_{ii}a_{jj}\right)^{1/2} \quad (1.4)$$

$$b_{ij} = \sum_{i=1}^{2}\sum_{j=1}^{2} w_{ij,b}\left(b_{ii}b_{jj}\right)^{1/2} \quad (1.5)$$

The advantages of the weighting matrix approach include simplification of the combining rules, since they have the same form for the covolume and energy parameters. Further, it provides more flexibility when fitting the weighting coefficients compared to the binary interaction parameters. Also, it can be shown that many of the combining rules in the literature may be reduced to the WMA proposed form with proper choice of the weighting matrix coefficients.

The main goal of this research is evaluating the performance of the weighting matrix approach to that of the binary interaction parameters approach for the energy and covolume. The research includes obtaining the values of the binary interaction parameters as well as the weighting matrix coefficients for the systems that will be studied, in addition, to comparing the two approaches together using the average absolute relative deviation (AARD) as well as the root mean square deviations (RMSD) in the mole fractions of the solid solutes in the supercritical fluid phase.

This thesis is divided into six chapters; a brief review of literature is given in the next chapter. The third chapter gives a background about the solubility of solids in supercritical fluid and the theory of determining the solubility using both modeling approaches, the binary interaction parameters approach with different combining rules and the weighting matrix approach. Solution methodology is presented in the fourth chapter. The fifth chapter consists of the results of this work and discussion of these results. The last chapter gives conclusions and recommendations for future directions to develop this work.

2. Literature Survey

Equations of state (EOS) are commonly applied in engineering practice, since they can be used to predict the thermodynamic properties of fluids and describe phase behaviour of mixtures over large ranges of temperature and pressure. Cubic EOS in combination with mixing rules are currently the most widely used models for the calculation of solubilities of components in SCF (Škerget *et al*., 2002). The form of the mixing rules that extend the use of equations of state developed for pure fluids to mixtures is, more important than the particular *P–V–T* relationship embodied in EOS (Anderko, 2000).

Until recent years, most of the applications of equations of state to mixtures considered the use of the classical van der Waals (vdW) mixing rules (Valderrama, 2003). Interaction parameters have been introduced into the energy parameter (*a*) and covolume parameter (*b*) in vdW-type equations, e.g,

$$P = \frac{RT}{v - b} - \frac{a(T)}{v(v + b) + b(v - b)} \qquad (2.1)$$

in order to improve predictions of mixture properties. However, it has been recognized that, even with the use of interaction parameters, the classical vdW one-fluid mixing rules do not provide accurate results for complex systems (Valderrama, 2003).

During the past 30 years, efforts have been made to extend the applicability of cubic equations of state and make them more useful in obtaining more accurate representations of phase equilibria in highly polar mixtures, associated mixtures, and other very complex systems. A number of empirical mixing rules have been discussed in reviews by (Orbey and Sandler, 1998), (Ashour *et al.*, 2000), (Škerget *et al*., 2002) and (Valderrama, 2003).

Recently, several mixing rules have been developed that make use the combination of the equations of state with activity coefficient models. For example, (Huron-Vidal , 1979) and (Wong-Sandler, 1992) mixing rules applied this approach and have been successful in describing the phase behavior of mixtures involving both polar and associating fluids (Escobedo-Alvarado *et al.*, 2001). It was concluded that these mixing rules are usually fairly reliable for the prediction of multicomponent phase equilibria from binary data, except for the most strongly nonideal systems (Škerget *et al*., 2002).

(Mohamed and Holder, 1987) proposed a simple form of mixing rule which adopted a linear density dependence for the binary parameter "k_{ij}" and used it together with the Peng-Robinson equation of state (PR EOS) to present vapour–liquid equilibria for systems containing carbon dioxide and aromatic hydrocarbons. On the average, the linear density dependent mixing rule reduced the deviations 2.2 times in relation to the classical one-parametric mixing rules (Mohamed and Holder, 1987). (Škerget *et al*., 2002) evaluated the performance of the Mohamed and Holder mixing rule with three adjustable parameters (MH3) to van der Waals one-fluid mixing rules with one (vdW1) and two adjustable binary parameters (vdW2) for solubility calculations of some nonpolar and polar solids; it was concluded that the best performing mixing rule among the three mixing rules investigated is the Mohamed and Holder density dependent mixing rule with three adjustable binary parameters, (Škerget *et al*., 2002).

(Mukhopadhyay and Rao, 1993) stated that increasing the number of binary adjustable parameters does not necessarily increases the accuracy of the calculations. They suggested a co-volume-dependent mixing rule with only one interaction parameter. In their mixing rule an inverse co-volume, "b_{ij}", dependency has been introduced for the attraction

energy parameter "a_{ij}" in order to account for the asymmetry and non-randomness. (Ashour *et al*., 2000) evaluated the performance of the Mukhopadhyay and Rao mixing rule to models that have only one adjustable parameter, such as Panagiotopoulos and Reid mixing rule (1986) and Solute–Solute interaction parameters (Brenneke and Eckert, 1989). It was concluded that the designed mixing rules for solid-supercritical fluids (SCF's) of Mukhopadhyay and Rao give better predictions compared to the other two models for most of the systems investigated (Ashour *et al*., 2000).

To the best of the researcher's knowledge; there has been no work done to study the thermodynamics of supercritical fluid extraction of solid solutes using the weighting matrix approach as an alternative to the traditional form of binary interaction parameters, but (Al-Matar and Sweis 2010), studied the solubility of naphthalene, aspirin, caffeine, C. I. Disperse Red 1 and C. I. Disperse Red 13 in supercritical carbon dioxide using their proposed weighting matrix approach, and also they compared their proposed approach against the binary interaction parameter approach for the energy parameter of the Peng-Robinson equation of state (PR-EOS) using the average absolute relative deviation (AARD) as well as the root mean square deviations (RMSD) in the mole fractions of the solid solutes in the supercritical fluid phase. (Al-Matar and Sweis, 2010) concluded that the weighting matrix approach performed slightly better, or at least equivalent, to the binary interaction parameters and the weighting matrix showed a behavior which is opposite to that of the binary interaction parameters.

3. Theoretical Background

3.1 Solubility of a Solid Species in a Supercritical Fluid

The matter of concern in this research is the prediction of the solubility of large size non-volatile organic solids in the supercritical phase. The fundamental thermodynamic relationship that represents phase equilibrium of a certain component and that must be satisfied for the proper presentation of the phase behavior of a component, regardless of the phases or the components involved is the iso-fugacity condition for each component in all the phases present. For the particular case of a solid and supercritical solvent phase, the iso-fugacity condition can be expressed as (Sandler, 2006) and (Prausnitz *et al*., 1999):

$$f_{i,\mathrm{s}}(T,P,\mathbf{x}) = f_{i,\mathrm{SCF}}(T,P,\mathbf{y}), \quad i = 1,\cdots,N. \qquad (3.1)$$

where subscript s refers to the solid phase, subscript SCF refers to the supercritical fluid phase, f is the fugacity, **x** is the vector of mole fractions in the solid phase, and **y** is the vector of mole fractions in the SCF phase.

Usually, the solid is modeled as a pure phase under the assumption that the SCF phase does not dissolve in the solid. For most purposes this is a very good assumption and introduces negligible error. Consequently, the equilibrium condition for the solute can be reduced to the following form (Sandler, 2006) and (Prausnitz *et al*., 1999):

$$\phi_{\mathrm{s}}(T,P_{\mathrm{s}}^{\mathrm{sat}})P_{\mathrm{s}}^{\mathrm{sat}}(T)\exp\left[\frac{v_s}{RT}(P-P_{\mathrm{s}}^{\mathrm{sat}})\right] = y_{\mathrm{s,SCF}}P\phi_{\mathrm{s,SCF}}(T,P,\mathbf{y}) \qquad (3.2)$$

where $y_{\mathrm{s,SCF}}$ is the mole fraction of the solid in SCF phase, $P_{\mathrm{s}}^{\mathrm{sat}}$ is the sublimation pressure of the pure solid at the system temperature, T. ϕ_{s} is the fugacity coefficient of pure solid at

temperature T, v_s is the molar volume of the pure solid, and $\phi_{s,SCF}$ is the fugacity coefficient of the solid in the SCF at the system temperature and pressure.

The computational difficulty in the evaluation of equation (3.2) is the calculation of the fugacity coefficients since these are the terms introduced to account for the deviations from ideal behavior. Hence the ability to accurately predict the solubility of solids in supercritical solvents depends on the method employed for the correct estimation of these terms.

3.2 Peng Robinson Equation of State (PR-EOS)

Using an equation of state (EOS) provides the means to the calculation of the fugacity coefficients. Cubic EOS's in combination with mixing rules are routinely used in the chemical and petrochemical industries to calculate thermophysical properties and phase equilibria (Sandler, 2001) and (Orbey and Sandler, 1998). One of the most widely used EOS in SFE calculations is the Peng-Robinson EOS (PR-EOS) which can be expressed as follows (Sandler, 2006):

$$P = \frac{RT}{v-b} - \frac{a(T)}{v(v+b)+b(v-b)} \tag{3.3}$$

The parameters of this equation are defined as follows (Sandler, 2006):

$$b = 0.07779\frac{RT_c}{P_c}$$

$$\kappa = 0.37464 + 1.5422\omega - 0.26992\omega^2$$

$$\alpha(T) = \left[1+\kappa\left(1-\sqrt{\frac{T}{T_c}}\right)\right]^2$$

$$a(T) = 0.45724\frac{(RT_c)^2}{P_c}\alpha(T)$$

where v is the molar volume, a is the energy parameter which accounts for intermolecular interactions between the species in the mixture, and b is the covolume which accounts for size differences between the species of the mixture, T_c is the critical temperature, P_c is the critical pressure, and ω is Pitzer's acentric factor.

3.3 Mixing Rules

For systems with more than one component, the fugacity in the supercritical solvent phase could also be calculated from the EOS, however, due to the presence of a mixture of components in the supercritical phase the interaction between components should be accounted for through the introduction of mixing rules for the parameters in equation (3.3) since the phase now consists of a mixture of components and is not a pure phase any more. Consequently, the mixing rules for a and b parameters can be written as:

$$a = \sum_{i=1}^{N}\sum_{j=1}^{N} x_i x_j a_{ij}(1-k_{ij}) \qquad (3.4)$$

$$b = \sum_{i=1}^{N}\sum_{j=1}^{N} x_i x_j b_{ij}(1-l_{ij}) \qquad (3.5)$$

The unlike terms (a_{ij}) and (b_{ij}) [where ($i \neq j$)] are obtained from the combining rules, and the k_{ij} (k_{ij} = 0 for like terms) and l_{ij} (l_{ij} = 0 for like terms) are binary interaction parameters obtained by fitting to experimental solubility data.

In this research, the weighting matrix approach (WMA) which was proposed by (Al-Matar and Sweis, 2010) is used as an alternative to the traditional form of the binary interaction parameters. The weighting matrix approach proposes that the binary interaction parameters be replaced by a weighting matrix such that (Al-Matar, 2002), (Al-Matar and Rockstraw, 2004) and (Al-Matar and Sweis, 2010):

$$a_{ij} = \sum_{i=1}^{2}\sum_{j=1}^{2} w_{ij,a}\left(a_{ii}a_{jj}\right)^{1/2} \quad (3.6)$$

$$b_{ij} = \sum_{i=1}^{2}\sum_{j=1}^{2} w_{ij,b}\left(b_{ii}b_{jj}\right)^{1/2} \quad (3.7)$$

from which the mixing rule changes form to:

$$a = \sum_{i=1}^{N}\sum_{j=1}^{N} x_i x_j a_{ij} \quad (3.4\text{ a})$$

$$b = \sum_{i=1}^{N}\sum_{j=1}^{N} x_i x_j b_{ij} \quad (3.5\text{ a})$$

Examples for the use of such weighting matrix are given below for the arithmetic and geometric mean rules:

Arithmetic Mean Rule	Geometric Mean Rule
$w_{ij,b} = \begin{bmatrix} 0.5 & 0 \\ 0 & 0.5 \end{bmatrix}$	$w_{ij,a} = \begin{bmatrix} 0 & 0.5 \\ 0.5 & 0 \end{bmatrix}$

Three combining rules and the weighting matrix approach were utilized together with the PR-EOS for evaluating the performance of the weighting matrix approach to that of the binary interaction parameters approach for the energy and covolume parameters. The used combining rules in this research can be expressed as follows:

1. Lorentz – Berthelot Combining Rules (Sandler, 2006) and (Prausnitz *et al*., 1999):

$$b_{ij} = \left(\frac{b_{ii} + b_{jj}}{2}\right) \quad (3.8)$$

$$a_{ij} = \left(a_{ii}a_{jj}\right)^{1/2} \quad (3.9)$$

2. The WHAK rules which are based on the molecularly proposed rules by Waldman and Hagler (1993) and developed for cubic EOS by Al-Matar (Al-Matar and Rockstraw, 2006):

$$b_{ij} = \left(\frac{b_{ii}^2 + b_{jj}^2}{2} \right)^{1/2} \tag{3.10}$$

$$a_{ij} = \left(a_{ii} a_{jj} \right)^{1/2} \left(\frac{b_{ii} b_{jj}}{b_{ij}^{\ 2}} \right) \tag{3.11}$$

3. MADAR–1 rules which are based on the molecularly proposed rules by Al-Matar and Rockstraw (Al-Matar, 2002), (Al-Matar and Rockstraw, 2004) and (Al-Matar and Rockstraw, 2006):

$$b_{ij} = \frac{1}{3} \sum_{L=0}^{2} \left(\frac{1}{4} \frac{(b_{ii} + b_{jj})^2}{b_{ii}^{L/3} b_{jj}^{L/3}} \right)^{\frac{1}{2-2L/3}} \tag{3.12}$$

$$a_{ij} = \left(a_{ii} a_{jj} \right)^{1/2} \left(\frac{b_{ii} b_{jj}}{b_{ij}^{\ 2}} \right) \tag{3.13}$$

3.4 Fugacity Coefficient

The PR-EOS can be used to derive the fugacity coefficient for each species in a mixture. The expression for the fugacity coefficient, and after much algebraic manipulation, can be written as (Sandler, 2006) and (Prausnitz *et al*., 1999):

$$\ln \phi_i = \frac{B_i}{B}(Z - 1) - \ln(Z - B) - \frac{A}{\sqrt{8}B} \left[\frac{2A_i}{A} - \frac{B_i}{B} \right] \ln \left[\frac{Z + (1+\sqrt{2})B}{Z + (1-\sqrt{2})B} \right] \tag{3.14}$$

where Z is the compressibility factor for the SCF phase, and the individual species reduced volume and energy parameters are expressed as (Sandler, 2006) and (Orbey and Sandler, 1998):

$$A = \frac{aP}{(RT)^2} \tag{3.15}$$

$$B = \frac{bP}{RT} \tag{3.16}$$

$$A_i = \frac{\left(2\sum_{k=1}^{N} x_k a_{ik} - a\right)P}{(RT)^2} \tag{3.17}$$

$$B_i = \frac{\left(2\sum_{k=1}^{N} x_k b_{ik} - b\right)P}{RT} \tag{3.18}$$

The compressibility factor (Z) is the maximum real root of the following cubic eqaution:

$$Z^3 + \alpha Z^2 + \beta Z + \gamma = 0 \tag{3.19}$$

The coefficients of the cubic equation for (Z) are defined as follows:

$$\alpha = -1 + B \tag{3.20}$$

$$\beta = A - 2B - 3B^2 \tag{3.21}$$

$$\gamma = -AB + B^2 + B^3 \tag{3.22}$$

4. Solution Methodology

Conceptually, the solution for the solubility is straightforward. The major difficulty is in the computational work demanded. The solution requires a nested iterative method to solve for the mole fraction of the solid in the supercritical fluid phase and for the compressibility factor in the cubic EOS. In this research, `MatLab`© Software was used to solve for the solid solubility in the supercritical fluid. `MatLab`© built-in functions `roots` which return all roots of polynomials, and `fminbnd` which is a Single-Variable Bounded Nonlinear Function Minimization Techinque were used for solution. The problem was converted to a minimization problem instead of a root finding problem since we can bind the search interval using the `fminbnd` function. Convergence was achieved typically in less than 20 iterations. More details about the used `MatLab`© codes are mentioned in Appendeix (B).

The fitted values of the binary interaction parameters and the weighting matrix coefficients were obtained by minimizing the average absolute relative deviations (AARD) and also by minimizing the root mean square deviations (RMSD) between the experimental and predicted solubilities, the AARD & the RMSD are defined as follows:

$$AARD\ (\%) = \frac{1}{n}\left[\sum_{n=1}^{n}\left|\frac{\{y_{2,n}^{\exp} - y_{2,n}^{cal}\}}{y_{2,n}^{\exp}}\right|\right] x\,100 \qquad (4.1)$$

$$RMSD = \frac{1}{n}\sum_{n=1}^{n}(y_{2,n}^{\exp} - y_{2,n}^{cal})^{2} \qquad (4.2)$$

The minimizing technique for the AARD & the RMSD was accomplished using `Solver Add-in` Analysis Tool in `Microsoft Excel`© Software, this tool finds the optimum value of a target cell by changing values in cells used to calculate the target cell.

The following algorithm presents the procedure of calculating the solubility of a solid solute in a SCF:

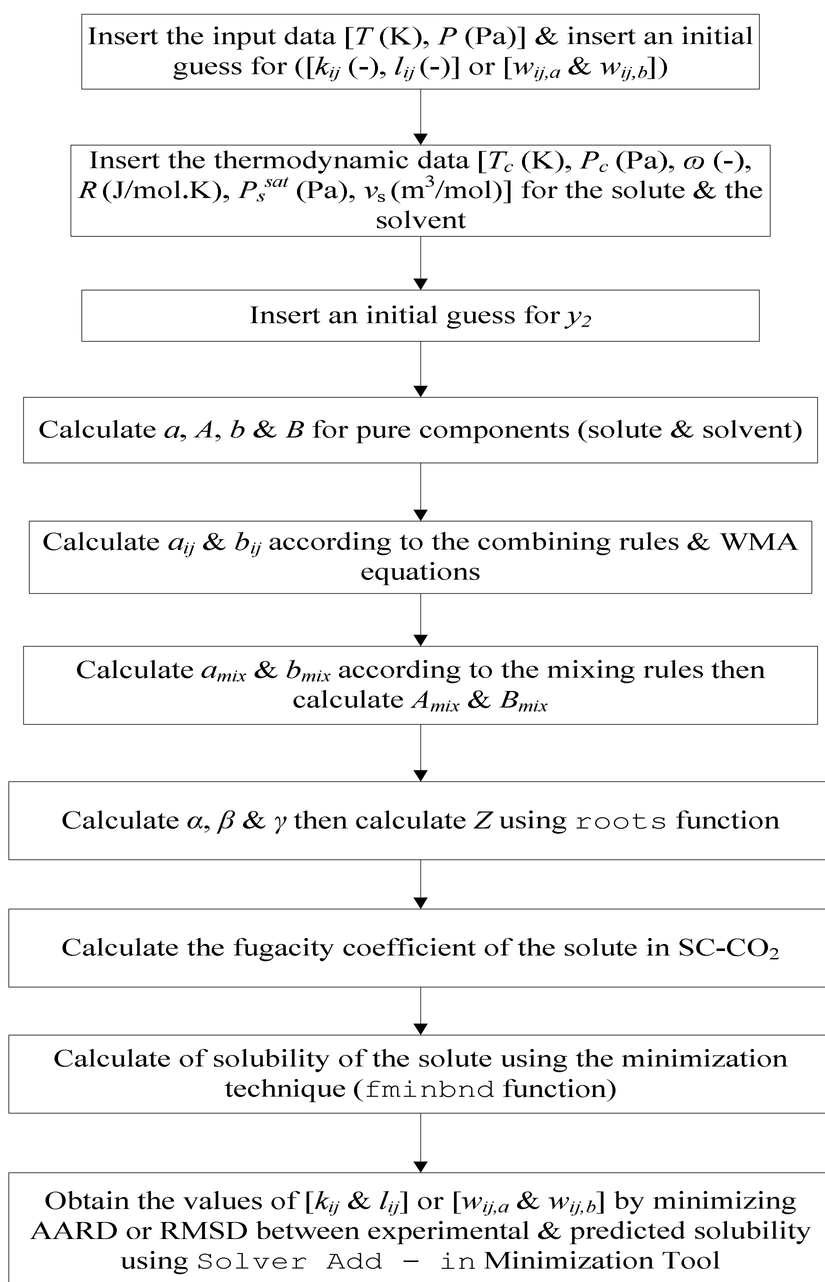

❖ Experimental Data Sources

The solubility of Aspirin, C. I. Disperse Red 1, C. I. Disperse Red 13, Naphthalene, Xanthene and Xanthone in supercritical carbon dioxide is predicted using the binary interaction parameters approach with Lorentz-Berthelot (LB), Waldman-Hagler (WH), and MADAR-1 combining rules as well as the weighting matrix approach. Experimental data for the solubility of these solid solutes in supercritical CO_2 were taken from the following literature sources:

- Aspirin in SC-CO_2: (Huang *et al.*, 2004).
- C. I. Disperse Red 1 and 13 in SC-CO_2: (Shinoda and Tamura, 2003).
- Naphthalene in SC-CO_2: (Gupta and Shim, 2007).
- Xanthene and Xanthone in SC-CO_2: (Huang *et al.*, 2005).

The critical constants and physical properties used in this research are provided in Table 4.1. The chemical structure of the compounds used in this research are shown in Table 4.2.

Table 4.1: Critical constants and sublimation pressures for the compounds considered in this research.

Solid Compound	**Critical Constants**			**Sublimation Pressure**		υ_s
	T_c (K)	P_c (bar)	ω (-)	P_s^{sat} (Pa)	T (K)	(cm^3/mol)
Aspirin (Huang *et al.*, 2004)	762.9	32.8	0.817	0.09021 0.2803 0.8011	308.15 318.15 328.15	129.64
C.I. Disperse Red 1 (Shinoda and Tamura, 2003)	928.6	19.07	1.391	2.556×10^{-8} 3.942×10^{-6} 2.419×10^{-4}	323. 15 353.15 383.15	251.1

C.I. Disperse Red 13 (Shinoda and Tamura, 2003)	937.0	18.20	1.409	1.078×10^{-8} 1.852×10^{-6} 1.242×10^{-4}	323.15 353.15 383.15	261.0
Naphthalene (Gupta and Shim, 2007)	748.2	40.5	0.302	$\log_{10} P = 13.583 - 3733.9/T$		110.3
Xanthene (Huang *et al*., 2005)	833.0	34.4	0.550	1.63×10^{-1} 1.48	308.15 328.15	144.3
Xanthone (Huang *et al*., 2005)	873.4	35.9	0.750	4.48×10^{-3} 5.27×10^{-2}	308.15 328.15	146.0
CO_2 (Solvent)	304.2	73.76	0.225	--		--

Table 4.2: Chemical structure of the compounds considered in this research.

Aspirin **CAS: 50-78-2**	**C.I. Disperse Red 1** **CAS: 2872-52-8**	**C.I. Disperse Red 13** **CAS: 3180-81-2**
Naphthalene **CAS: 91-20-3**	**Xanthene** **CAS: 92-83-1**	**Xanthone** **CAS: 90-47-1**
	O=C=O carbon dioxide **CAS: 124-38-9**	

5. Results and Discussion

The solubilities of Aspirin, C.I. Disperse Red 1, C.I. Disperse Red 13, Naphthalene, Xanthene and Xanthone in supercritical CO_2 have been calculated at various temperature and pressure ranges using the PR – EOS with two modeling approaches, binary interaction parameters approach using Lorentz-Berthelot (LB), Waldman-Hagler (WH), and MADAR-1 combining rules as well as the Weighting Matrix Approach (WMA), very good agreement between models calculations and experimentally measured solubility was observed.

The optimum values of the binary interaction parameters and the weighting matrix approach coefficients for all systems studied in this research were obtained by minimizing the average absolute relative deviations (AARD) and also by minimizing the root mean square deviations (RMSD) between the experimental solubility and predicted solubility. It was noticed that fitting the binary interaction parameters values and the weighting matrix approach coefficients by minimizing the AARD gives better results than fitting by minimizing the RMSD; the fitting results which were obtained by minimizing the RMSD are mentioned in Appendix (A).

Table 5.1 compares the average absolute relative deviations (AARD) in the solubility mole fraction for both modeling approaches, binary interaction parameters approach using Lorentz-Berthelot (LB), Waldman-Hagler (WH), and MADAR-1 combining rules as well as the Weighting Matrix Approach (WMA) for the energy parameter, a, only, with the AARD values for the purely predictive approach, i.e., ($k_{ij} = 0$ and $w_{ij,a} = 0$). Table 5.1 also provides the optimum values of the energy binary interaction

parameters, k_{ij}, as well as the weighting approach matrix coefficients for energy parameter, $w_{ij,a}$, for Aspirin, C.I. Disperse Red 1, C.I. Disperse Red 13, Naphthalene, Xanthene and Xanthone.

Table 5.2 compares the average absolute relative deviations (AARD) in the solubility mole fraction for both modeling approaches, binary interaction parameters approach using LB, WH, and MADAR-1 combining rules as well as the weighting matrix approach for both energy parameter, *a*, and covolume parameter, *b*, with the AARD values for the purely predictive approach, i.e., (k_{ij} = 0, l_{ij} = 0, $w_{ij,a}$ = 0 and $w_{ij,b}$ = 0). Table 5.2 also provides the optimum values of the binary interaction parameters for the energy parameter, k_{ij}, and also for the covolume parameter, l_{ij}, as well as the weighting matrix approach coefficients for the energy parameter, $w_{ij,a}$, and also for the covolume parameter, $w_{ij,b}$, for all systems studied in this research.

The following figures show the solubility of Aspirin, C.I. Disperse Red 1, C.I. Disperse Red 13, Naphthalene, Xanthene and Xanthone in supercritical CO_2 at various temperatures as a function of pressure together with both modeling approaches, binary interaction parameters approach using Lorentz-Berthelot (LB), Waldman-Hagler (WH), and MADAR-1 combining rules as well as the Weighting Matrix Approach (WMA).

From table 5.1, table 5.2 and also from the purely predictive figures for all systems studied in this research; it can be noticed that the purely predictive approach gives the worst behavior and also the worst AARD, as expected, with two to three orders of magnitude of overestimation or underestimation, this emphasizes the rule that supercritical conditions can play in testing equations of state due to the extreme pressures and asymmetry between the

mixture components. It also appears that the purely predictive approach, for all systems studied in this research, yields better estimates at higher temperatures. This may be attributed to the nature of molecular interactions taking place at such temperatures.

Form table 5.1, and also from energy parameter, *a*, figures for all systems studied in this research; it can be noticed that both modeling approaches provide better estimates compared to the purely predictive approach. It also appears from table 5.1 that the values of the energy binary interaction parameters for all systems studied in this research using WH and MADAR-1 combining rules are negative which are opposite to that using LB combining rules and the weighting matrix approach.

From table 5.1; it can be noticed that using WH combining rules with the energy binary interaction parameter (k_{ij}) for all systems leads to superior estimates compared to LB & MADAR-1 combining rules as well as the WMA with the minimum overall average of AARD (17.0 %).

From table 5.1, it can be noticed that for Aspirin, using LB combining rules with the energy binary interaction parameter (k_{ij}) leads to suerior estimates compared to WMA as well as WH & MADAR-1 combining rules with the overall average of AARD of (6.0 %, 9.6 %, 18.1 % & 27.5 %) respectively.

From table 5.1, it can be noticed that for C.I. Disperse Red 1, using WH combining rules with the energy binary interaction parameter (k_{ij}) leads to suerior estimates compared to LB combining rules, WMA & MADAR-1 combining rules with the overall average of AARD of (20.1 %, 29.7 %, 57.2 % & 64.4 %) respectively.

From table 5.1, it can be noticed that for C.I. Disperse Red 13, using WH combining rules with the energy binary interaction parameter (k_{ij}) leads to suerior estimates compared to LB & MADAR-1 combining rules as well as the WMA with the overall average of AARD of (25.6 %, 41.8 %, 58.7 % & 66.1 %) respectively.

From table 5.1, it can be noticed that for Naphthalene, using WH combining rules with the energy binary interaction parameter (k_{ij}) leads to suerior estimates compared to MADAR-1 & LB combining rules as well as the WMA with the overall average of AARD of (7.3 %, 9.4 %, 11.0 % & 19.7 %) respectively.

From table 5.1, it can be noticed that for Xanthene, using LB combining rules with the energy binary interaction parameter (k_{ij}) leads to suerior estimates compared to WH combining rules, WMA & MADAR-1combining rules with the overall average of AARD of (7.9 %, 13.6 %, 24.4 % & 28.7 %) respectively.

From table 5.1, it can be noticed that for Xanthone, using LB combining rules with the energy binary interaction parameter (k_{ij}) leads to suerior estimates compared to WH combining rules, WMA & MADAR-1combining rules with the overall average of AARD of (11.5 %, 17.3 %, 27.6 % & 30.6 %) respectively.

Form table 5.2, and also from energy parameter, *a*, and covolume parameter, *b*, figures for all systems studied in this research; it can be noticed that both modeling approaches provide superior estimates compared to the purely predictive approach and to the energy parameter using approach with almost the same values of the solubility of the solid solute in SC-CO_2 (e.g., Figure 5.1.1.3 for Aspirin with both (*a*) & (*b*) parameters) and also the same values of the AARD.

From table 5.2; it can be noticed that the energy binary interaction parameter, k_{ij}, values using WH, and MADAR-1 combining rules are almost the same for all systems studied in this research by modeling with both (a) & (b) parameters.

It also appears from table 5.1 and table 5.2 that modeling with MADAR-1 combining rules doesn't give values for both energy and covolume binary interaction parameters (k_{ij} & l_{ij}) for both C.I. Disperse Red 1 and C.I. Disperse Red 13 at 323.15 K for both energy and covolume binary interaction parameters by minimizing the AARD.

From table A.1 and table A.2 in Appendix (A); it can be noticed that modeling with Waldman-Hagler (WH) combining rules doesn't give values for both energy and covolume binary interaction parameters (k_{ij} & l_{ij}) for both C.I. Disperse Red 1 and C.I. Disperse Red 13 at 323.15 K and at 353.15 K for both energy and covolume binary interaction parameters by minimizing the RMSD. It also can be noticed that modeling with MADAR-1 combining rules doesn't give values for both energy and covolume binary interaction parameters (k_{ij} & l_{ij}) for both C.I. Disperse Red 1 and C.I. Disperse Red 13 at all temperatures, 323.15 K, 353.15 K and 383.15 K, for both energy and covolume binary interaction parameters by minimizing the RMSD.

Table 5.1: Modeling results for solids solubility in SC – CO_2 using the PR – EOS with the energy binary interaction parameter and WMA coefficient by minimizing AARD.

Solid Compound	T (K)	P (bar)	n	Pure Predictive	LB (k_{ij})		WH (k_{ij})		MADAR-1 (k_{ij})		WMA ($w_{ij,a}$)	
				AARD (%)	k_{ij}	AARD (%)	k_{ij}	AARD (%)	k_{ij}	AARD (%)	$w_{ij,a}$	AARD (%)
Aspirin	308.15	120.0 - 250.0	8	16668	0.2085	2.1357	-1.5593	12.7305	-2.5013	21.1955	0.5329	11.5633
	318.15	120.0 - 250.0	8	8329	0.2051	8.3361	-1.5524	21.6604	-2.4735	32.1876	0.5319	7.7642
	328.15	120.0 - 250.0	8	4886	0.2054	7.5599	-1.5440	19.9129	-2.4564	29.0359	0.5315	9.4274
	Overall		**24**	**Avg. = 9961**	**Average = 6.0105**		**Average = 18.1013**		**Average = 27.4730**		**Average = 9.5849**	
C.I. Disperse Red 1	323.15	100.0 - 300.0	6	12294	0.1235	26.5343	-4.9037	33.4488	0	100.0	0.5157	55.1017
	353.15	100.0 - 300.0	6	1286	0.1013	37.1241	-5.0608	14.5316	-14.9296	48.6656	0.5143	66.0755
	383.15	100.0 - 300.0	6	210	0.0678	25.4392	-5.2150	12.2267	-15.1986	44.5823	0.5121	50.4792
	Overall		**18**	**Avg. = 4597**	**Average = 29.6992**		**Average = 20.0690**		**Average = 64.4160**		**Average = 57.2188**	
C.I. Disperse Red 13	323.15	100.0 - 300.0	6	4023	0.0934	35.3281	-5.4962	28.1959	0	100.0	0.5143	65.1474
	353.15	100.0 - 300.0	6	490	0.0717	49.9927	-5.6364	26.7481	-17.8591	45.9179	0.5128	69.9079
	383.15	100.0 - 300.0	6	96	0.0393	39.9399	-5.8012	21.9274	-18.2903	30.0470	0.5108	63.3717
	Overall		**18**	**Avg. = 1536**	**Average = 41.7536**		**Average = 25.6238**		**Average = 58.6550**		**Average = 66.1423**	
Naphthalene	308	71.9 - 321.5	87	227.91	0.0735	18.7383	-1.3686	10.2211	-1.8246	11.8945	0.5254	32.8342
	313	124.2 - 261.3	8	236.08	0.0722	10.2291	-1.3742	2.1872	-1.8360	3.6395	0.5247	20.7431
	318	98.3 - 297.0	20	161.76	0.0634	15.2577	-1.3935	5.7532	-1.8568	3.8197	0.5235	26.9667
	323	120.1 - 304.7	11	138.62	0.0573	11.1393	-1.4107	1.2206	-1.8780	4.9453	0.5227	23.2655
	328	76.9 - 278.8	27	53.14	0.0341	12.3498	-1.4508	9.4537	-1.9152	12.6218	0.5185	24.3141
	333.55	108.4 - 291.4	19	12.26	0.0086	5.7446	-1.5107	13.2540	-1.9858	17.3490	0.5147	6.1409
	338.05	151.8 - 232.2	7	3.63	0.0103	3.6298	-1.4992	8.8568	-1.9699	11.2301	0.5141	3.7343
	Overall		**179**	**Avg. = 119**	**Average = 11.0126**		**Average = 7.2781**		**Average = 9.3571**		**Average = 19.7141**	
Xanthene	308.15	80.0 - 240.0	7	310.44	0.0619	9.4782	-2.1059	9.5899	-3.3093	25.9202	0.5185	26.5537

	328.15	90.0 - 210.0	6	131.10	0.0526	6.4206	-2.0977	17.5844	-3.2614	31.5668	0.5160	22.2551
	Overall		**13**	**Avg. = 221**	**Average = 7.9494**		**Average = 13.5872**		**Average = 28.7435**		**Average = 24.4044**	
Xanthone	308.15	120.0 - 300.0	8	7106	0.1550	8.4472	-1.8206	24.7837	-2.9407	36.5311	0.5243	21.3456
	328.15	120.0 - 300.0	8	2626	0.1513	14.5482	-1.8256	9.7665	-2.9339	24.6304	0.5236	33.8890
	Overall		**16**	**Avg. = 4866**	**Average = 11.4977**		**Average = 17.2751**		**Average = 30.5807**		**Average = 27.6173**	
Overall			**268**	**Avg. = 3550**	**Average = 17.9872**		**Average = 16.9891**		**Average = 36.5376**		**Average = 34.1137**	

Table 5.2: Modeling results for solids solubility in SC – CO_2 using the PR – EOS with the energy and covolume binary interaction parameters and WMA coefficients by minimizing AARD.

Solid Compound	***T*** **(K)**	***P*** **(bar)**	**n**	**Pure Predictive**	**LB (k_{ij} , l_{ij})**			**WH (k_{ij} , l_{ij})**			**MADAR-1 (k_{ij} , l_{ij})**			**WMA ($w_{ij,a}$, $w_{ij,b}$)**		
				AARD (%)	k_{ij}	l_{ij}	**AARD (%)**	k_{ij}	l_{ij}	**AARD (%)**	k_{ij}	l_{ij}	**AARD (%)**	$w_{ij,a}$	$w_{ij,b}$	**AARD (%)**
Aspirin	308.15	120.0 - 250.0	8	16668	0.2209	0.0305	1.2564	-0.4304	0.2054	1.2645	-0.4321	0.2967	1.2569	0.5223	0.4012	1.2559
	318.15	120.0 - 250.0	8	8329	0.2662	0.1574	2.9729	-0.0180	0.3093	2.9714	-0.0192	0.3887	2.9695	0.5268	0.4505	2.9733
	328.15	120.0 - 250.0	8	4886	0.2447	0.1049	4.5463	-0.1824	0.2663	4.5463	-0.1840	0.3505	4.5554	0.5246	0.4301	4.5452
	Overall		**24**	**Avg. = 9961**	**Average = 2.9252**			**Average = 2.9274**			**Average = 2.9273**			**Average = 2.9248**		
C.I. Disperse Red 1	323.15	100.0 - 300.0	6	12294	0.0725	-0.1292	25.0757	-3.1132	0.1365	25.1000	0	0	100.0	0.5035	0.2973	24.8800
	353.15	100.0 - 300.0	6	1286	-0.0430	-0.3732	12.2222	-5.8355	-0.0498	12.2340	-5.8370	0.2941	12.2362	0.4981	0.2175	11.9377
	383.15	100.0 - 300.0	6	210	-0.0369	-0.2846	12.2748	-4.9444	0.0181	12.2744	-4.9429	0.3399	12.2778	0.4982	0.2444	12.2748
	Overall		**18**	**Avg. = 4597**	**Average = 16.5242**			**Average = 16.5361**			**Average = 41.5047**			**Average = 16.3642**		
C.I. Disperse Red 13	323.15	100.0 - 300.0	6	4023	-0.0146	-0.2630	27.0023	-4.9371	0.0356	27.0869	0	0	100.0	0.4992	0.2484	27.0828
	353.15	100.0 - 300.0	6	490	-0.1407	-0.5355	17.8852	-8.7999	-0.1694	17.8758	-8.7931	0.2350	17.8780	0.4935	0.1574	17.8864
	383.15	100.0 - 300.0	6	96	-0.1712	-0.5567	13.6581	-9.3343	-0.1852	13.6583	-9.3401	0.2243	13.6610	0.4921	0.1502	13.6578
	Overall		**18**	**Avg. = 1536**	**Average = 19.5152**			**Average = 19.5403**			**Average = 43.8463**			**Average = 19.5424**		
Naphthalene	308	71.9 - 321.5	87	227.91	0.0101	-0.1436	10.7580	-1.1697	0.0345	10.7537	-1.1693	0.1003	10.7560	0.5014	0.3489	10.7590
	313	124.2 - 261.3	8	236.08	-0.0203	-0.2088	1.9745	-1.5012	-0.0209	1.9769	-1.4989	0.0489	1.9747	0.4971	0.3223	1.9740

	318	98.3 - 297.0	20	161.76	-0.0544	-0.2695	3.8264	-1.8491	-0.0719	3.8255	-1.8485	0.0012	3.8258	0.4924	0.2976	3.8266
	323	120.1 - 304.7	11	138.62	-0.0281	-0.1911	1.1444	-1.4462	-0.0058	1.1400	-1.4441	0.0630	1.1426	0.4961	0.3295	1.1450
	328	76.9 - 278.8	27	53.14	-0.0150	-0.1176	9.4433	-1.1249	0.0564	9.4421	-1.1252	0.1206	9.4413	0.4979	0.3594	9.4435
	333.55	108.4 - 291.4	19	12.26	0.0405	0.0757	4.2005	-0.3757	0.2192	4.2071	-0.3756	0.2724	4.2095	0.5056	0.4382	4.1999
	338.05	151.8 - 232.2	7	3.63	0.0522	0.1047	1.9161	-0.2731	0.2442	1.9173	-0.2738	0.2955	1.9147	0.5073	0.4500	1.9161
	Overall		**179**	**Avg. = 119**	**Average = 4.7519**			**Average = 4.7518**			**Average = 4.7521**			**Average = 4.7520**		
Xanthene	308.15	80.0 - 240.0	7	310.44	0.0195	-0.1048	4.7568	-1.4086	0.0983	4.7337	-1.4063	0.2111	4.7541	0.5019	0.3457	4.7581
	328.15	90.0 - 210.0	6	131.10	0.0447	-0.0219	6.8321	-1.0055	0.1663	6.8320	-1.0076	0.2700	6.8422	0.5044	0.3777	6.8316
	Overall		**13**	**Avg. = 221**	**Average = 5.7944**			**Average = 5.7829**			**Average = 5.7982**			**Average = 5.7948**		
Xanthone	308.15	120.0 - 300.0	8	7106	0.1711	0.0418	8.8864	-0.5372	0.2183	8.8778	-0.5352	0.3170	8.8869	0.5153	0.4020	8.8869
	328.15	120.0 - 300.0	8	2626	0.1011	-0.1358	7.0254	-1.3405	0.0737	7.0225	-1.3407	0.1902	7.0220	0.5090	0.3334	7.0259
	Overall		**16**	**Avg. = 4866**	**Average = 7.9559**			**Average = 7.9501**			**Average = 7.9544**			**Average = 7.9564**		
Overall			**268**	**Avg. = 3550**	**Average = 9.5778**			**Average = 9.5814**			**Average = 17.7972**			**Average = 9.5558**		

5.1 Solubility of Solid Compounds in Supercritical CO_2 Using Combining Rules and Weighting Matrix Approach

5.1.1 Solubility of Aspirin Using Combining Rules and Weighting Matrix Approach

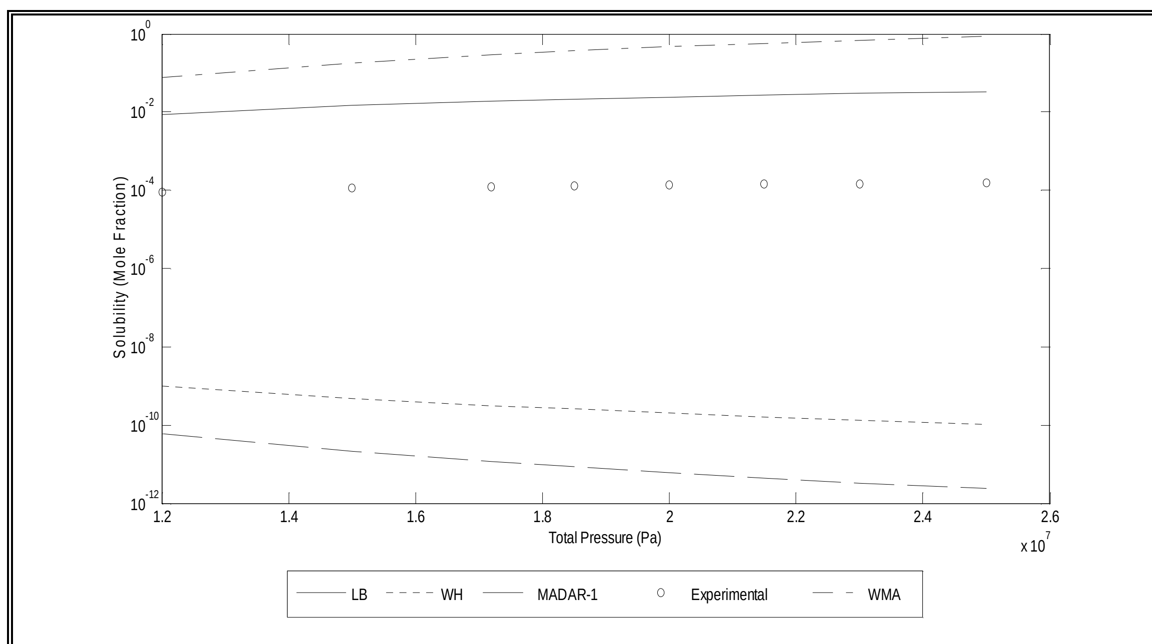

Figure 5.1.1.1: Solubility of Aspirin in SC – CO_2 at 308.15 K (Pure Predictive)

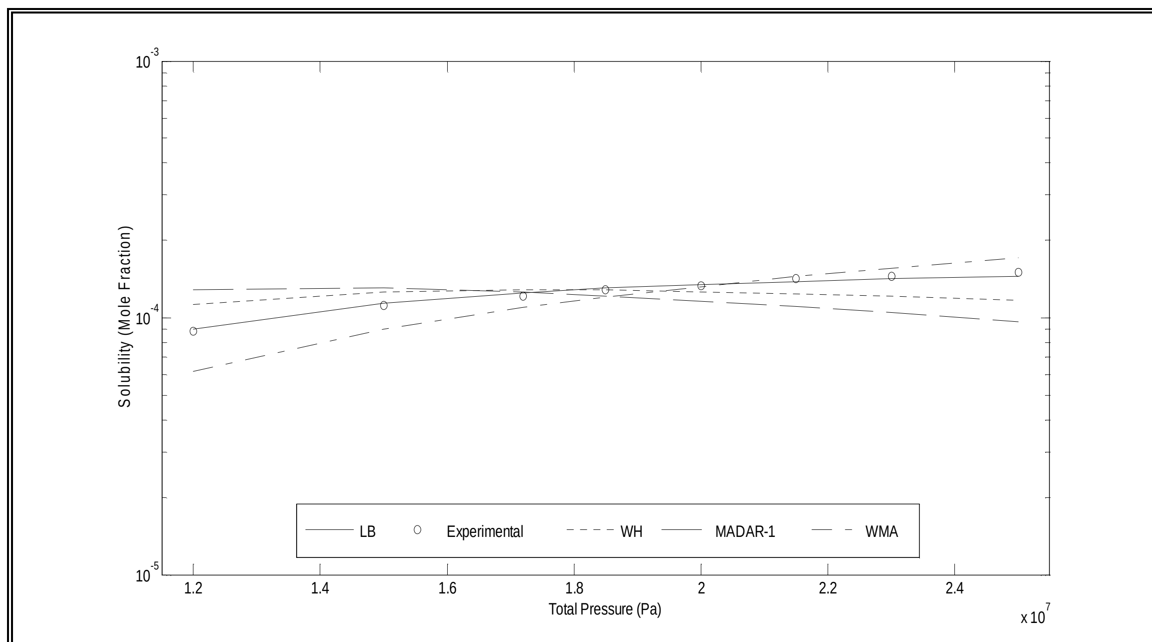

Figure 5.1.1.2: Solubility of Aspirin in SC – CO_2 at 308.15 K with (a) parameters only

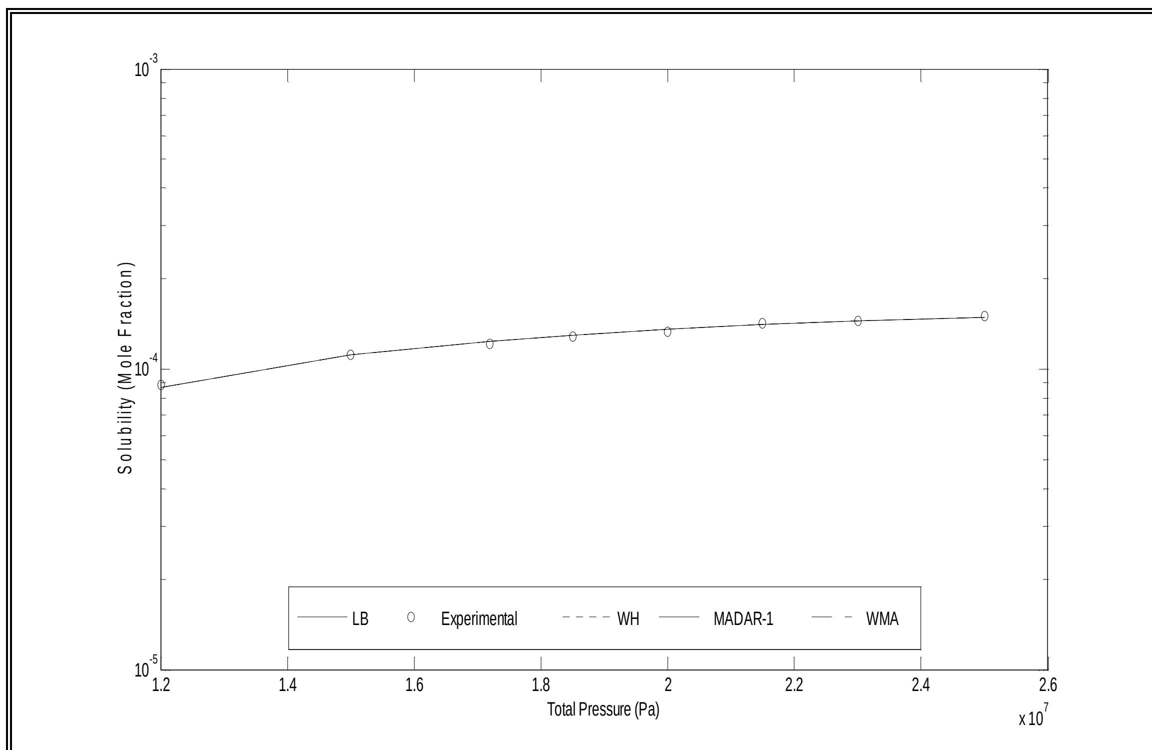

Figure 5.1.1.3: Solubility of Aspirin in SC – CO_2 at 308.15 K with (a) & (b) parameters

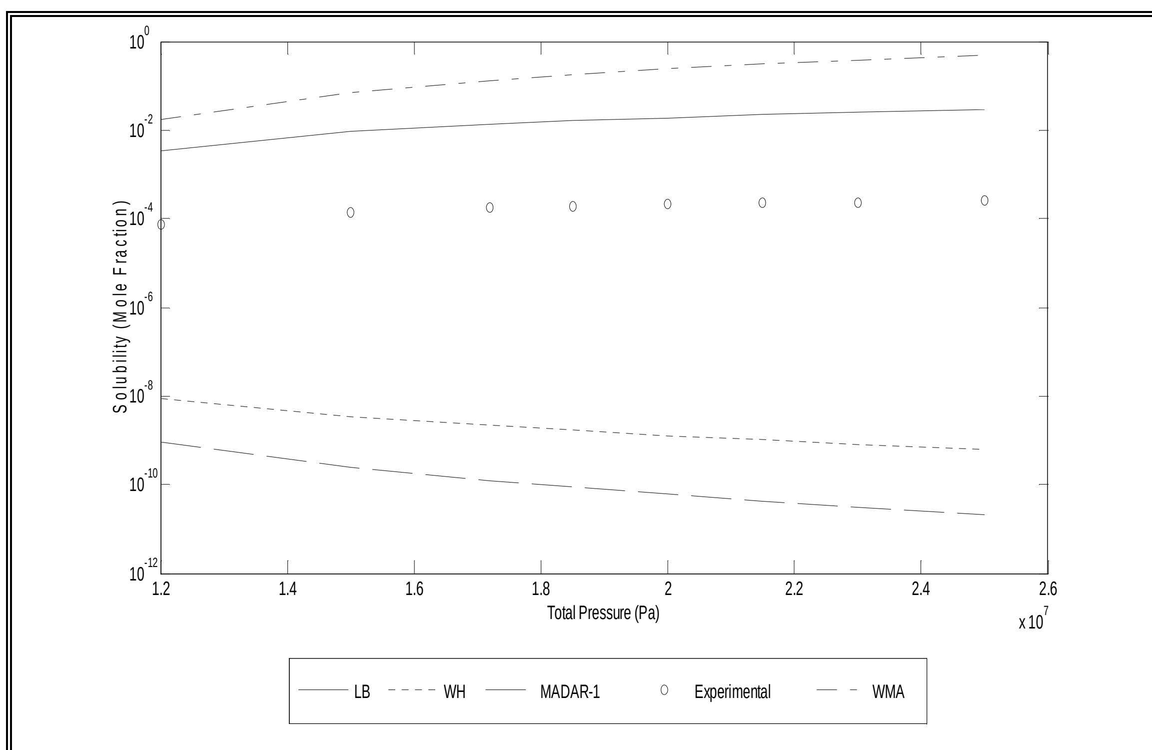

Figure 5.1.1.4: Solubility of Aspirin in SC – CO_2 at 318.15 K (Pure Predictive)

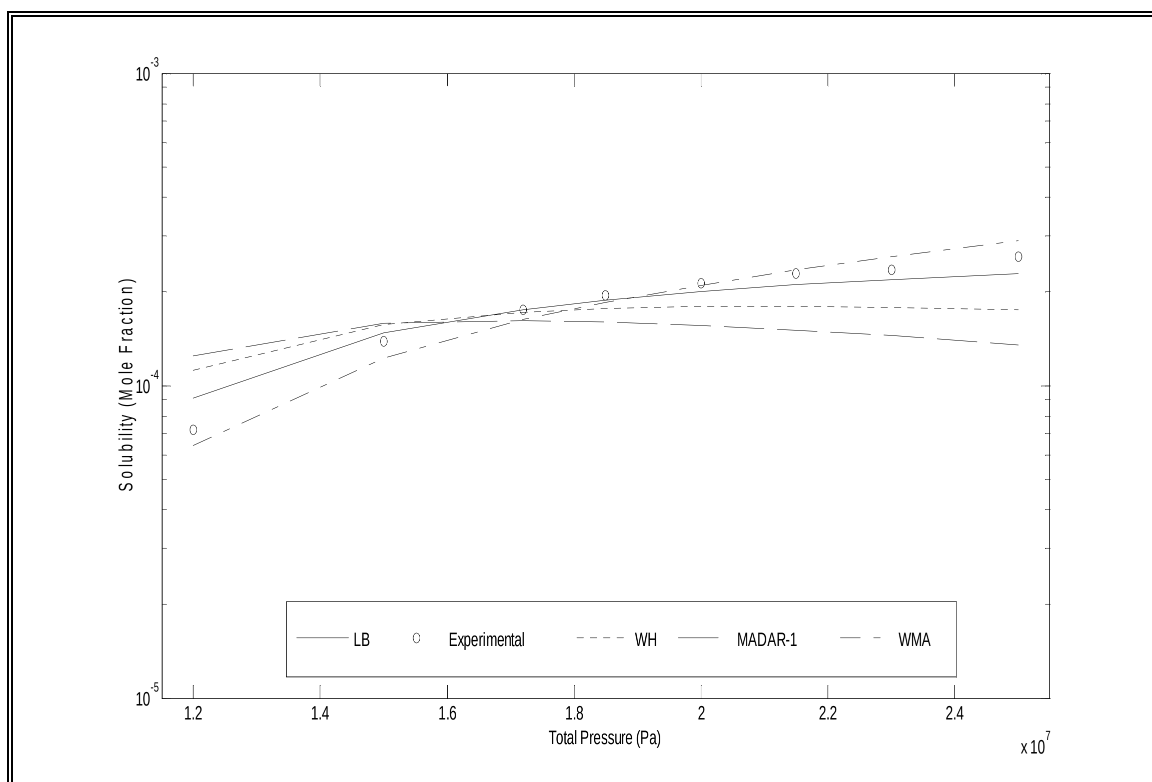

Figure 5.1.1.5: Solubility of Aspirin in SC – CO_2 at 318.15 K with (a) parameters only

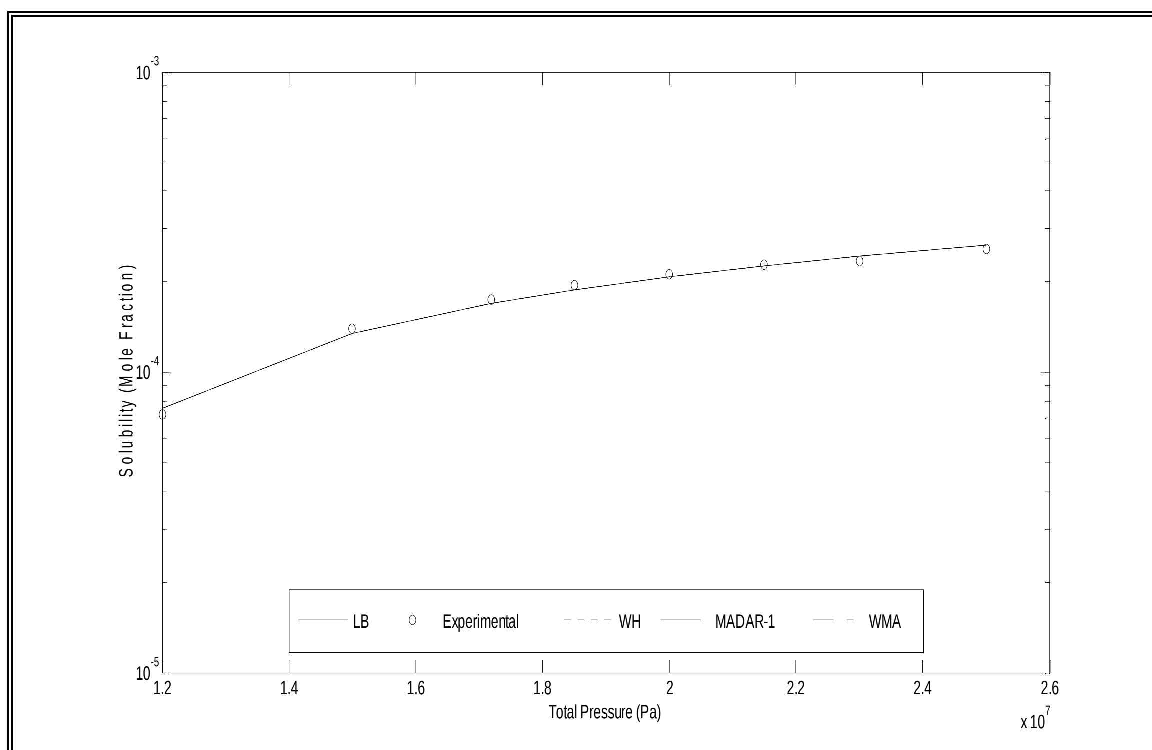

Figure 5.1.1.6: Solubility of Aspirin in SC – CO_2 at 318.15 K with (a) & (b) parameters

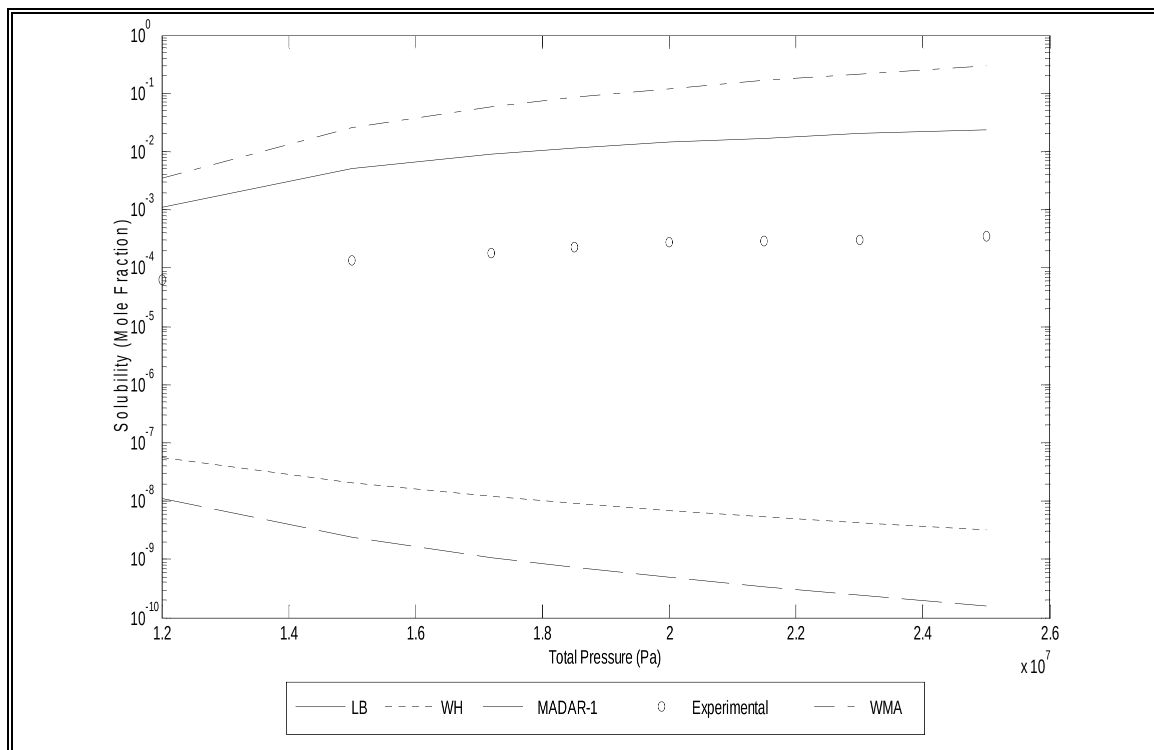

Figure 5.1.1.7: Solubility of Aspirin in SC – CO_2 at 328.15 K (Pure Predictive)

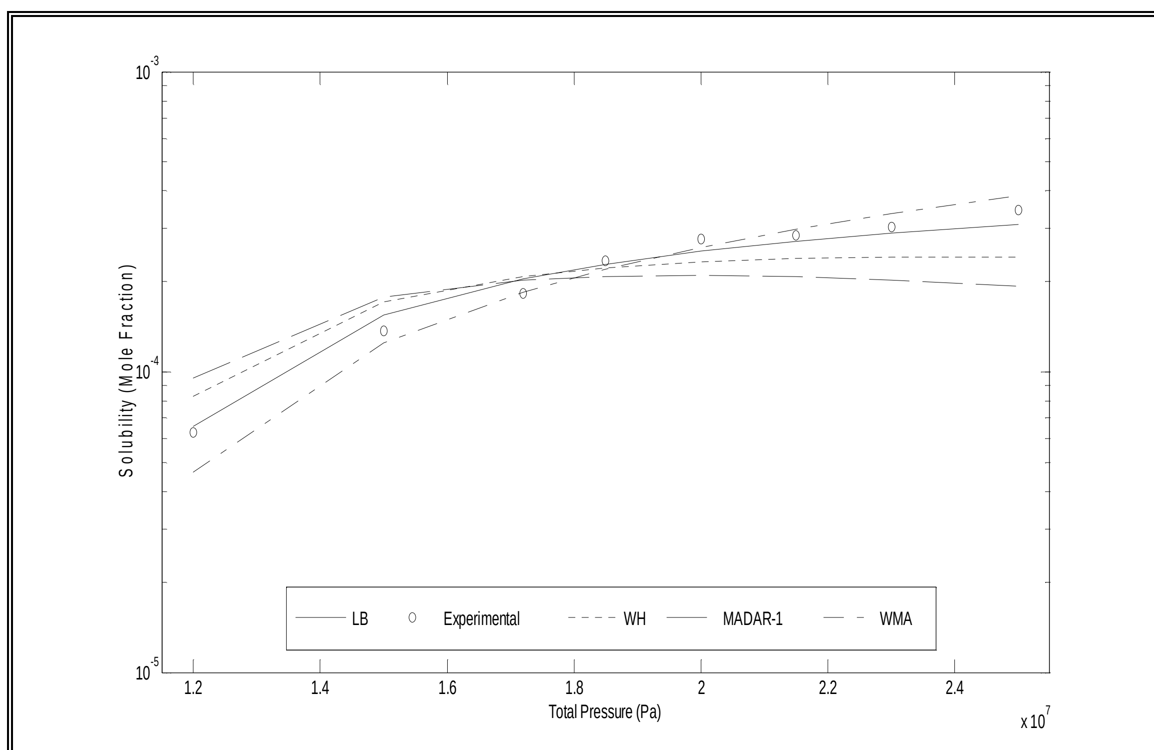

Figure 5.1.1.8: Solubility of Aspirin in SC – CO_2 at 328.15 K with (a) parameters only

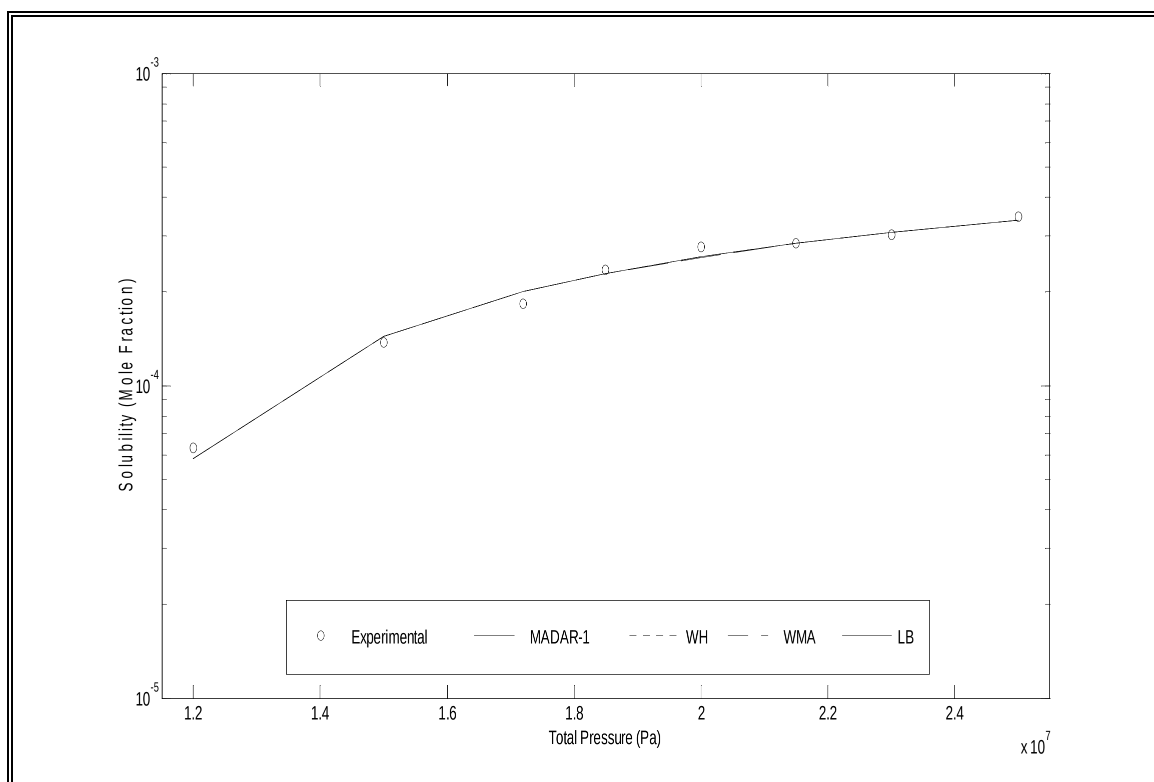

Figure 5.1.1.9: Solubility of Aspirin in SC – CO_2 at 328.15 K with (a) & (b) parameters

5.1.2 Solubility of C.I. Disperse Red 1 Using Combining Rules and Weighting Matrix Approach

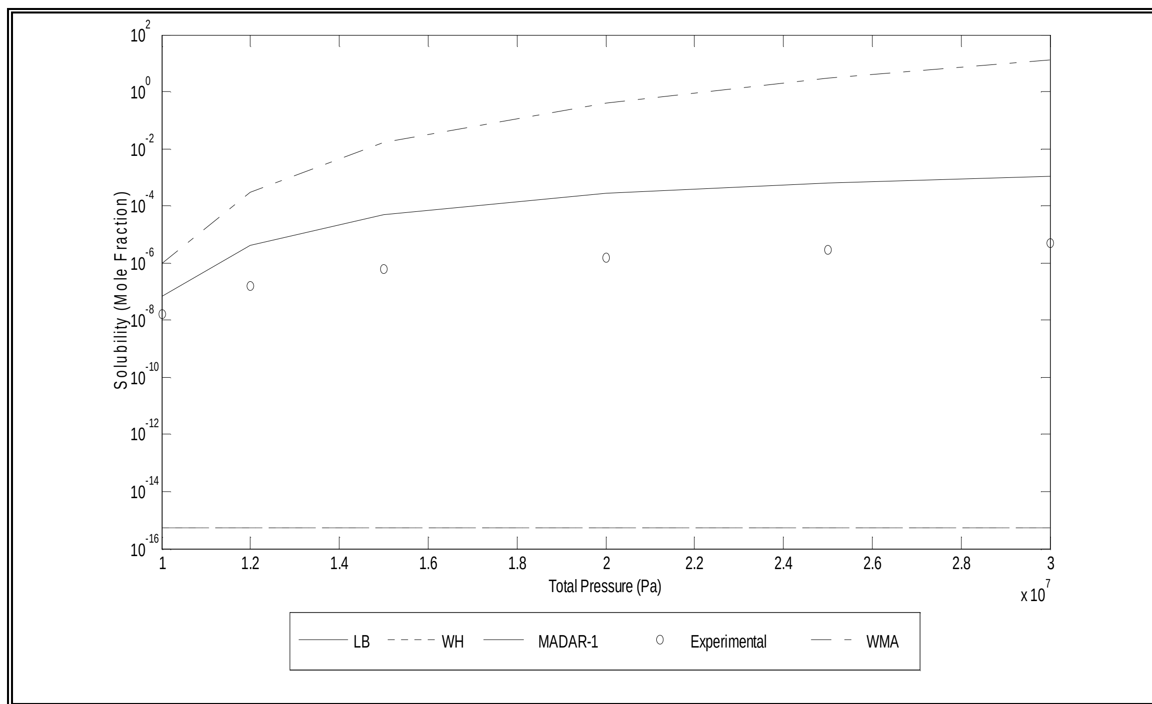

Figure 5.1.2.1: Solubility of C.I. Disperse Red 1 in SC – CO_2 at 323.15 K (Pure Predictive)

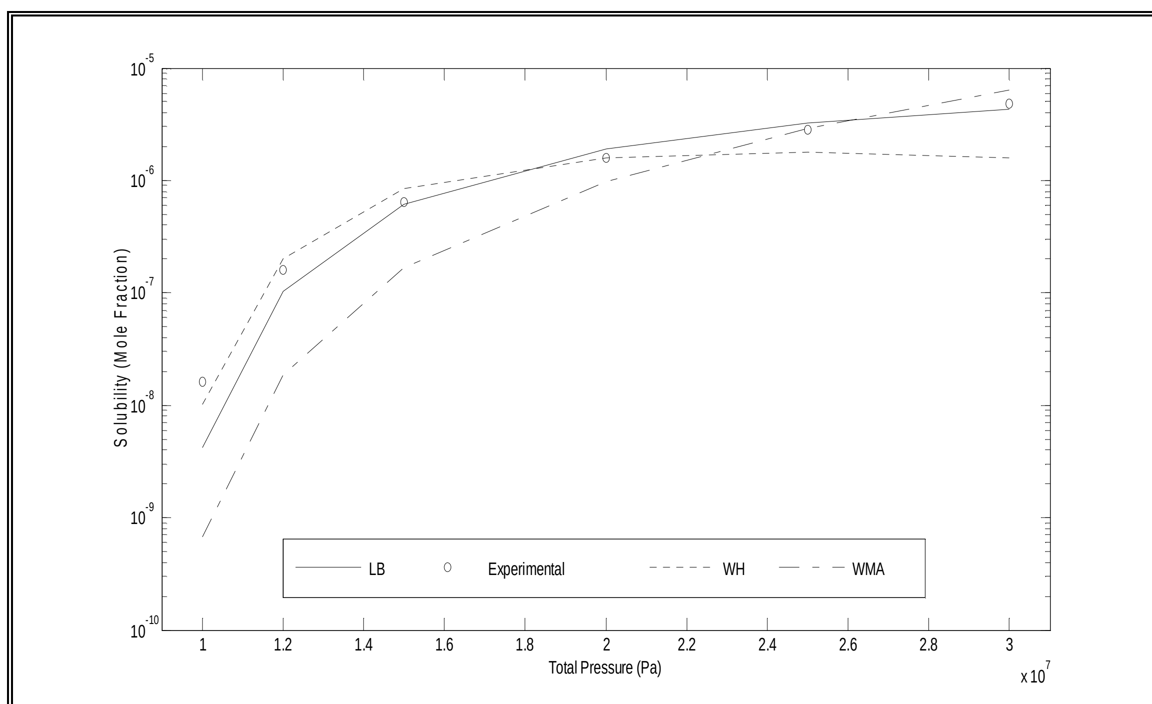

Figure 5.1.2.2: Solubility of C.I. Disperse Red 1 in SC – CO_2 at 323.15 K with (a) parameters only

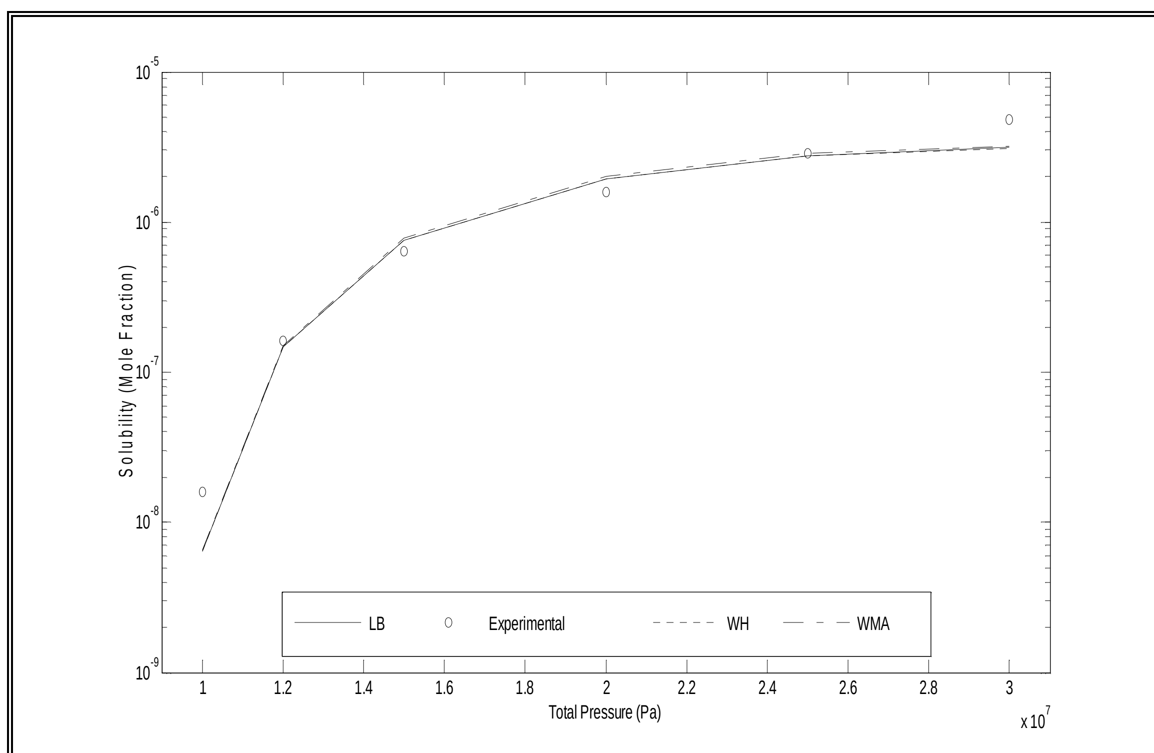

Figure 5.1.2.3: Solubility of C.I. Disperse Red 1 in SC – CO_2 at 323.15 K with (a) & (b) parameters

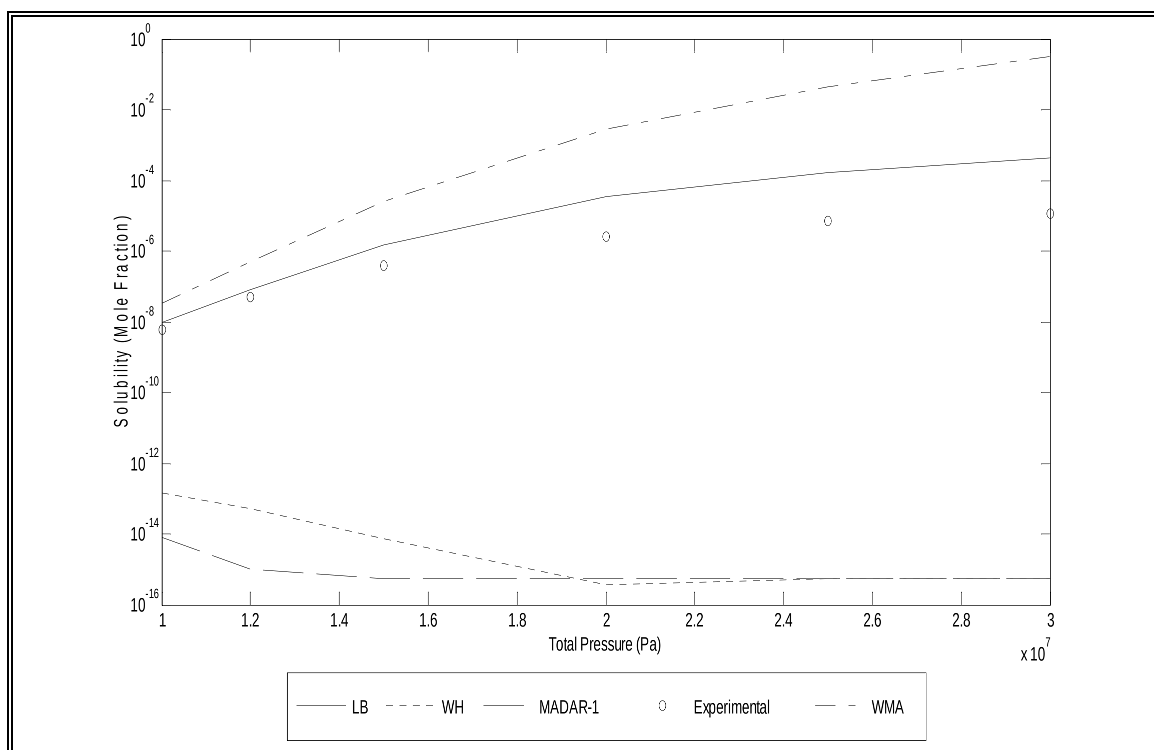

Figure 5.1.2.4: Solubility of C.I. Disperse Red 1 in SC – CO_2 at 353.15 K (Pure Predictive)

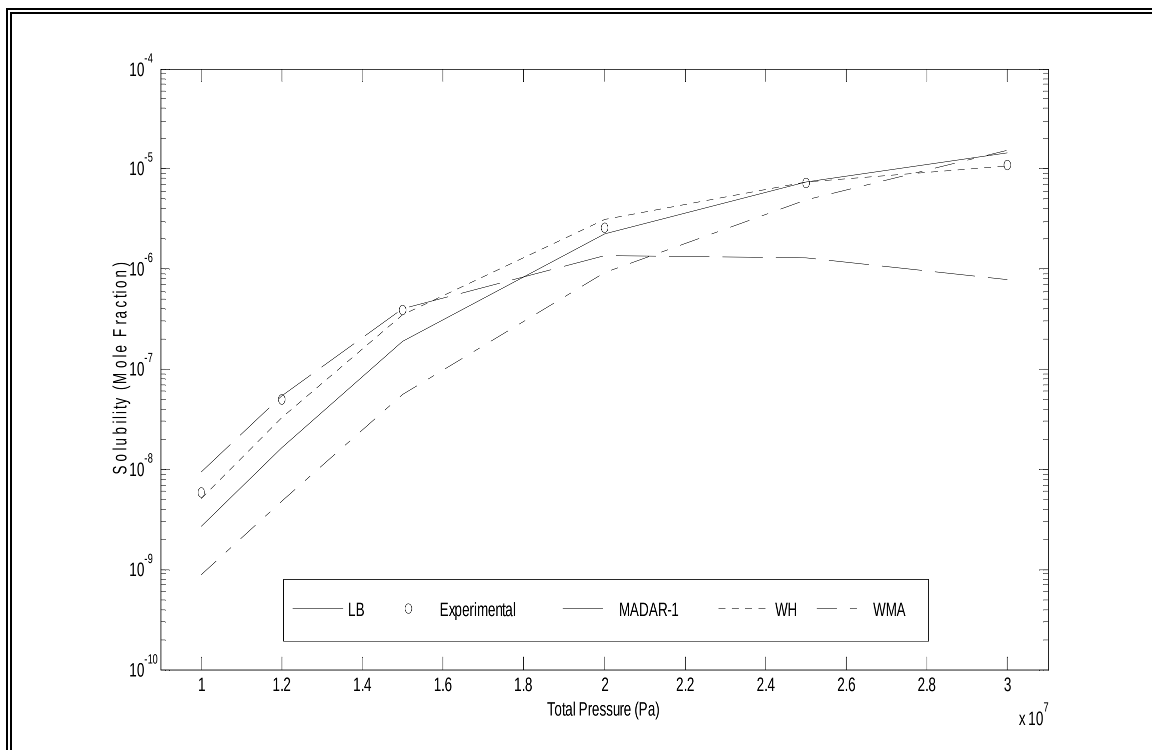

Figure 5.1.2.5: Solubility of C.I. Disperse Red 1 in SC – CO_2 at 353.15 K with (a) parameters only

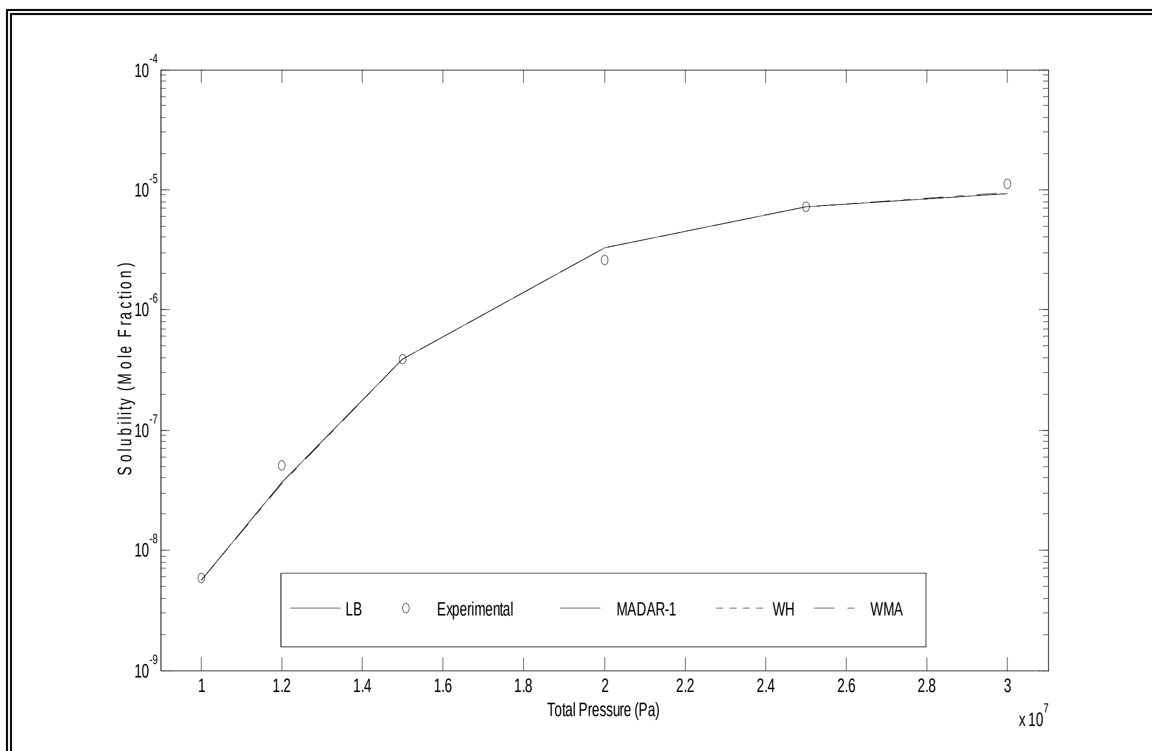

Figure 5.1.2.6: Solubility of C.I. Disperse Red 1 in SC – CO_2 at 353.15 K with (a) & (b) parameters

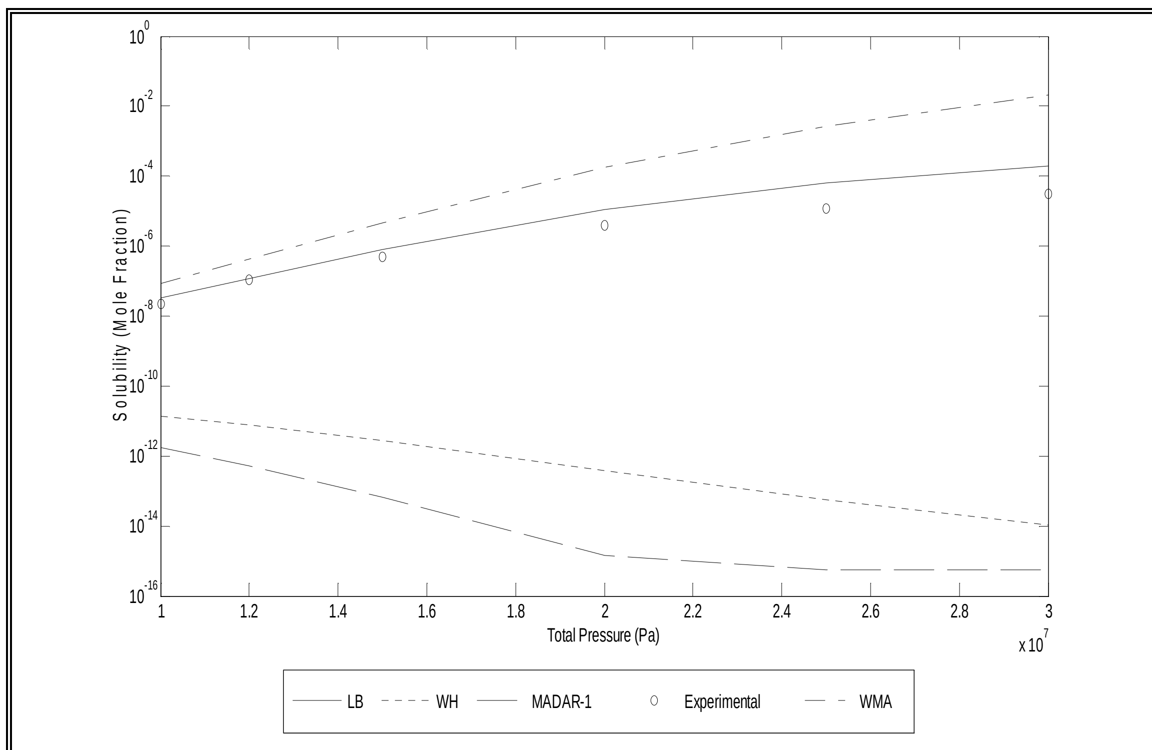

Figure 5.1.2.7: Solubility of C.I. Disperse Red 1 in SC – CO_2 at 383.15 K (Pure Predictive)

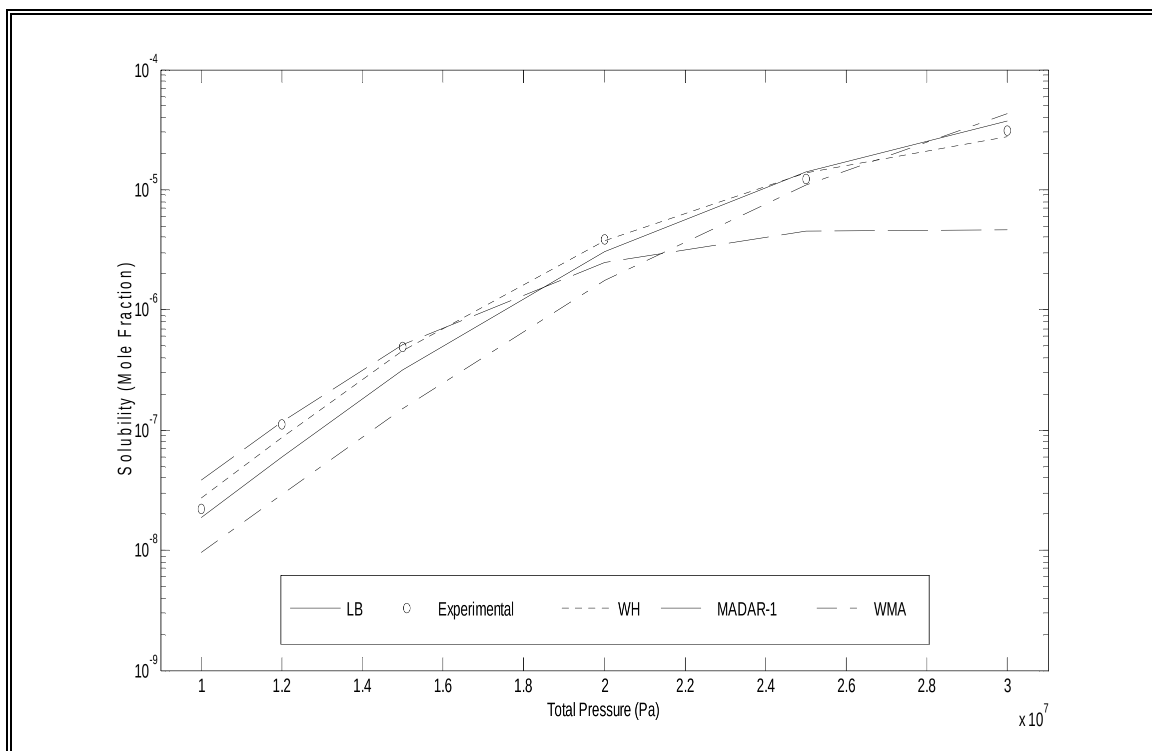

Figure 5.1.2.8: Solubility of C.I. Disperse Red 1 in SC – CO_2 at 383.15 K with (a) parameters only

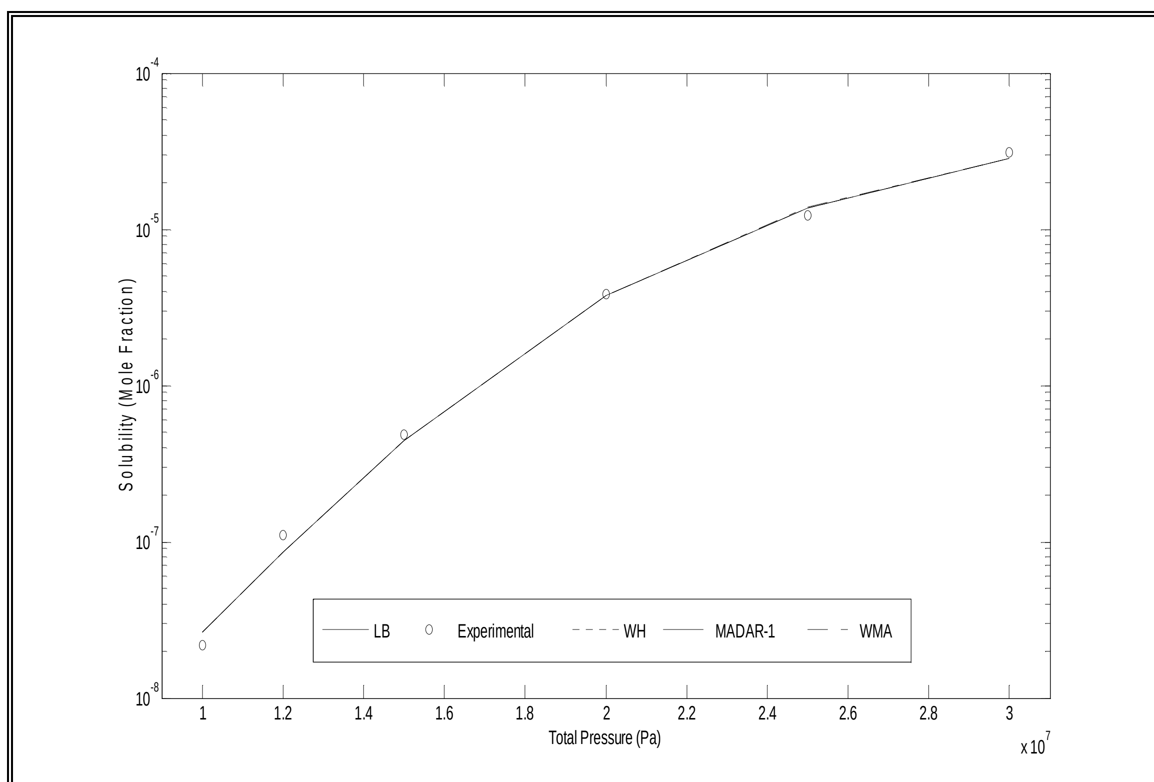

Figure 5.1.2.9: Solubility of C.I. Disperse Red 1 in SC – CO_2 at 383.15 K with (a) & (b) parameters

5.1.3 Solubility of C.I. Disperse Red 13 Using Combining Rules and Weighting Matrix Approach

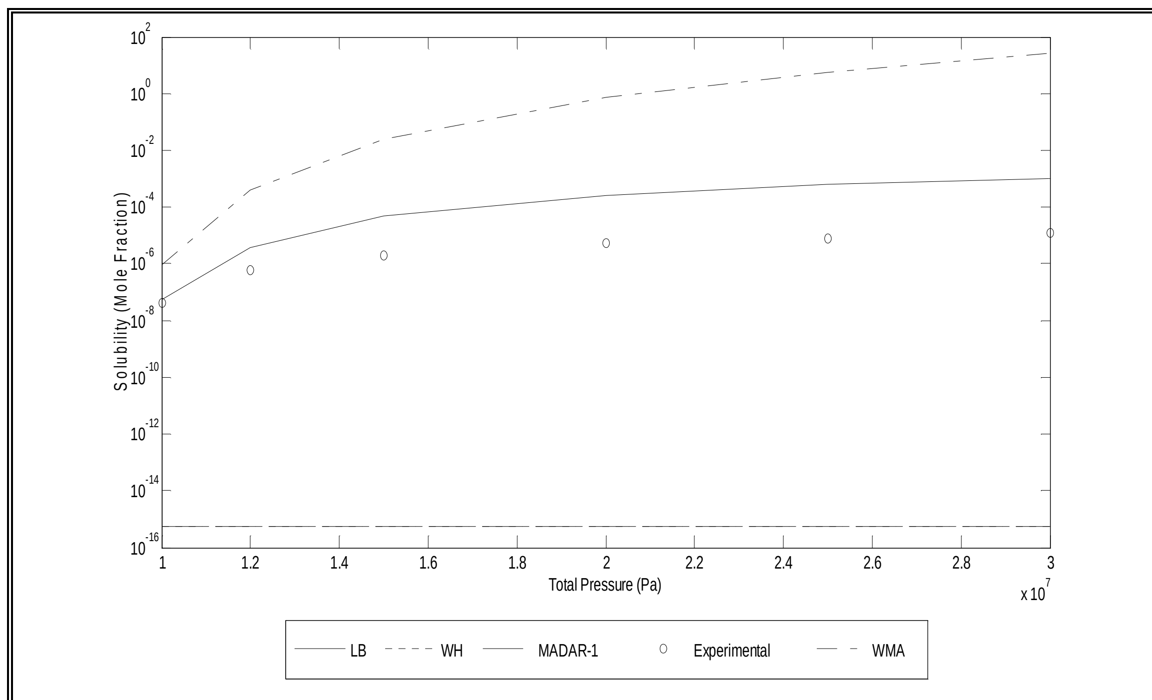

Figure 5.1.3.1: Solubility of C.I. Disperse Red 13 in SC – CO_2 at 323.15 K (Pure Predictive)

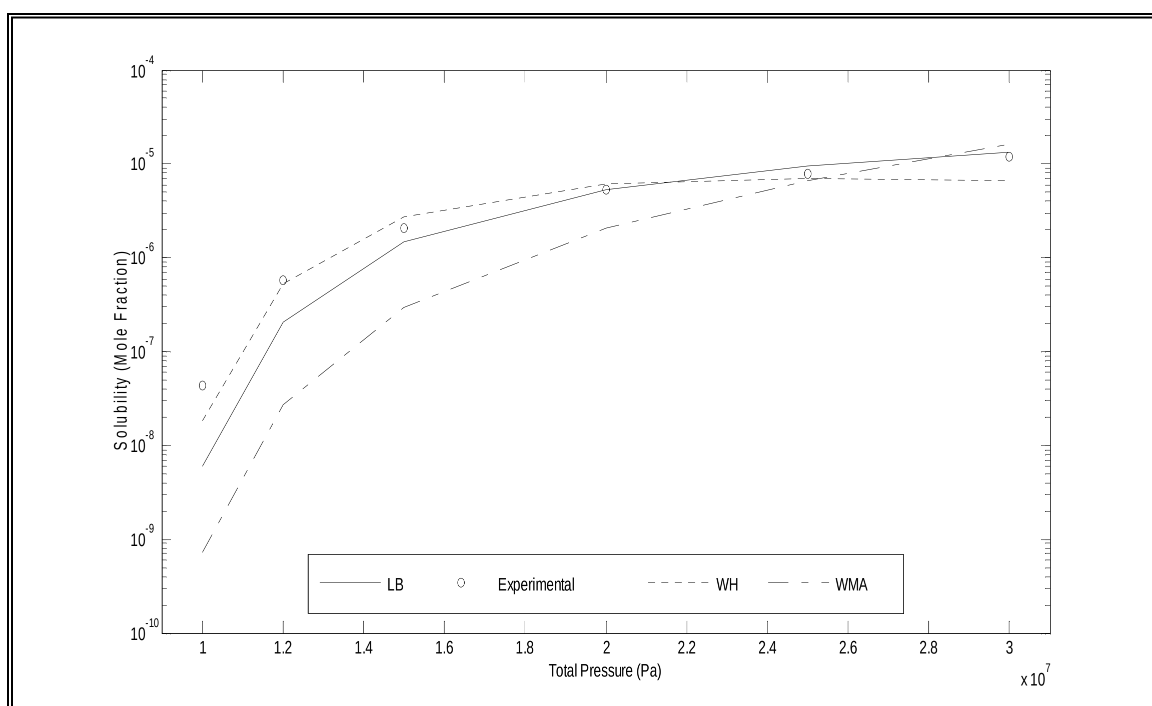

Figure 5.1.3.2: Solubility of C.I. Disperse Red 13 in SC – CO_2 at 323.15 K with (a) parameters only

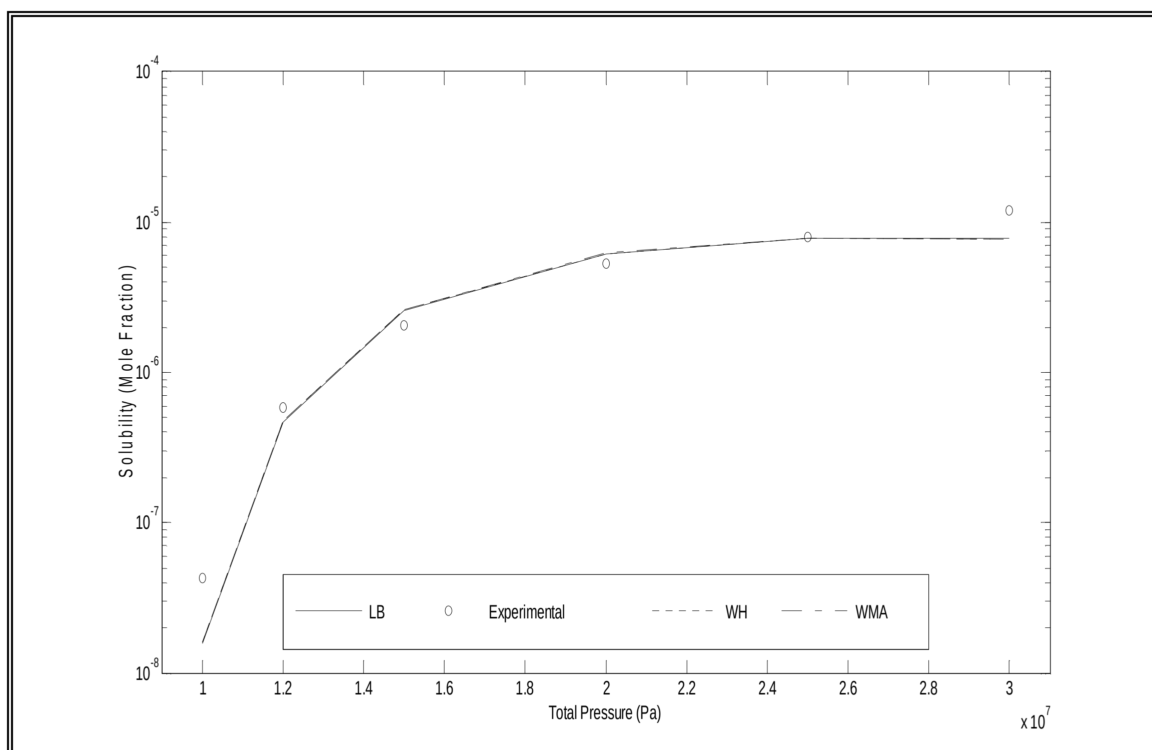

Figure 5.1.3.3: Solubility of C.I. Disperse Red 13 in SC – CO_2 at 323.15 K with (a) & (b) parameters

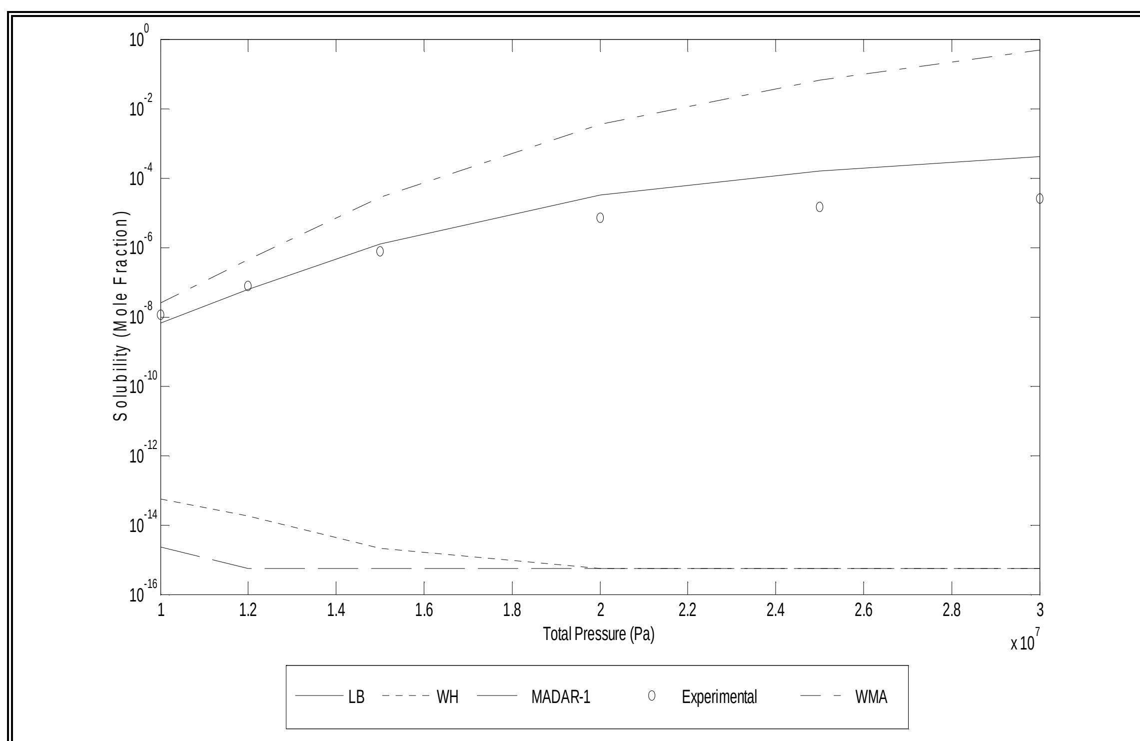

Figure 5.1.3.4: Solubility of C.I. Disperse Red 13 in SC – CO_2 at 353.15 K (Pure Predictive)

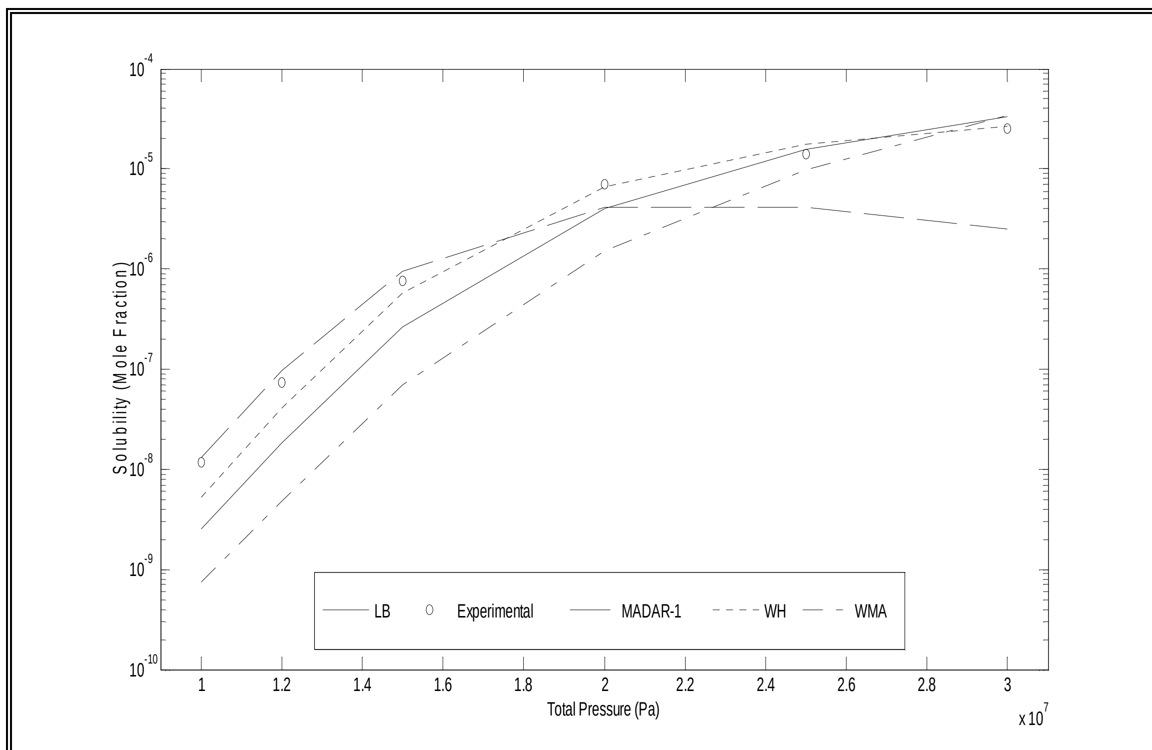

Figure 5.1.3.5: Solubility of C.I. Disperse Red 13 in SC – CO_2 at 353.15 K with (a) parameters only

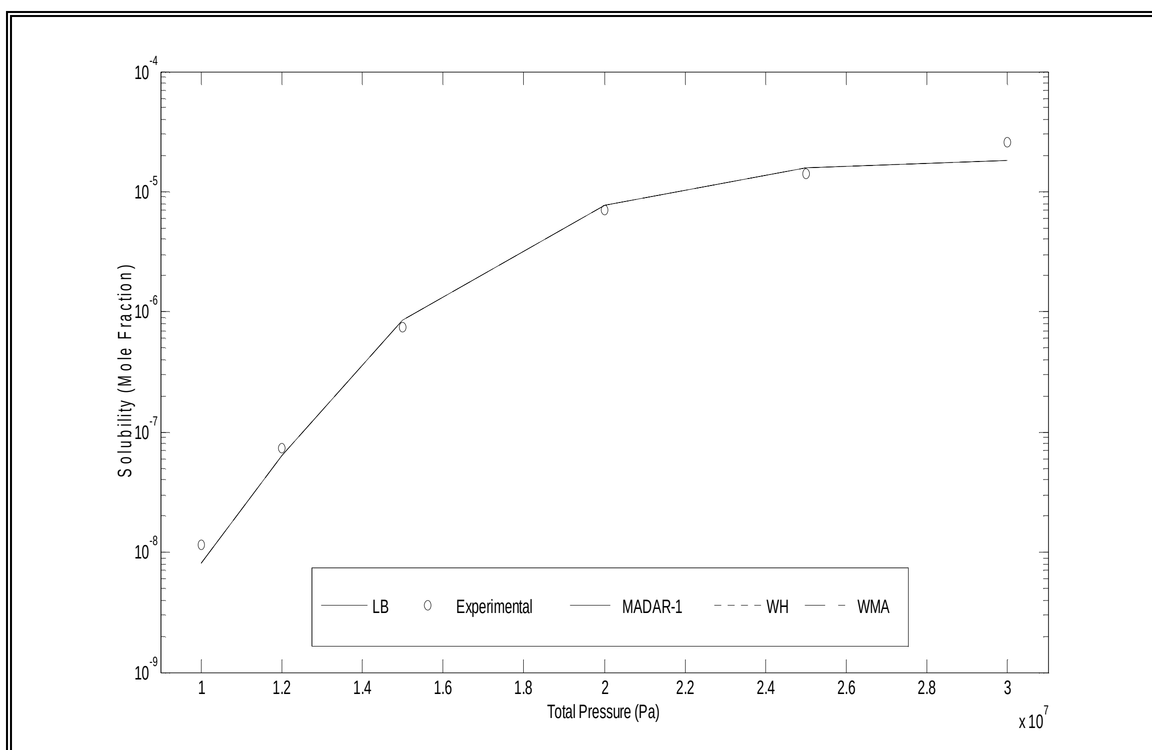

Figure 5.1.3.6: Solubility of C.I. Disperse Red 13 in SC – CO_2 at 353.15 K with (a) & (b) parameters

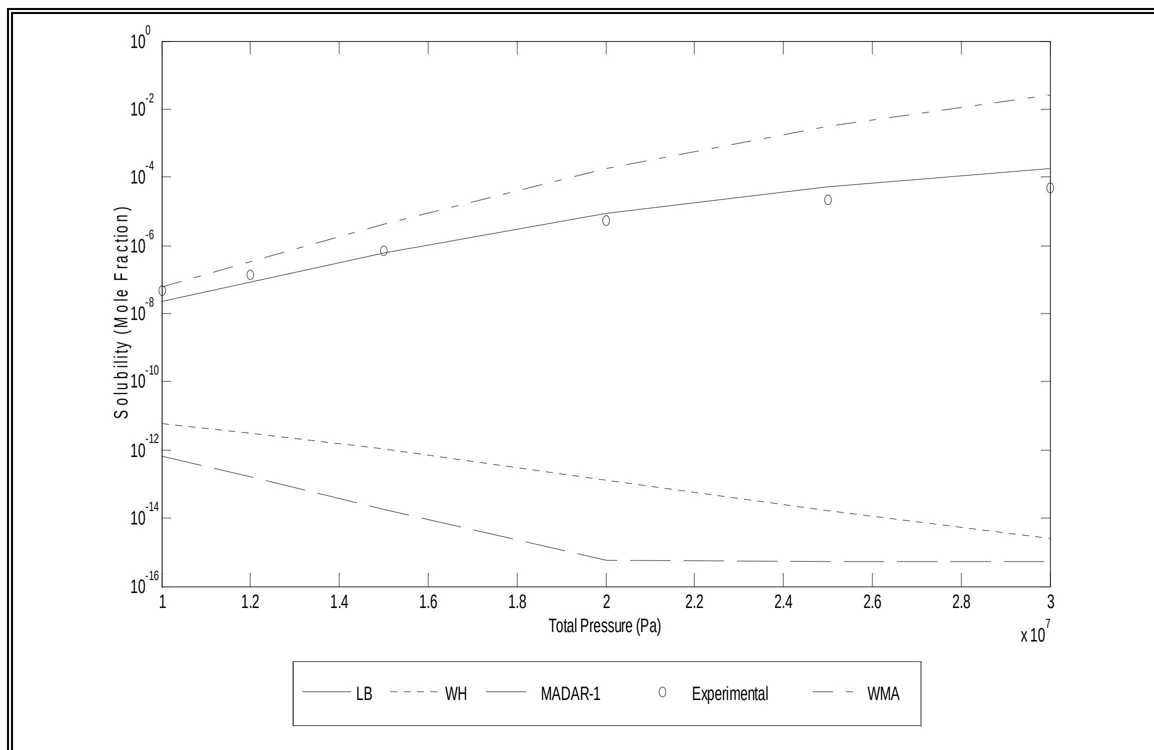

Figure 5.1.3.7: Solubility of C.I. Disperse Red 13 in SC – CO_2 at 383.15 K (Pure Predictive)

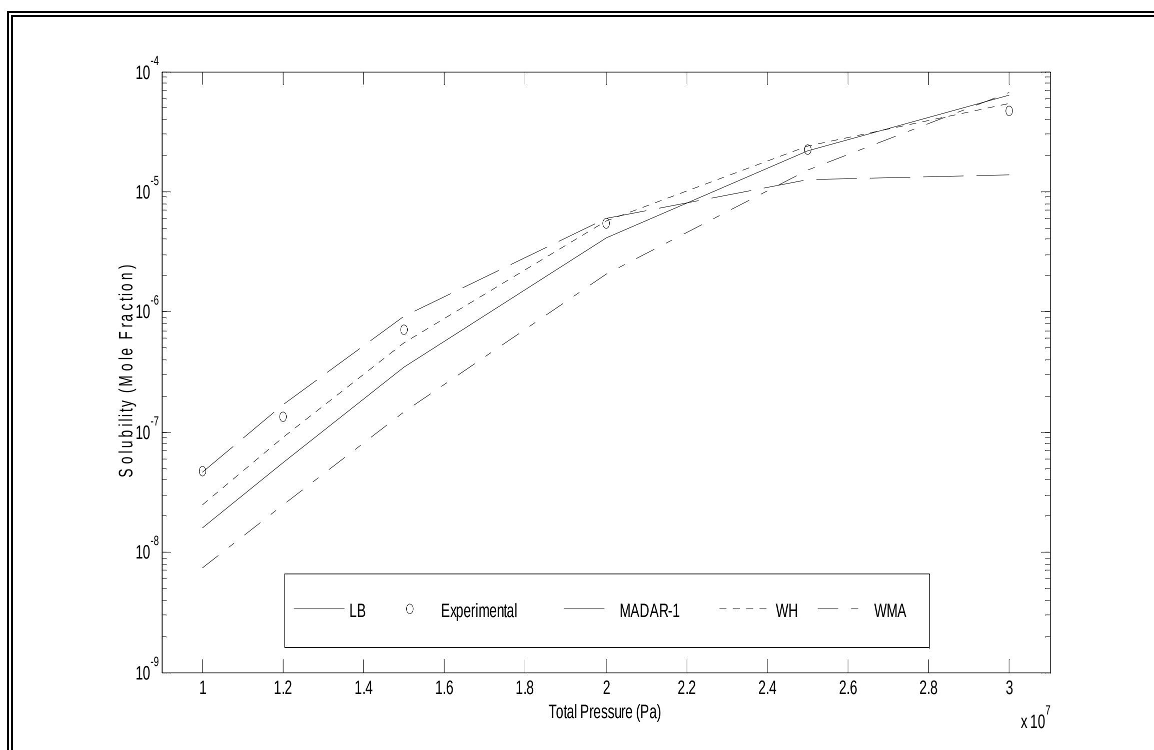

Figure 5.1.3.8: Solubility of C.I. Disperse Red 13 in SC – CO_2 at 383.15 K with (a) parameters only

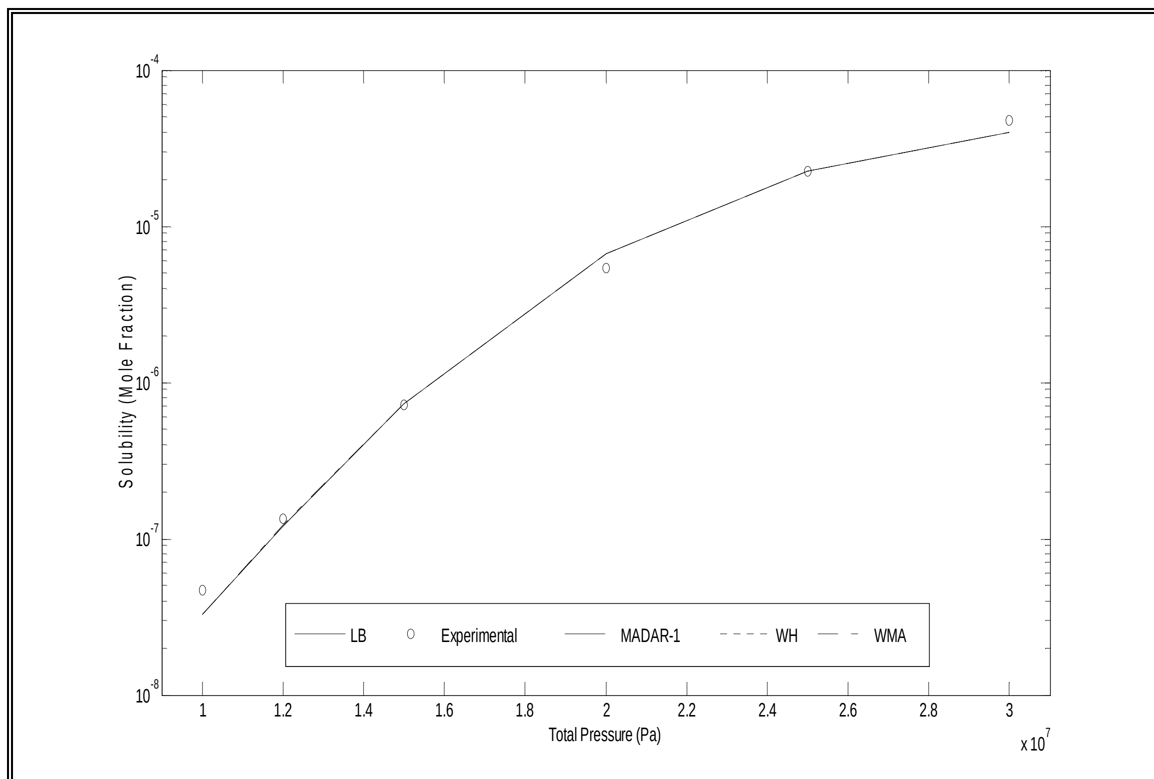

Figure 5.1.3.9: Solubility of C.I. Disperse Red 13 in SC – CO_2 at 383.15 K with (a) & (b) parameters

5.1.4 Solubility of Naphthalene Using Combining Rules and Weighting Matrix Approach

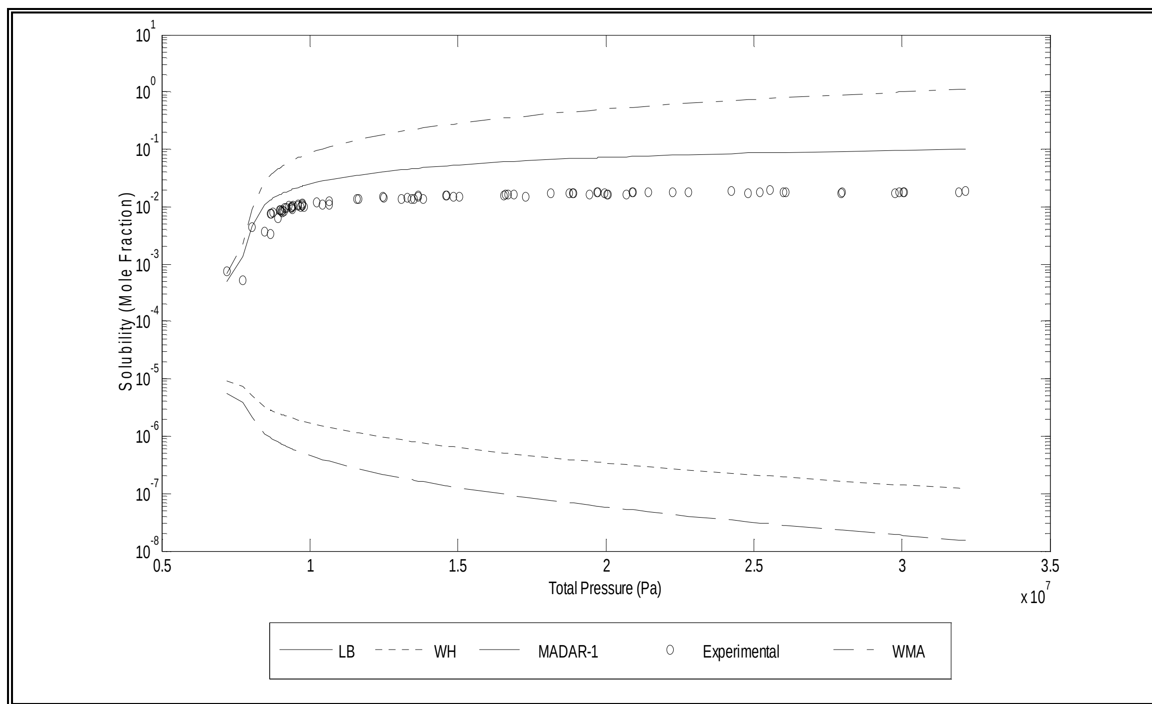

Figure 5.1.4.1: Solubility of Naphthalene in SC – CO_2 at 308 K (Pure Predictive)

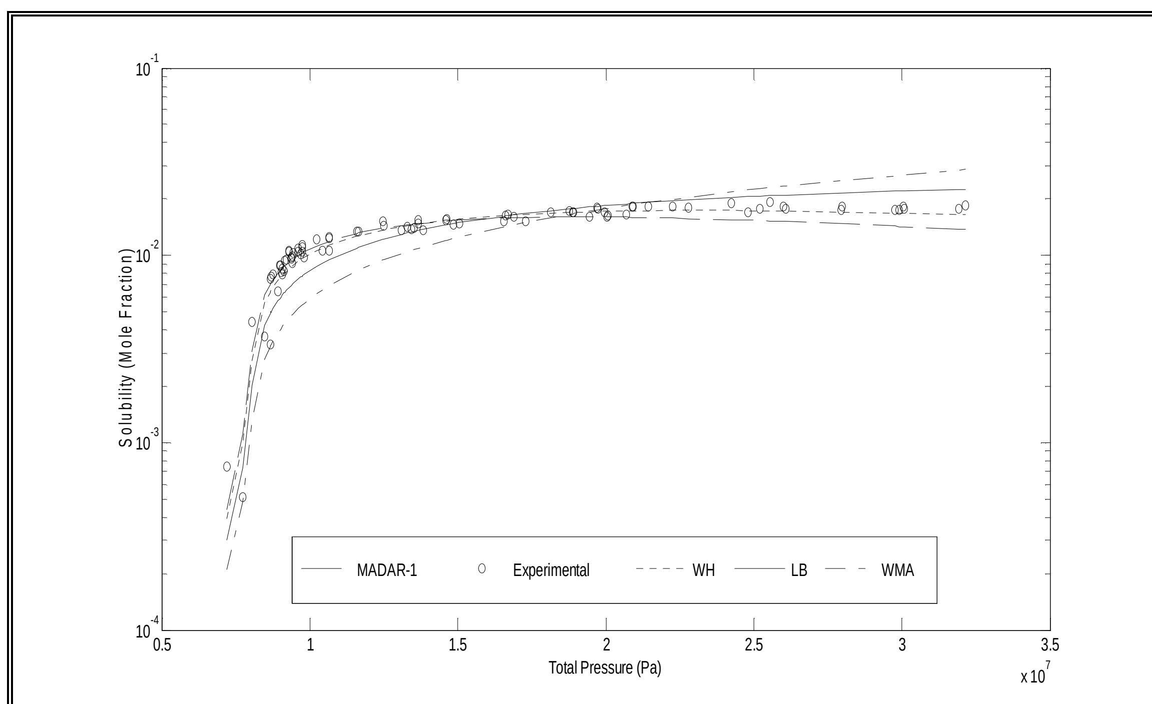

Figure 5.1.4.2: Solubility of Naphthalene in SC – CO_2 at 308 K with (a) parameters only

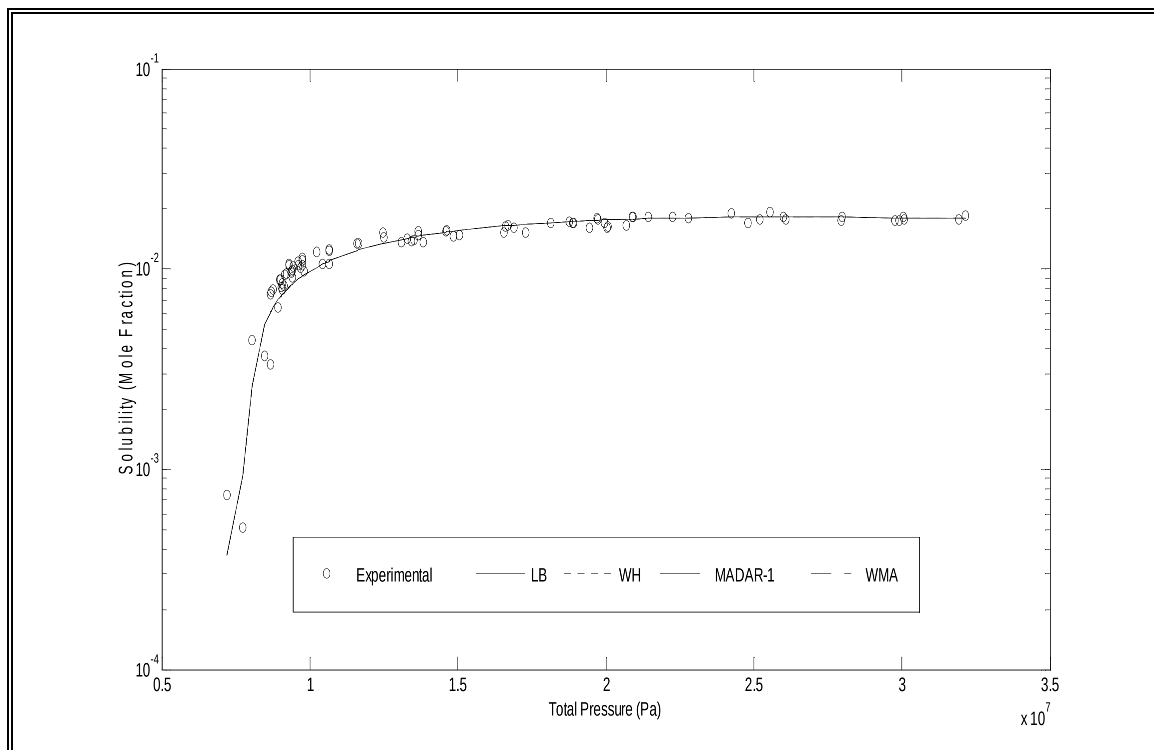

Figure 5.1.4.3: Solubility of Naphthalene in SC – CO_2 at 308 K with (a) & (b) parameters

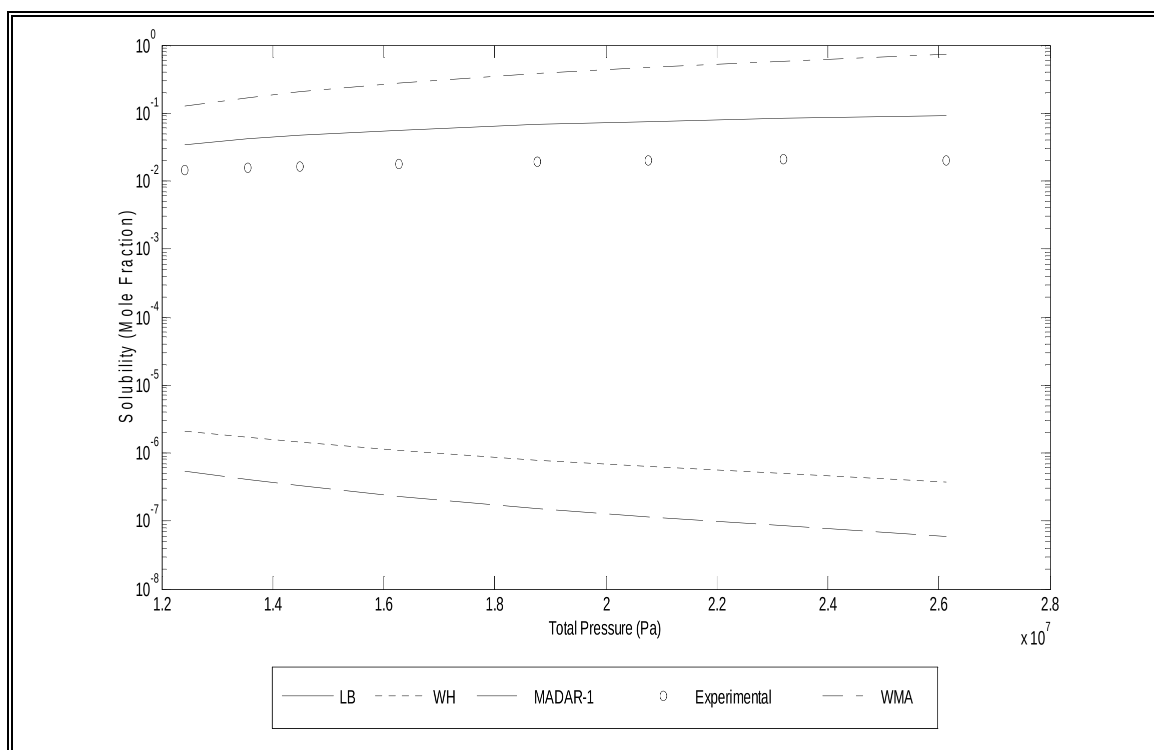

Figure 5.1.4.4: Solubility of Naphthalene in SC – CO_2 at 313 K (Pure Predictive)

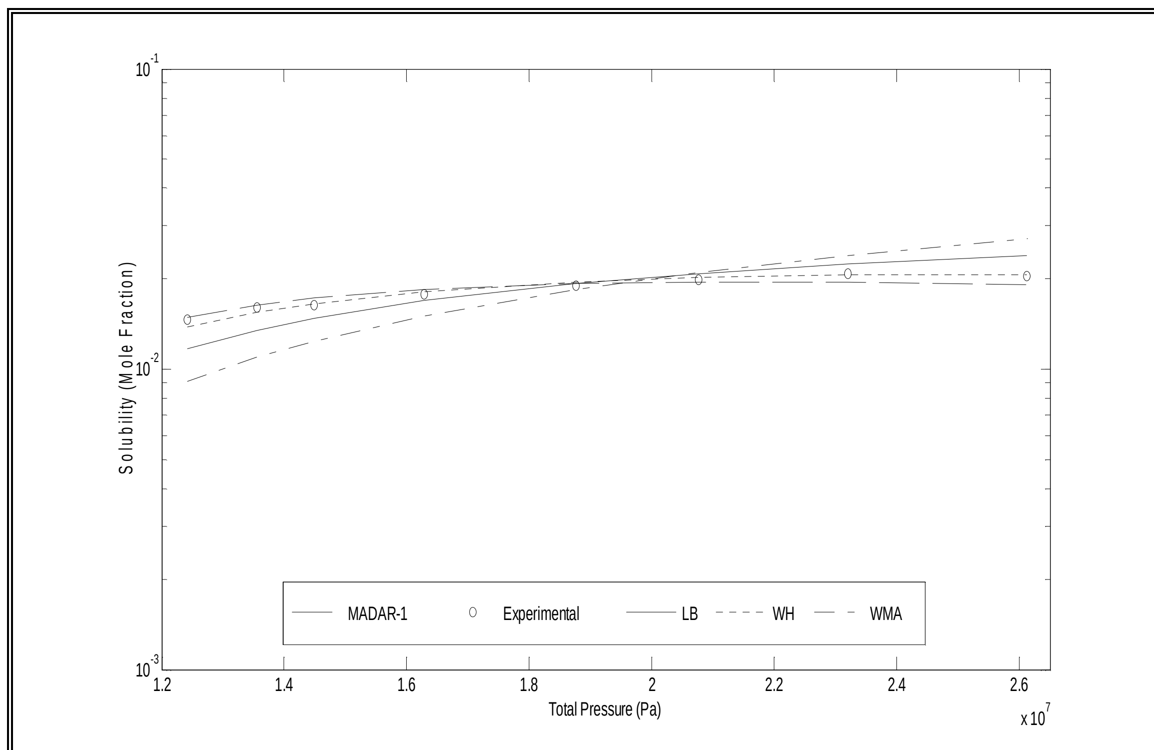

Figure 5.1.4.5: Solubility of Naphthalene in SC – CO_2 at 313 K with (a) parameters only

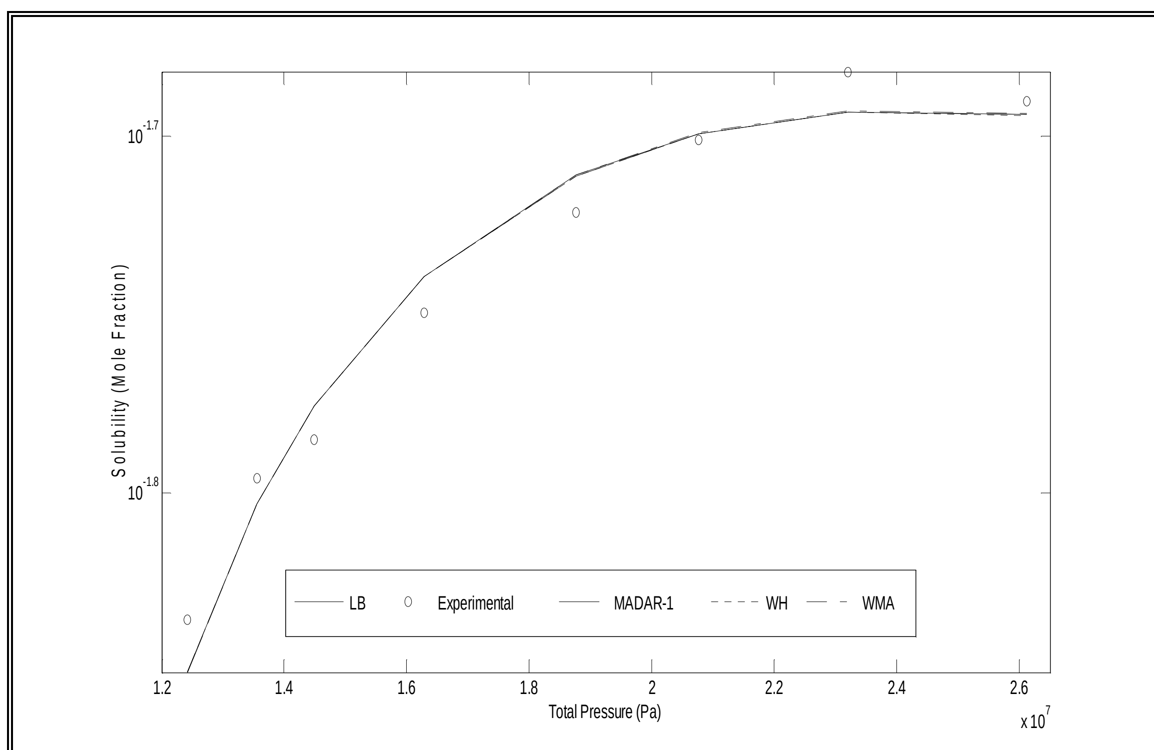

Figure 5.1.4.6: Solubility of Naphthalene in SC – CO_2 at 313 K with (a) & (b) parameters

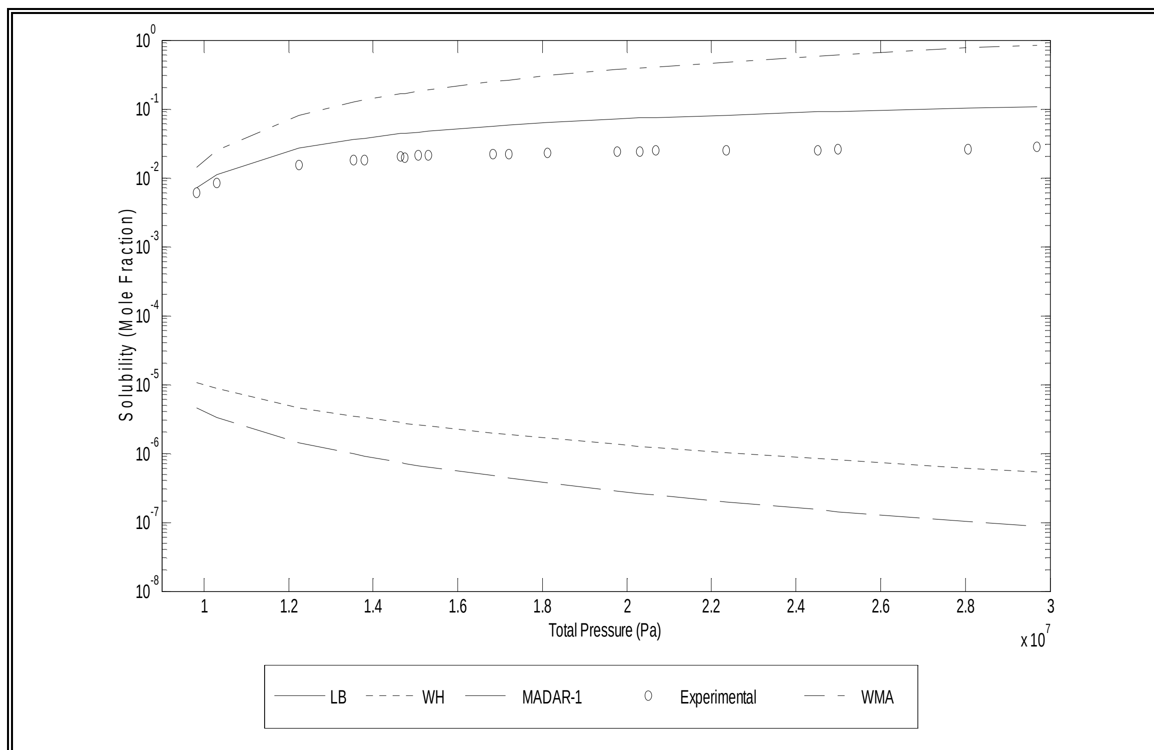

Figure 5.1.4.7: Solubility of Naphthalene in SC – CO_2 at 318 K (Pure Predictive)

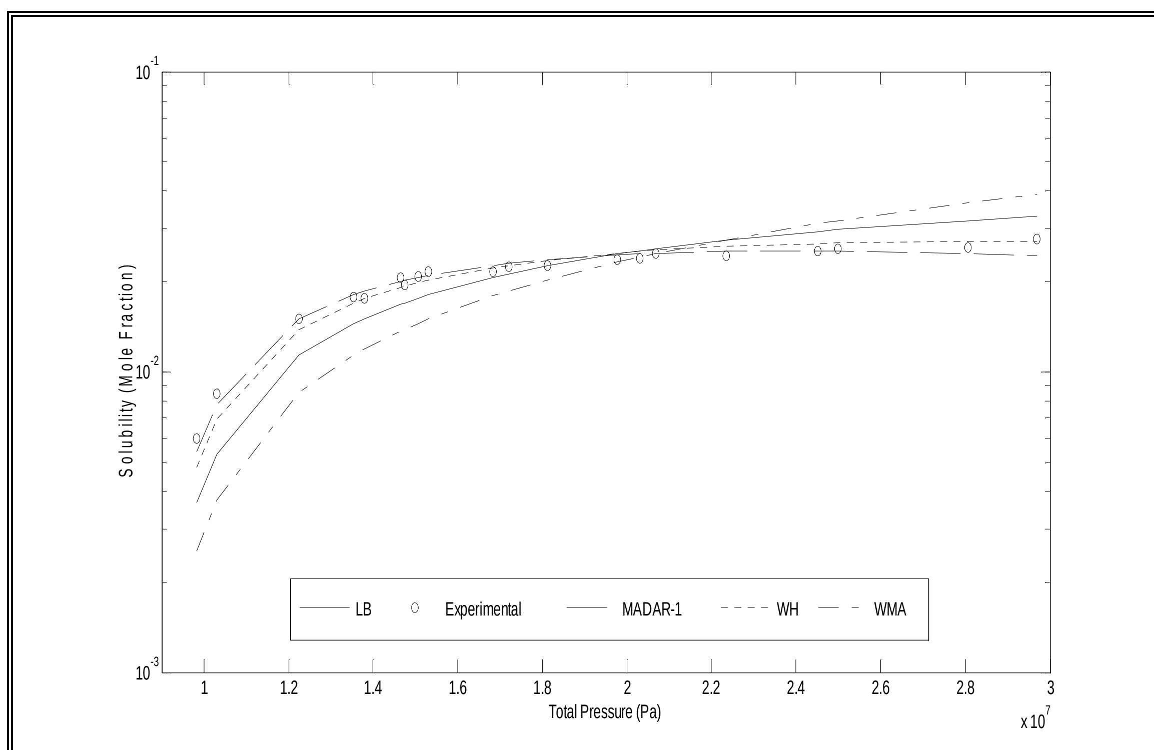

Figure 5.1.4.8: Solubility of Naphthalene in SC – CO_2 at 318 K with (a) parameters only

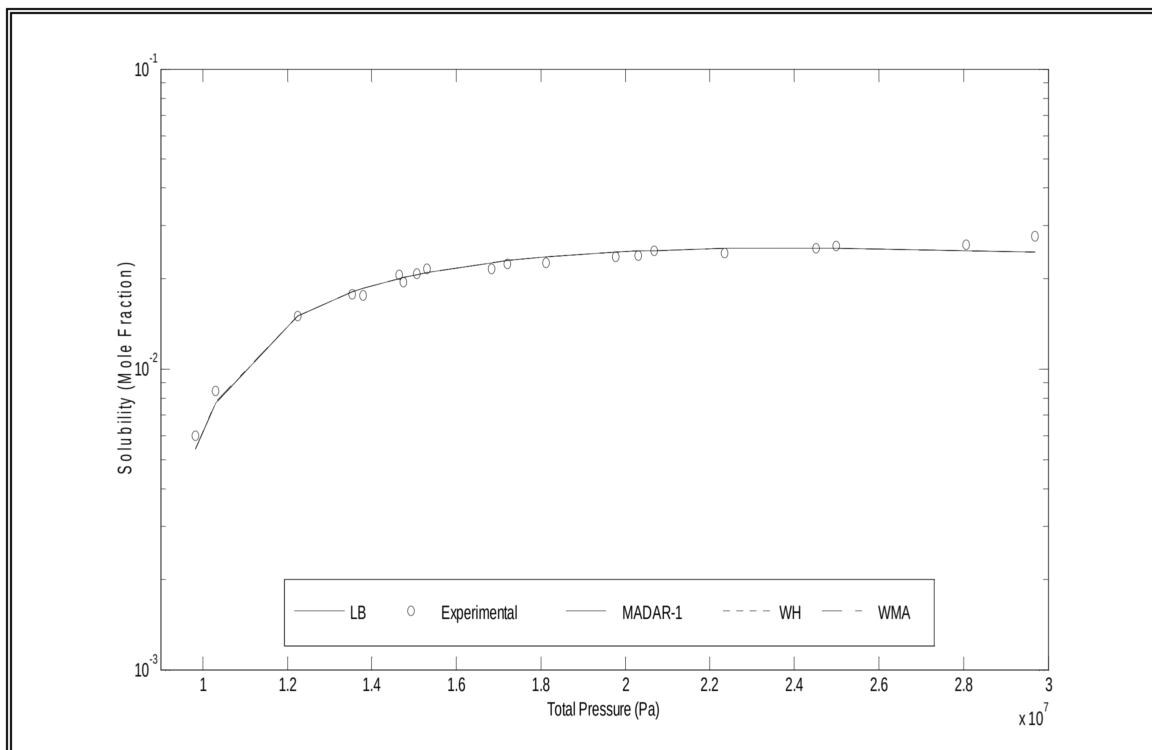

Figure 5.1.4.9: Solubility of Naphthalene in SC – CO_2 at 318 K with (a) & (b) parameters

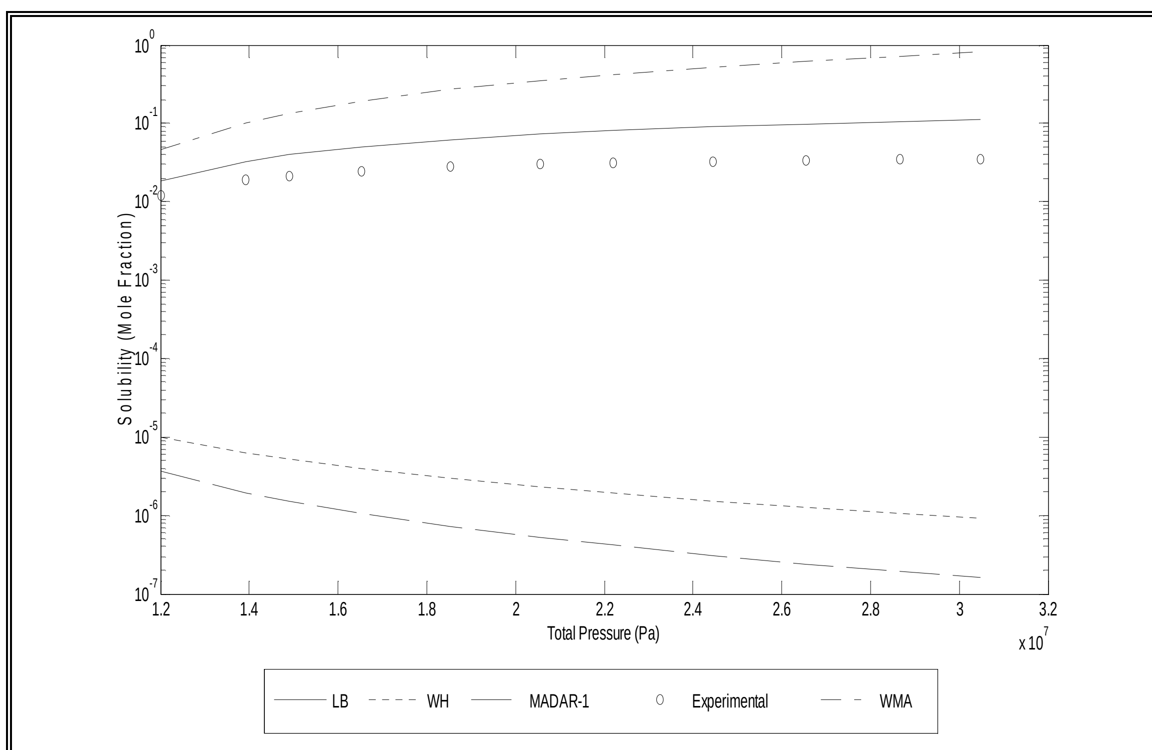

Figure 5.1.4.10: Solubility of Naphthalene in SC – CO_2 at 323 K (Pure Predictive)

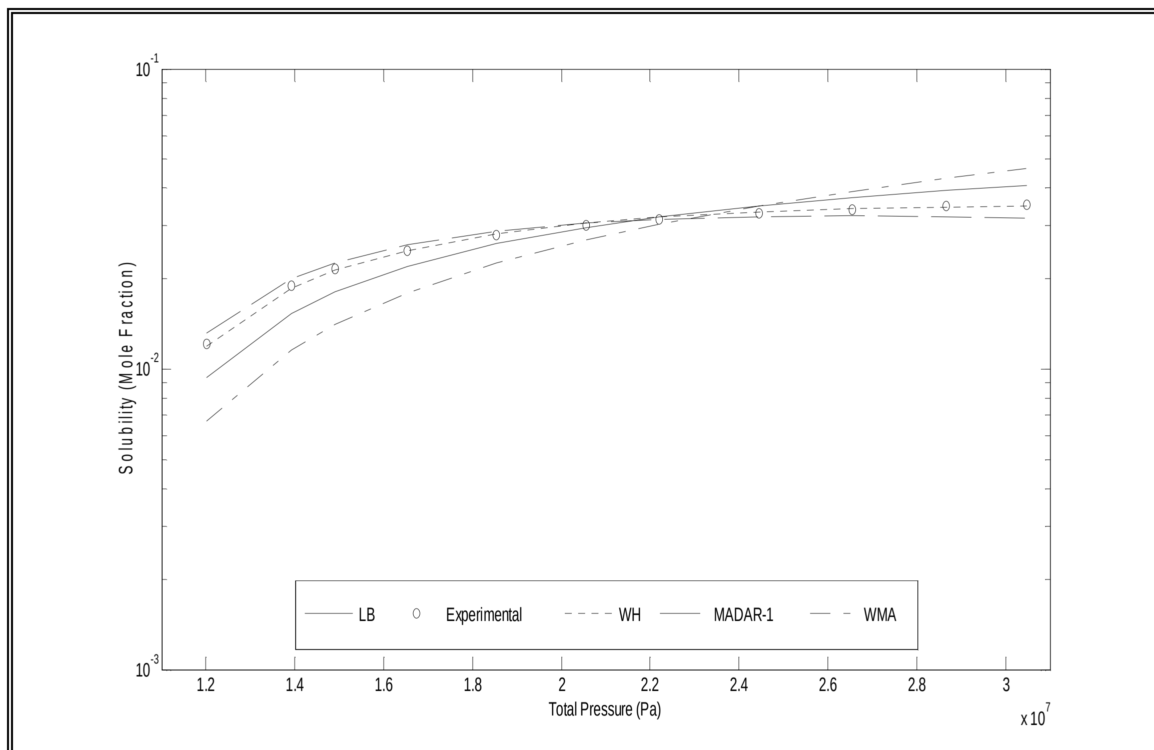

Figure 5.1.4.11: Solubility of Naphthalene in SC – CO_2 at 323 K with (a) parameters only

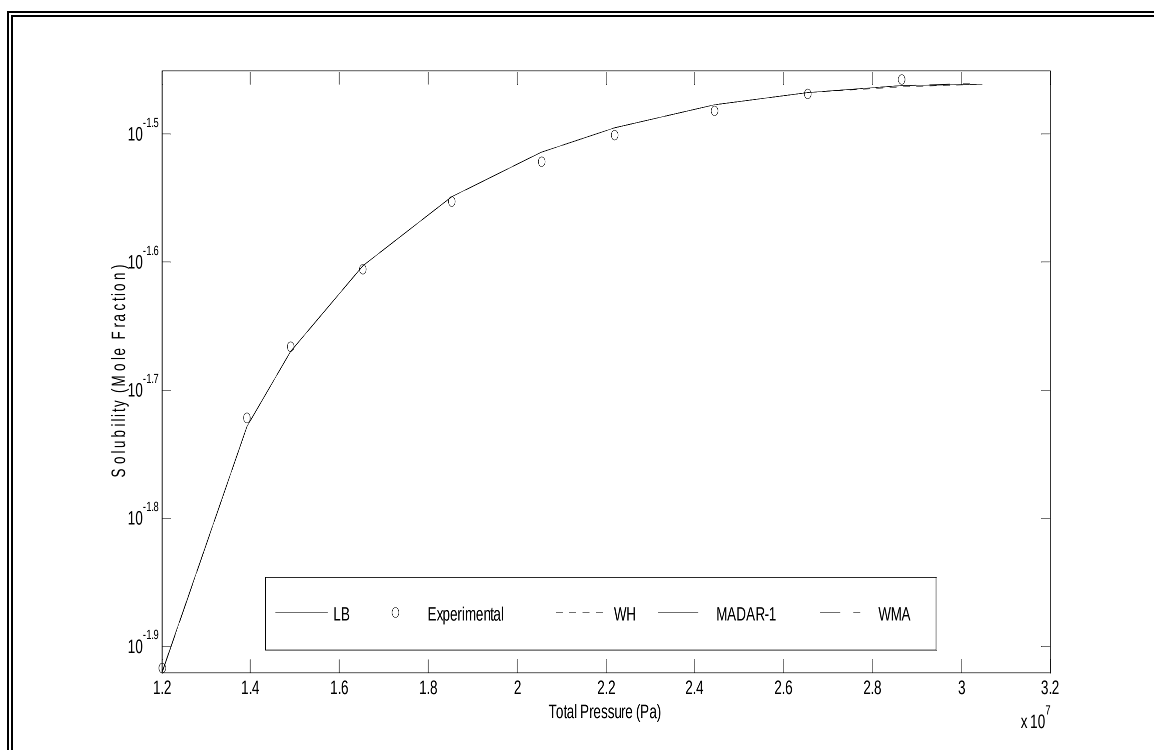

Figure 5.1.4.12: Solubility of Naphthalene in SC – CO_2 at 323 K with (a) & (b) parameters

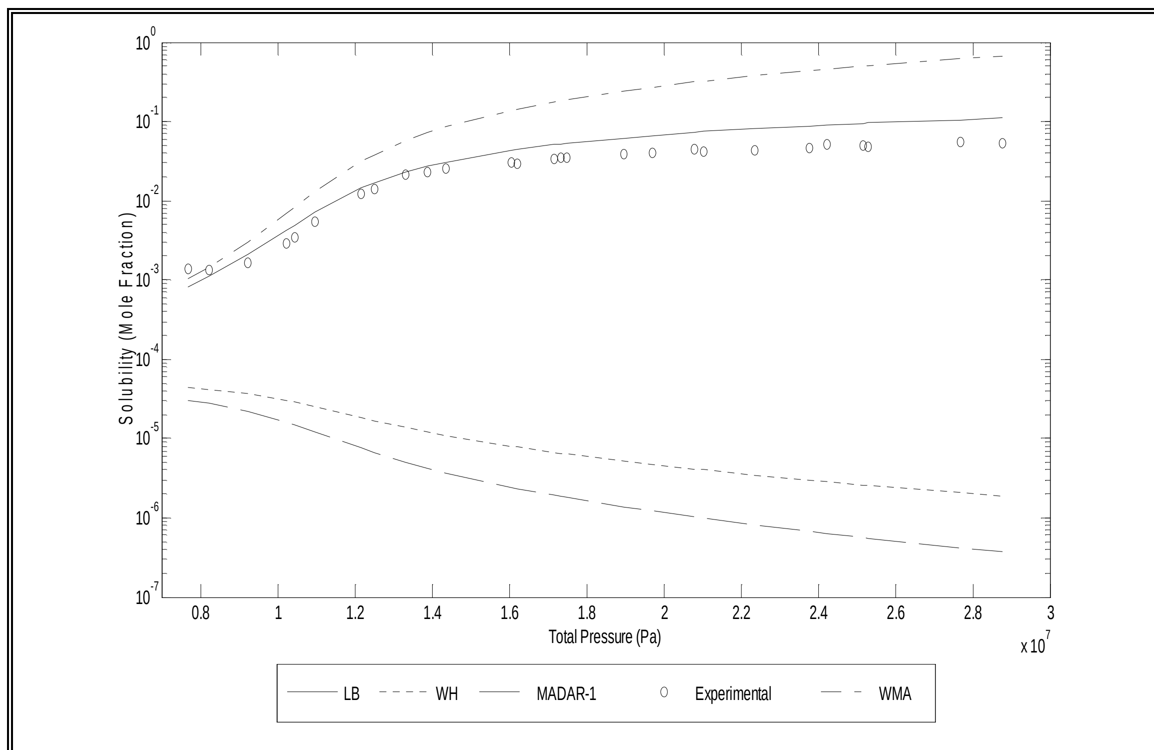

Figure 5.1.4.13: Solubility of Naphthalene in SC – CO_2 at 328 K (Pure Predictive)

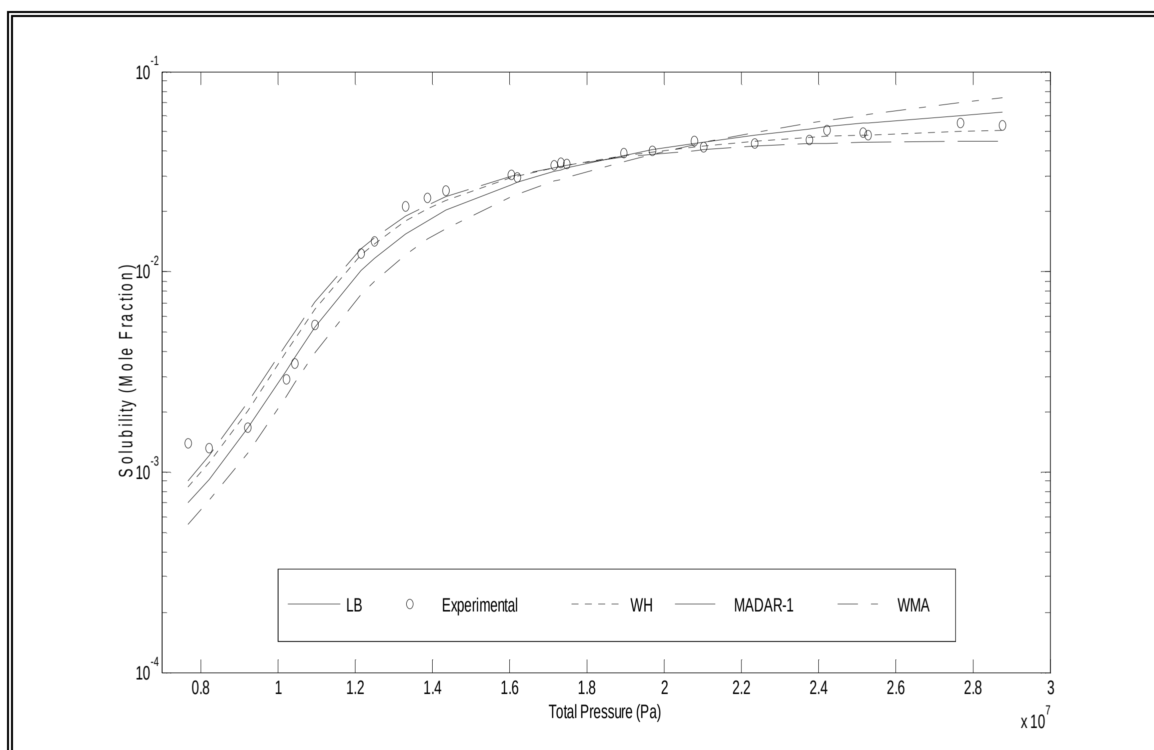

Figure 5.1.4.14: Solubility of Naphthalene in SC – CO_2 at 328 K with (a) parameters only

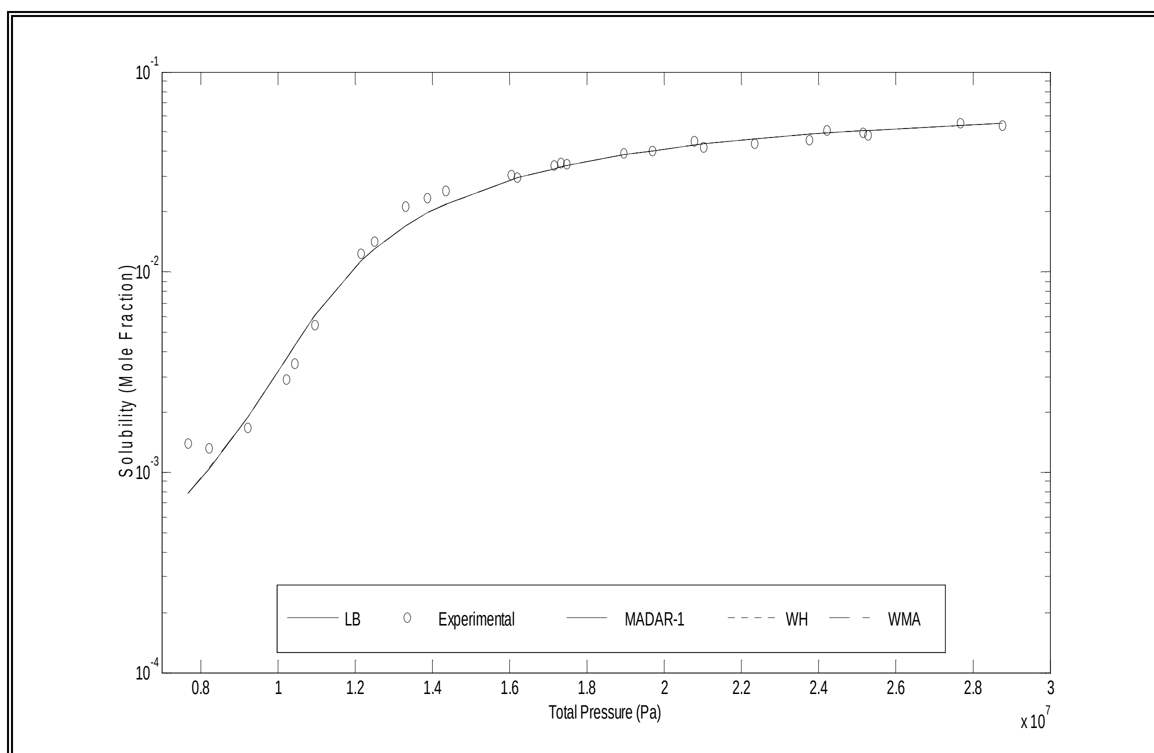

Figure 5.1.4.15: Solubility of Naphthalene in SC – CO_2 at 328 K with (a) & (b) parameters

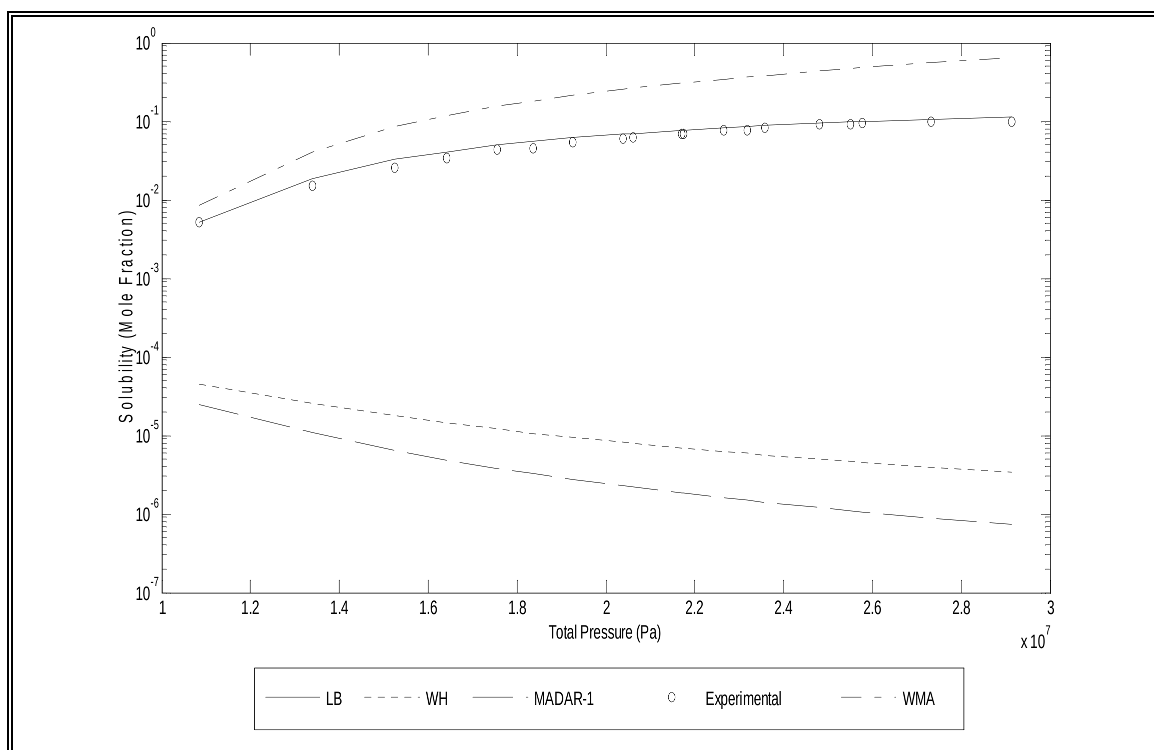

Figure 5.1.4.16: Solubility of Naphthalene in SC – CO_2 at 333.55 K (Pure Predictive)

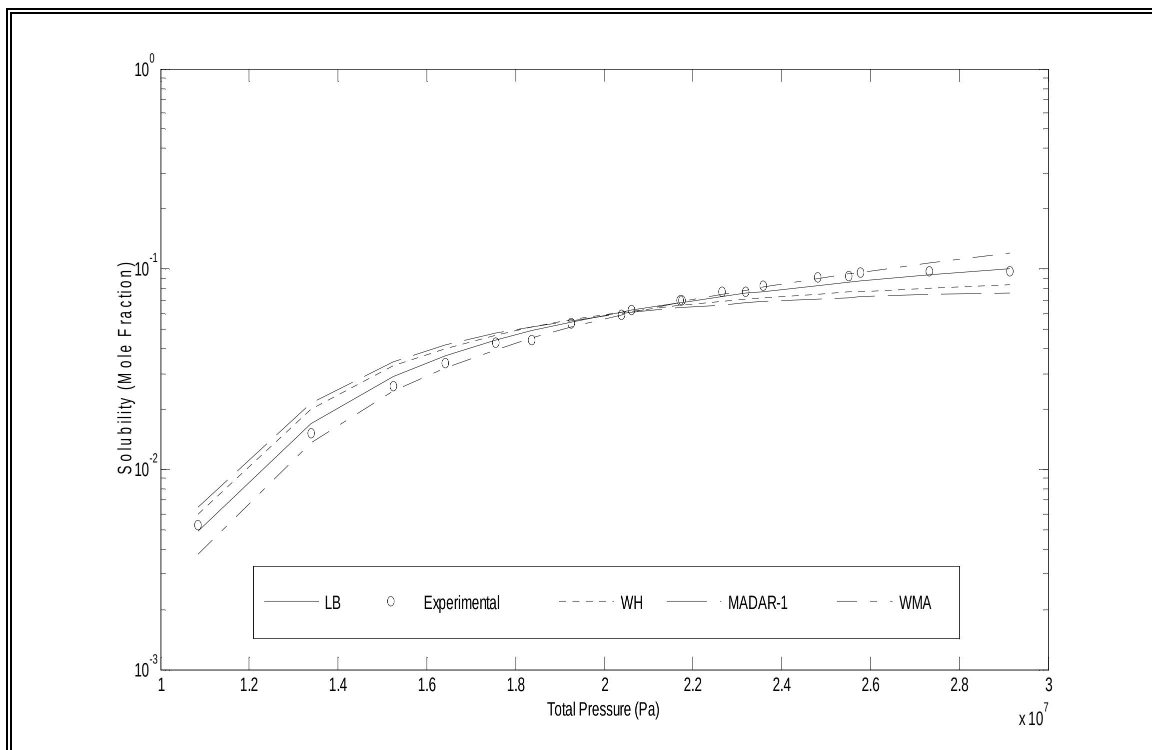

Figure 5.1.4.17: Solubility of Naphthalene in SC – CO_2 at 333.55 K with (a) parameters only

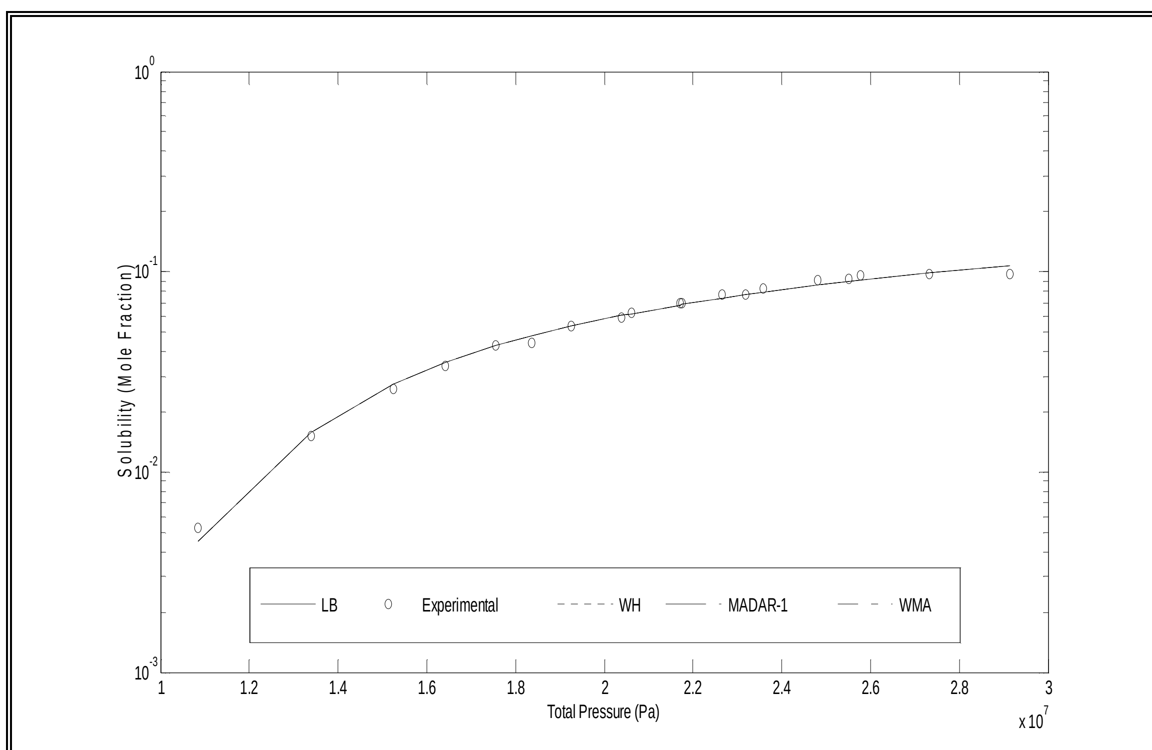

Figure 5.1.4.18: Solubility of Naphthalene in SC – CO_2 at 333.55 K with (a) & (b) parameters

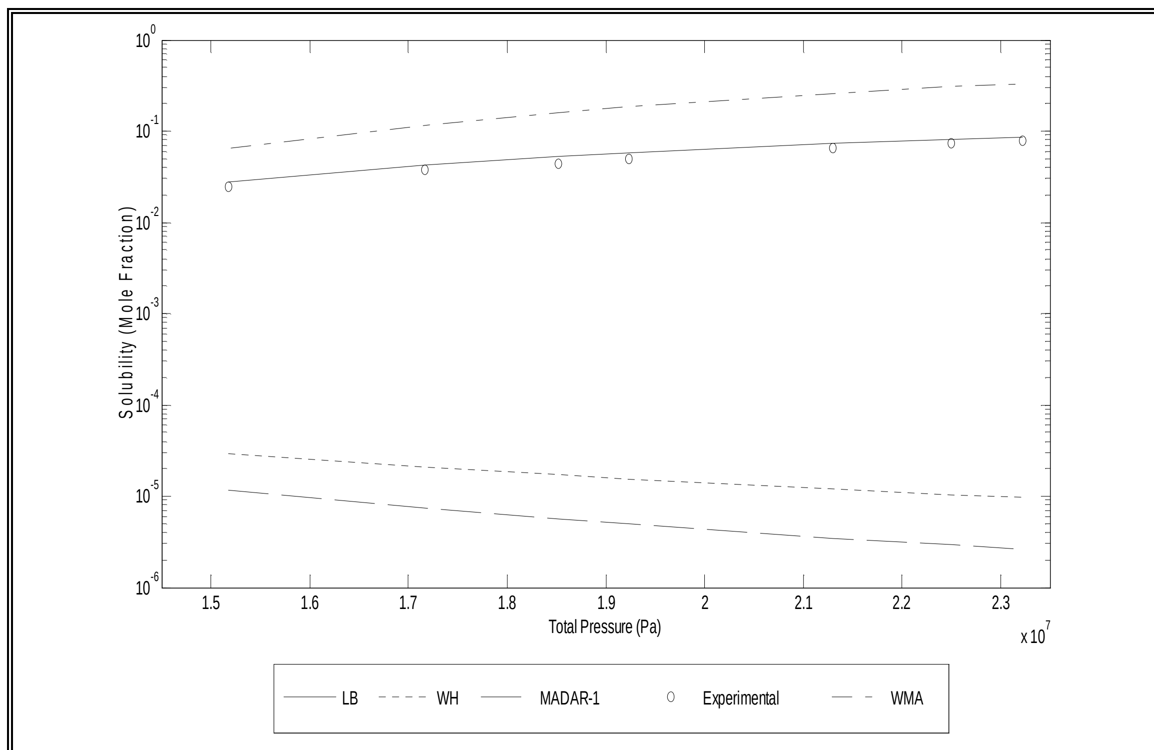

Figure 5.1.4.19: Solubility of Naphthalene in SC – CO_2 at 338.05 K (Pure Predictive)

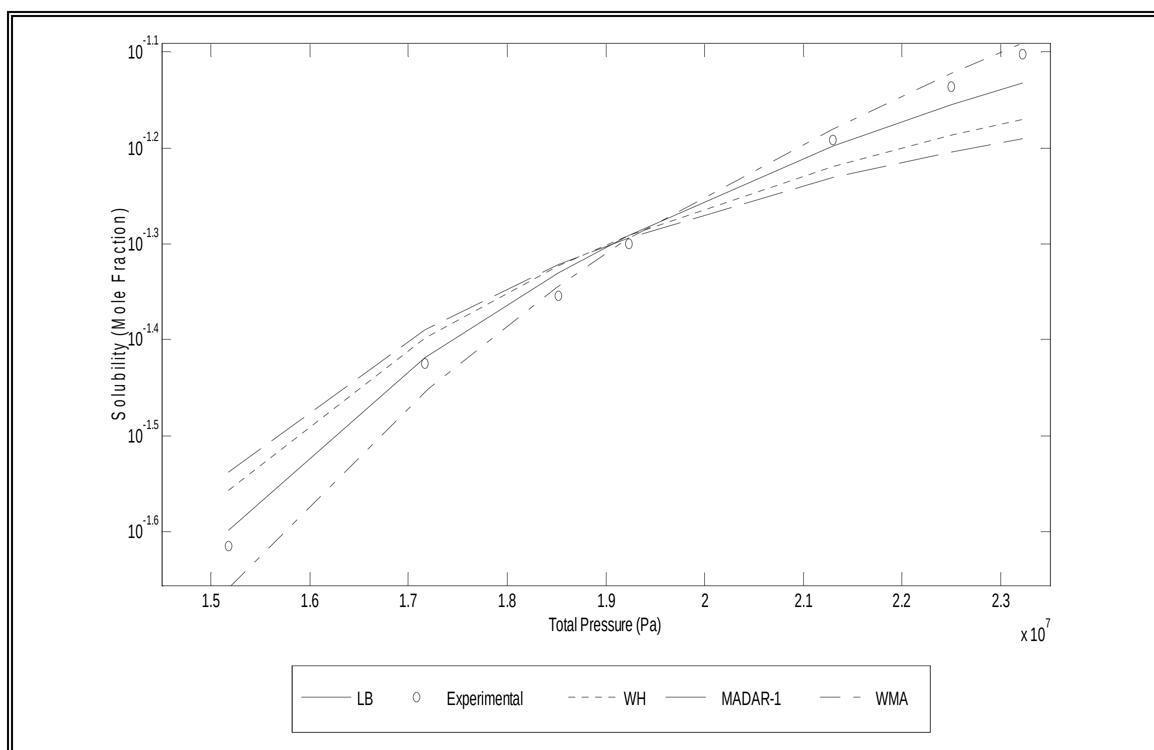

Figure 5.1.4.20: Solubility of Naphthalene in SC – CO_2 at 338.05 K with (a) parameters only

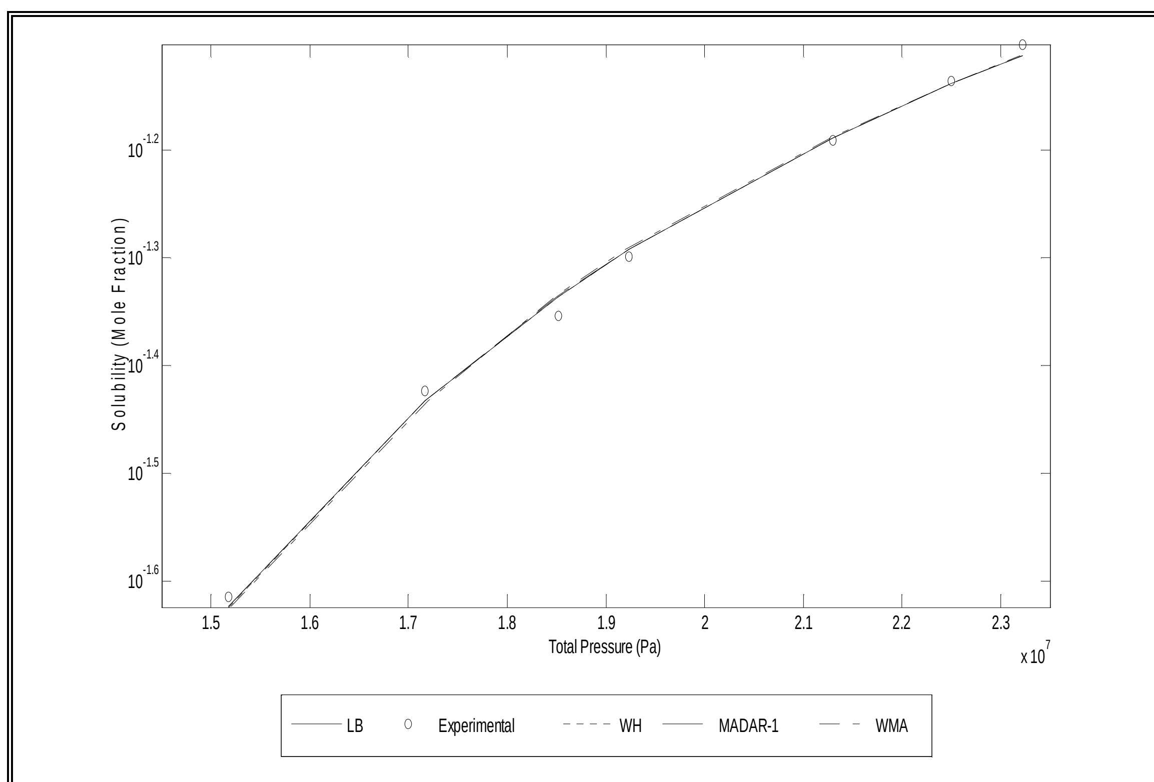

Figure 5.1.4.21: Solubility of Naphthalene in SC – CO_2 at 338.05 K with (a) & (b) parameters

5.1.5 Solubility of Xanthene Using Combining Rules and Weighting Matrix Approach

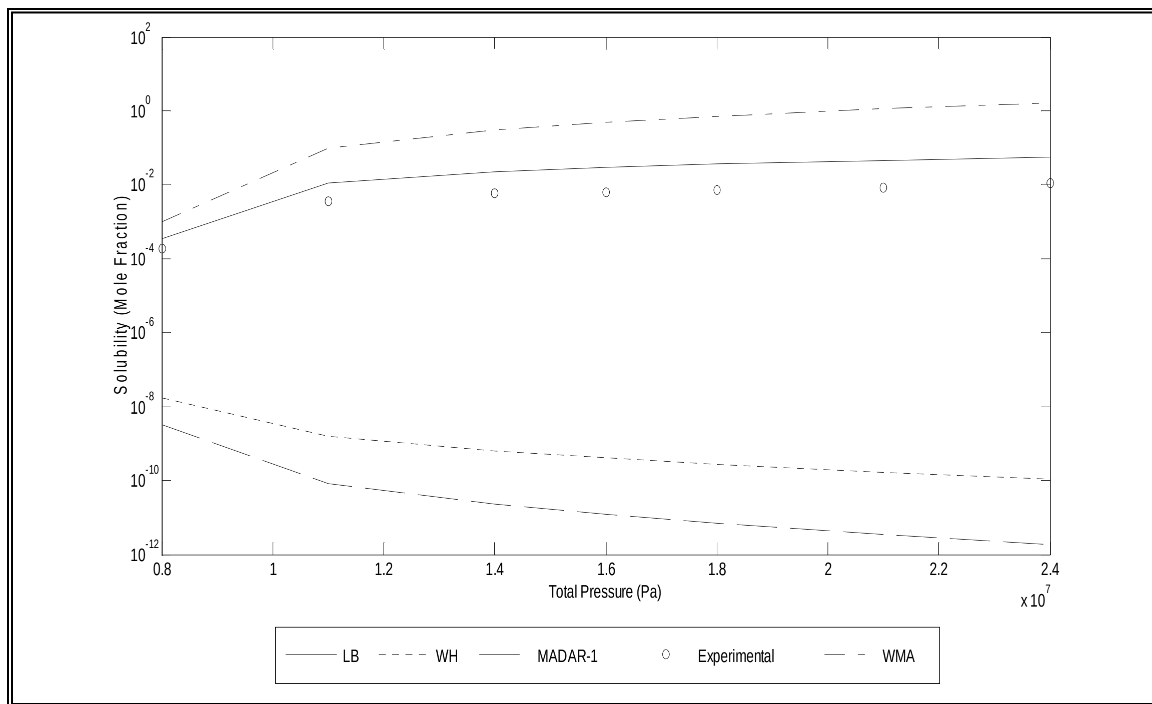

Figure 5.1.5.1: Solubility of Xanthene in SC – CO_2 at 308.15 K (Pure Predictive)

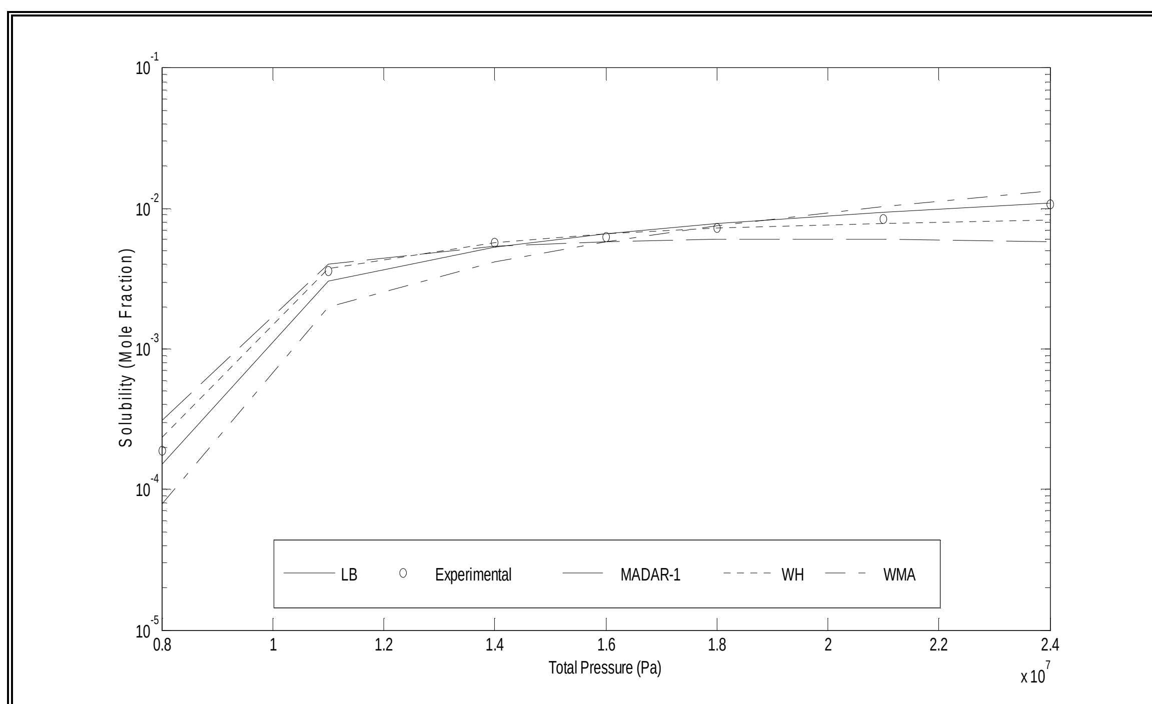

Figure 5.1.5.2: Solubility of Xanthene in SC – CO_2 at 308.15 K with (a) parameters only

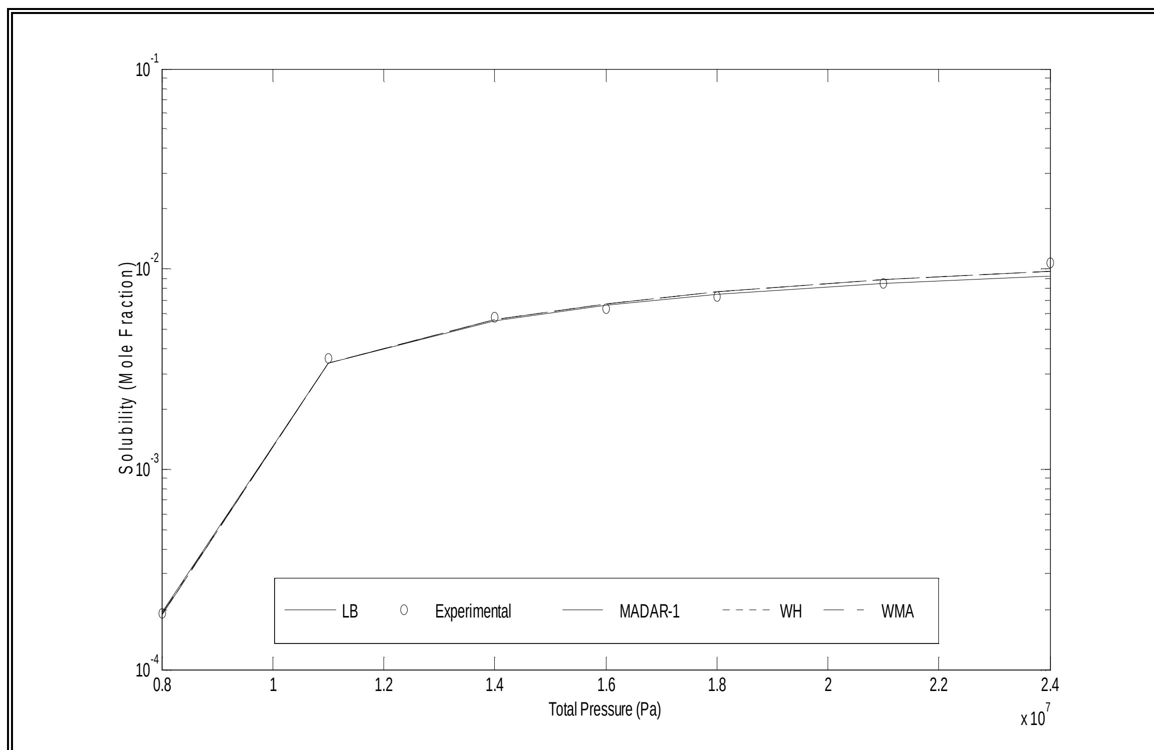

Figure 5.1.5.3: Solubility of Xanthene in SC – CO_2 at 308.15 K with (a) & (b) parameters

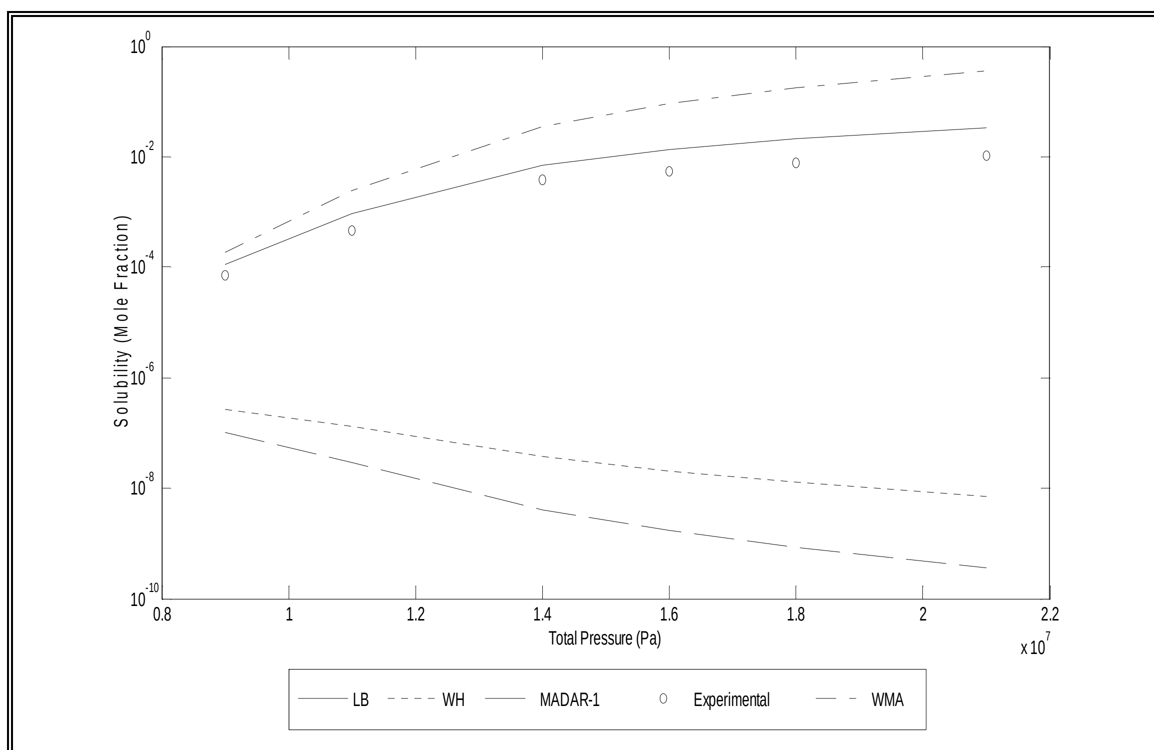

Figure 5.1.5.4: Solubility of Xanthene in SC – CO_2 at 328.15 K (Pure Predictive)

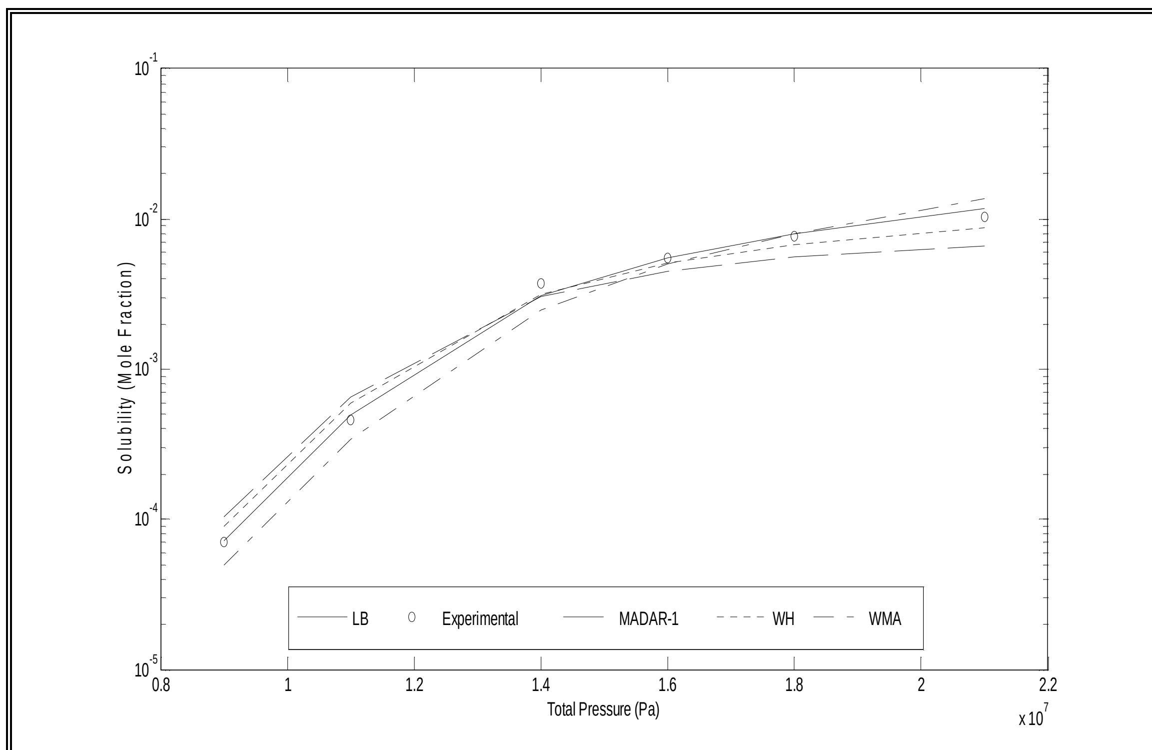

Figure 5.1.5.5: Solubility of Xanthene in SC – CO_2 at 328.15 K with (a) parameters only

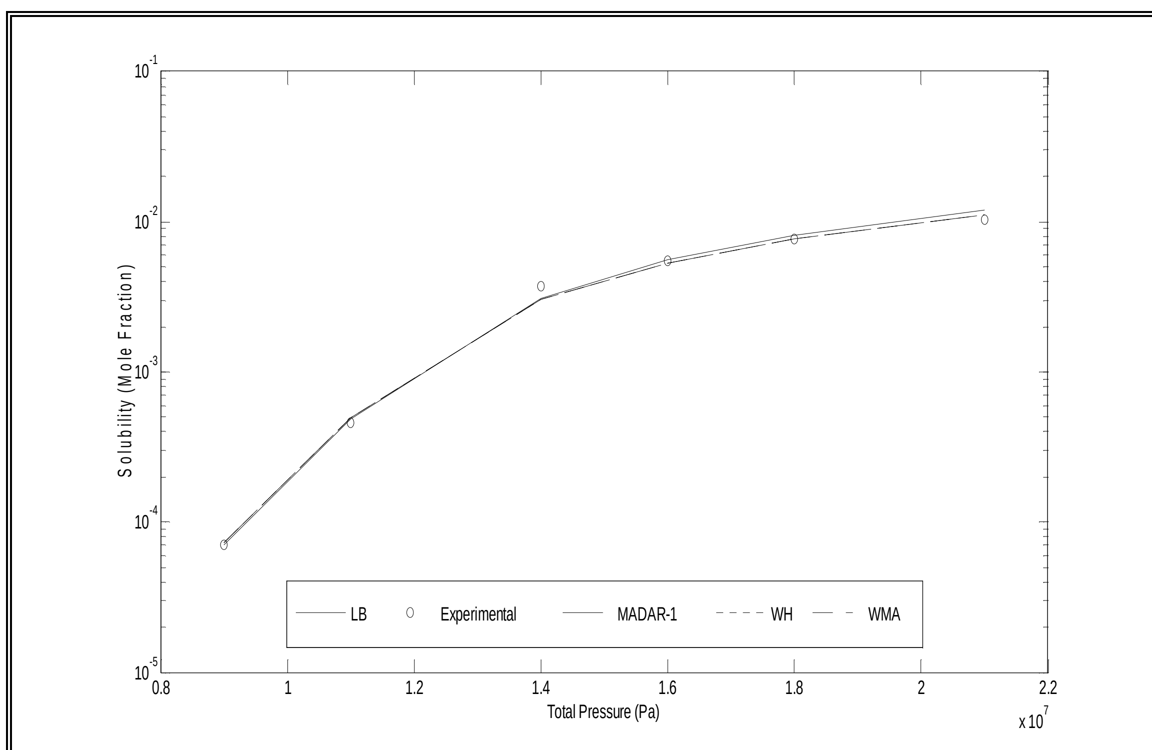

Figure 5.1.5.6: Solubility of Xanthene in SC – CO_2 at 328.15 K with (a) & (b) parameters

5.1.6 Solubility of Xanthone Using Combining Rules and Weighting Matrix Approach

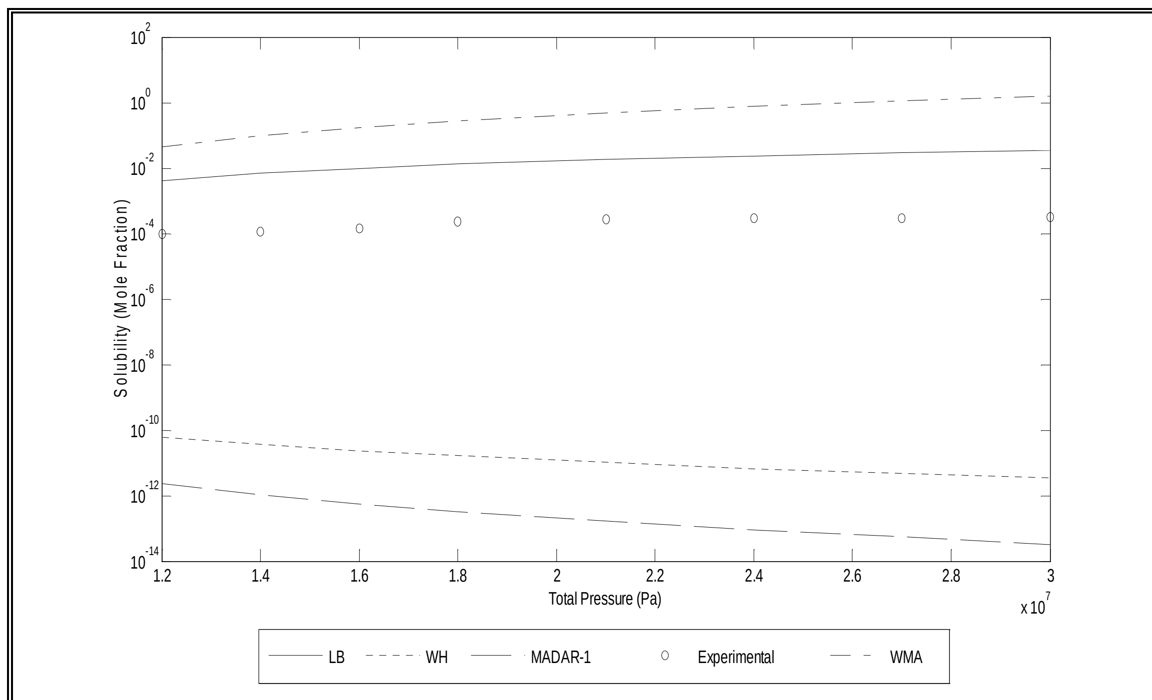

Figure 5.1.6.1: Solubility of Xanthone in SC – CO_2 at 308.15 K (Pure Predictive)

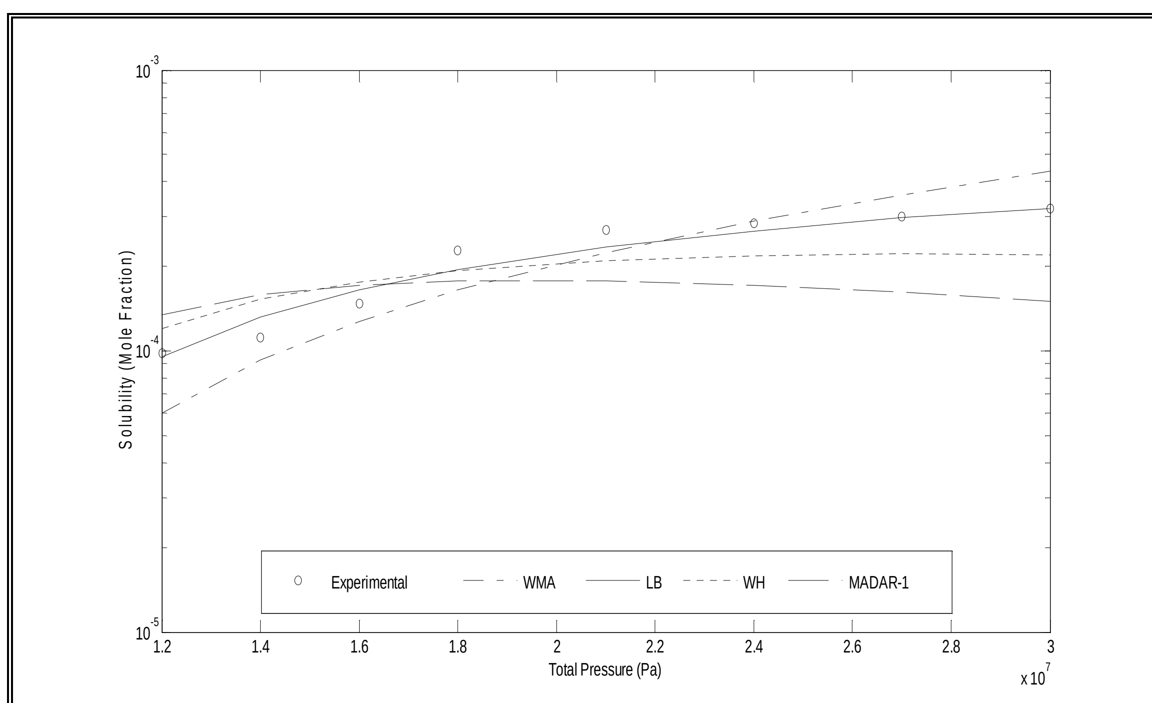

Figure 5.1.6.2: Solubility of Xanthone in SC – CO_2 at 308.15 K with (a) parameters only

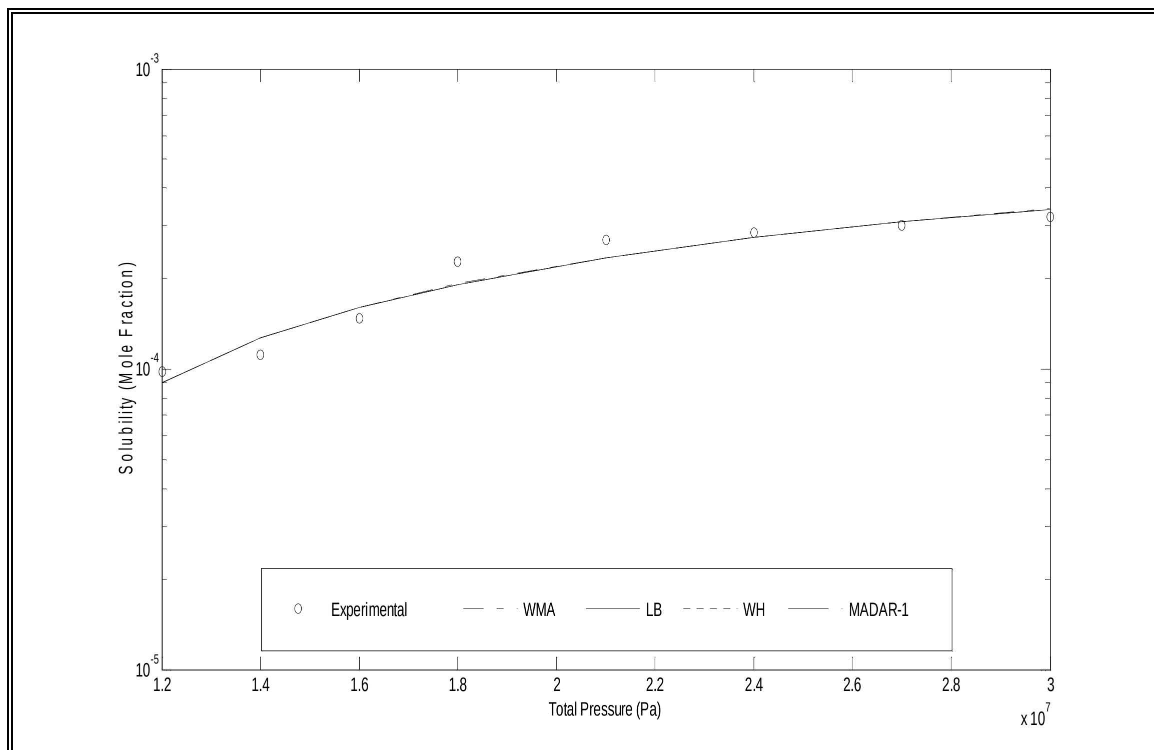

Figure 5.1.6.3: Solubility of Xanthone in SC – CO_2 at 308.15 K with (a) & (b) parameters

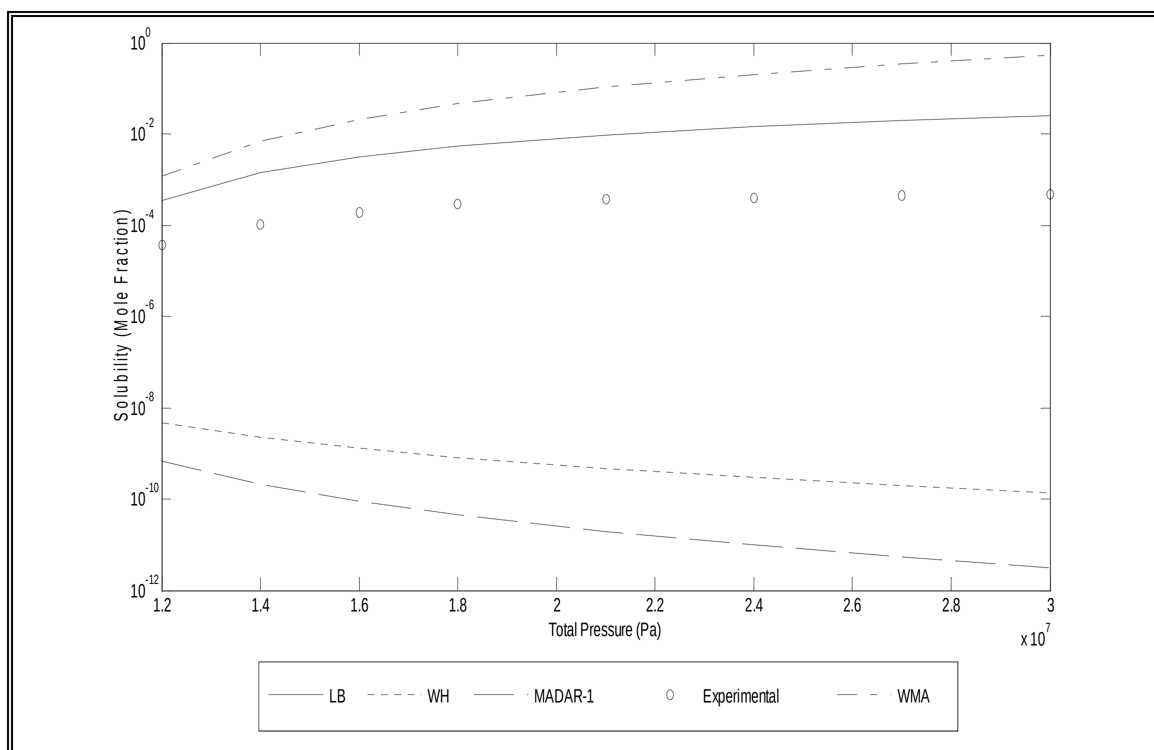

Figure 5.1.6.4: Solubility of Xanthone in SC – CO_2 at 328.15 K (Pure Predictive)

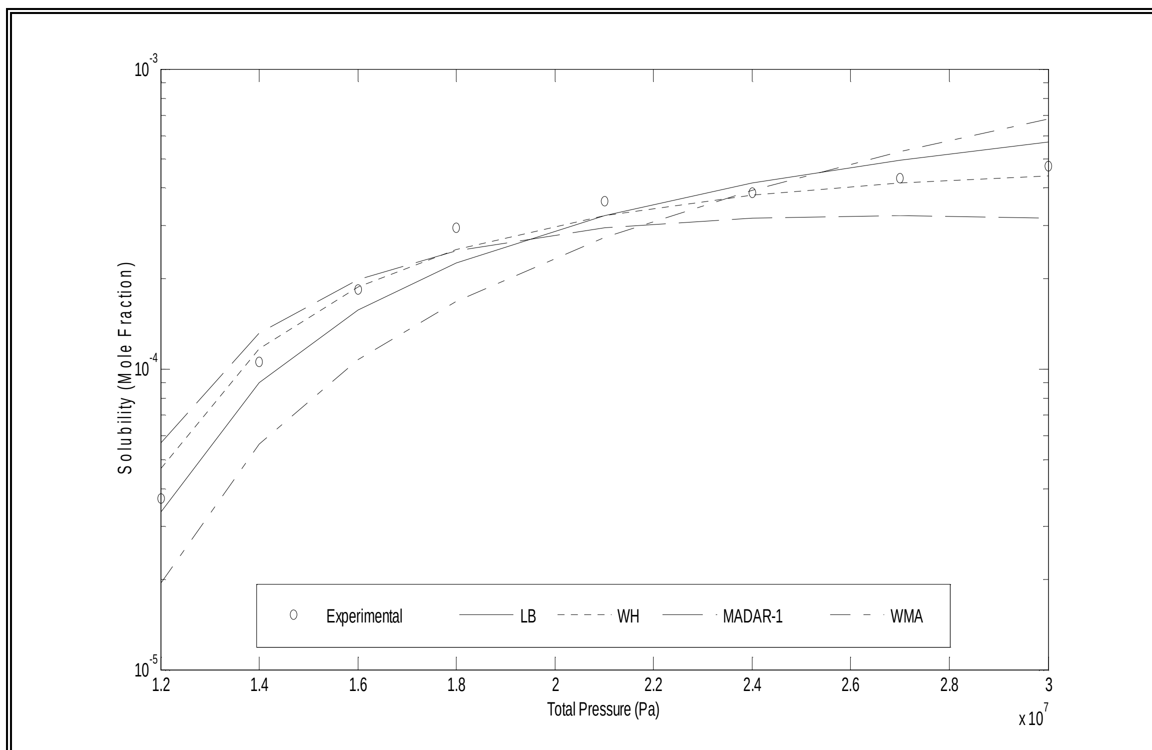

Figure 5.1.6.5: Solubility of Xanthone in SC – CO_2 at 328.15 K with (a) parameters only

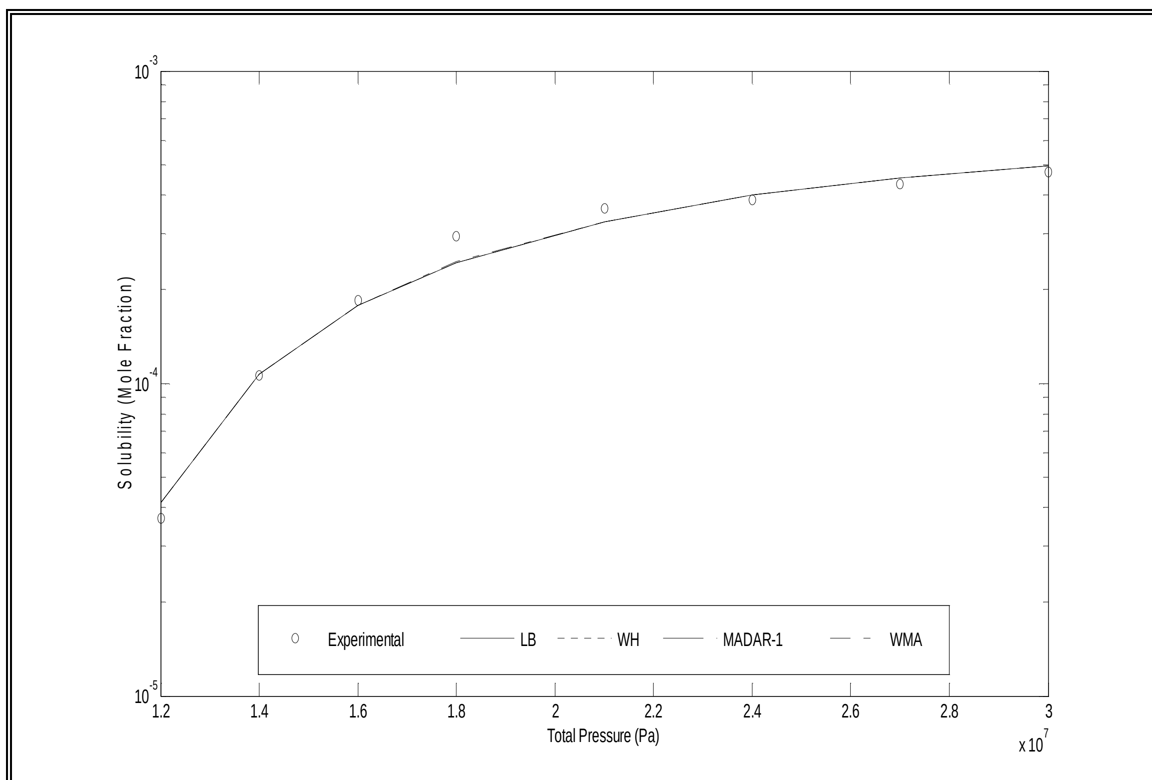

Figure 5.1.6.6: Solubility of Xanthone in SC – CO_2 at 328.15 K with (a) & (b) parameters

5.2 Effect of Temperature on the Binary Interaction Parameters and Weighting Matrix Approach Coefficients for Solid Compounds in Supercritical CO_2

The binary interaction parameters using LB, WH, and MADAR-1 combining rules in addition to the weighting matrix approach coefficients for Aspirin, C.I. Disperse Red 1 and 13, Naphthalene, Xanthene and Xanthone respectively were fitted as linear functions of temperature, the results of regression are given in tables 5.2.1 to 5.2.6. The dependence of the binary interaction parameters and the weighting matrix approach coefficients on temperature for all systems studied in this research can be shown in figures 5.2.1 to 5.2.18.

It can be noticed from the results that the dependence of the binary interaction parameters on temperature is higher than that for the weighting matrix approach coefficients.

Table 5.2.1: Dependence of the binary interaction parameters and the WMA coefficients on temperature for **Aspirin** in SC – CO_2 at **[T = 308.15 – 328.15 K]**.

Combining Rules	**(*a*) parameter only**	**(*a*) & (*b*) parameters**	
	k_{ij} & $w_{ij,a}$	k_{ij} & $w_{ij,a}$	l_{ij} & $w_{ij,b}$
LB	$k_{ij} = -2.0\text{x}10^{-4}T + 0.2552$	$k_{ij} = 1.2\text{x}10^{-3}T - 0.1348$	$l_{ij} = 3.7\text{x}10^{-3}T - 1.0865$
WH	$k_{ij} = 8.0\text{x}10^{-4}T - 1.7951$	$k_{ij} = 1.24\text{x}10^{-2}T - 4.1584$	$l_{ij} = 3.0\text{x}10^{-3}T - 0.7081$
MADAR-1	$k_{ij} = 2.2\text{x}10^{-3}T - 3.1915$	$k_{ij} = 1.24\text{x}10^{-2}T - 4.1544$	$l_{ij} = 2.7\text{x}10^{-3}T - 0.5111$
WMA	$w_{ij,a} = -7.0\text{x}10^{-5}T + 0.5542$	$w_{ij,a} = 1.0\text{x}10^{-4}T + 0.4881$	$w_{ij,b} = 1.4\text{x}10^{-3}T - 0.0323$

Table 5.2.2: Dependence of the binary interaction parameters and the WMA coefficients on temperature for **C.I. Disperse Red 1** in SC – CO_2 at **[T = 323.15 – 353.15 K]**.

Combining Rules	**(*a*) parameter only**	**(*a*) & (*b*) parameters**	
	k_{ij} & $w_{ij,a}$	k_{ij} & $w_{ij,a}$	l_{ij} & $w_{ij,b}$
LB	$k_{ij} = -9.0\text{x}10^{-4}T + 0.4252$	$k_{ij} = -1.8\text{x}10^{-3}T + 0.6413$	$l_{ij} = -2.6\text{x}10^{-3}T + 0.6523$
WH	$k_{ij} = -5.2\text{x}10^{-3}T - 3.2279$	$k_{ij} = -3.05\text{x}10^{-2}T + 6.1468$	$l_{ij} = -2.0\text{x}10^{-3}T + 0.7317$
MADAR-1	$k_{ij} = -0.25T + 79.413$	$k_{ij} = -8.24\text{x}10^{-2}T + 25.5$	$l_{ij} = 5.7\text{x}10^{-3}T - 1.789$
WMA	$w_{ij,a} = -6.0\text{x}10^{-5}T + 0.5354$	$w_{ij,a} = -9.0\text{x}10^{-5}T + 0.5309$	$w_{ij,b} = -9.0\text{x}10^{-4}T + 0.5643$

Table 5.2.3: Dependence of the binary interaction parameters and the WMA coefficients on temperature for **C.I. Disperse Red 13** in SC – CO_2 at **[T = 323.15 – 353.15 K]**.

Combining Rules	(a) parameter only	(a) & (b) parameters	
	k_{ij} & $w_{ij,a}$	k_{ij} & $w_{ij,a}$	l_{ij} & $w_{ij,b}$
LB	$k_{ij} = –9.0\text{x}10^{-4}T + 0.3864$	$k_{ij} = –2.6\text{x}10^{-3}T + 0.813$	$l_{ij} = –4.9\text{x}10^{-3}T + 1.2771$
WH	$k_{ij} = –5.1\text{x}10^{-3}T – 3.8498$	$k_{ij} = –7.33\text{x}10^{-2}T + 18.191$	$l_{ij} = –3.7\text{x}10^{-3}T + 1.193$
MADAR-1	$k_{ij} = –0.305T + 95.604$	$k_{ij} = –0.156T + 48.93$	$l_{ij} = –3.7\text{x}10^{-3}T – 1.1672$
WMA	$w_{ij,a} = –6.0\text{x}10^{-5}T + 0.533$	$w_{ij,a} = –1.0\text{x}10^{-4}T + 0.5371$	$w_{ij,b} = –1.6\text{x}10^{-3}T + 0.7636$

Table 5.2.4: Dependence of the binary interaction parameters and the WMA coefficients on temperature for **Naphthalene** in SC – CO_2 at **[T = 308.00 – 338.05 K]**.

Combining Rules	(a) parameter only	(a) & (b) parameters	
	k_{ij} & $w_{ij,a}$	k_{ij} & $w_{ij,a}$	l_{ij} & $w_{ij,b}$
LB	$k_{ij} = –2.5\text{x}10^{-3}T + 0.8401$	$k_{ij} = 2.1\text{x}10^{-3}T – 0.6652$	$l_{ij} = 1.04\text{x}10^{-2}T – 3.4798$
WH	$k_{ij} = –5.1\text{x}10^{-3}T + 0.2291$	$k_{ij} = –4.04\text{x}10^{-2}T – 14.146$	$l_{ij} = 8.8\text{x}10^{-3}T – 2.7825$
MADAR-1	$k_{ij} = –5.6\text{x}10^{-3}T – 0.0714$	$k_{ij} = –4.03\text{x}10^{-2}T – 14.126$	$l_{ij} = 8.2\text{x}10^{-3}T – 2.5215$
WMA	$w_{ij,a} = –4.0\text{x}10^{-4}T + 0.6556$	$w_{ij,a} = 3.0\text{x}10^{-4}T + 0.4074$	$w_{ij,b} = 4.3\text{x}10^{-3}T – 1.01$

Table 5.2.5: Dependence of the binary interaction parameters and the WMA coefficients on temperature for **Xanthene** in SC – CO_2 at **[T = 308.15 – 328.15 K]**.

Combining Rules	(a) parameter only	(a) & (b) parameters	
	k_{ij} & $w_{ij,a}$	k_{ij} & $w_{ij,a}$	l_{ij} & $w_{ij,b}$
LB	$k_{ij} = –5.0\text{x}10^{-4}T + 0.2058$	$k_{ij} = 1.3\text{x}10^{-3}T – 0.3701$	$l_{ij} = 4.1\text{x}10^{-3}T – 1.3816$
WH	$k_{ij} = 4.0\text{x}10^{-4}T – 2.2324$	$k_{ij} = 2.02\text{x}10^{-2}T – 7.6196$	$l_{ij} = 3.4\text{x}10^{-3}T – 0.9494$
MADAR-1	$k_{ij} = –5.6\text{x}10^{-3}T – 0.0714$	$k_{ij} = 1.99\text{x}10^{-2}T – 7.55$	$l_{ij} = 2.9\text{x}10^{-3}T – 0.6965$
WMA	$w_{ij,a} = –1.0\text{x}10^{-4}T + 0.5577$	$w_{ij,a} = 1.0\text{x}10^{-4}T + 0.4636$	$w_{ij,b} = 1.6\text{x}10^{-3}T + 0.1473$

Table 5.2.6: Dependence of the binary interaction parameters and the WMA coefficients on temperature for **Xanthone** in SC – CO_2 at **[T = 308.15 – 328.15 K]**.

Combining Rules	(*a*) parameter only	(*a*) & (b) parameters	
	k_{ij} & $w_{ij,a}$	k_{ij} & $w_{ij,a}$	l_{ij} & $w_{ij,b}$
LB	$k_{ij} = –2.0\text{x}10^{-4}T + 0.2113$	$k_{ij} = –3.5\text{x}10^{-3}T + 1.2491$	$l_{ij} = –8.9\text{x}10^{-3}T + 2.7781$
WH	$k_{ij} = –3.0\text{x}10^{-4}T – 1.7433$	$k_{ij} = –4.02\text{x}10^{-2}T + 11.84$	$l_{ij} = –7.2\text{x}10^{-3}T + 2.4465$
MADAR-1	$k_{ij} = 3.0\text{x}10^{-3}T – 3.0457$	$k_{ij} = –4.03\text{x}10^{-2}T + 11.876$	$l_{ij} = –6.3\text{x}10^{-3}T + 2.271$
WMA	$w_{ij,a} = –3.0\text{x}10^{-5}T + 0.5349$	$w_{ij,a} = –3.0\text{x}10^{-4}T + 0.6124$	$w_{ij,b} = –3.4\text{x}10^{-3}T + 1.4576$

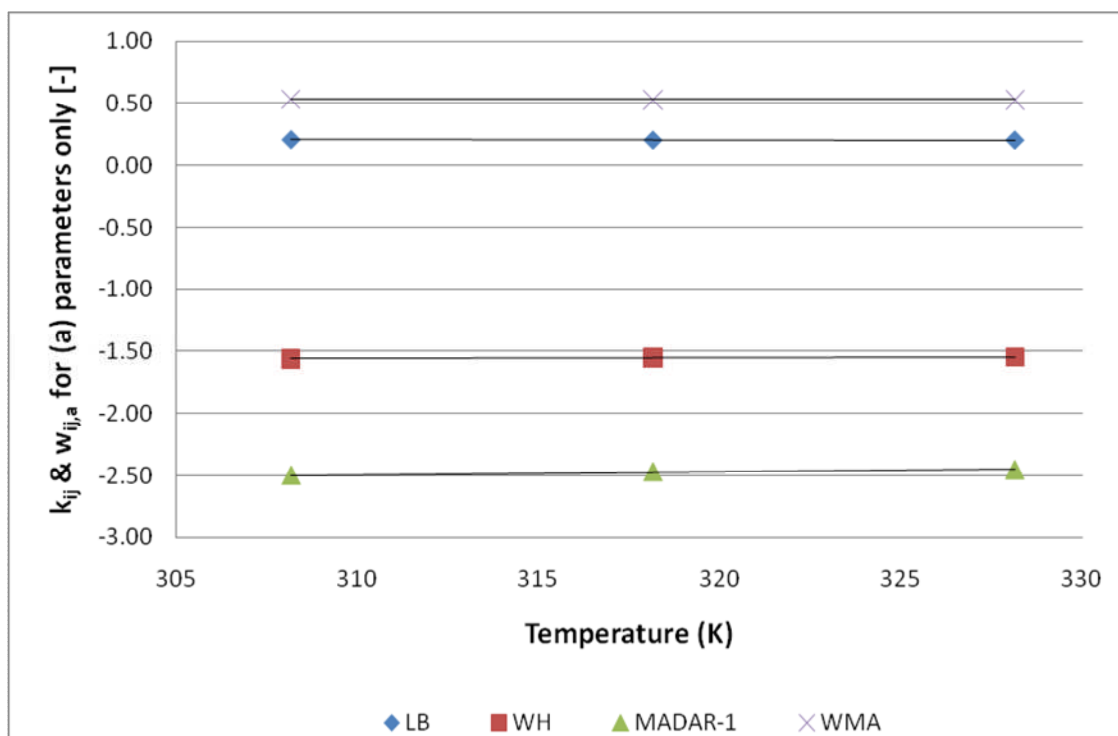

Figure 5.2.1: Dependence of the binary interaction parameter and the WMA coefficient for energy (*a*) only [l_{ij} & $w_{ij,b}$ = 0] on the temperature for the solubility of **Aspirin** in SC – CO_2.

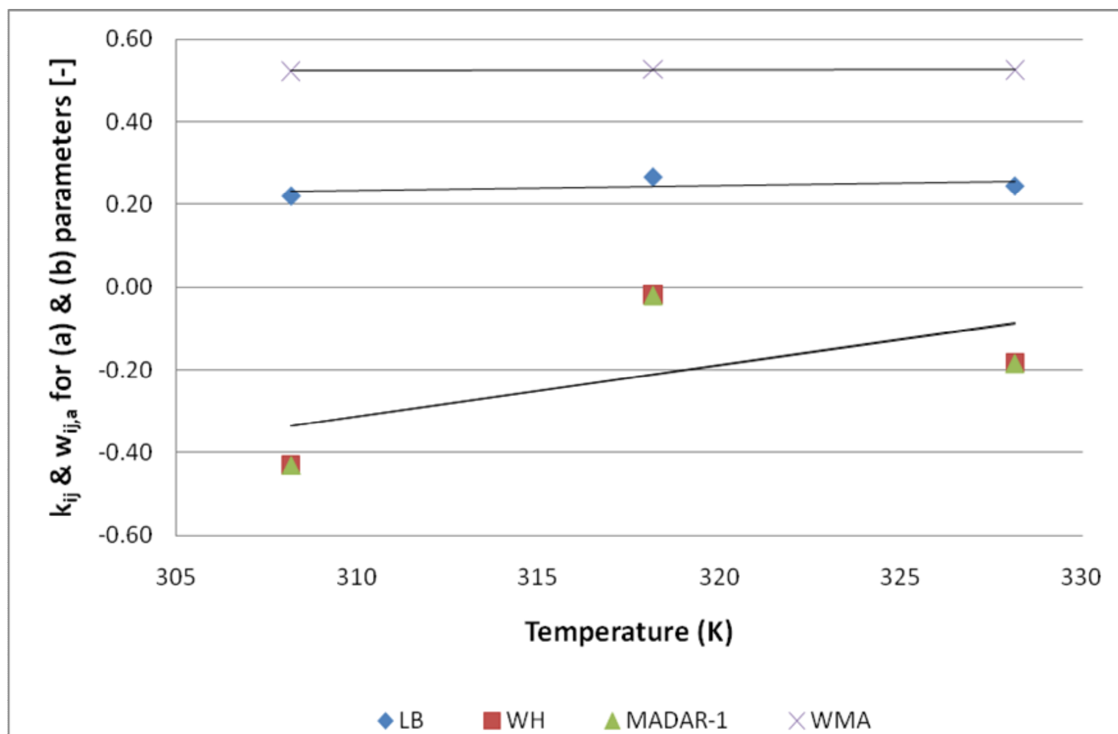

Figure 5.2.2: Dependence of the binary interaction parameter and the WMA coefficient for energy (*a*) on the temperature for the solubility of **Aspirin** in SC – CO_2.

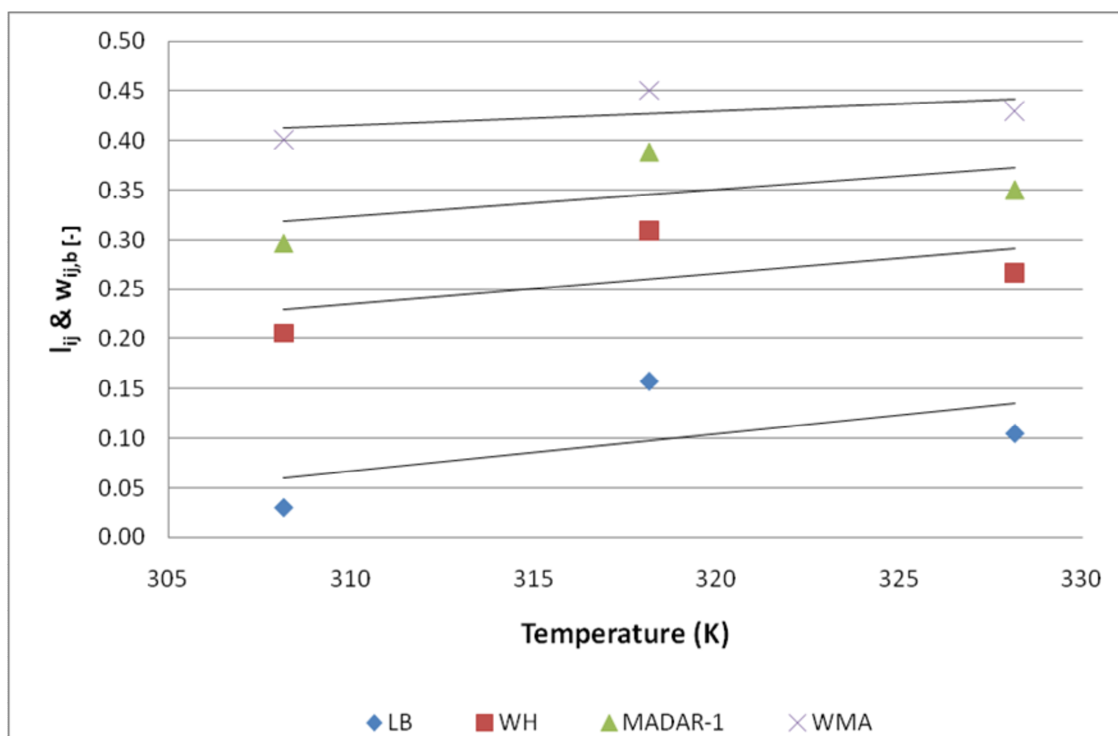

Figure 5.2.3: Dependence of the binary interaction parameter and the WMA coefficient for covolume (*b*) on the temperature for the solubility of **Aspirin** in SC – CO_2.

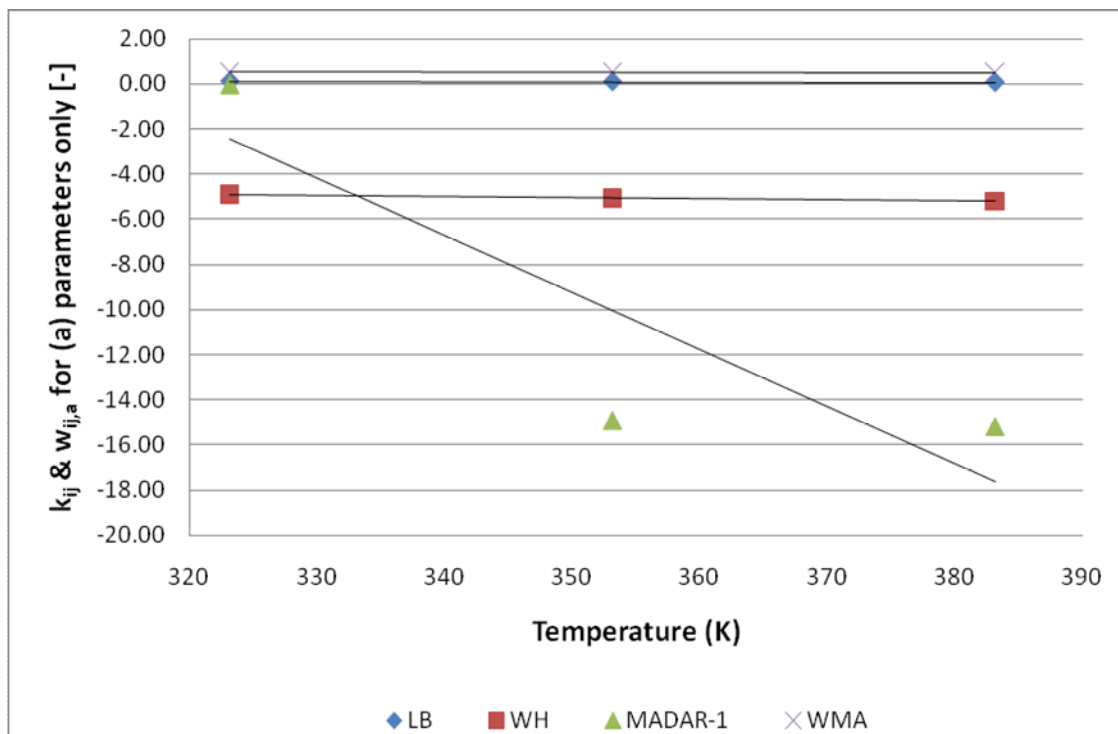

Figure 5.2.4: Dependence of the binary interaction parameter and the WMA coefficient for energy (*a*) only [l_{ij} & $w_{ij,b} = 0$] on the temperature for the solubility of **C.I. Disperse Red 1** in SC – CO_2.

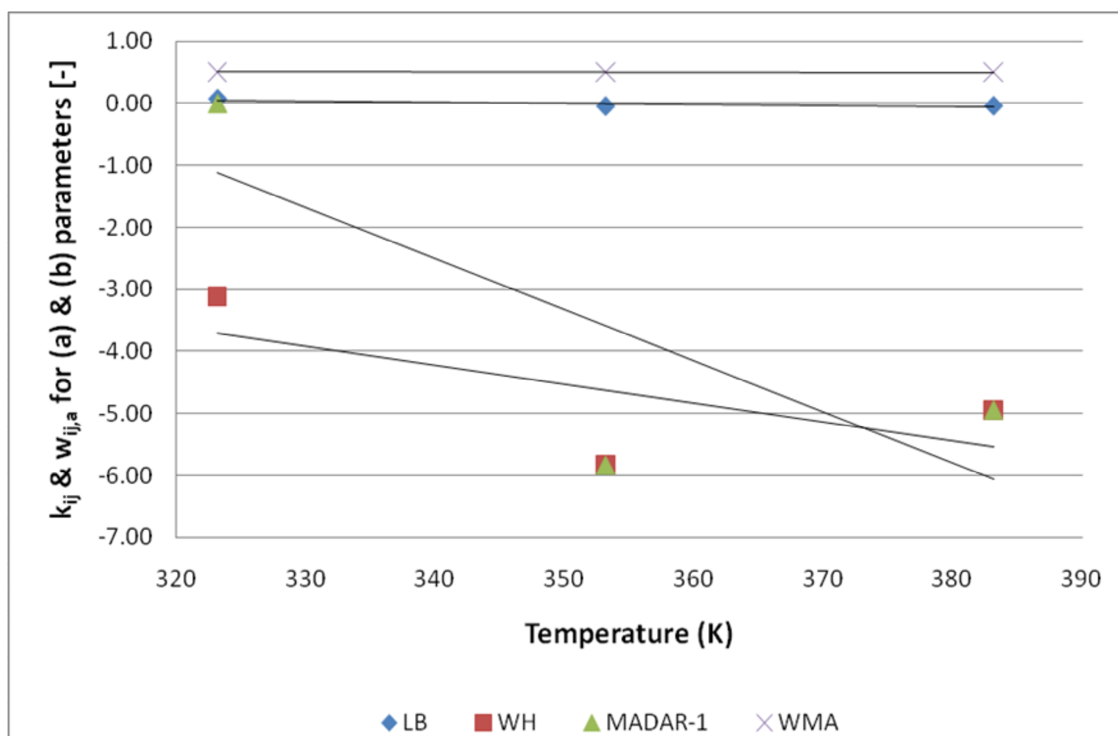

Figure 5.2.5: Dependence of the binary interaction parameter and the WMA coefficient for energy (*a*) on the temperature for the solubility of **C.I. Disperse Red 1** in SC – CO_2.

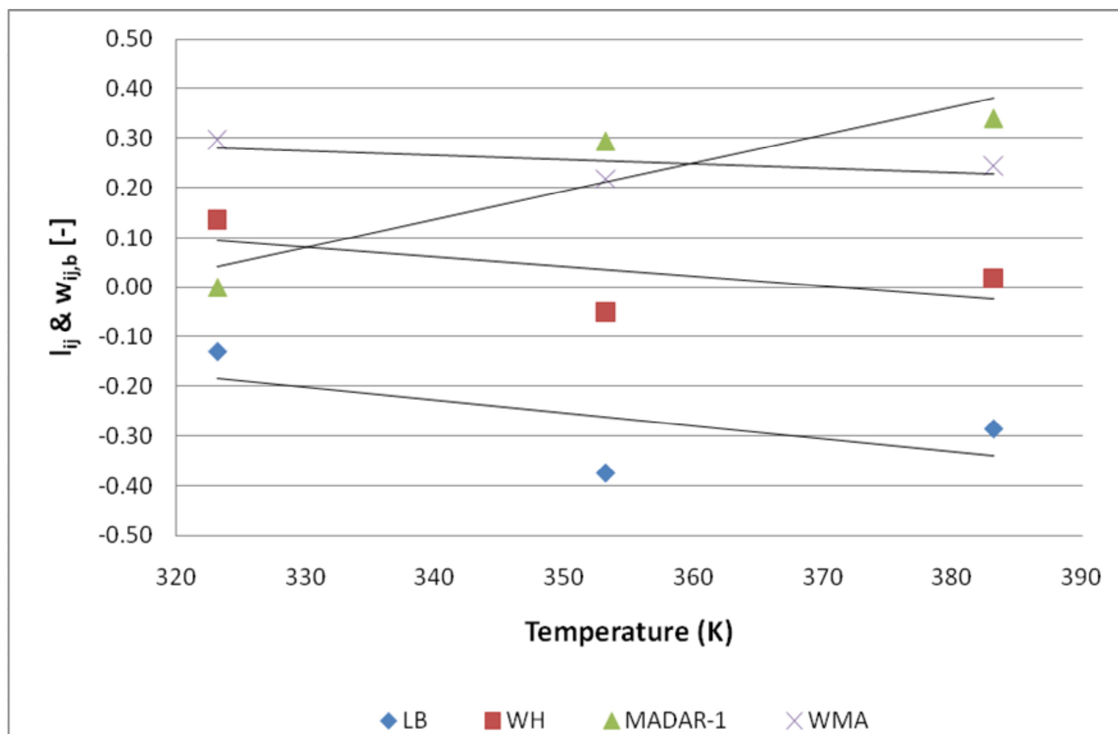

Figure 5.2.6: Dependence of the binary interaction parameter and the WMA coefficient for covolume (*b*) only on the temperature for the solubility of **C.I. Disperse Red 1** in SC – CO_2.

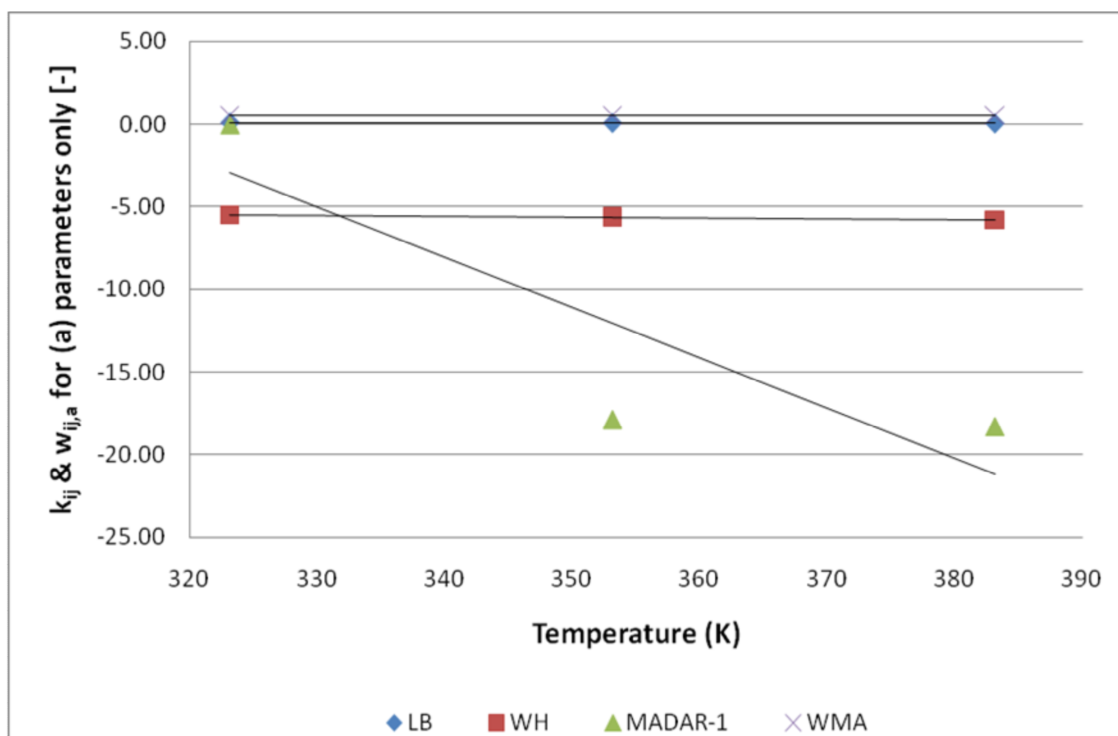

Figure 5.2.7: Dependence of the binary interaction parameter and the WMA coefficient for energy (*a*) only [l_{ij} & $w_{ij,b}$ = 0] on the temperature for the solubility of **C.I. Disperse Red 13** in SC – CO_2.

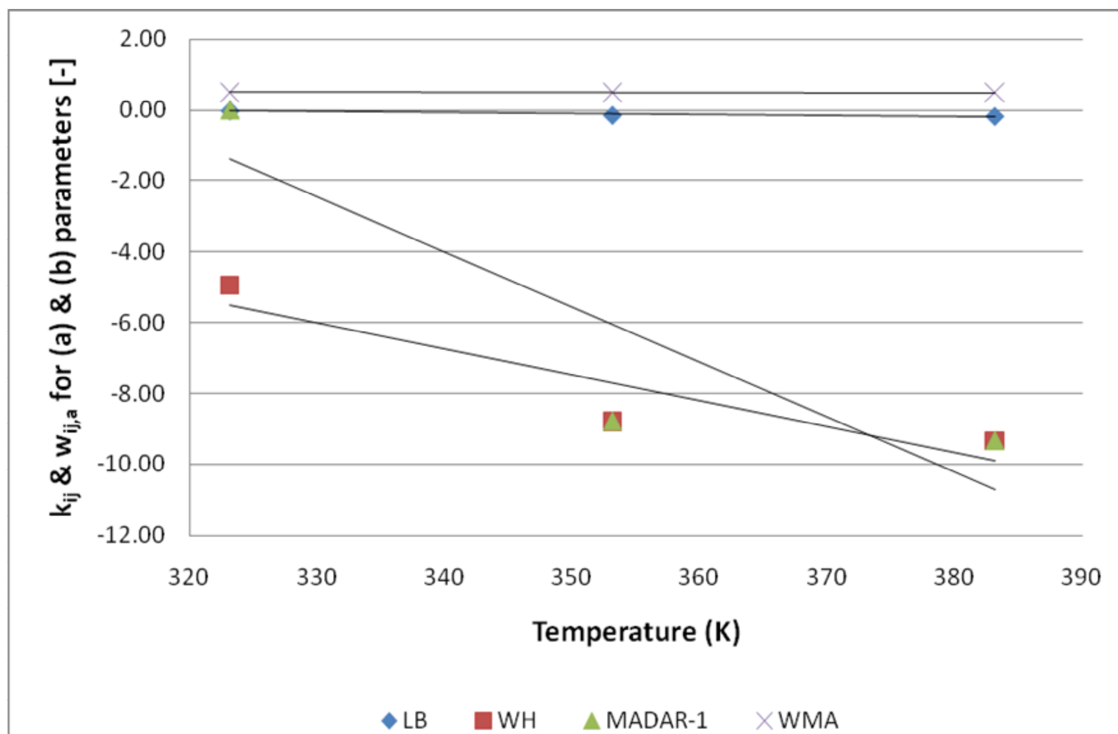

Figure 5.2.8: Dependence of the binary interaction parameter and the WMA coefficient for energy (*a*) on the temperature for the solubility of **C.I. Disperse Red 13** in SC – CO_2.

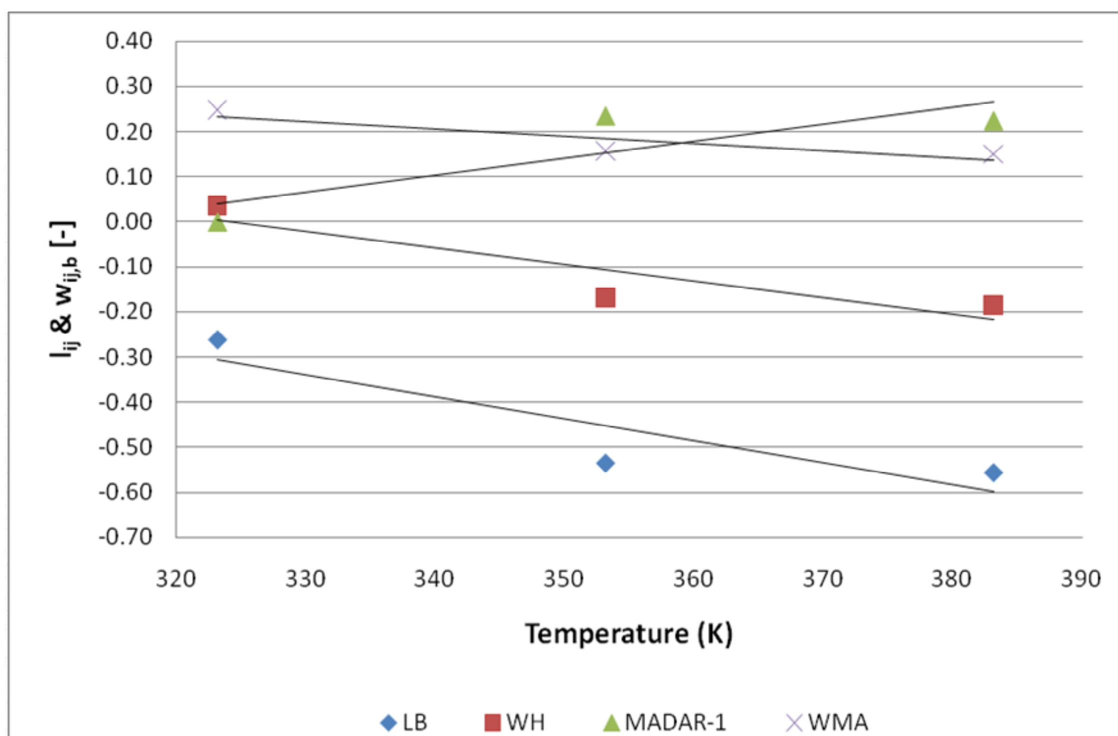

Figure 5.2.9: Dependence of the binary interaction parameter and the WMA coefficient for covolume (*b*) on the temperature for the solubility of **C.I. Disperse Red 13** in SC – CO_2.

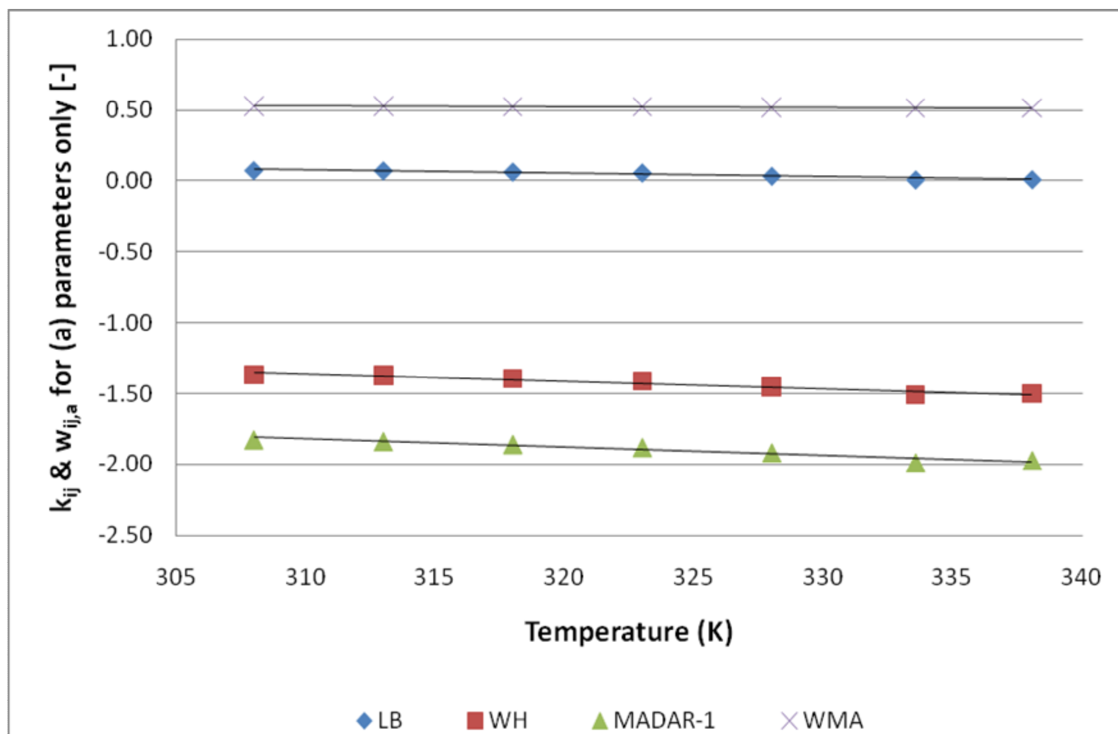

Figure 5.2.10: Dependence of the binary interaction parameter and the WMA coefficient for energy (*a*) only [l_{ij} & $w_{ij,b}$ = 0] on the temperature for the solubility of **Naphthalene** in SC – CO_2.

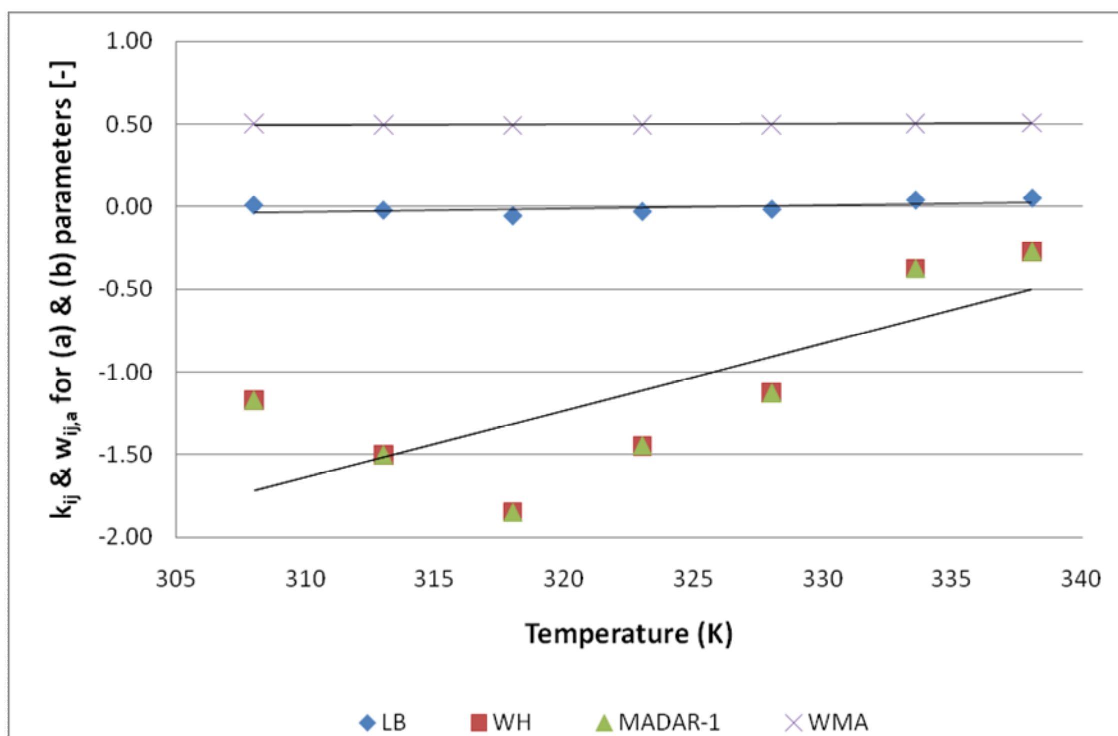

Figure 5.2.11: Dependence of the binary interaction parameter and the WMA coefficient for energy (*a*) on the temperature for the solubility of **Naphthalene** in SC – CO_2.

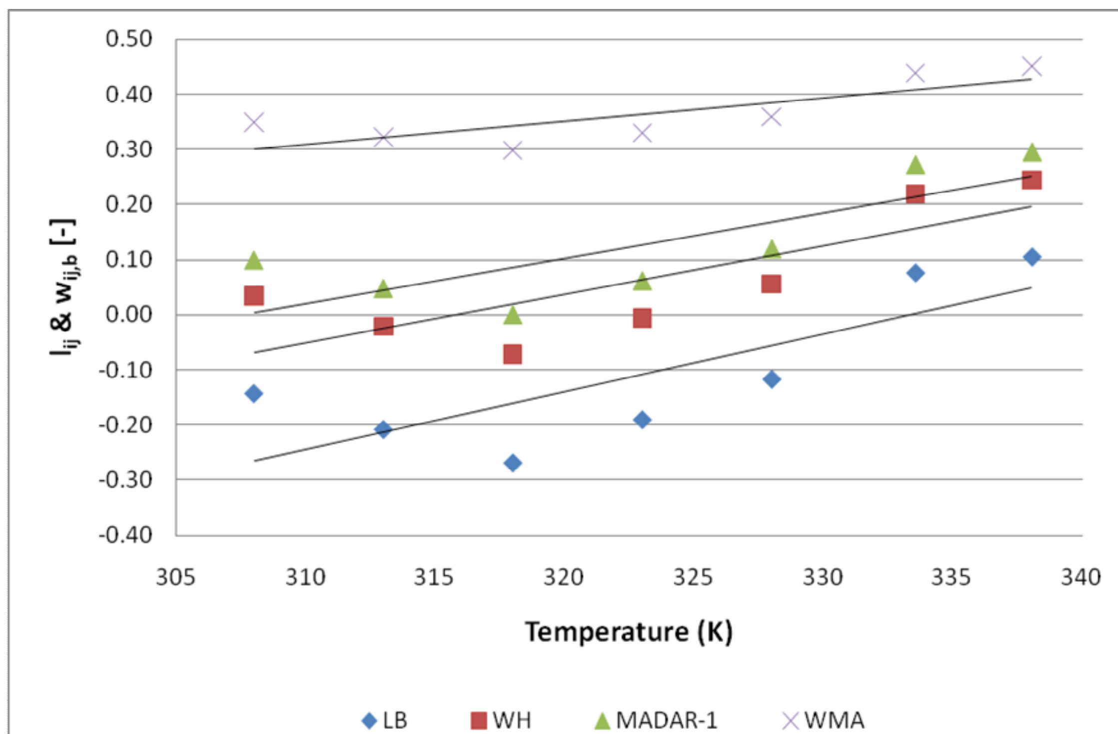

Figure 5.2.12: Dependence of the binary interaction parameter and the WMA coefficient for covolume (*b*) on the temperature for the solubility of **Naphthalene** in SC – CO_2.

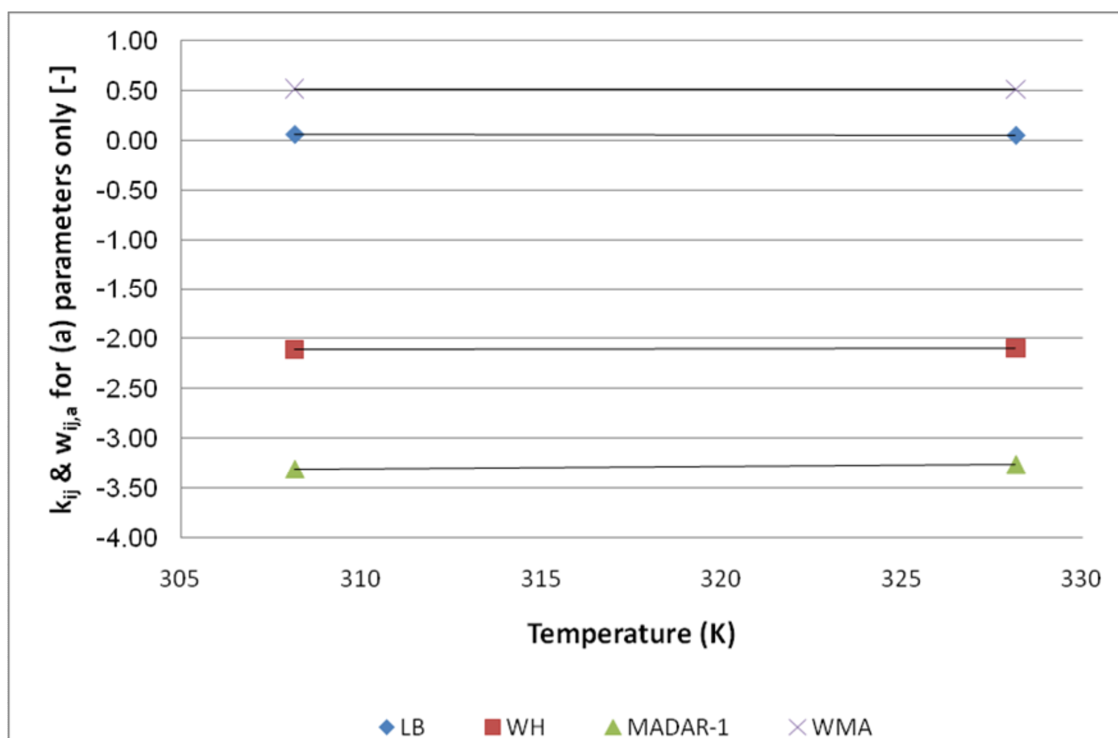

Figure 5.2.13: Dependence of the binary interaction parameter and the WMA coefficient for energy (*a*) only [l_{ij} & $w_{ij,b}$ = 0] on the temperature for the solubility of **Xanthene** in SC – CO_2.

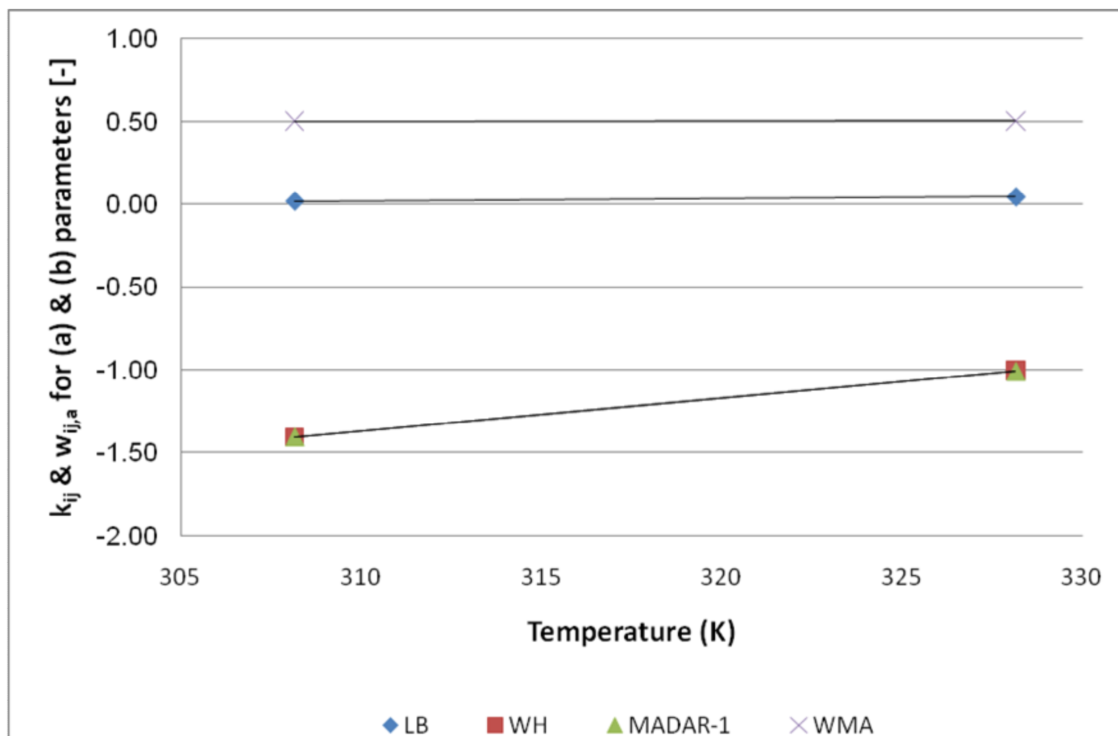

Figure 5.2.14: Dependence of the binary interaction parameter and the WMA coefficient for energy (*a*) on the temperature for the solubility of **Xanthene** in SC – CO_2.

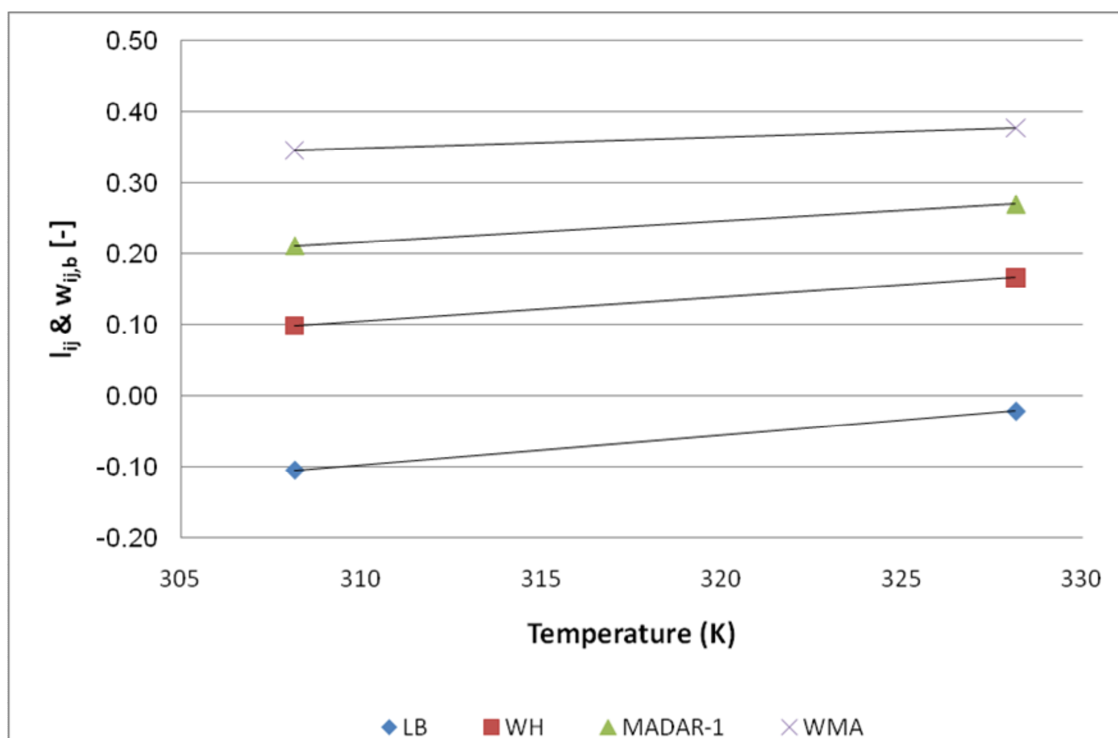

Figure 5.2.15: Dependence of the binary interaction parameter and the WMA coefficient for covolume (*b*) on the temperature for the solubility of **Xanthene** in SC – CO_2.

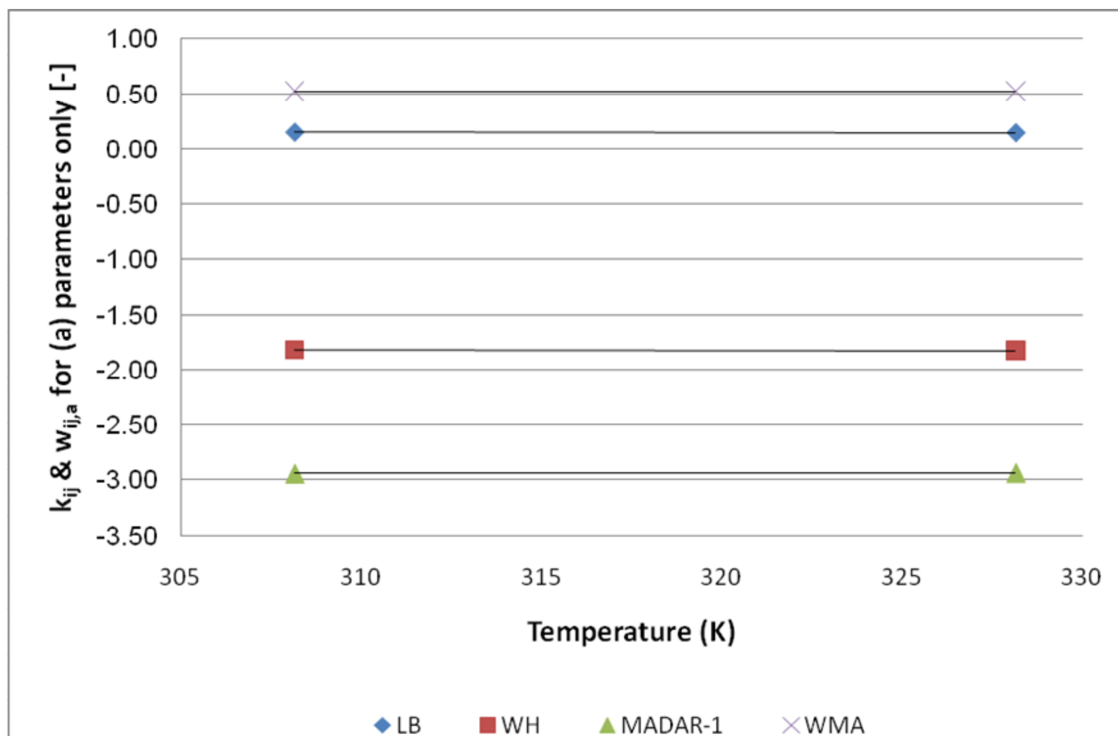

Figure 5.2.16: Dependence of the binary interaction parameter and the WMA coefficient for energy (*a*) only [l_{ij} & $w_{ij,b} = 0$] on the temperature for the solubility of **Xanthone** in SC – CO_2.

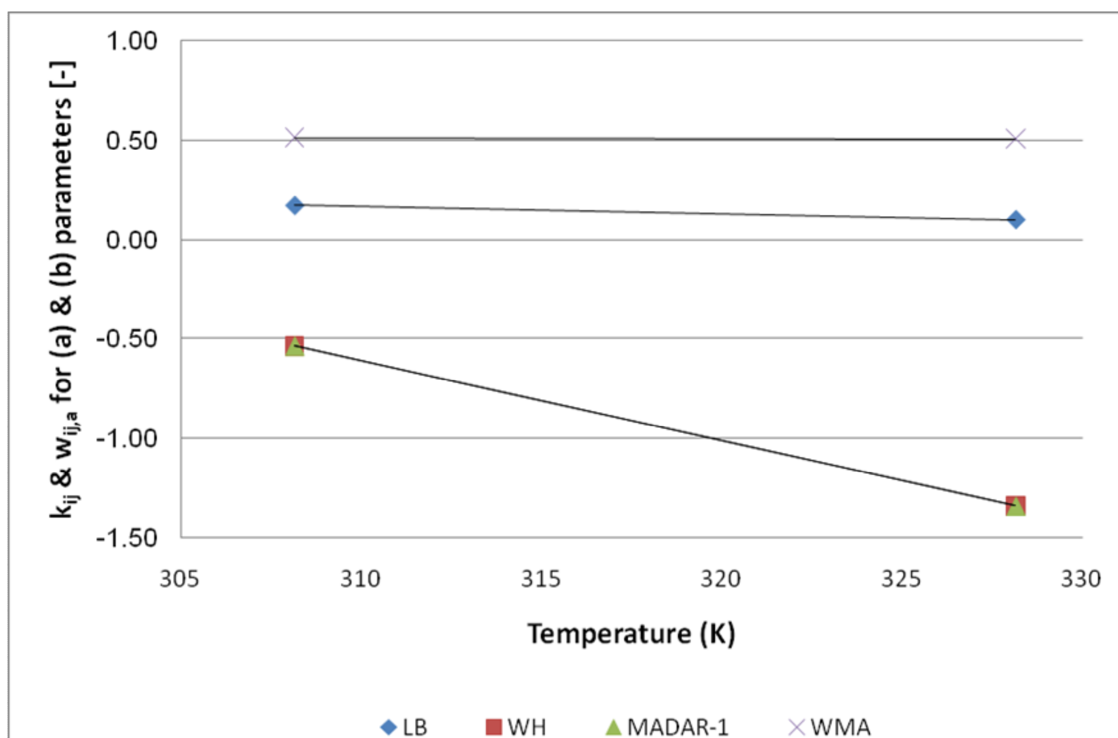

Figure 5.2.17: Dependence of the binary interaction parameter and the WMA coefficient for energy (*a*) on the temperature for the solubility of **Xanthone** in SC – CO_2.

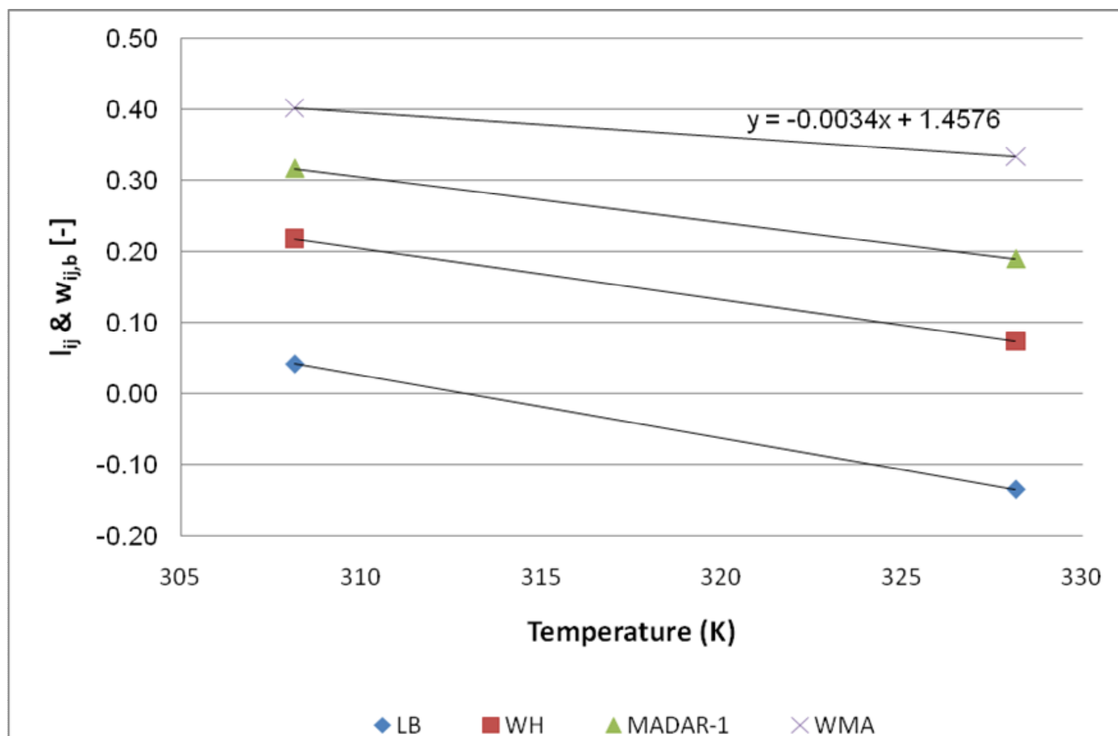

Figure 5.2.18: Dependence of the binary interaction parameter and the WMA coefficient for covolume (*b*) on the temperature for the solubility of **Xanthone** in SC – CO_2.

6. Conclusions and Recommendations

This section gives the main conclusions and the possible future directions in order to develop and improve this work.

6.1 Conclusions

- For all systems studied in this research, the binary interaction parameters modeling approach provide better estimates than the weighting matrix approach compared to the purely predictive approach .

- For Aspirin, Xanthene and Xanthone; Lorentz-Berthelot (LB) combining rules with the energy binary interaction parameter (k_{ij}) gives the best estimates compared to Waldman-Hagler (WH) and MADAR-1 combining rules as well as the weighting matrix approach.

- For both C.I. Disperse Red 1, C.I. Disperse Red 13 and Naphthalene; Waldman-Hagler (WH) combining rules with the energy binary interaction parameter (k_{ij}) gives the best estimates compared to Lorentz-Berthelot (LB) and MADAR-1 combining rules as well as the weighting matrix approach.

- For both binary interaction parameters and weighting matrix modeling approaches, using both energy and covolume parameters together leads to superior estimates compared to the purely predictive approach as well as to the energy parameter using approach with almost the same values of the solubility of the solid solute in SC-CO_2 using both modeling approaches.

- For both binary interaction parameters and weighting matrix approaches, the energy parameter, *a*, has more contribution than the covolume parameter, *b*, to provide better estimates compared to the purely predictve approach.

- For all systems studied in this research, the dependence of the binary interaction parameters on temperature is higher than that for the weighting matrix approach coefficients.

- The weighting matrix approach was applicable for all systems studied in this research for both energy and covolume binary interaction parameters by minimizing the average absolute relative deviations (AARD) and also by minimizing the root mean square deviations (RMSD) between the experimental solubility and predicted solubility, this concludes that the weighting matrix approach is more flexible than both Waldman-Hagler (WH), and MADAR-1 combining rules which were not applicable for some systems.

6.2 Recommendations

- To find a relationship between the binary interaction parameters and weighting matrix coefficients in order to make use of available databanks of binary interaction parameters.

- To test the Peng Robinson EOS with both binary interaction parameters and weighting matrix modeling approaches on different systems.

- To test both binary interaction parameters and weighting matrix modeling approaches on other equations of state.

References

Al-Matar, A. Kh. (2002), A Generating Equation for Mixing Rules and Assessment of Their Effect on the Second Virial Coefficient, **Ph. D. Thesis**, New Mexico State University, Las Cruces, New Mexico, USA.

Al-Matar, A. Kh. and Rockstraw, D. A. (2004), A Generating Equation for Mixing Rules and Two New Mixing Rules for Interatomic Potential Energy Parameters, **Journal of Computational Chemistry**, 25(5), 660-668.

Al-Matar, A. Kh. and Rockstraw, D. A. (2006), Assessment of the Effect of Mixing Rules on Predicting the Second Virial Coefficient and a Further Evidence of the Inadequacy of the Lorentz-Berthelot Rules, **Dirasat-Engineering Sciences**, 33(1):27-36.

Al-Matar, A. Kh. and Sweis, F. K. (2010), Thermodynamics of supercritical fluid extraction of some dyes and pharmaceutical compounds using the weighting matrix approach, **Chemical Product and Process Modeling**, 5(1), Article 26.

Anderko, A. (2000), Cubic and Generalized van der Waals Equations, in: Sengers, J.V., Kayser, R.F., Peters, C.J. and White, H.J. (Eds.), **Equations of State for Fluids and Fluid Mixtures (Experimental Thermodynamics)**, Elsevier Science, Amsterdam, 2000, pp. 75–126.

Ashour, I., Almehaideba, R., Fateenb, S.E., and Alya, G. (2000), Representation of solid-supercritical fluid phase equilibria using cubic equations of state, **Fluid Phase Equilibria**, 167, 41–61.

Brennecke, J.F. and Eckert, C.A. (1989), Phase equilibria for supercritical process design, **AIChE Journal**, 35, 1409.

Escobedo-Alvarado, G. N., Sandler, S. I. and, Scurto, A. M. (2001), Modeling of solid–supercritical fluid phase equilibria with a cubic equation of state – G^{ex} model, **Journal of Supercritical Fluids**, 21, 123–134.

Gupta, R.B. and Shim, J.J. (2007), **Solubility in Supercritical Carbon Dioxide**, CRC Press.

Huang, Z., Lu, W. D., Kawi, S. and Chiew Y. C. (2004), Solubility of Aspirin in Supercritical Carbon Dioxide with and without Acetone, **Journal of Chemical Engineering Data**, 49, 1323-1327.

Huang, Z., Sun, G.B, Kawi, S., Shi, Y., Wen , R. and Song, S.W. (2005), Solubilities of xanthone and xanthene in supercritical CO_2, **Fluid Phase Equilibria**, 238, 26–32.

Huron, M.J. and Vidal, J. (1979), New mixing rules in simple equations of state for representing vapor-liquid equilibria of strongly non-ideal solutions. **Fluid Phase Equilibria**, 3, 255.

Martinez, J.L. (2008), **Supercritical Fluid Extraction of Nutraceuticals and Bioactive Compounds**, CRC Press

Mohamed, R.S. and Holder, G.D. (1987), High pressure phase behavior in systems containing CO_2 and heavier compounds with similar vapor pressures, **Fluid Phase Equilibria,** 32, 295–317.

Mukhopadhyay, M. (2000), **Natural Extracts Using Supercritical Carbon Dioxide**, Boca Raton: CRC Press.

Mukhopadhyay, M. and Rao, G.V.R. (1993), Thermodynamic modeling for supercritical fluid process design, **Industrial and Engineering Chemistry Research**, 32(5), 922–930.

Orbey, H. and Sandler, S. I., (1998), **Modelling Vapor Liquid Equilibria**, Cambridge: Cambridge University Press.

Panagiotopoulos, A.Z. and Reid, R.C. (1986), New Mixing Rule for Cubic Equations of State for Highly Polar, Asymmetric Systems, in: Chao, K.C. and R. L. Robinson (Eds.), **Equations of State – Theories and Applications, ACS Symposium Series**: New York, 1986, 300, 571-582.

Prausnitz, J. M., Lichtenthaler, R. N., and de Azeved, E. G. (1999), **Molecular Thermodynamics of Fluid-Phase Equilibria,** 3rd Edition, Upper Saddle River: Prentice Hall PTR.

Sandler, S.I. (2006), **Chemical, Biochemical and Engineering Thermodynamics**, 4th Edition, New York: John Wiley and Sons.

Shinoda, T. and Tamura, K. (2003), Solubilities of C.I. Disperse Red 1 and C.I. Disperse Red 13 in supercritical carbon dioxide, **Fluid Phase Equilibria**, 213, 115–123.

Škerget, M., Novak-Pintaric, Z., Knez., Ž., and Kravanja, Z. (2002), Estimation of solid solubilities in supercritical carbon dioxide: Peng–Robinson adjustable binary parameters in the near critical region, **Fluid Phase Equilibria**, 203, 111–132.

Valderrama, J. O. (2003), The State of the Cubic Equations of State, **Industrial and Engineering Chemistry Research**, 42, 1603-1618.

Waldman, M. and Hagler, A. T. (1993), New combining rules for rare gas van der Waals parameters, **Journal of Computational Chemistry**, 14 (9), 1077–1084.

Wong, D.S.H. and Sandler, S.I. (1992), A theoretically correct mixing rule for cubic equations of state, **AIChE Journal**, 38, 671-680.

Appendices

Appendix A

Fitting Results by Minimizing RMSD

Table A.1: Modeling results for solids solubility in SC – CO_2 using the PR – EOS with the energy binary interaction parameter and WMA coefficient by minimizing RMSD.

Solid Compound	*T* (K)	*P* (bar)	N	Pure Predictive	LB (k_{ij})		WH (k_{ij})		MADAR-1 (k_{ij})		WMA ($w_{ij,a}$)	
				RMSD	k_{ij}	RMSD	k_{ij}	RMSD	k_{ij}	RMSD	$w_{ij,a}$	RMSD
Aspirin	308.15	120.0 - 250.0	8	2.3305E-02	0.2083	3.1104E-06	-1.5646	1.8179E-05	-2.5135	2.9896E-05	0.5330	1.5669E-05
	318.15	120.0 - 250.0	8	1.8500E-02	0.2027	1.2102E-05	-1.5737	3.3978E-05	-2.5185	5.1020E-05	0.5320	1.5426E-05
	328.15	120.0 - 250.0	8	1.4384E-02	0.2032	1.6824E-05	-1.5658	3.9276E-05	-2.5032	5.7428E-05	0.5317	1.8546E-05
	Overall		**24**	**1.8729E-02**		**1.0679E-05**		**3.0478E-05**		**4.6115E-05**		**1.6547E-05**
C.I. Disperse Red 1	323.15	100.0 - 300.0	6	5.3364E-04	0.1230	3.0487E-07	0	2.3871E-06	0	2.3871E-06	0.5164	9.4965E-07
	353.15	100.0 - 300.0	6	1.8614E-04	0.1079	6.2313E-07	0	5.5200E-06	0	5.5200E-06	0.5147	1.6007E-06
	383.15	100.0 - 300.0	6	7.2276E-05	0.0753	5.2947E-07	-5.2326	1.0216E-06	0	1.3654E-05	0.5127	1.9132E-06
	Overall		**18**	**2.6402E-04**		**4.8582E-07**		**2.9762E-06**		**7.1872E-06**		**1.4879E-06**
C.I. Disperse Red 13	323.15	100.0 - 300.0	6	5.0343E-04	0.0960	4.6719E-07	0	6.2954E-06	0	6.2954E-06	0.5145	1.9769E-06
	353.15	100.0 - 300.0	6	1.6368E-04	0.0780	1.6291E-06	0	1.2223E-05	0	1.2223E-05	0.5131	3.4930E-06
	383.15	100.0 - 300.0	6	5.4274E-05	0.0498	2.4210E-06	-5.7802	8.431E-07	0	2.1491E-05	0.5113	4.7362E-06
	Overall		**18**	**2.4046E-04**		**1.5058E-06**		**6.4538E-06**		**1.3336E-05**		**3.4020E-06**
Naphthalene	308	71.9 - 321.5	87	4.2475E-02	0.0763	2.3207E-03	-1.3719	1.0075E-03	-1.8358	1.3585E-03	0.5261	4.4065E-03
	313	124.2 - 261.3	8	4.7425E-02	0.0735	2.0207E-03	-1.3738	4.1394E-04	-1.8371	7.8199E-04	0.5250	4.0770E-03
	318	98.3 - 297.0	20	4.3482E-02	0.0663	2.9952E-03	-1.3910	1.0411E-03	-1.8571	1.0187E-03	0.5241	5.5903E-03
	323	120.1 - 304.7	11	4.7870E-02	0.0598	2.8840E-03	-1.4104	3.5164E-04	-1.8817	1.5151E-03	0.5233	6.0701E-03

	328	76.9 - 278.8	27	2.6753E-02	0.0376	3.2743E-03	-1.4555	1.4692E-03	-1.9303	2.0884E-03	0.5196	6.4438E-03
	333.55	108.4 - 291.4	19	7.6370E-03	0.0065	3.4114E-03	-1.5274	6.8022E-03	-2.0232	9.7294E-03	0.5150	5.2843E-03
	338.05	151.8 - 232.2	7	7.1656E-03	0.0086	2.2334E-03	-1.5102	4.8362E-03	-1.9866	6.1357E-03	0.5143	1.5034E-03
	Overall		**179**	**3.1830E-02**		**2.7343E-03**		**2.2745E-03**		**3.2325E-03**		**4.7679E-03**
Xanthene	308.15	80.0 - 240.0	7	2.6529E-02	0.0634	4.3800E-04	-2.1168	8.2210E-04	-3.3521	1.4773E-03	0.5190	1.2110E-03
	328.15	90.0 - 210.0	6	1.1248E-02	0.0547	4.3815E-04	-2.1187	1.7695E-04	-3.3331	5.1028E-04	0.5168	9.9327E-04
	Overall		**13**	**1.8888E-02**		**4.3807E-04**		**4.9953E-04**		**9.9378E-04**		**1.1021E-03**
Xanthone	308.15	120.0 - 300.0	8	1.9691E-02	0.1537	1.8913E-05	-1.8418	4.3421E-05	-2.9887	7.4521E-05	0.5246	5.0180E-05
	328.15	120.0 - 300.0	8	1.2611E-02	0.1546	4.5376E-05	-1.8335	1.6607E-05	-2.9754	3.8703E-05	0.5241	8.8512E-05
	Overall		**16**	**1.6151E-02**		**3.2145E-05**		**3.0014E-05**		**5.6612E-05**		**6.9346E-05**
Overall			**268**	**1.4350E-02**		**5.3619E-04**		**4.7400E-04**		**7.2493E-04**		**9.9347E-04**

Table A.2: Modeling results for solids solubility in SC – CO_2 using the PR – EOS with the energy and covolume binary interaction parameters and WMA coefficients by minimizing RMSD.

Solid Compound	T (K)	P (bar)	N	Pure Predictive	LB (k_{ij} , l_{ij})			WH (k_{ij} , l_{ij})			MADAR-1 (k_{ij} , l_{ij})			WMA ($w_{ij,a}$, $w_{ij,b}$)		
				AARD (%)	k_{ij}	l_{ij}	AARD (%)	k_{ij}	l_{ij}	AARD (%)	k_{ij}	l_{ij}	AARD (%)	$w_{ij,a}$	$w_{ij,b}$	AARD (%)
Aspirin	308.15	120.0 - 250.0	8	2.3305E-02	0.2241	0.0381	1.7409E-06	-0.4046	0.2112	1.7413E-06	-0.4058	0.3019	1.7419E-06	0.5226	0.4041	1.7409E-06
	318.15	120.0 - 250.0	8	1.8500E-02	0.2506	0.1187	4.2571E-06	-0.1384	0.2774	4.2579E-06	-0.1377	0.3608	4.2573E-06	0.5253	0.4356	4.2572E-06
	328.15	120.0 - 250.0	8	1.4384E-02	0.2535	0.1282	1.0048E-05	-0.1096	0.2852	1.0048E-05	-0.1136	0.3666	1.0050E-05	0.5255	0.4392	1.0048E-05
	Overall		**24**	**1.8729E-02**			**5.3488E-06**			**5.3492E-06**			**5.3499E-06**			**5.3488E-06**

C.I. Disperse Red 1	323.15	100.0 - 300.0	6	5.3364E-04	0.1882	0.1499	1.3706E-07	0	0	2.3871E-06	0	0	2.3871E-06	0.5092	0.3929	1.3706E-07
	353.15	100.0 - 300.0	6	1.8614E-04	0.0197	-0.2126	7.1761E-08	0	0	5.5200E-06	0	0	5.5200E-06	0.5010	0.2692	7.1778E-08
	383.15	100.0 - 300.0	6	7.2276E-05	0.0376	-0.0937	3.7742E-07	-1.2932	0.3353	9.5311E-07	0	0	1.3654E-05	0.5009	0.2943	7.0054E-07
	Overall		**18**	**2.6402E-04**			**1.9541E-07**			**2.9534E-06**			**7.1872E-06**			**3.0313E-07**
C.I. Disperse Red 13	323.15	100.0 - 300.0	6	5.0343E-04	0.0802	-0.0357	4.6226E-07	0	0	6.2954E-06	0	0	6.2954E-06	0.5015	0.2898	8.3625E-07
	353.15	100.0 - 300.0	6	1.6368E-04	-0.0154	-0.2218	9.3459E-07	0	0	1.2223E-05	0	0	1.2223E-05	0.4984	0.2483	9.8432E-07
	383.15	100.0 - 300.0	6	5.4274E-05	-0.0964	-0.3589	1.1292E-07	-0.3770	0.4821	4.1854E-06	0	0	2.1491E-05	0.4958	0.2223	8.5635E-07
	Overall		**18**	**2.4046E-04**			**5.0325E-07**			**7.5678E-06**			**1.3336E-05**			**8.9231E-07**
Naphthalene	308	71.9 - 321.5	87	4.2475E-02	-0.0118	-0.1913	1.0045E-03	-1.4065	-0.0057	1.0045E-03	-1.4073	0.0626	1.0045E-03	0.4983	0.3294	1.0045E-03
	313	124.2 - 261.3	8	4.7425E-02	-0.0176	-0.2027	3.7241E-04	-1.4664	-0.0153	3.7241E-04	-1.4678	0.0536	3.7245E-04	0.4975	0.3248	3.7241E-04
	318	98.3 - 297.0	20	4.3482E-02	-0.0369	-0.2296	8.7114E-04	-1.6270	-0.0380	8.7114E-04	-1.6291	0.0323	8.7116E-04	0.4948	0.3138	8.7114E-04
	323	120.1 - 304.7	11	4.7870E-02	-0.0241	-0.1824	3.4984E-04	-1.3997	0.0018	3.4986E-04	-1.4012	0.0695	3.4989E-04	0.4966	0.3330	3.4984E-04
	328	76.9 - 278.8	27	2.6753E-02	-0.0435	-0.1827	1.4688E-03	-1.4470	0.0014	1.4688E-03	-1.4213	0.0733	1.4713E-03	0.4939	0.3330	1.4688E-03
	333.55	108.4 - 291.4	19	7.6370E-03	0.0298	0.0527	3.1487E-03	-0.4592	0.2002	3.1487E-03	-0.4615	0.2542	3.1488E-03	0.5041	0.4288	3.1487E-03
	338.05	151.8 - 232.2	7	7.1656E-03	0.0678	0.1427	9.6072E-04	-0.1500	0.2758	9.6077E-04	-0.1477	0.3256	9.6073E-04	0.5094	0.4655	9.6072E-04
	Overall		**179**	**3.1830E-02**			**1.1680E-03**			**1.1680E-03**			**1.1684E-03**			**1.1680E-03**
Xanthene	308.15	80.0 - 240.0	7	2.6529E-02	0.0461	-0.0407	4.1180E-04	-1.0825	0.1501	4.1182E-04	-1.0790	0.2566	4.1180E-04	0.5046	0.3706	4.1180E-04
	328.15	90.0 - 210.0	6	1.1248E-02	-0.0187	-0.1901	1.5771E-04	-1.9002	0.0292	1.5771E-04	-1.9018	0.1500	1.5771E-04	0.4982	0.3129	1.5771E-04
	Overall		**13**	**1.8888E-02**			**2.8476E-04**			**2.8477E-04**			**2.8476E-04**			**2.8476E-04**
Xanthone	308.15	120.0 - 300.0	8	1.9691E-02	0.1506	-0.0079	1.8867E-05	-0.7407	0.1782	1.8867E-05	-0.7404	0.2816	1.8867E-05	0.5134	0.3828	1.8867E-05
	328.15	120.0 - 300.0	8	1.2611E-02	0.0641	-0.2318	1.6576E-05	-1.8647	-0.0044	1.6576E-05	-1.8643	0.1220	1.6576E-05	0.5057	0.2965	1.6576E-05

	Overall	**16**	**1.6151E-02**		**1.7721E-05**		**1.7721E-05**		**1.7721E-05**		**1.7721E-05**
Overall		**268**	**1.4350E-02**		**2.4609E-04**		**2.4773E-04**		**2.4946E-04**		**2.4617E-04**

A.1 Solubility of Solid Compounds in Supercritical CO_2 Using Combining Rules and Weighting Matrix Approach

A.1.1 Solubility of Aspirin Using Combining Rules and Weighting Matrix Approach

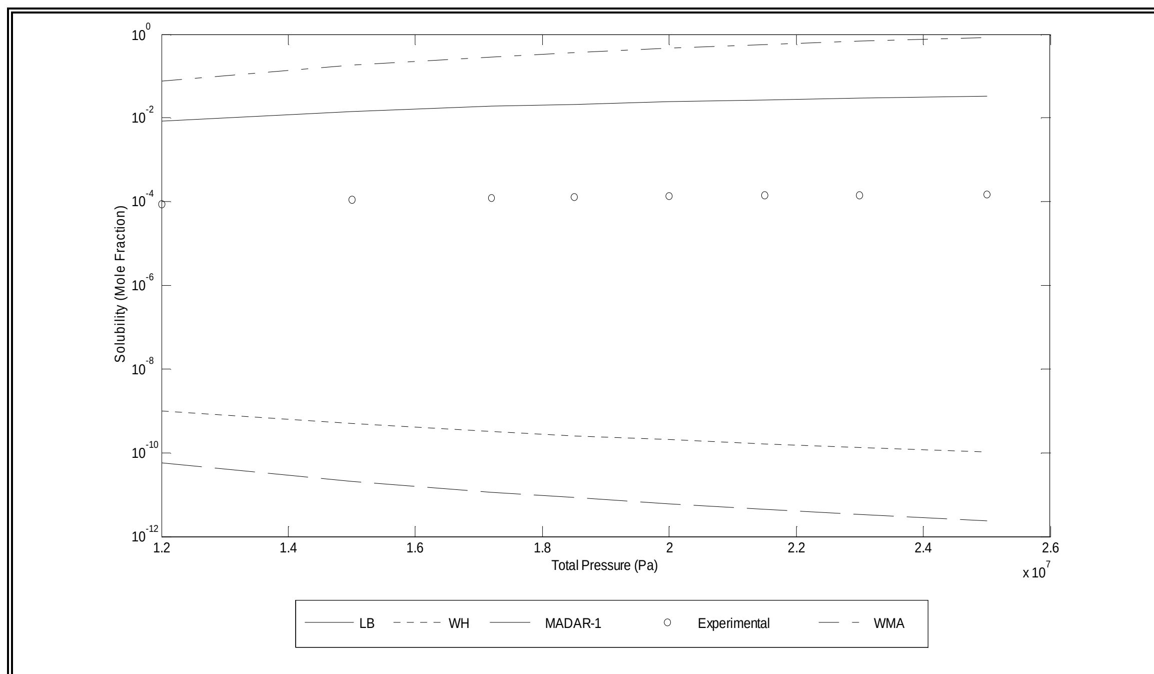

Figure A.1.1.1: Solubility of Aspirin in SC – CO_2 at 308.15 K (Pure Predictive)

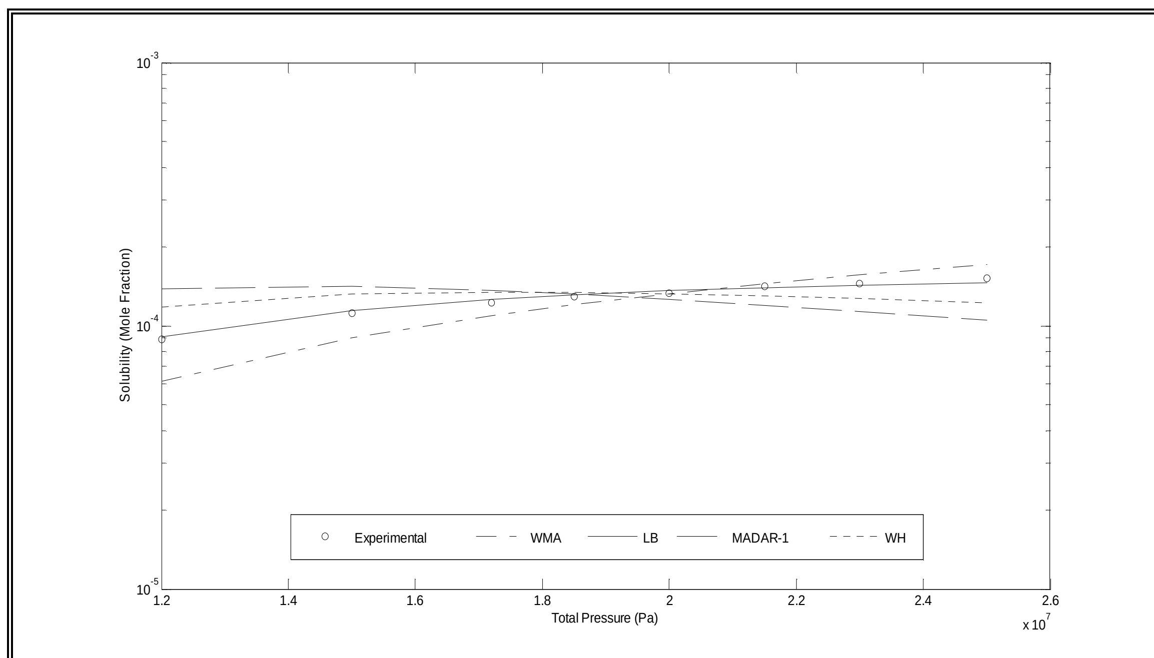

Figure A.1.1.2: Solubility of Aspirin in SC – CO_2 at 308.15 K with (a) parameters only

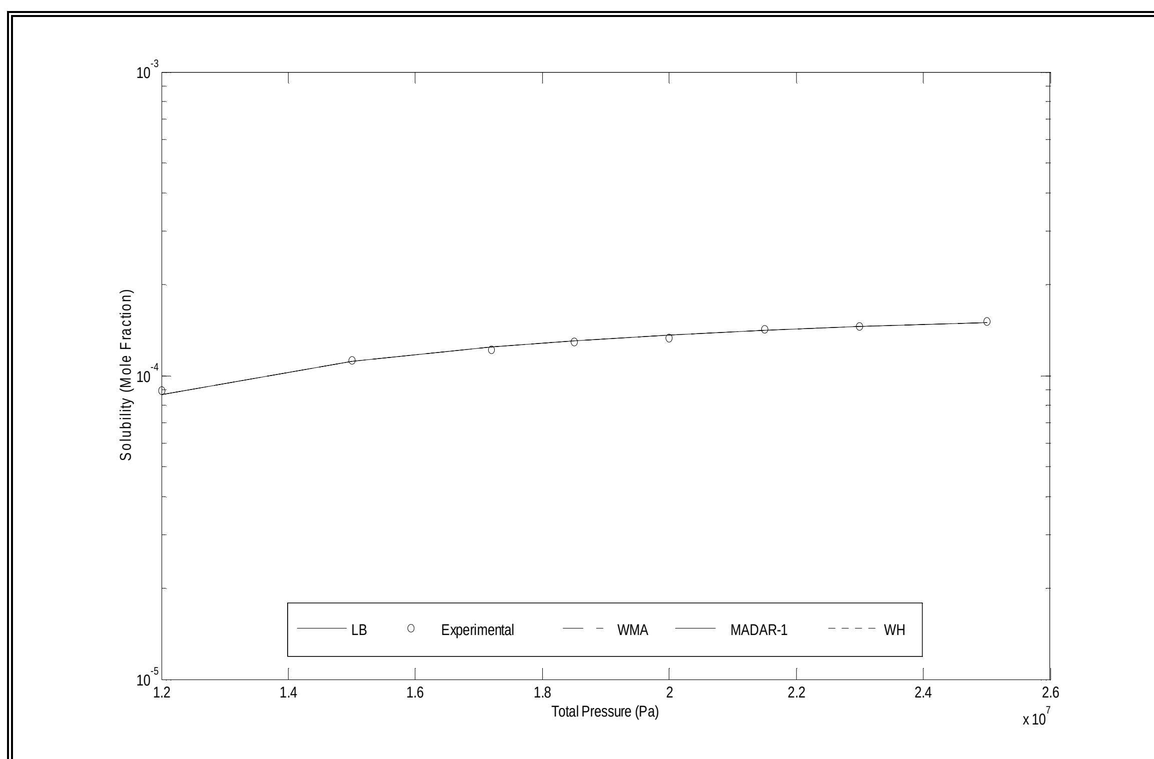

Figure A.1.1.3: Solubility of Aspirin in SC – CO_2 at 308.15 K with (a) & (b) parameters

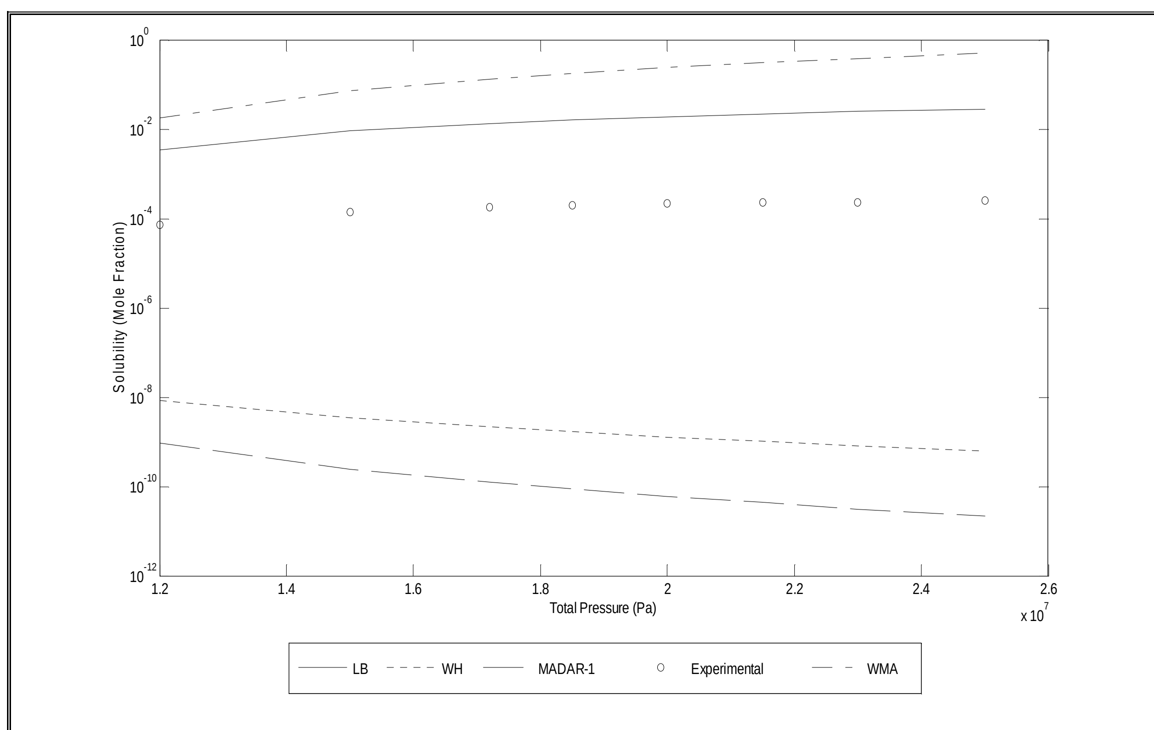

Figure A.1.1.4: Solubility of Aspirin in SC – CO_2 at 318.15 K (Pure Predictive)

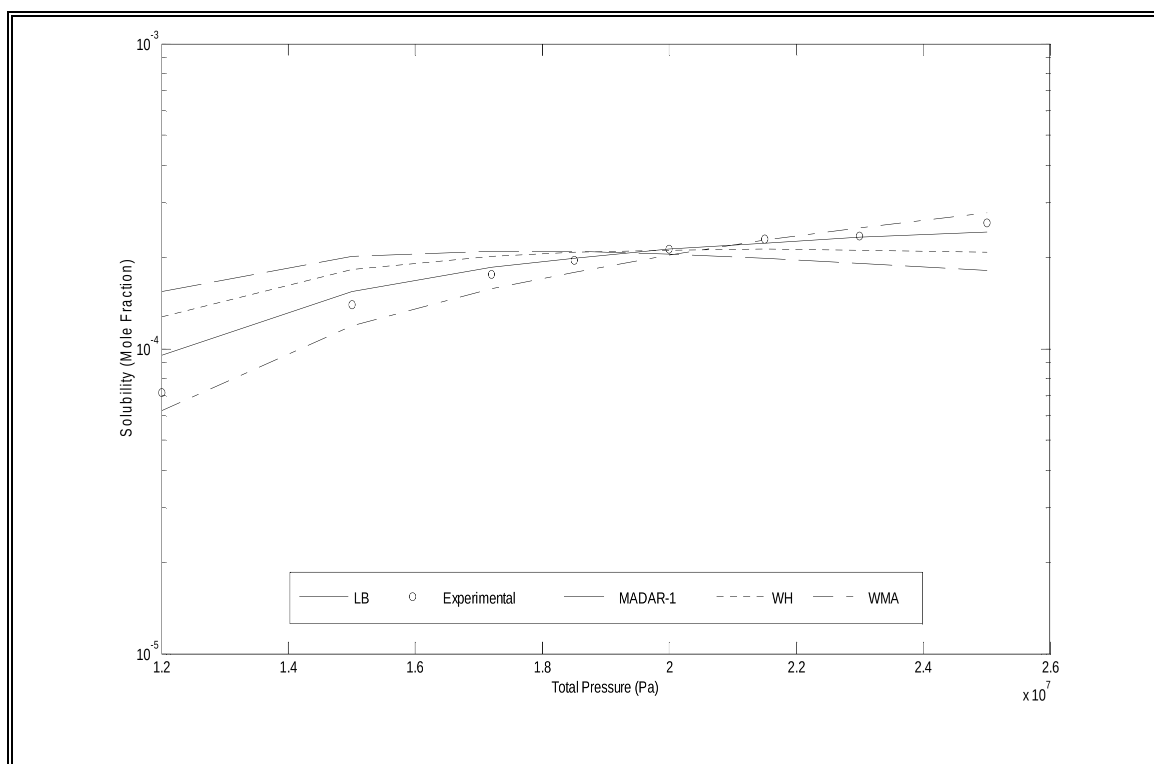

Figure A.1.1.5: Solubility of Aspirin in SC – CO_2 at 318.15 K with (a) parameters only

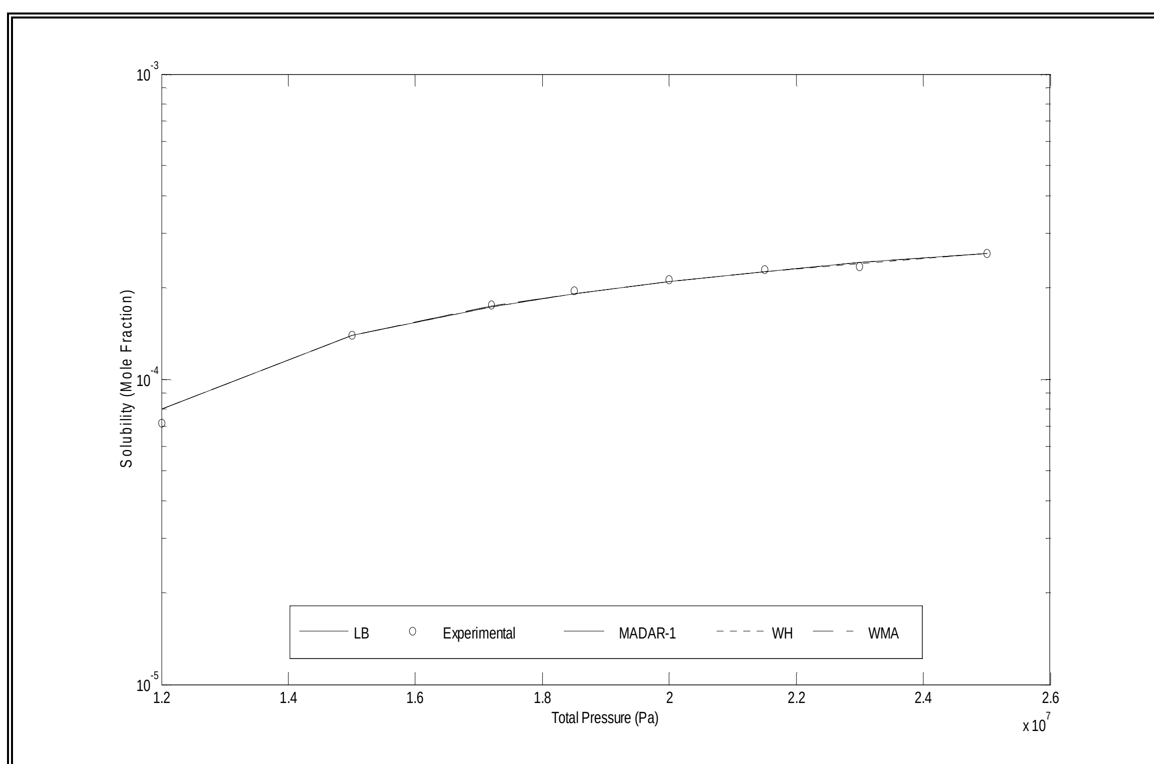

Figure A.1.1.6: Solubility of Aspirin in SC – CO_2 at 318.15 K with (a) & (b) parameters

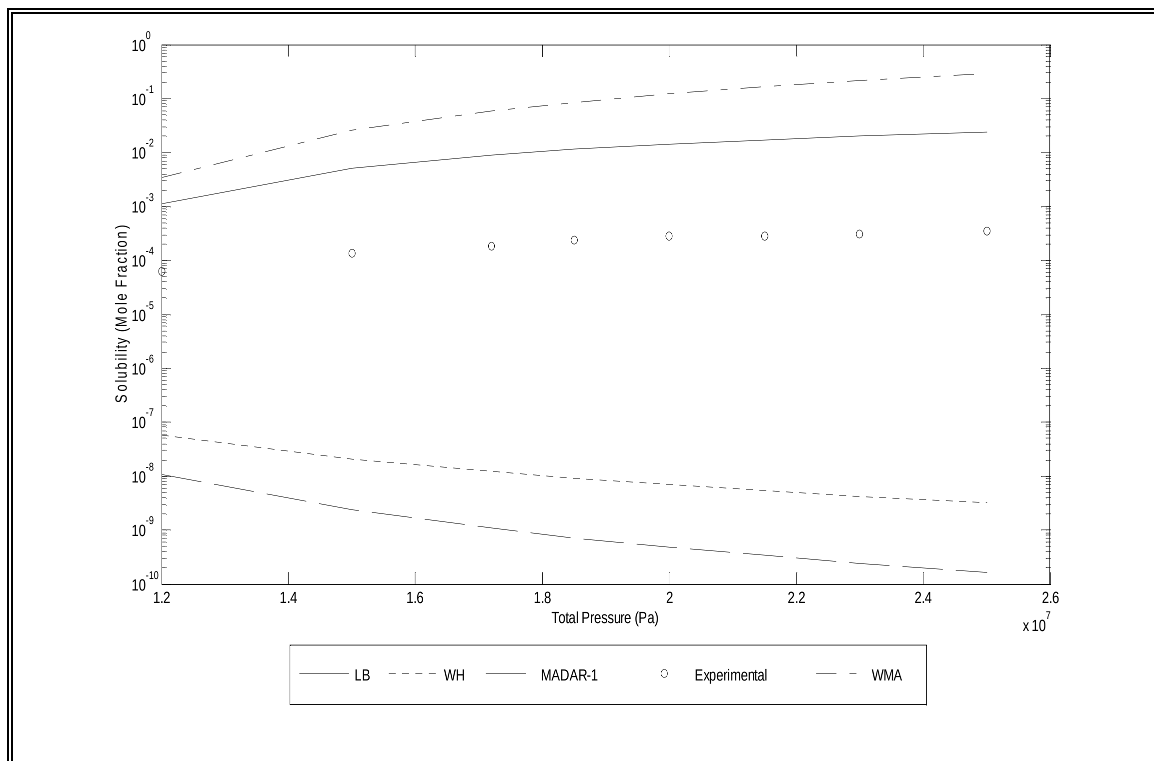

Figure A.1.1.7: Solubility of Aspirin in SC – CO_2 at 328.15 K (Pure Predictive)

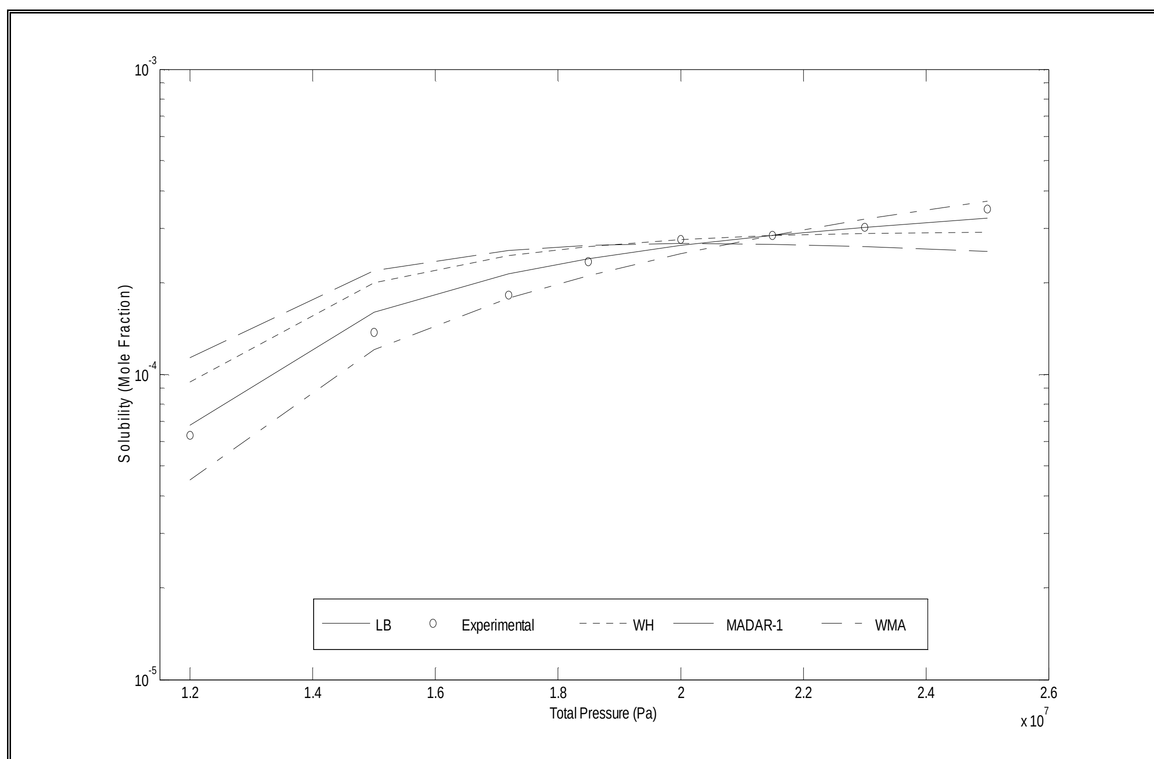

Figure A.1.1.8: Solubility of Aspirin in SC – CO_2 at 328.15 K with (a) parameters only

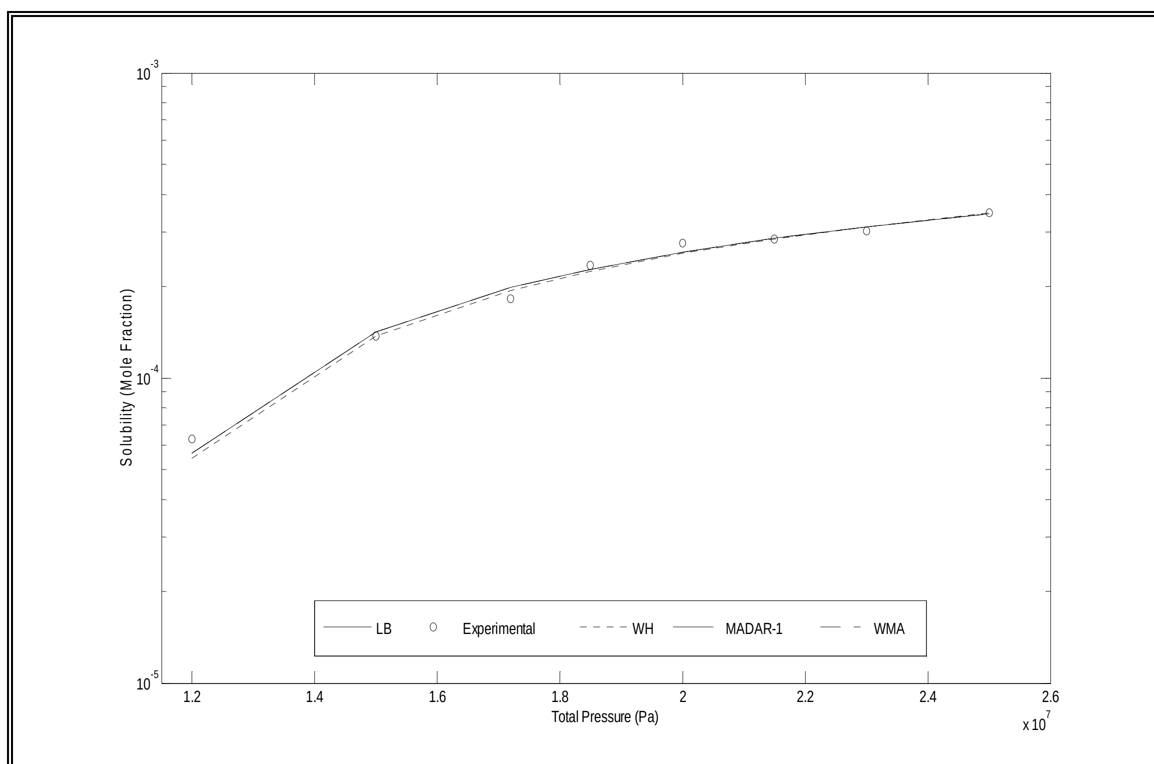

Figure A.1.1.9: Solubility of Aspirin in SC – CO_2 at 328.15 K with (a) & (b) parameters

A.1.2 Solubility of C.I. Disperse Red 1 Using Combining Rules and Weighting Matrix Approach

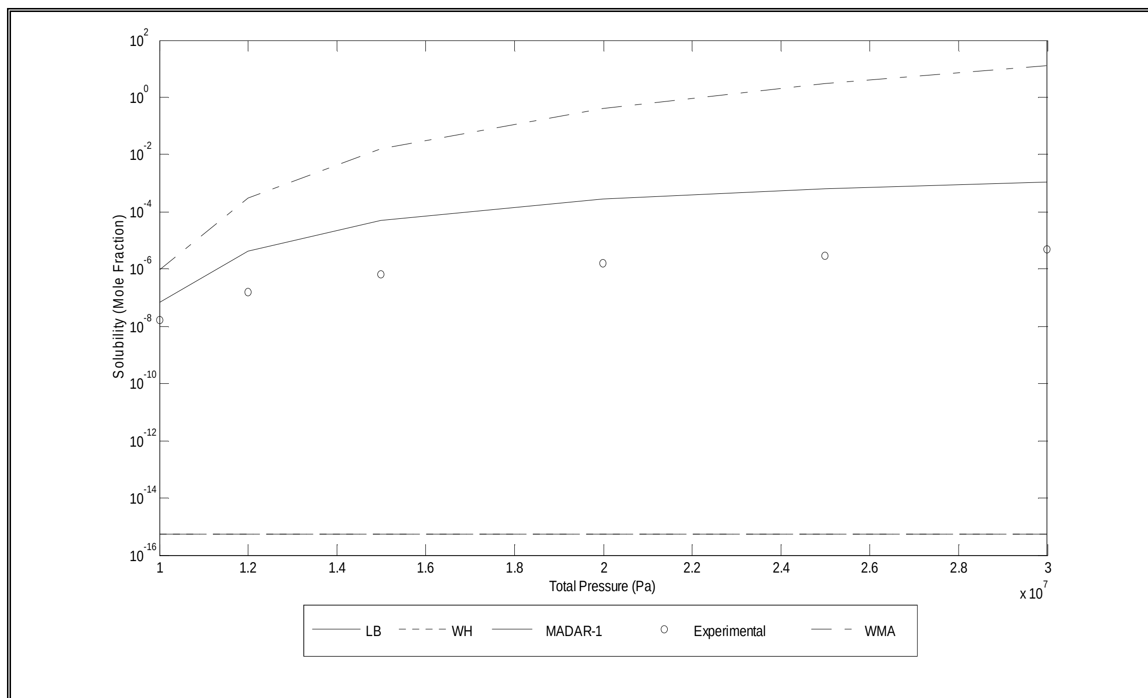

Figure A.1.2.1: Solubility of C.I. Disperse Red 1 in SC – CO_2 at 323.15 K (Pure Predictive)

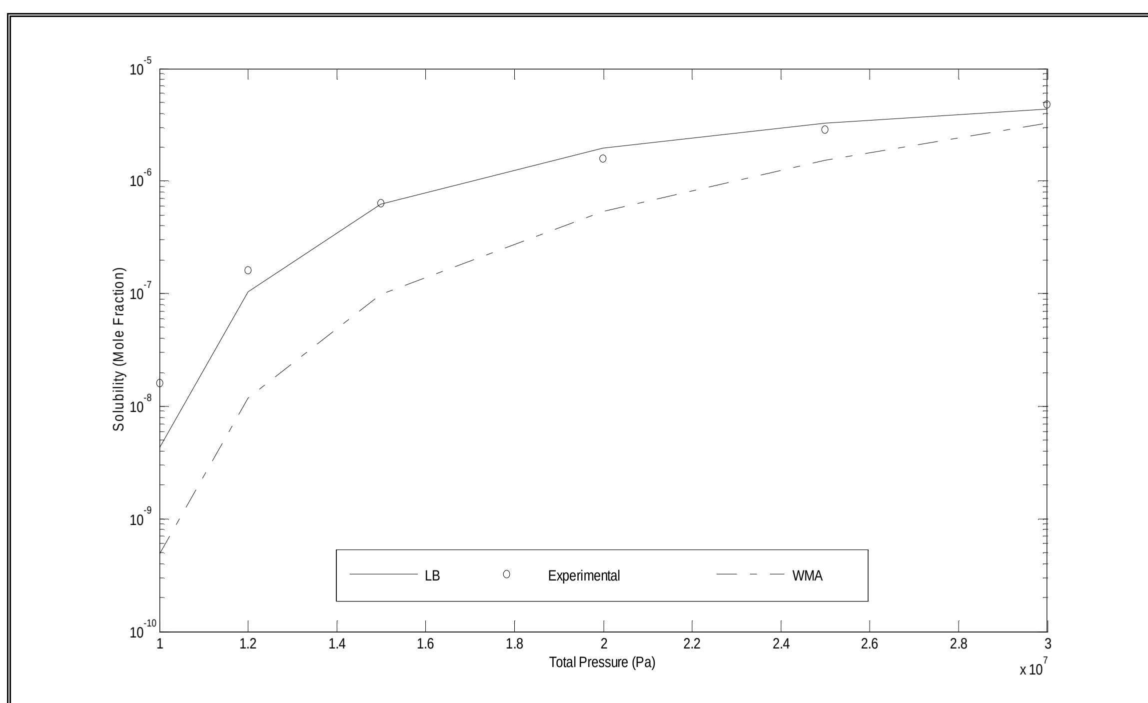

Figure A.1.2.2: Solubility of C.I. Disperse Red 1 in SC – CO_2 at 323.15 K with (a) parameters only

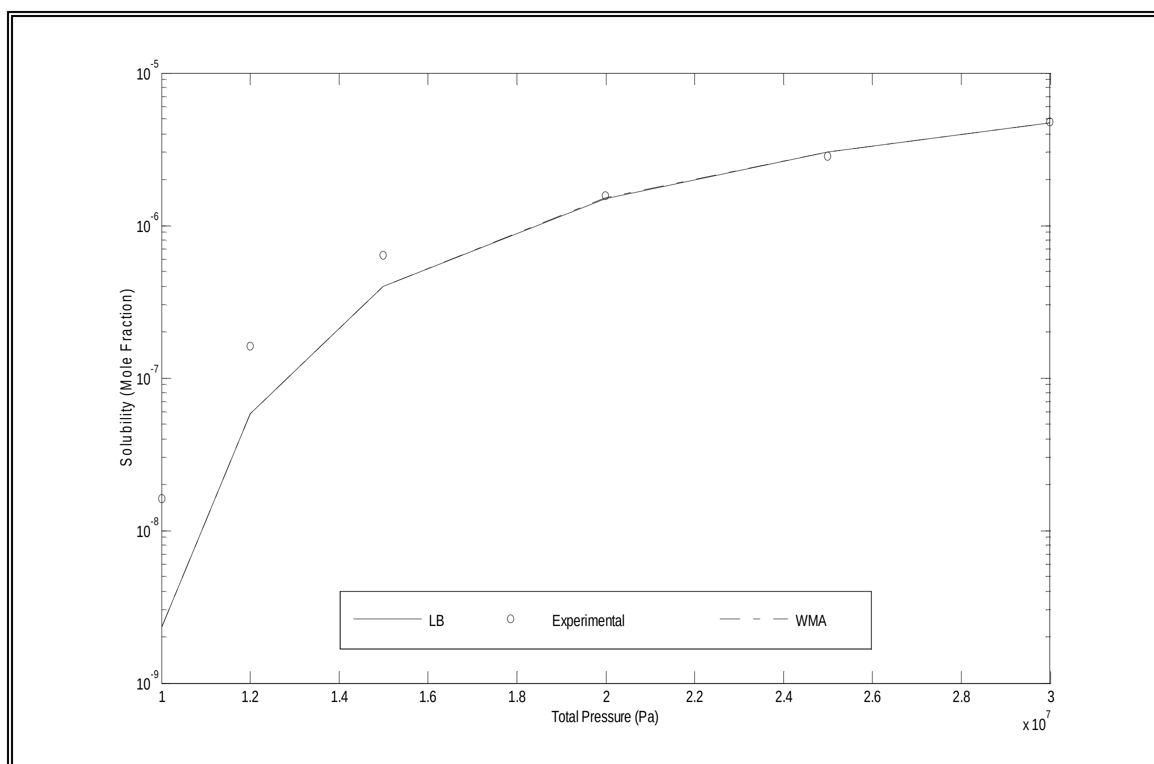

Figure A.1.2.3: Solubility of C.I. Disperse Red 1 in SC – CO_2 at 323.15 K with (a) & (b) parameters

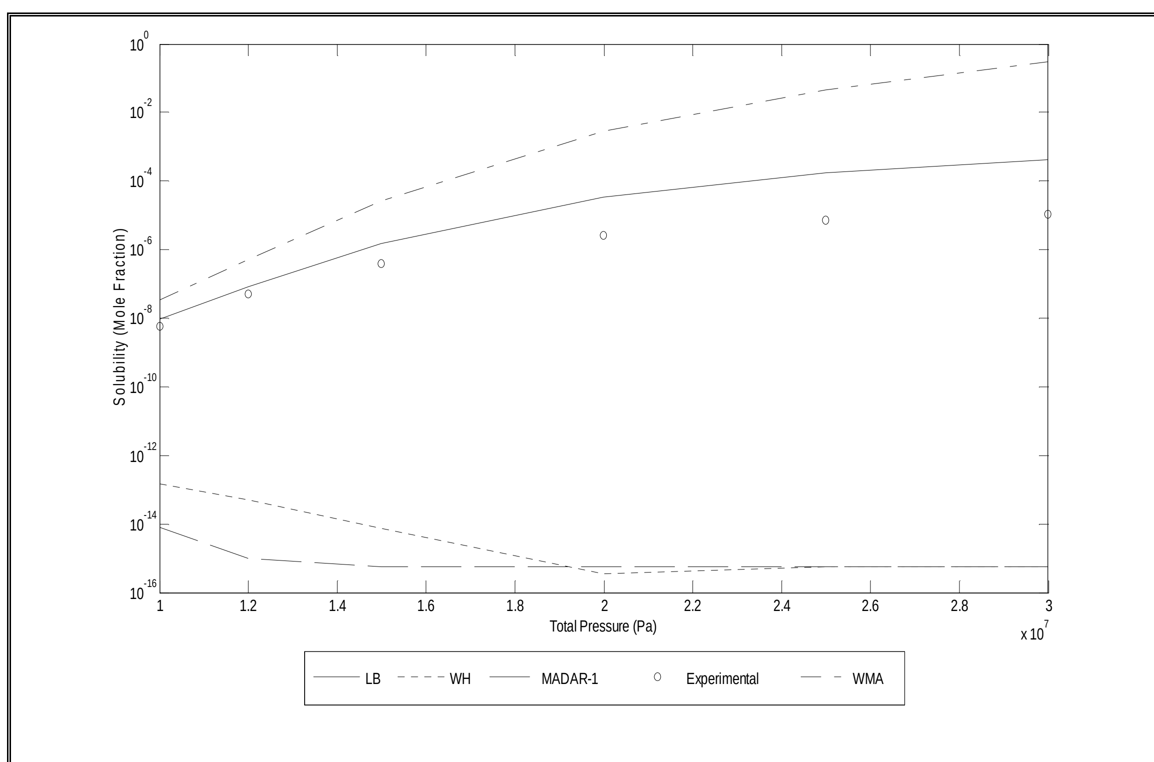

Figure A.1.2.4: Solubility of C.I. Disperse Red 1 in SC – CO_2 at 353.15 K (Pure Predictive)

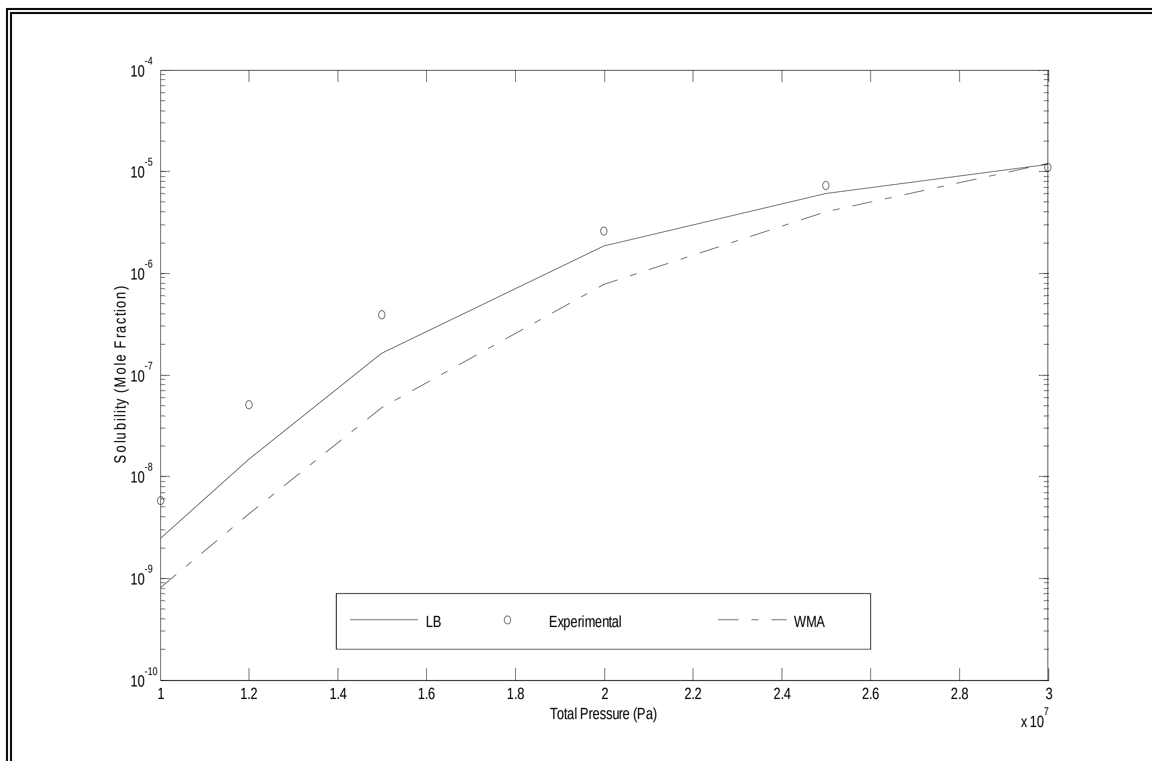

Figure A.1.2.5: Solubility of C.I. Disperse Red 1 in SC – CO_2 at 353.15 K with (a) parameters only

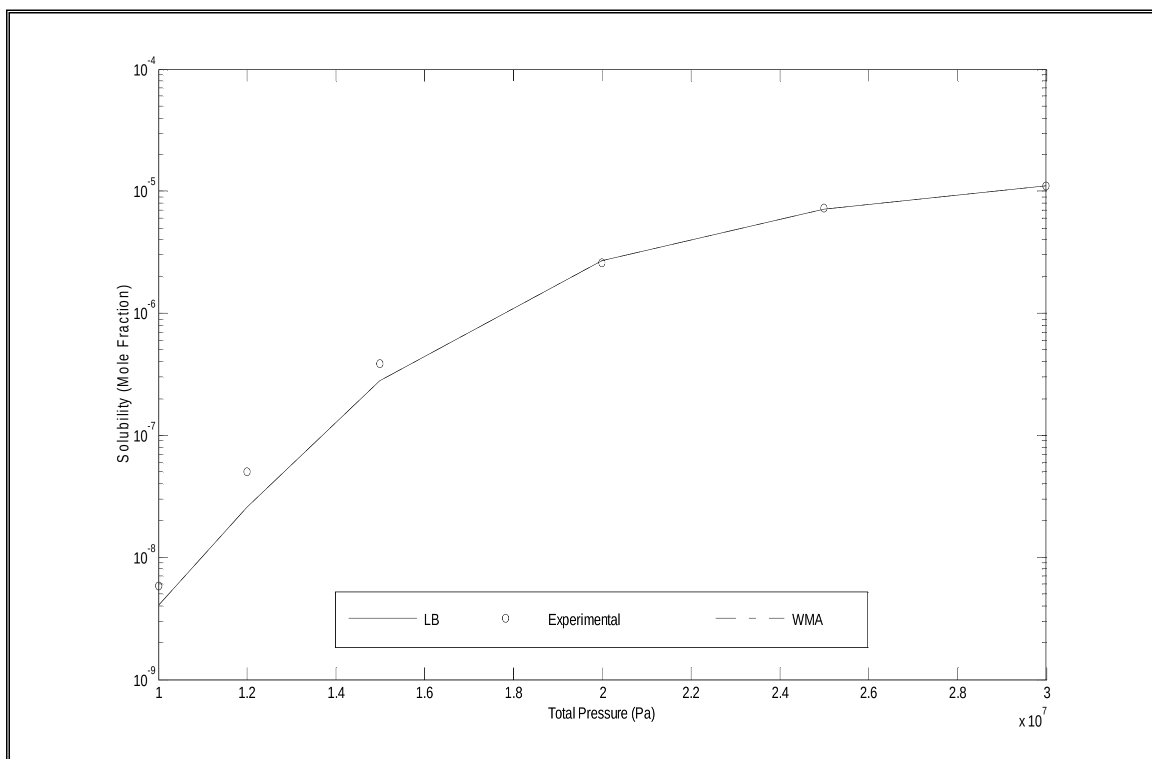

Figure A.1.2.6: Solubility of C.I. Disperse Red 1 in SC – CO_2 at 353.15 K with (a) & (b) parameters

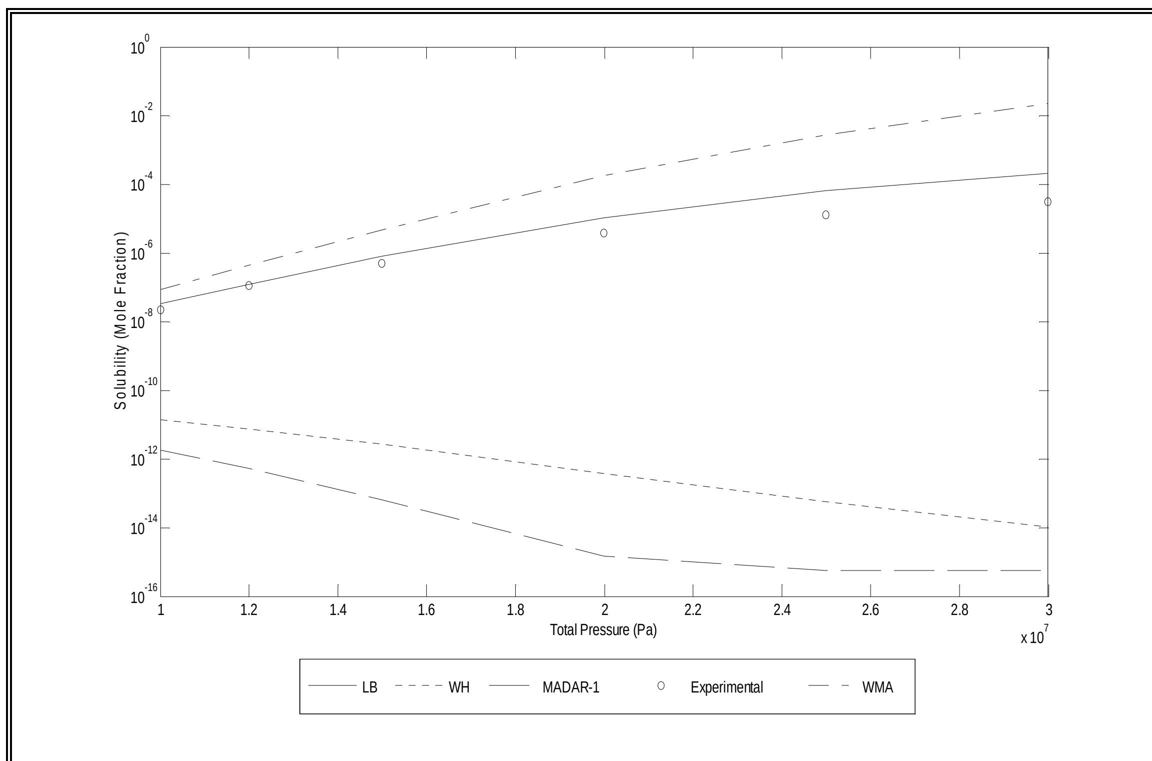

Figure A.1.2.7: Solubility of C.I. Disperse Red 1 in SC – CO_2 at 383.15 K (Pure Predictive)

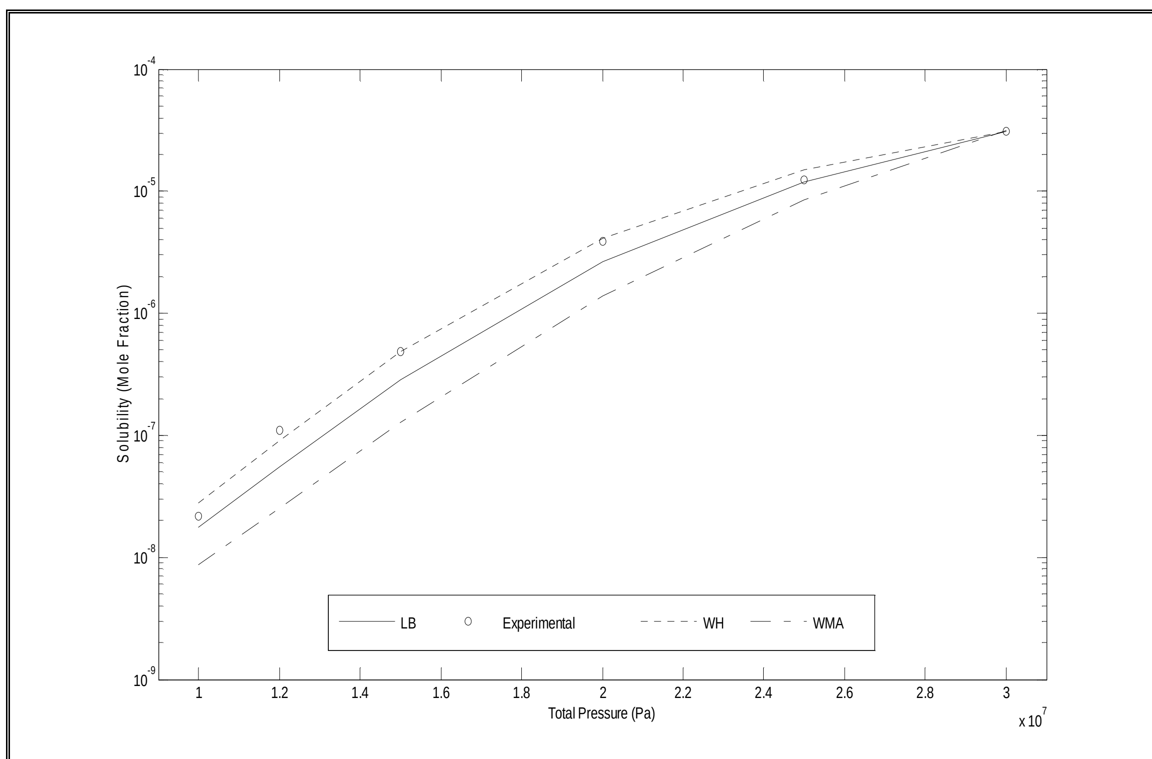

Figure A.1.2.8: Solubility of C.I. Disperse Red 1 in SC – CO_2 at 383.15 K with (a) parameters only

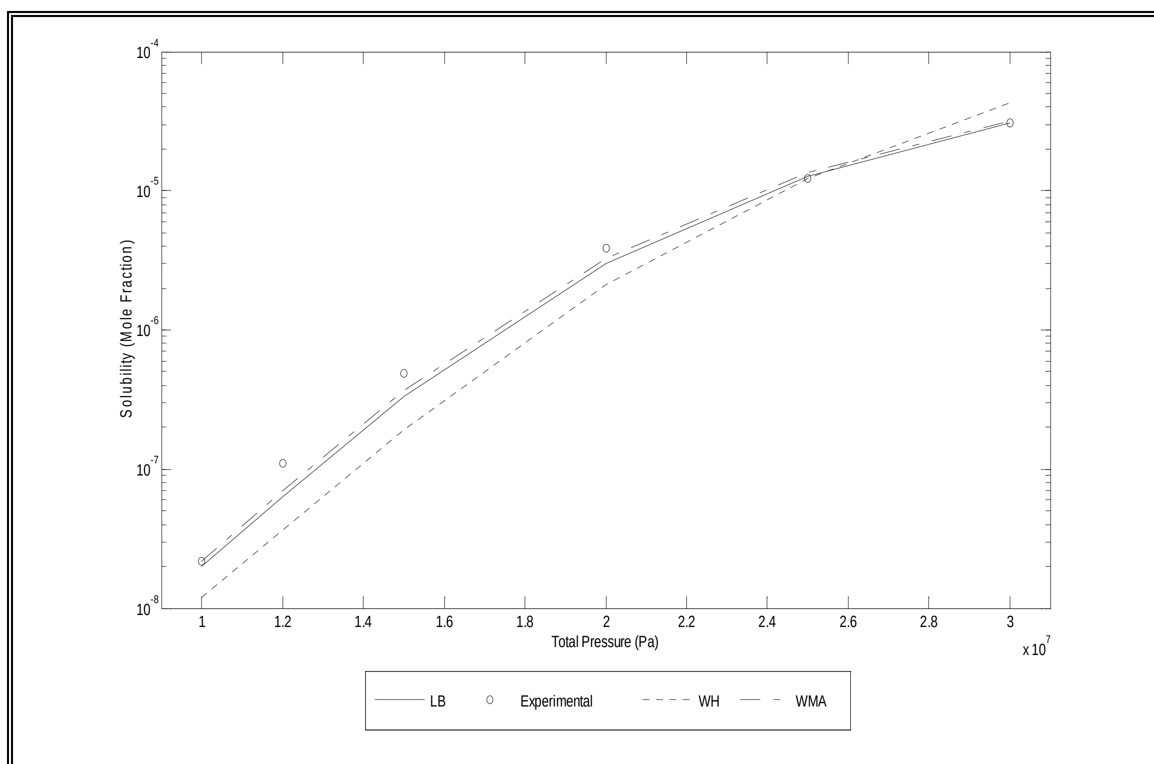

Figure A.1.2.9: Solubility of C.I. Disperse Red 1 in SC – CO_2 at 383.15 K with (a) & (b) parameters

A.1.3 Solubility of C.I. Disperse Red 13 Using Combining Rules and Weighting Matrix Approach

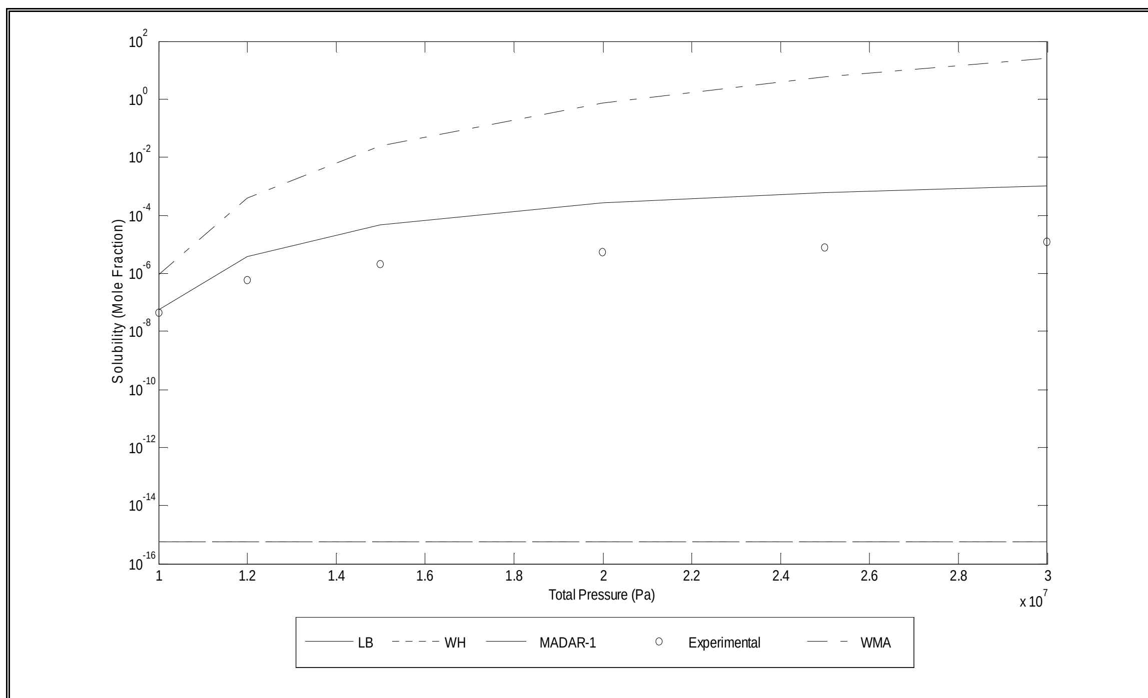

Figure A.1.3.1: Solubility of C.I. Disperse Red 13 in SC – CO_2 at 323.15 K (Pure Predictive)

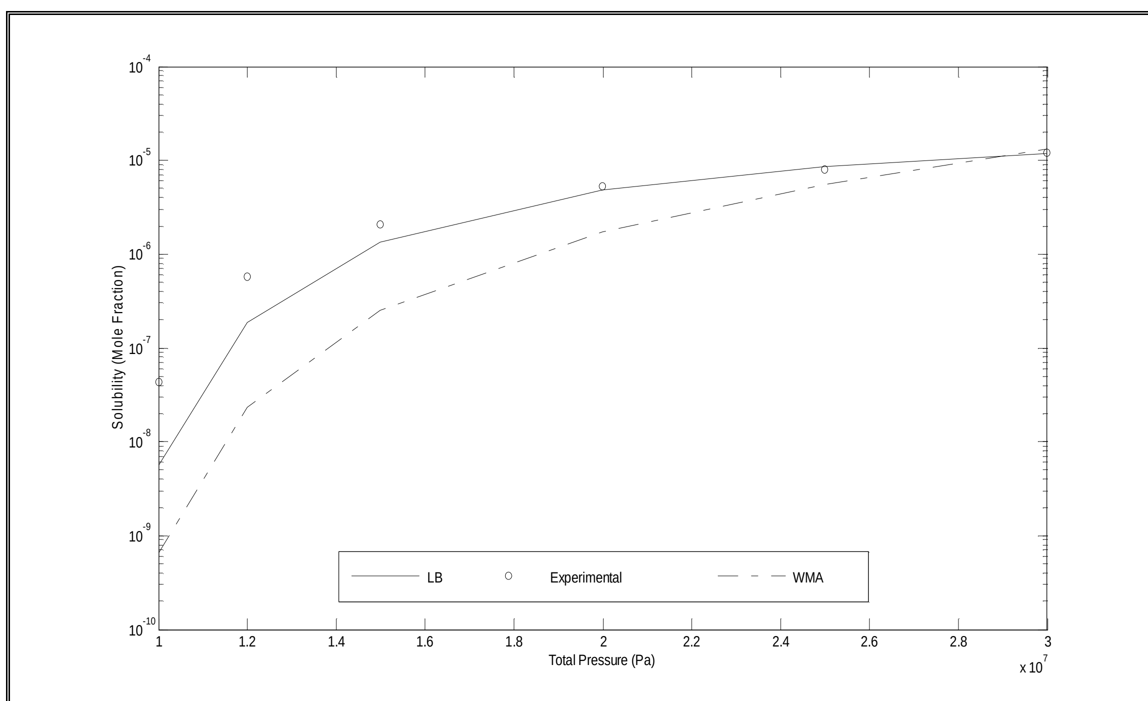

Figure A.1.3.2: Solubility of C.I. Disperse Red 13 in SC – CO_2 at 323.15 K with (a) parameters only

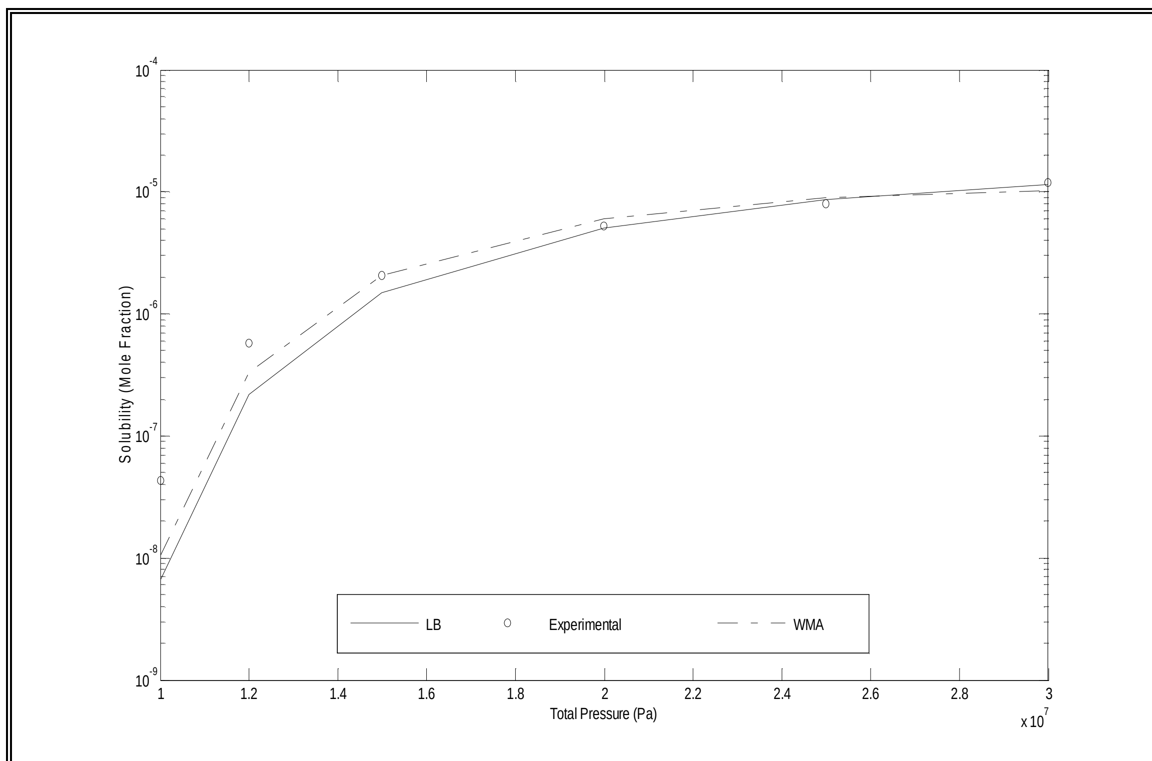

Figure A.1.3.3: Solubility of C.I. Disperse Red 13 in SC – CO_2 at 323.15 K with (a) & (b) parameters

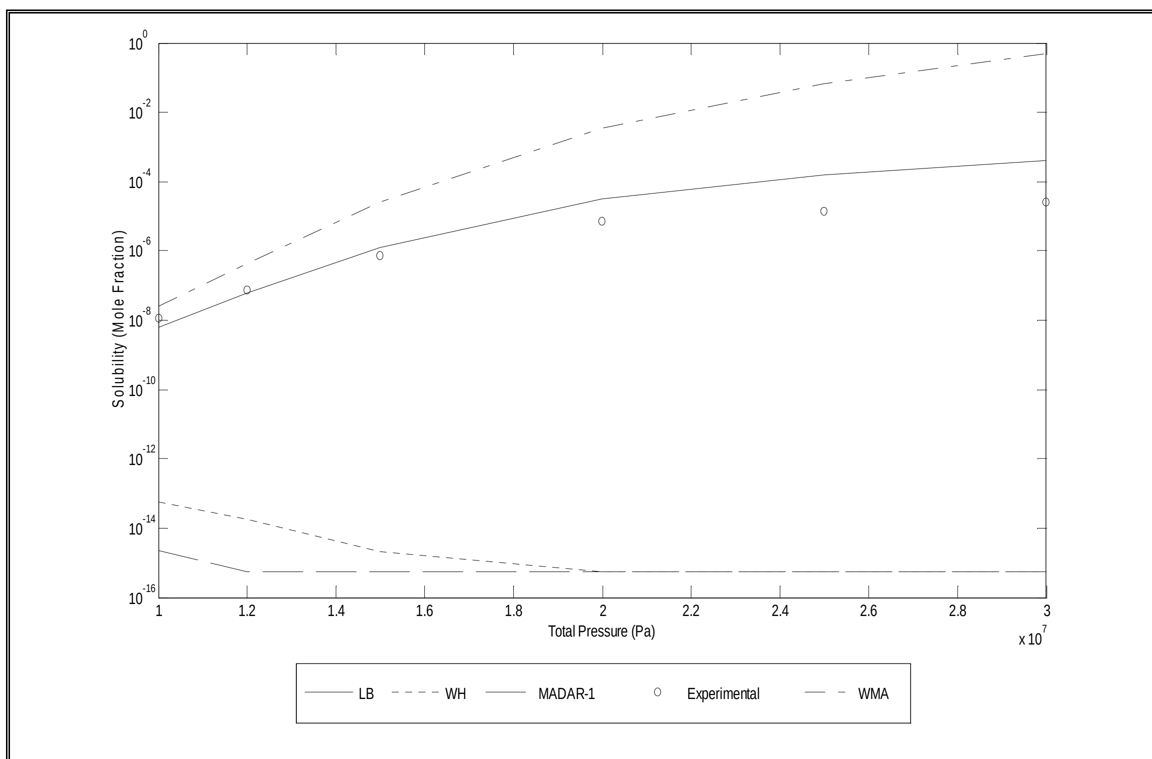

Figure A.1.3.4: Solubility of C.I. Disperse Red 13 in SC – CO_2 at 353.15 K (Pure Predictive)

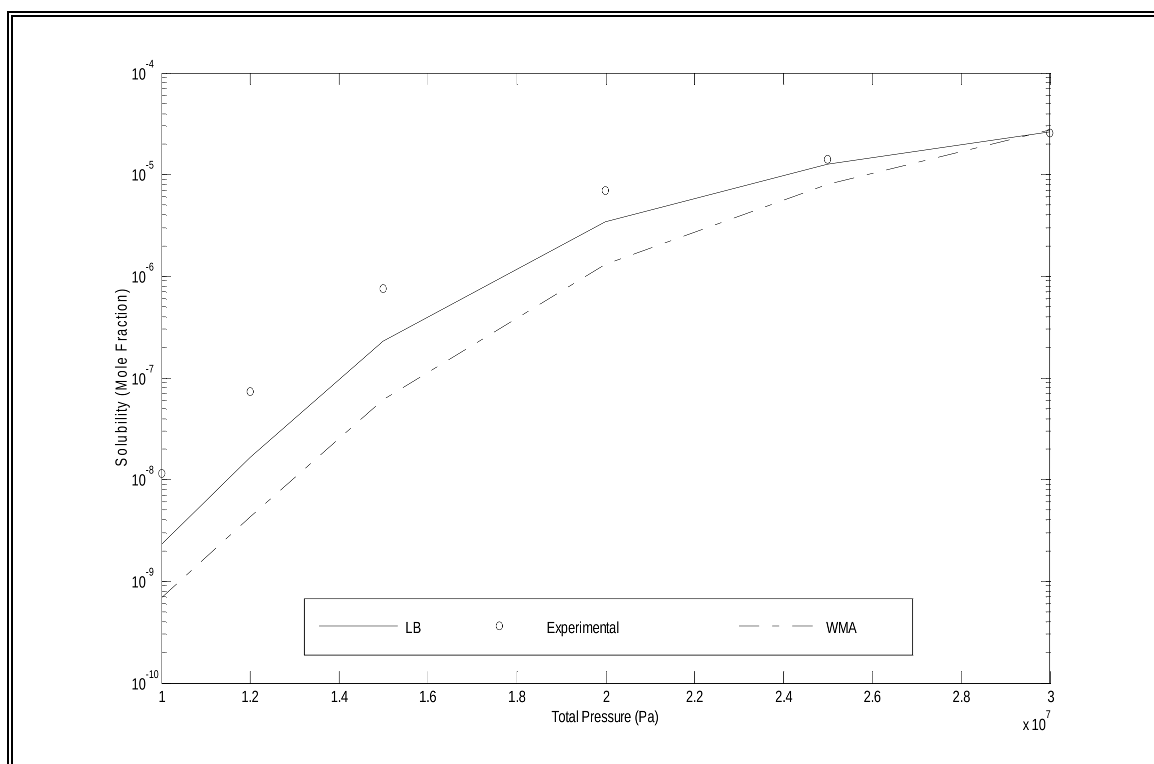

Figure A.1.3.5: Solubility of C.I. Disperse Red 13 in SC – CO_2 at 353.15 K with (a) parameters only

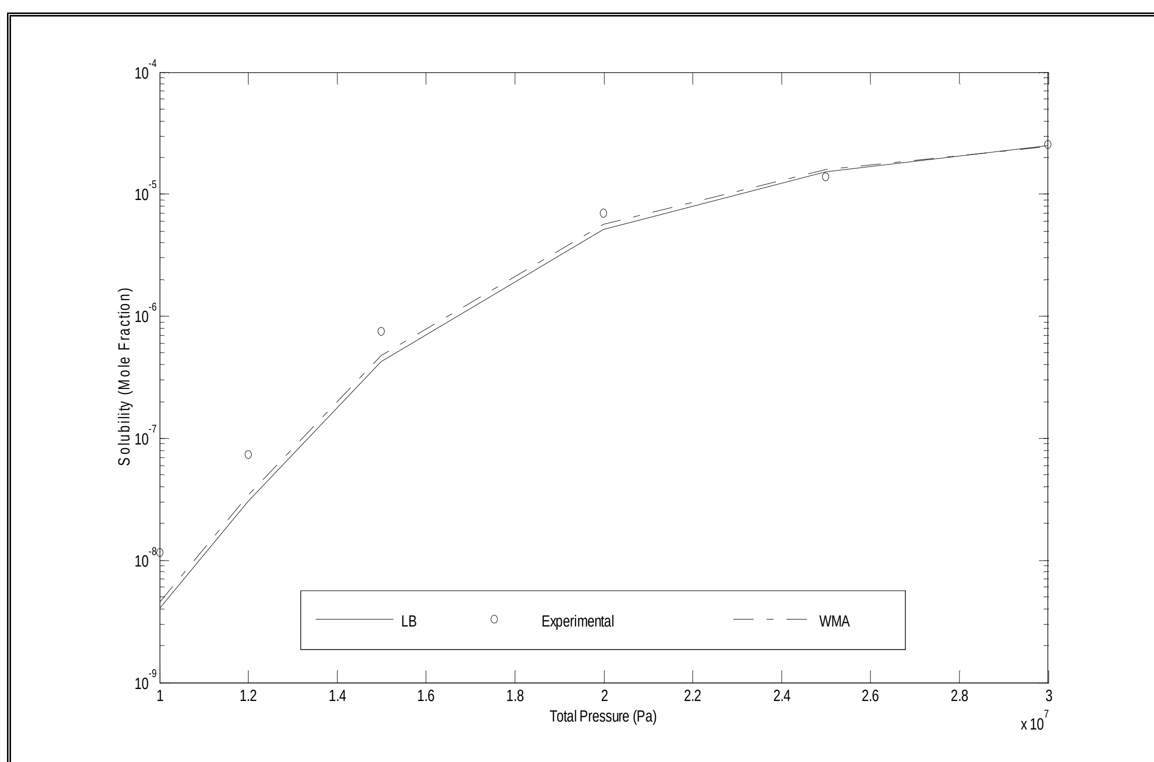

Figure A.1.3.6: Solubility of C.I. Disperse Red 13 in SC – CO_2 at 353.15 K with (a) & (b) parameters

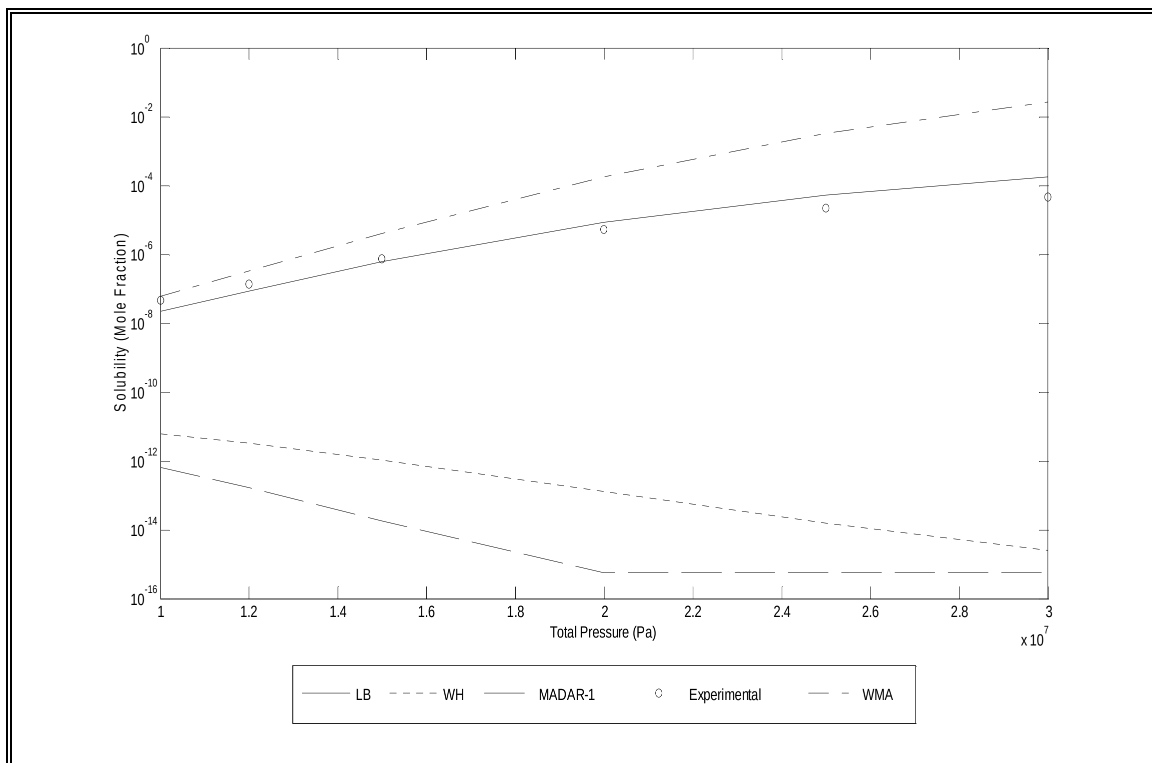

Figure A.1.3.7: Solubility of C.I. Disperse Red 13 in SC – CO_2 at 383.15 K (Pure Predictive)

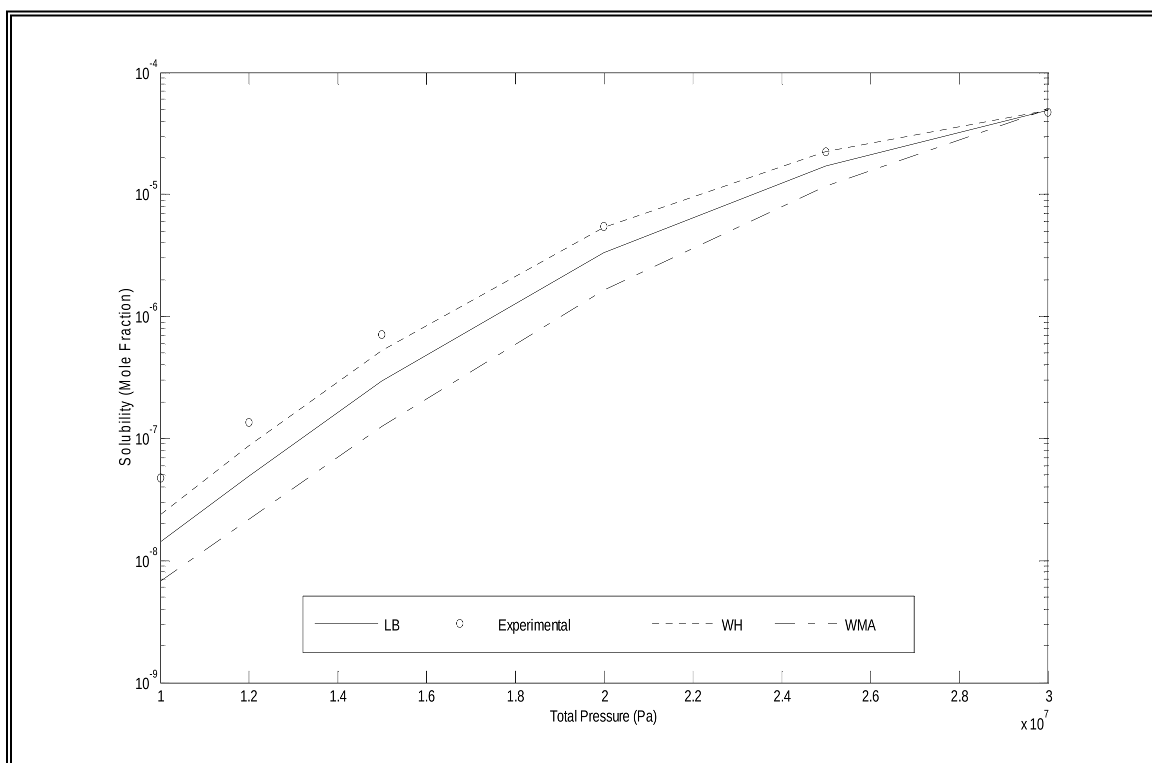

Figure A.1.3.8: Solubility of C.I. Disperse Red 13 in SC – CO_2 at 383.15 K with (a) parameters only

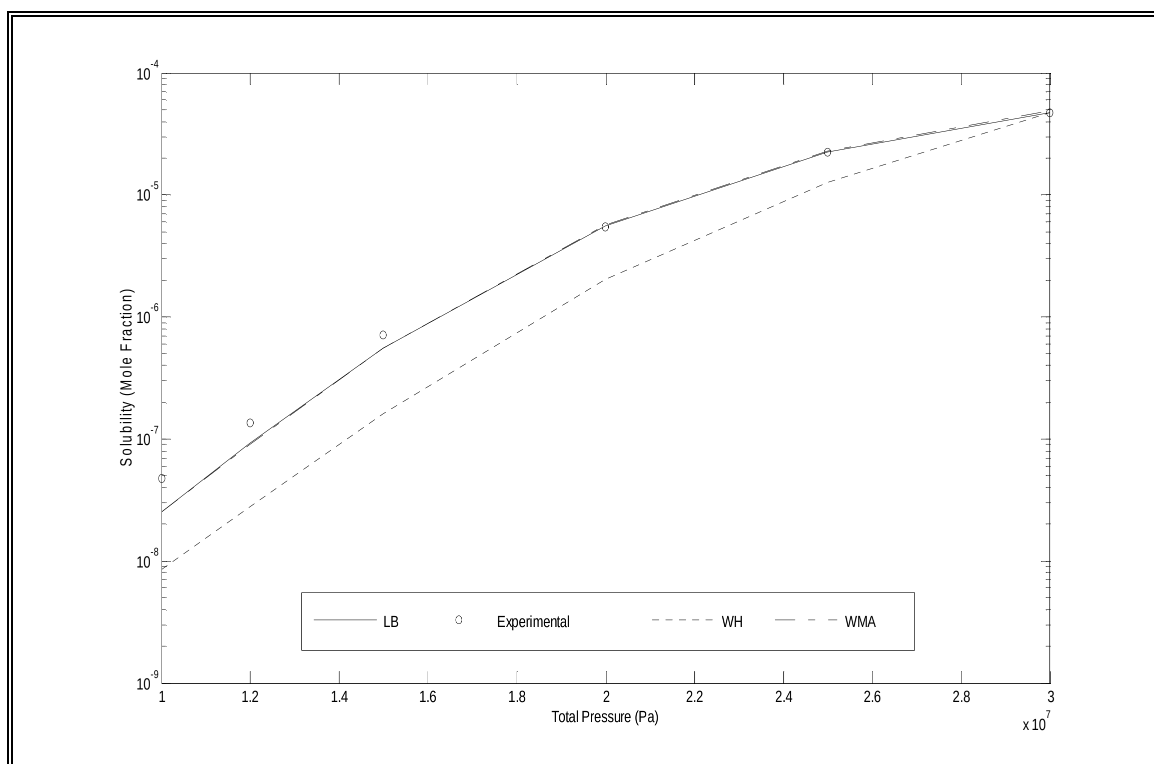

Figure A.1.3.9: Solubility of C.I. Disperse Red 13 in SC – CO_2 at 383.15 K with (a) & (b) parameters

A.1.4 Solubility of Naphthalene Using Combining Rules and Weighting Matrix Approach

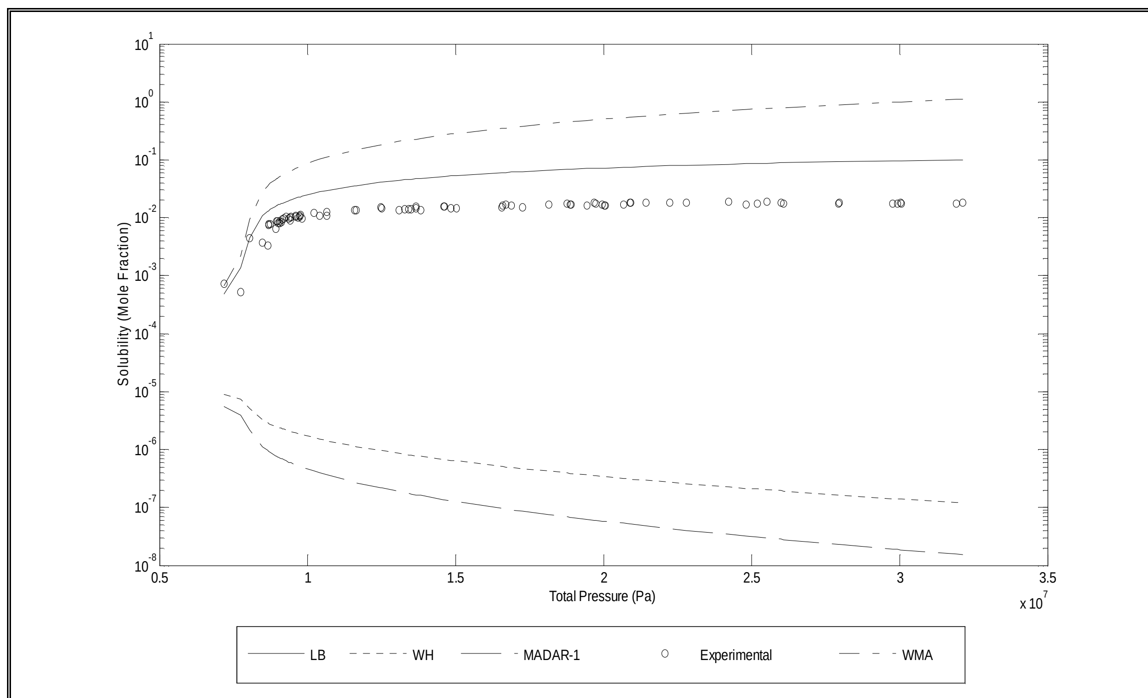

Figure A.1.4.1: Solubility of Naphthalene in SC – CO_2 at 308 K (Pure Predictive)

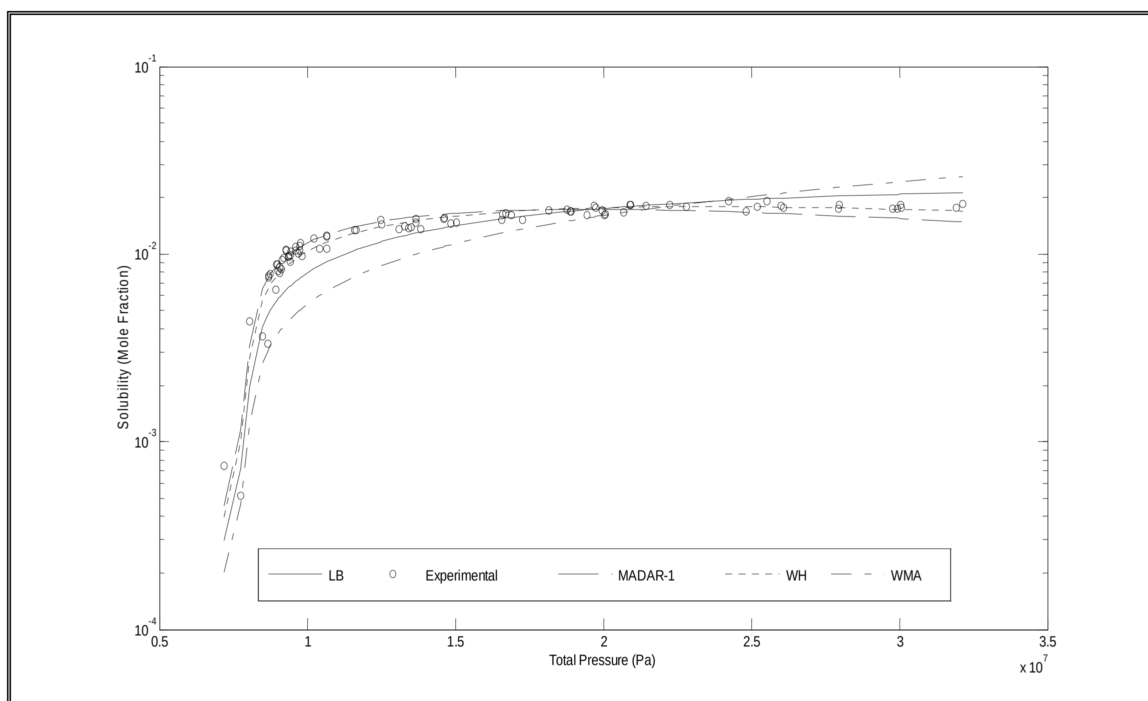

Figure A.1.4.2: Solubility of Naphthalene in SC – CO_2 at 308 K with (a) parameters only

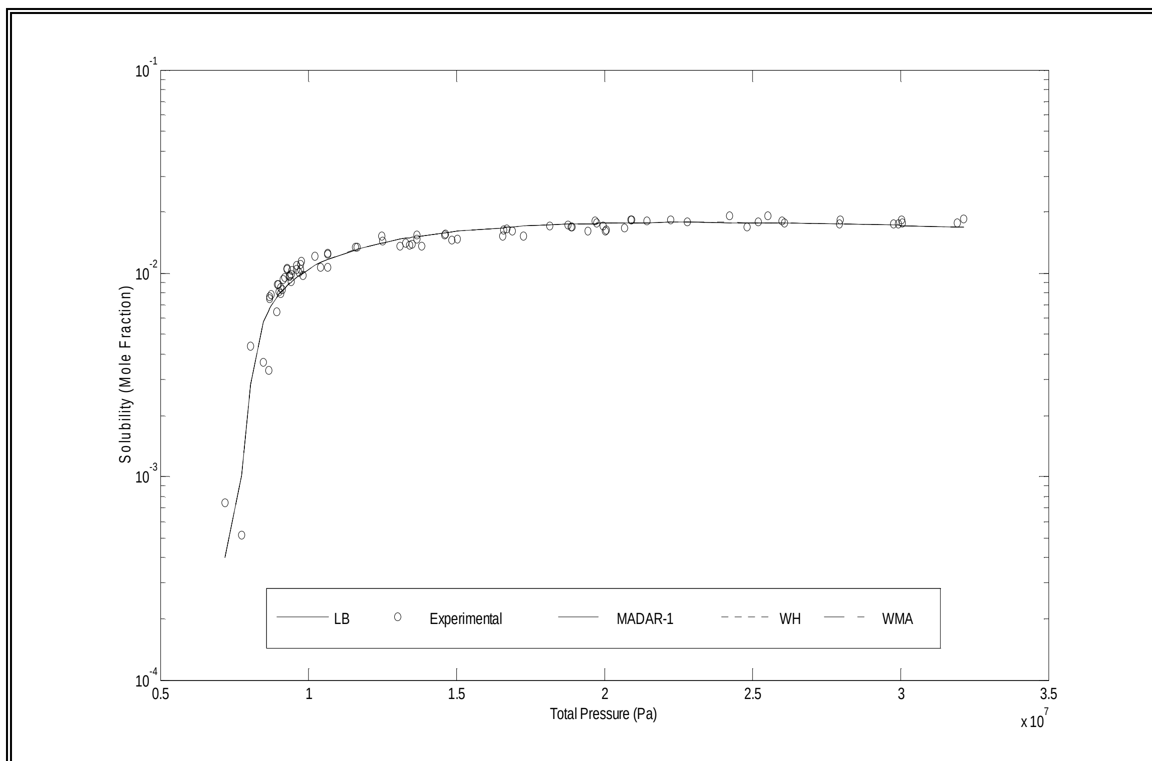

Figure A.1.4.3: Solubility of Naphthalene in SC – CO_2 at 308 K with (a) & (b) parameters

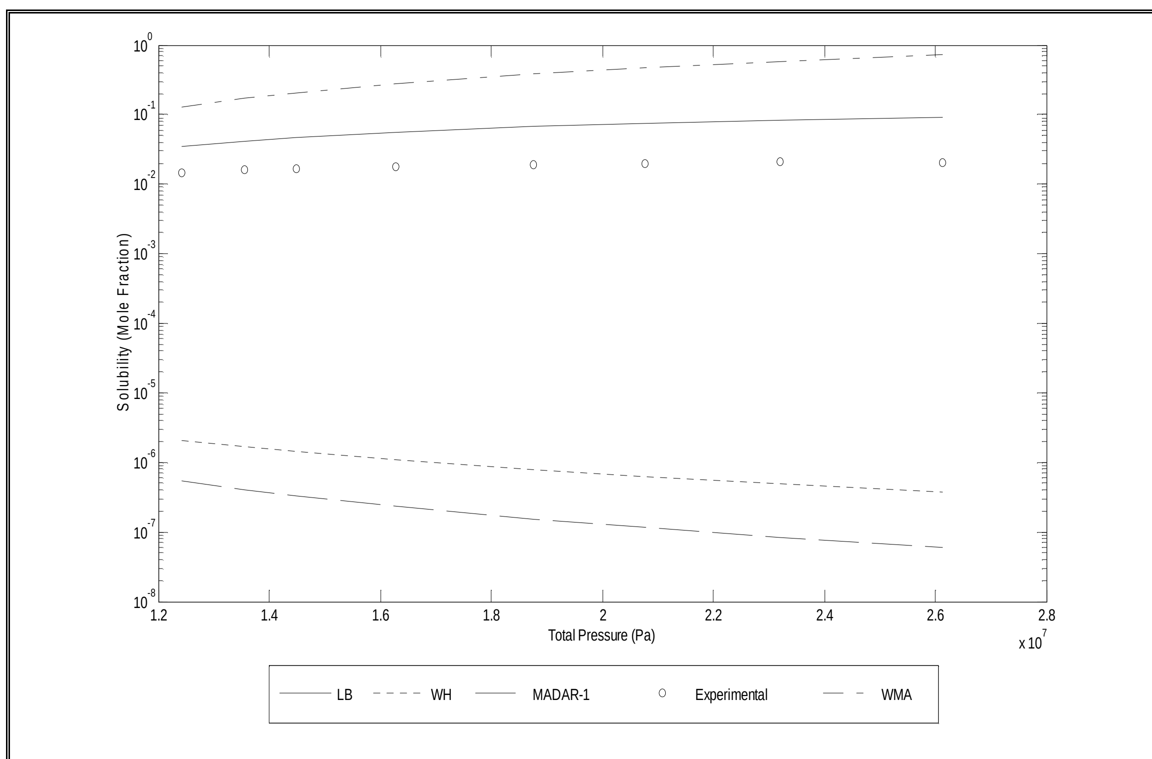

Figure A.1.4.4: Solubility of Naphthalene in SC – CO_2 at 313 K (Pure Predictive)

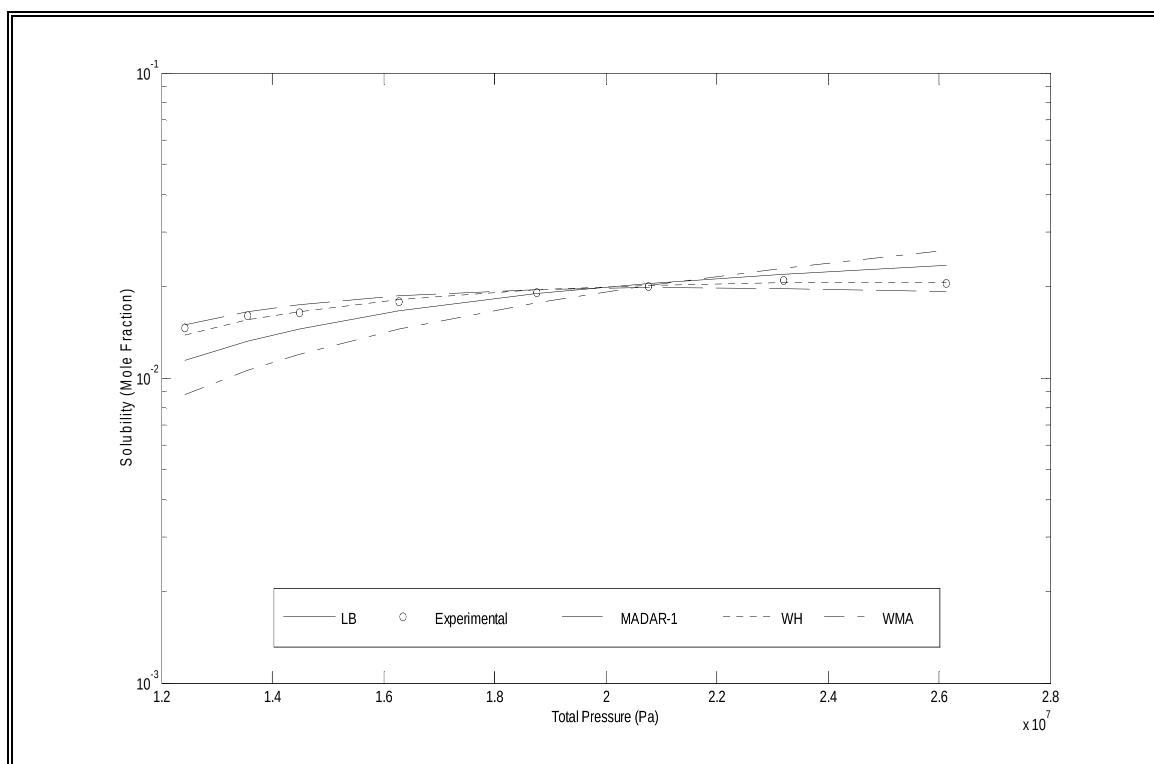

Figure A.1.4.5: Solubility of Naphthalene in SC – CO_2 at 313 K with (a) parameters only

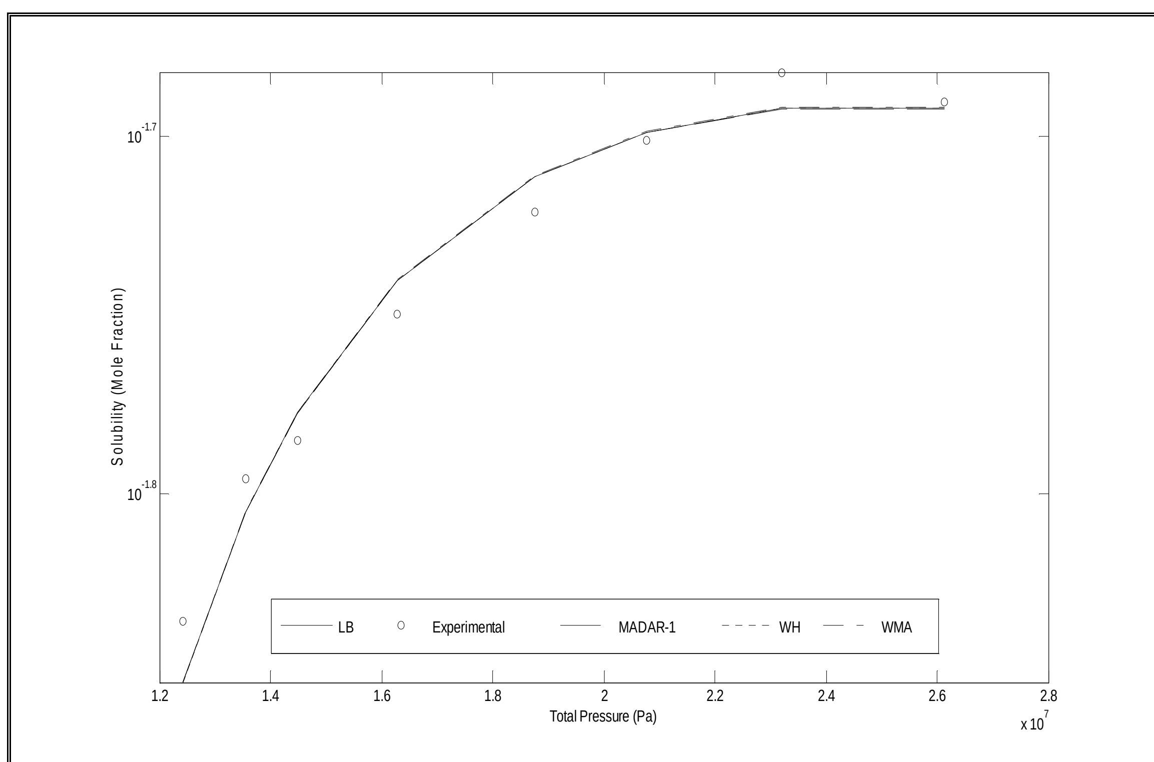

Figure A.1.4.6: Solubility of Naphthalene in SC – CO_2 at 313 K with (a) & (b) parameters

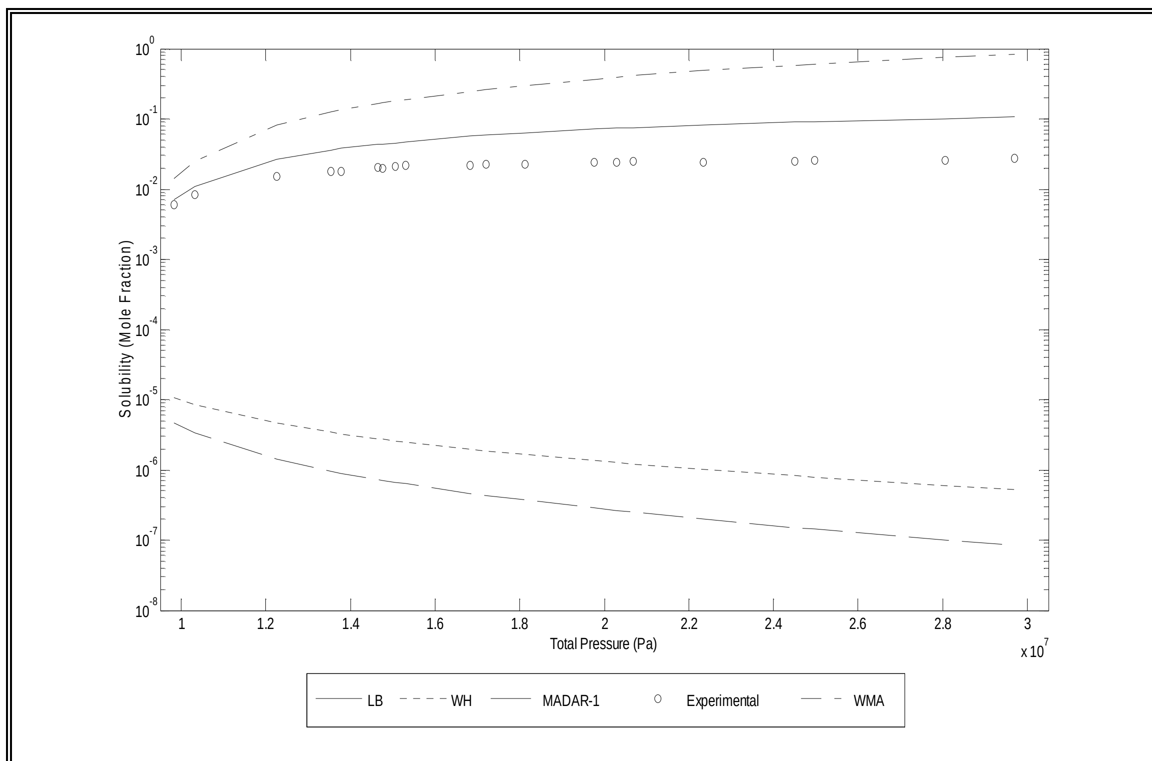

Figure A.1.4.7: Solubility of Naphthalene in SC – CO_2 at 318 K (Pure Predictive)

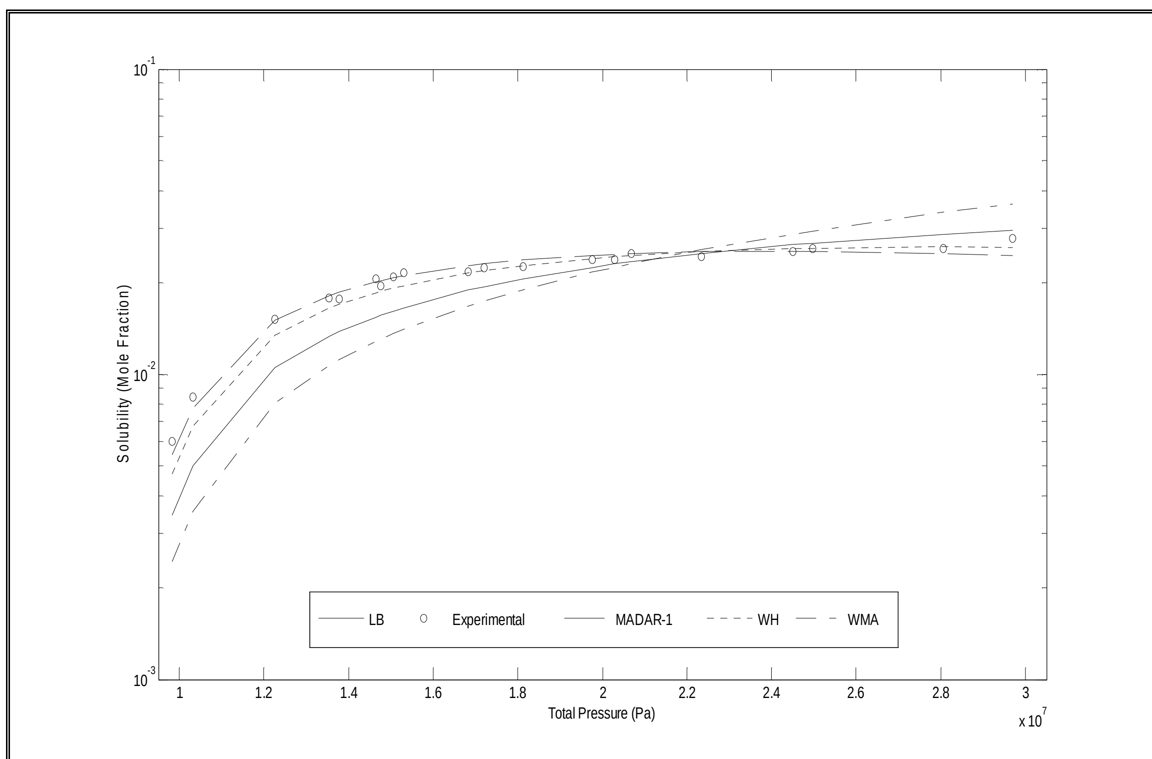

Figure A.1.4.8: Solubility of Naphthalene in SC – CO_2 at 318 K with (a) parameters only

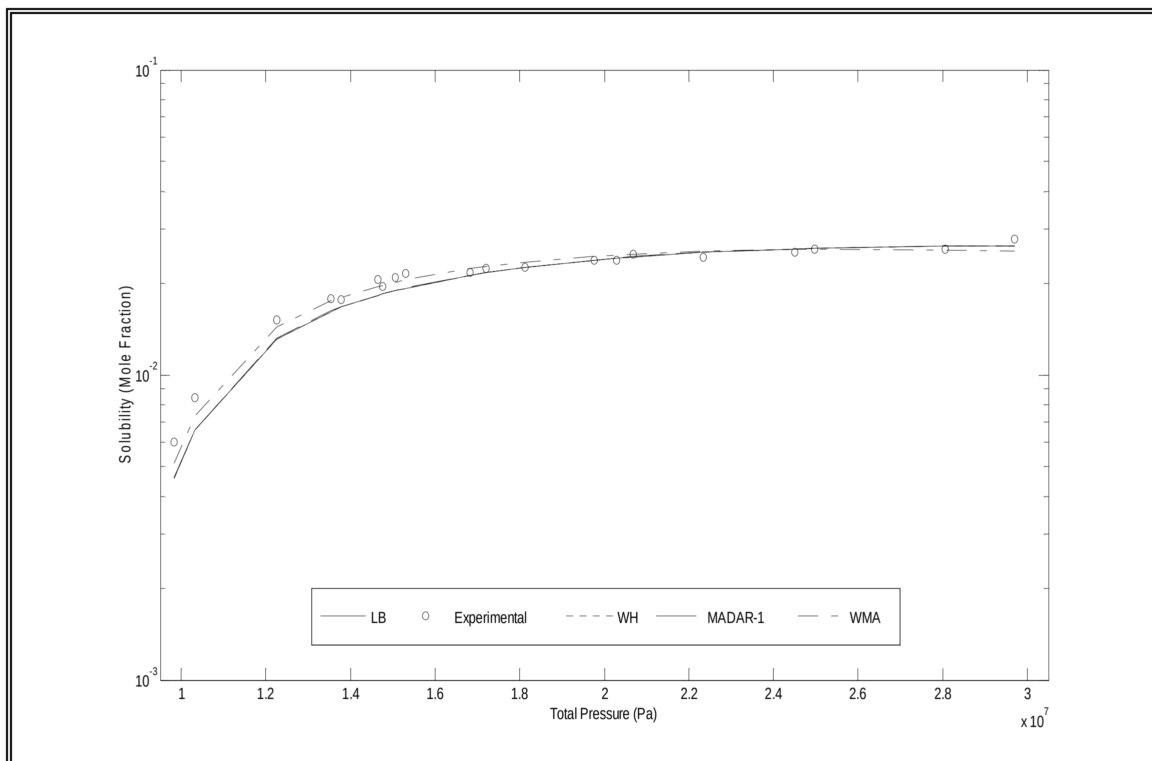

Figure A.1.4.9: Solubility of Naphthalene in SC – CO_2 at 318 K with (a) & (b) parameters

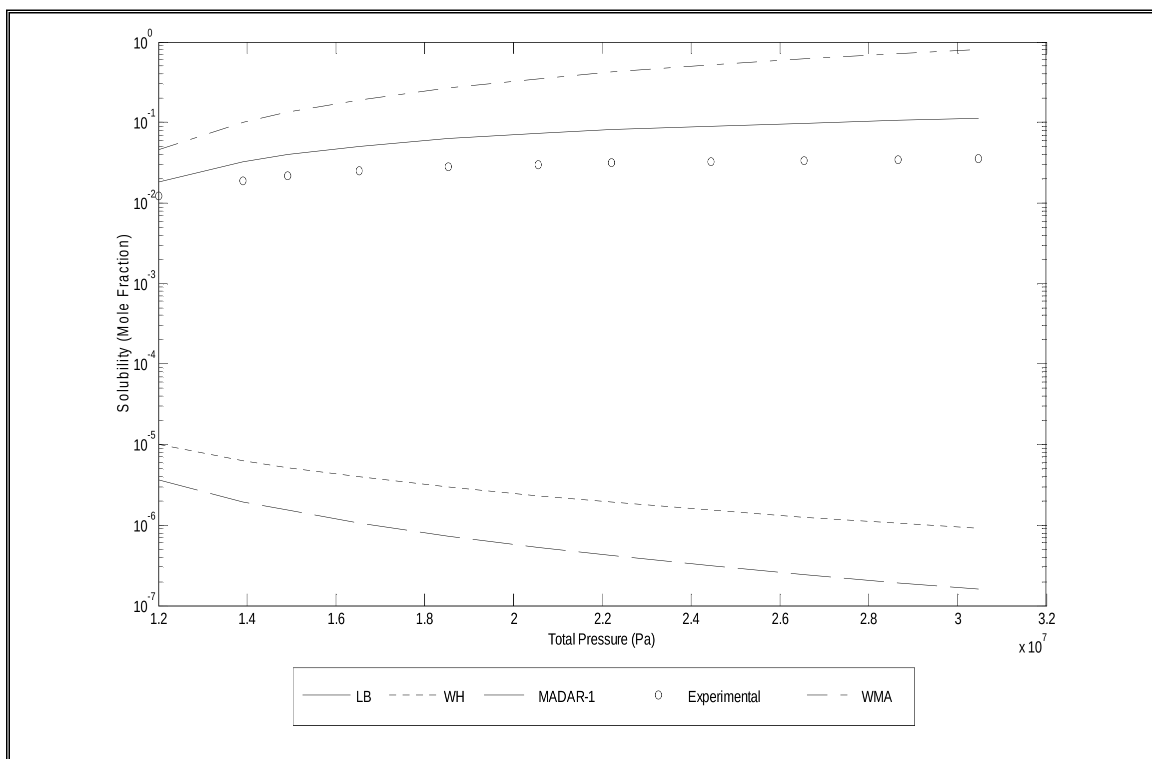

Figure A.1.4.10: Solubility of Naphthalene in SC – CO_2 at 323 K (Pure Predictive)

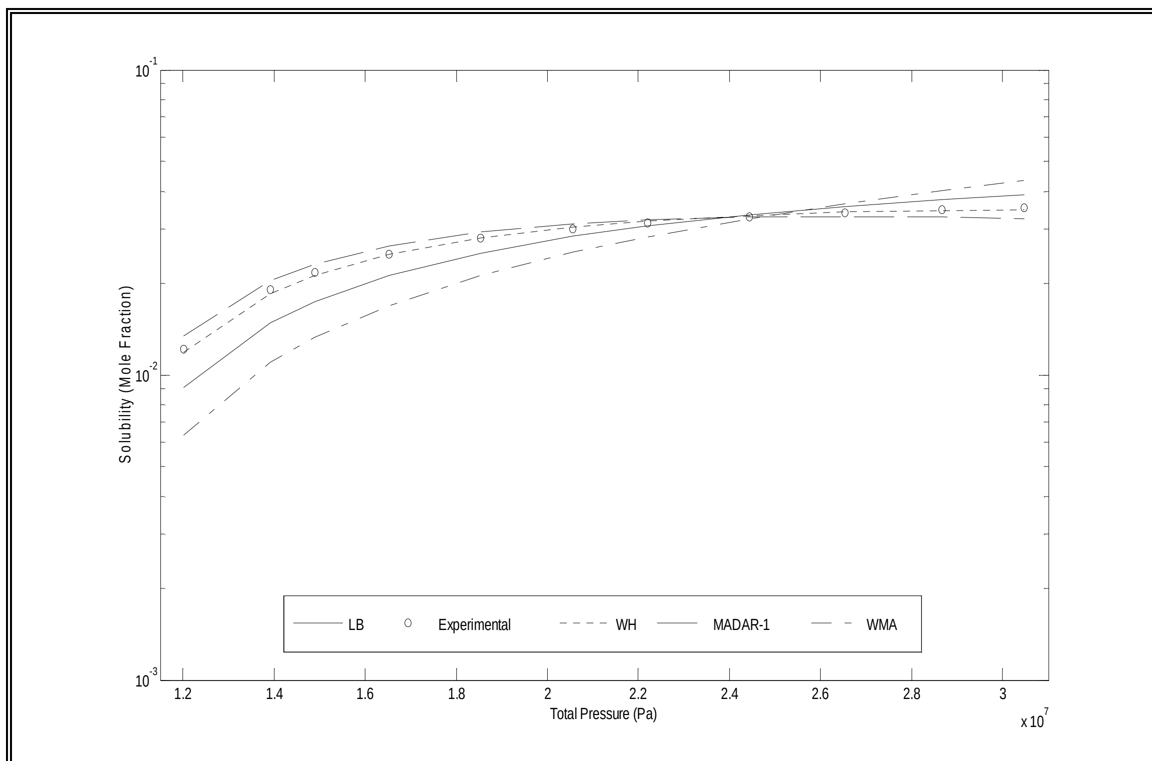

Figure A.1.4.11: Solubility of Naphthalene in SC – CO_2 at 323 K with (a) parameters only

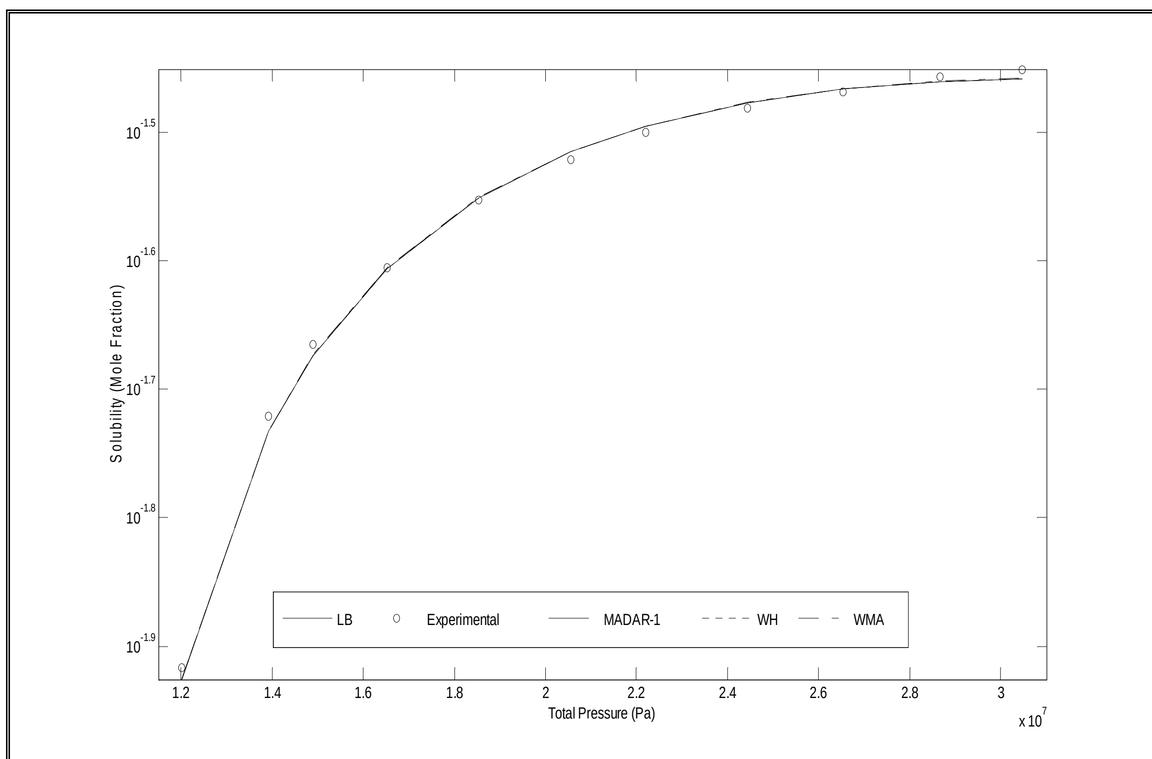

Figure A.1.4.12: Solubility of Naphthalene in SC – CO_2 at 323 K with (a) & (b) parameters

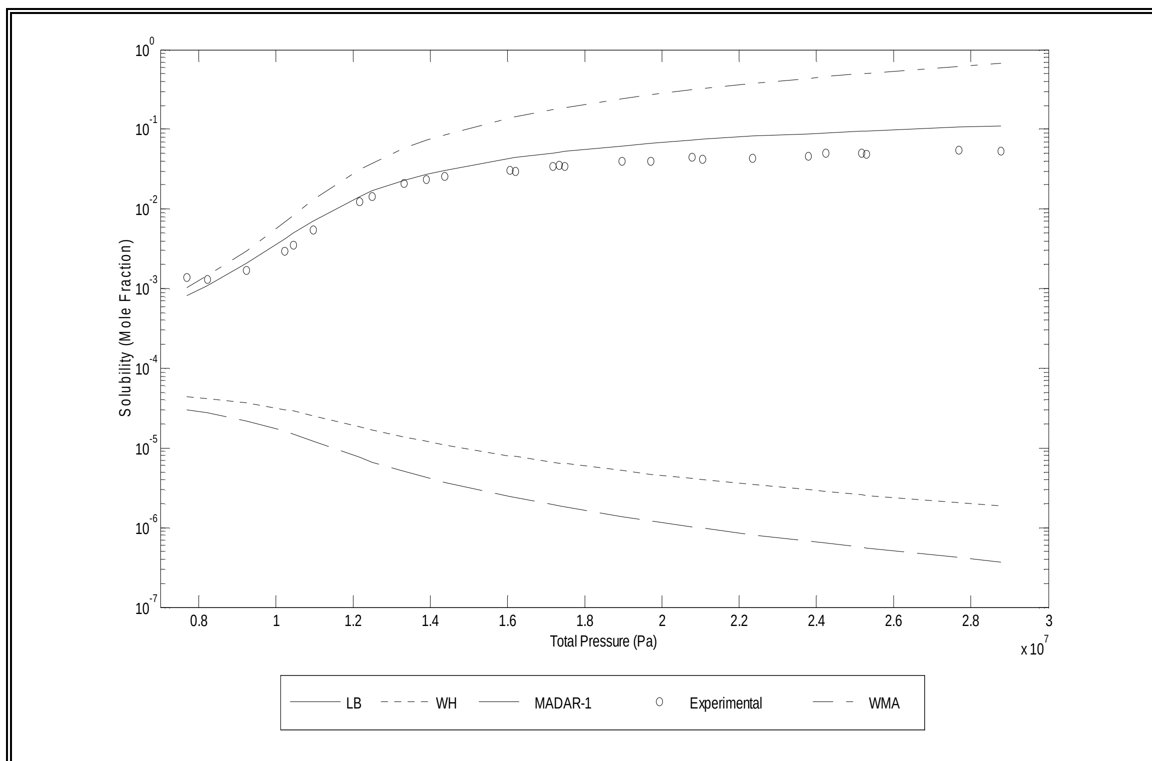

Figure A.1.4.13: Solubility of Naphthalene in SC – CO_2 at 328 K (Pure Predictive)

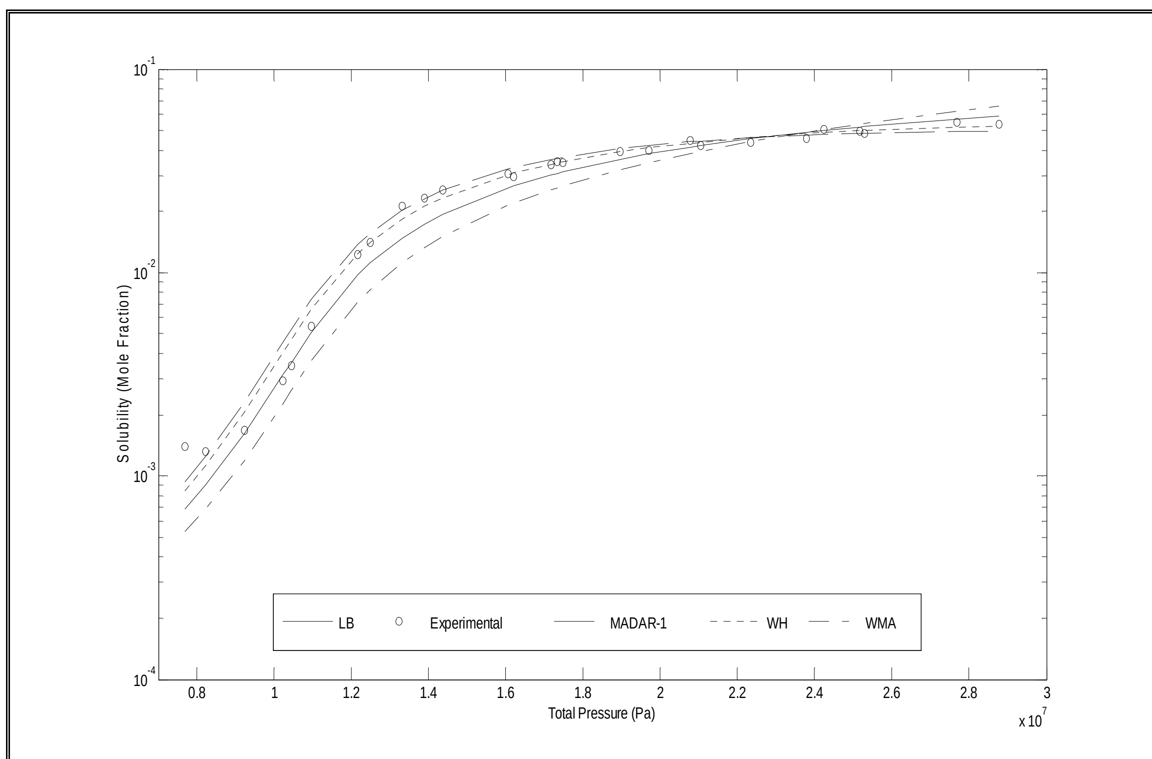

Figure A.1.4.14: Solubility of Naphthalene in SC – CO_2 at 328 K with (a) parameters only

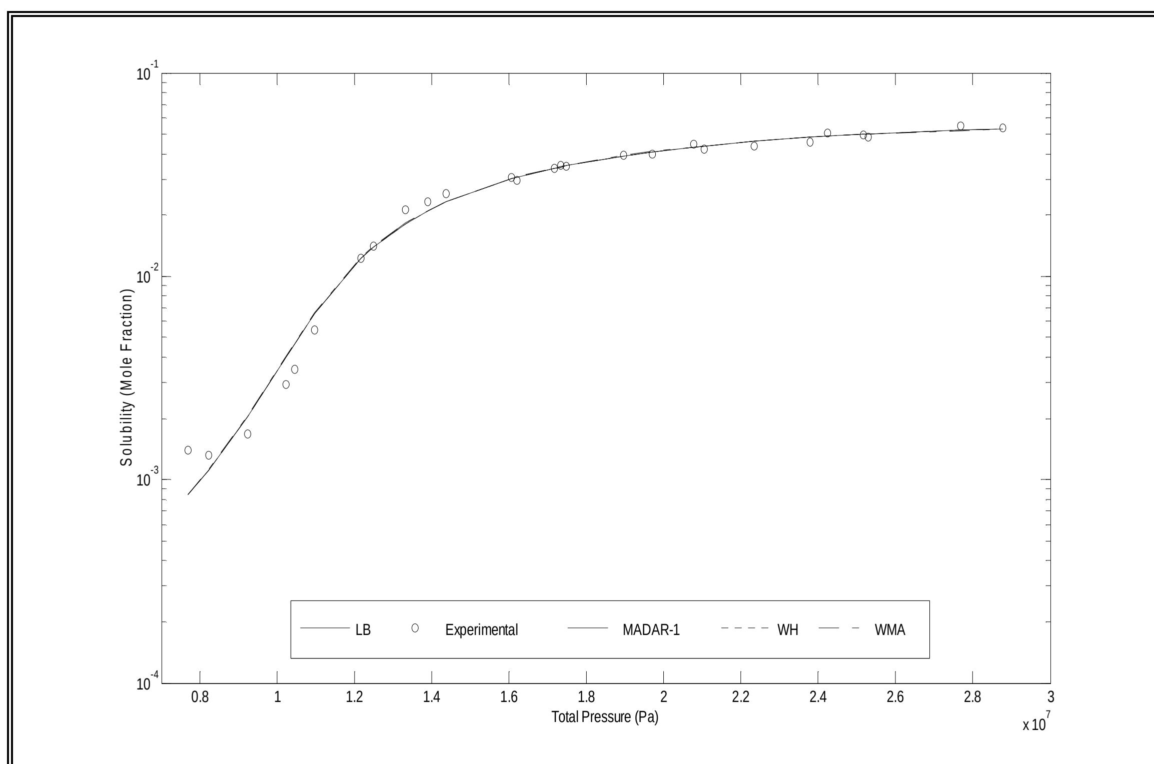

Figure A.1.4.15: Solubility of Naphthalene in SC – CO_2 at 328 K with (a) & (b) parameters

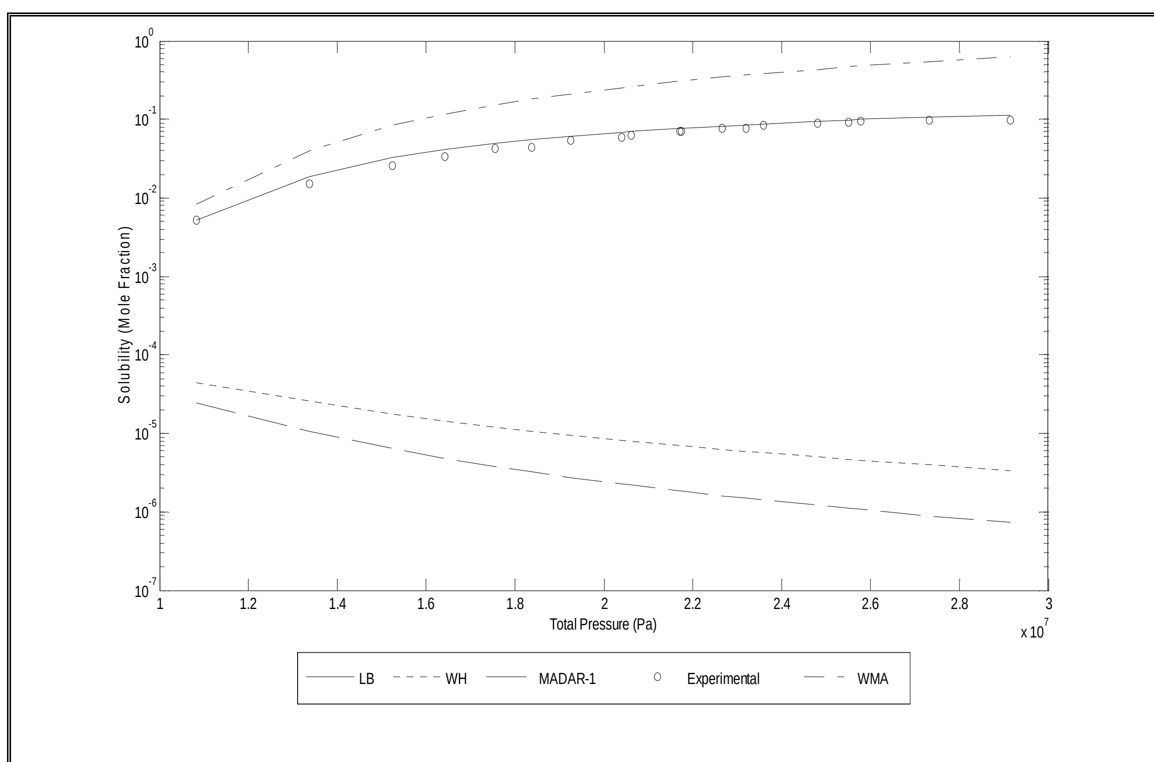

Figure A.1.4.16: Solubility of Naphthalene in SC – CO_2 at 333.55 K (Pure Predictive)

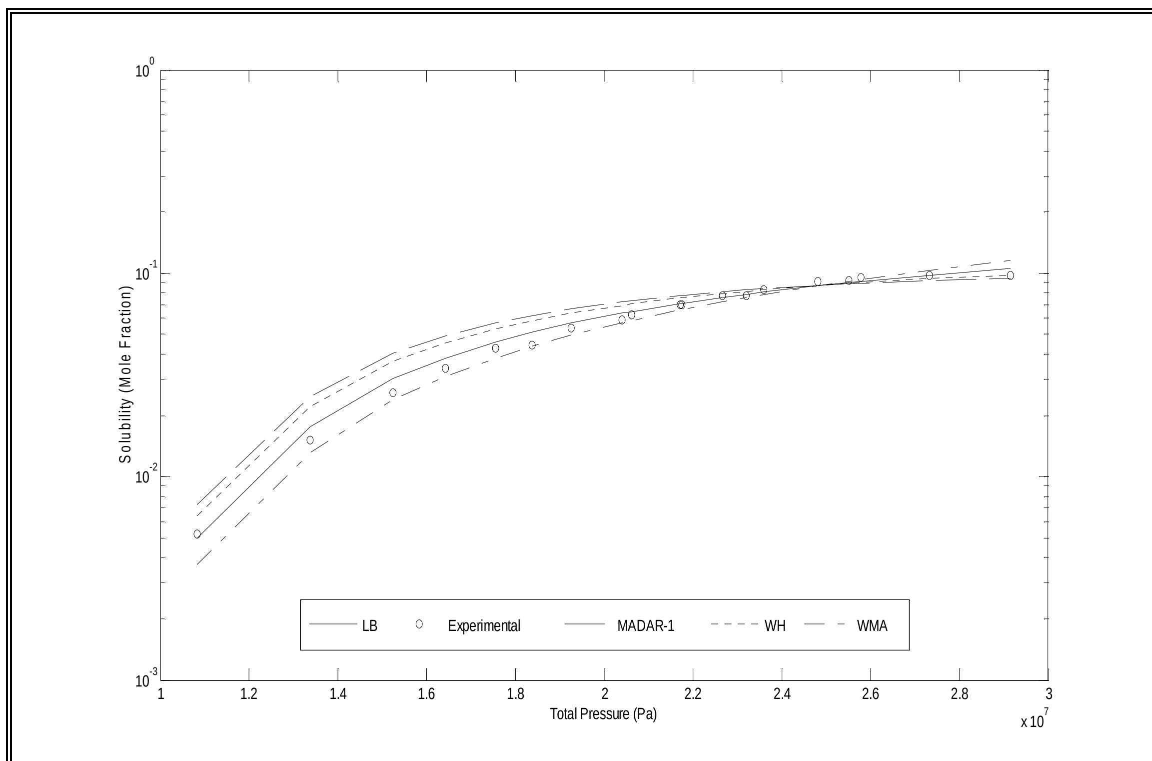

Figure A.1.4.17: Solubility of Naphthalene in SC – CO_2 at 333.55 K with (a) parameters only

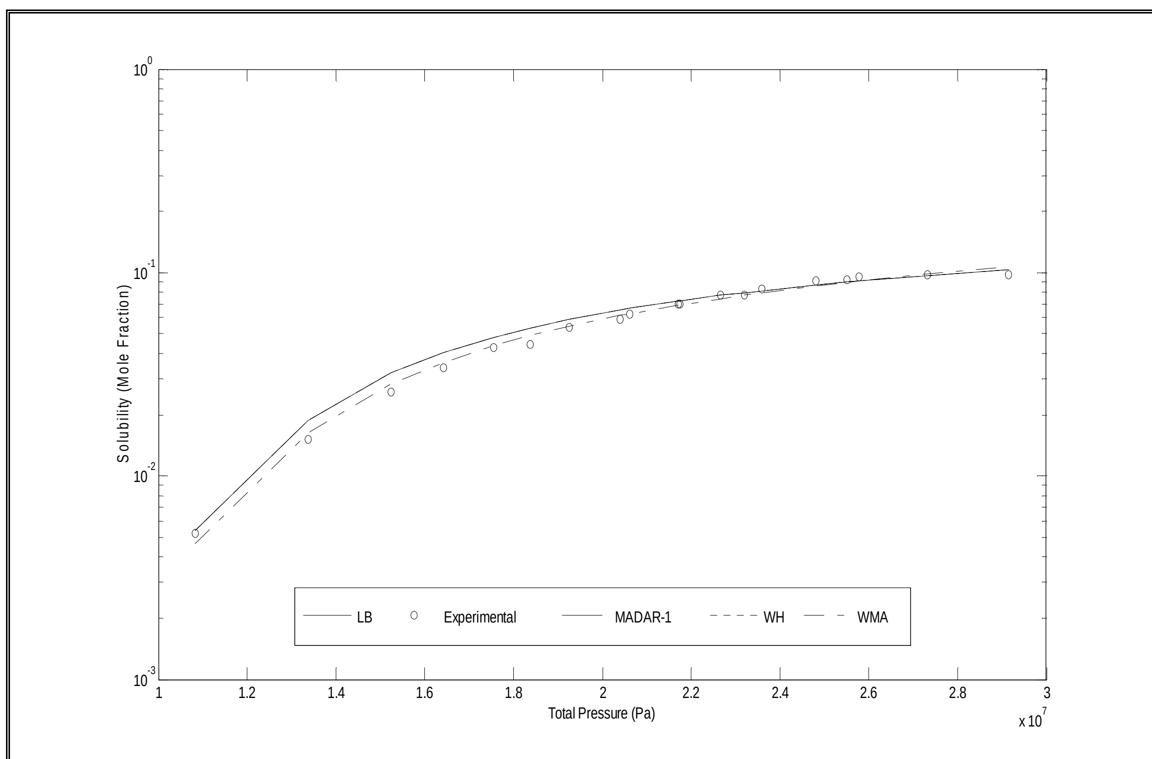

Figure A.1.4.18: Solubility of Naphthalene in SC – CO_2 at 333.55 K with (a) & (b) parameters

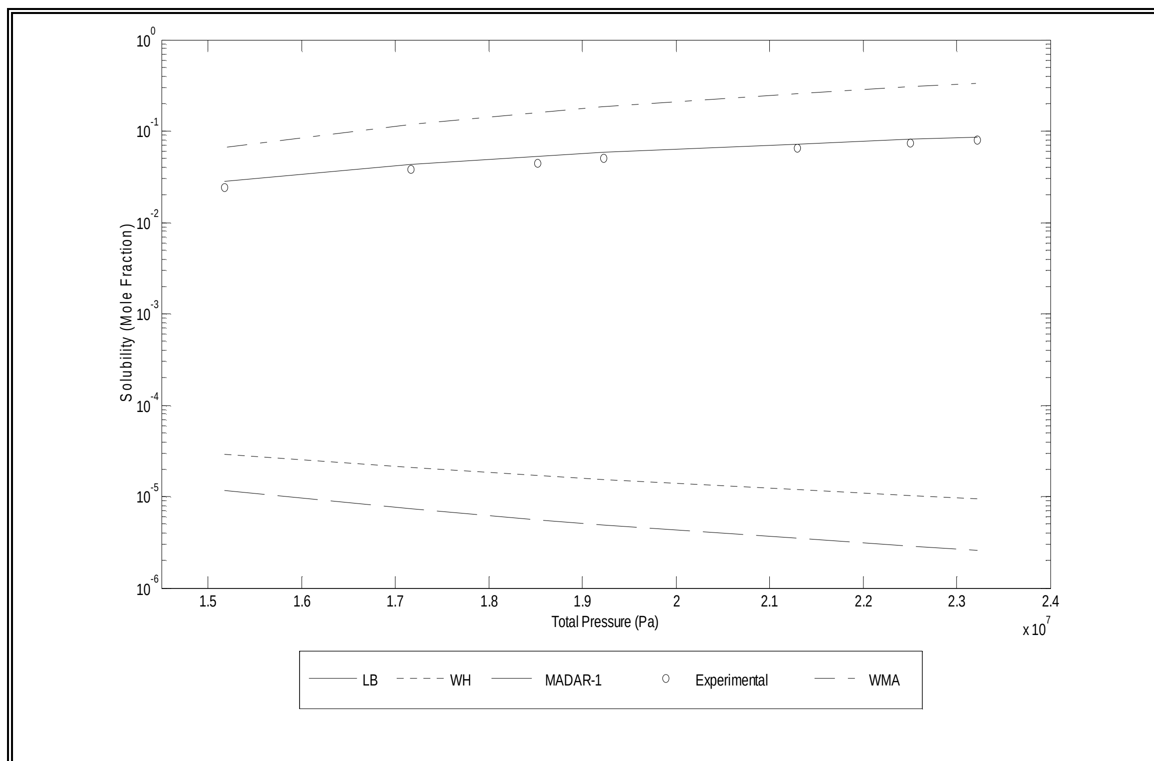

Figure A.1.4.19: Solubility of Naphthalene in SC – CO_2 at 338.05 K (Pure Predictive)

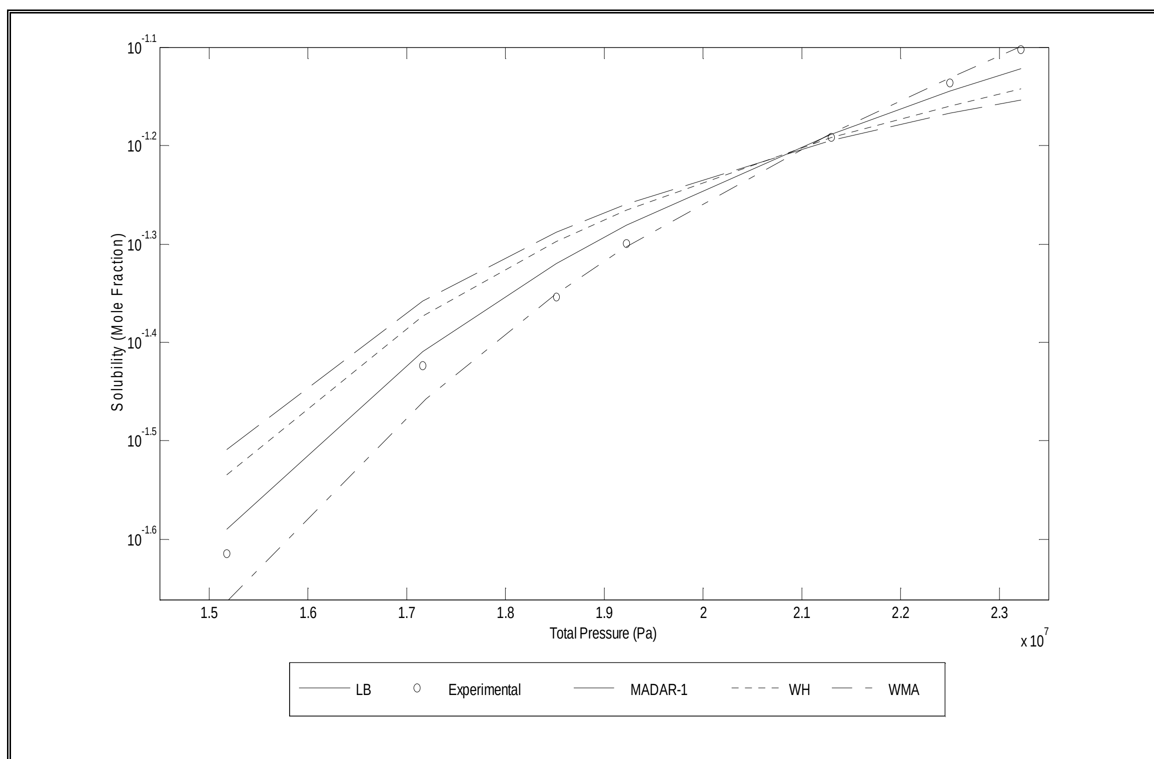

Figure A.1.4.20: Solubility of Naphthalene in SC – CO_2 at 338.05 K with (a) parameters only

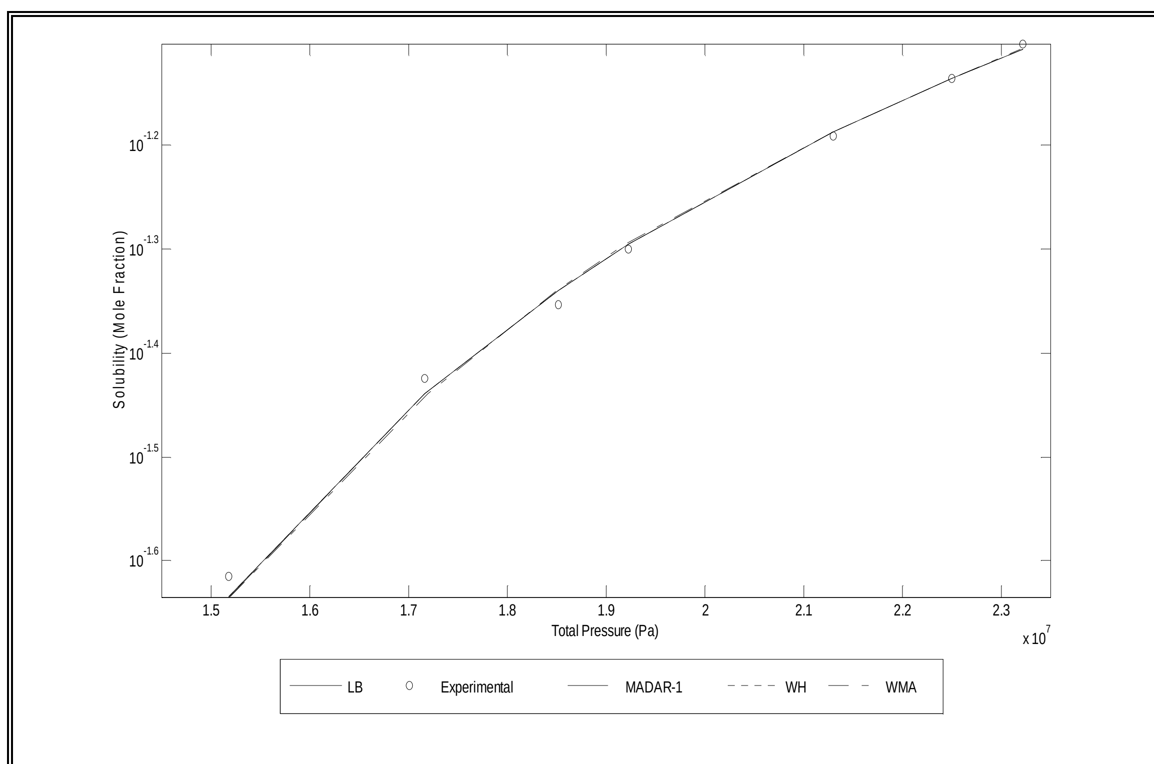

Figure A.1.4.21: Solubility of Naphthalene in SC – CO_2 at 338.05 K with (a) & (b) parameters

A.1.5 Solubility of Xanthene Using Combining Rules and Weighting Matrix Approach

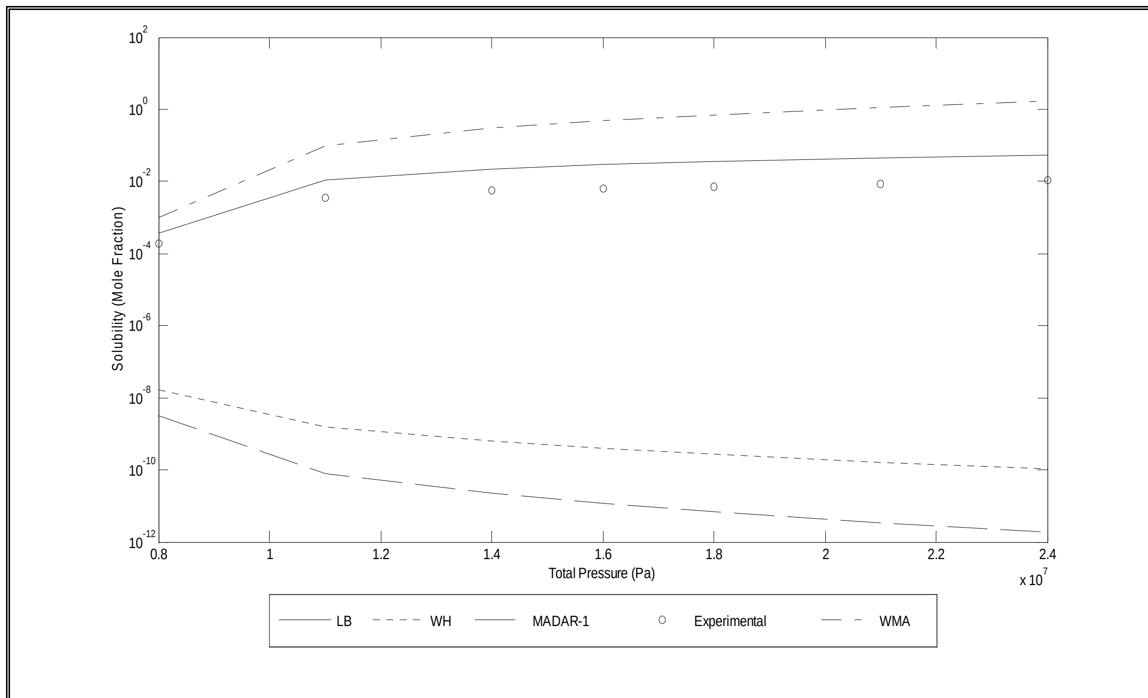

Figure A.1.5.1: Solubility of Xanthene in SC – CO_2 at 308.15 K (Pure Predictive)

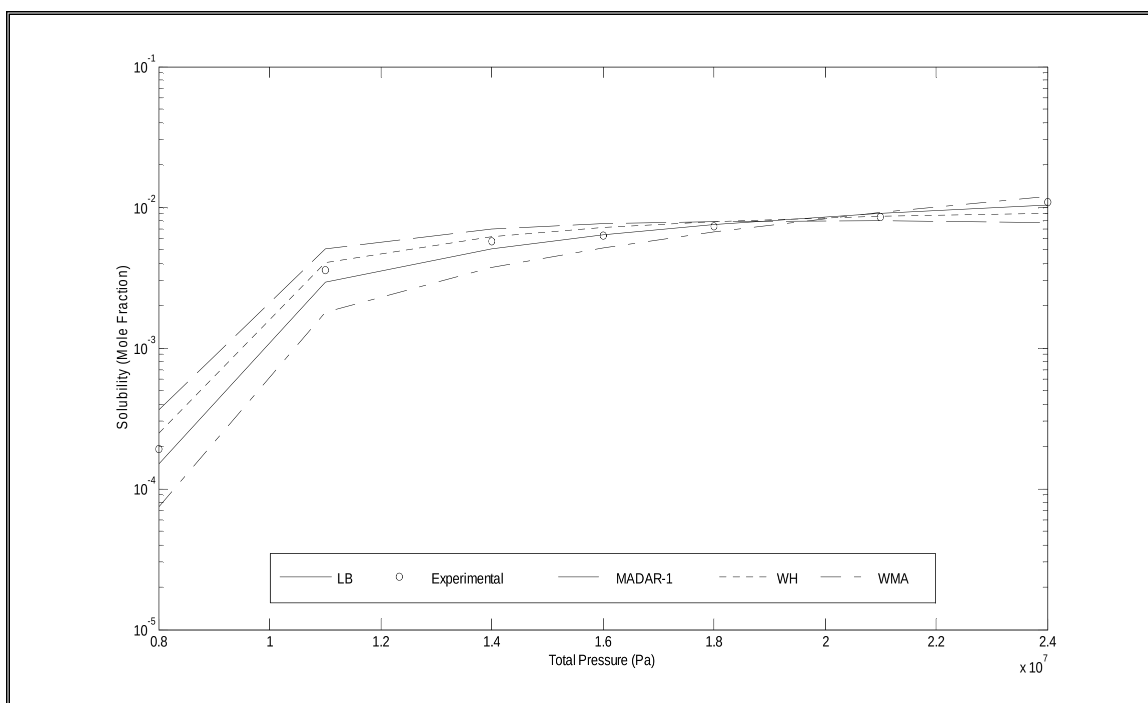

Figure A.1.5.2: Solubility of Xanthene in SC – CO_2 at 308.15 K with (a) parameters only

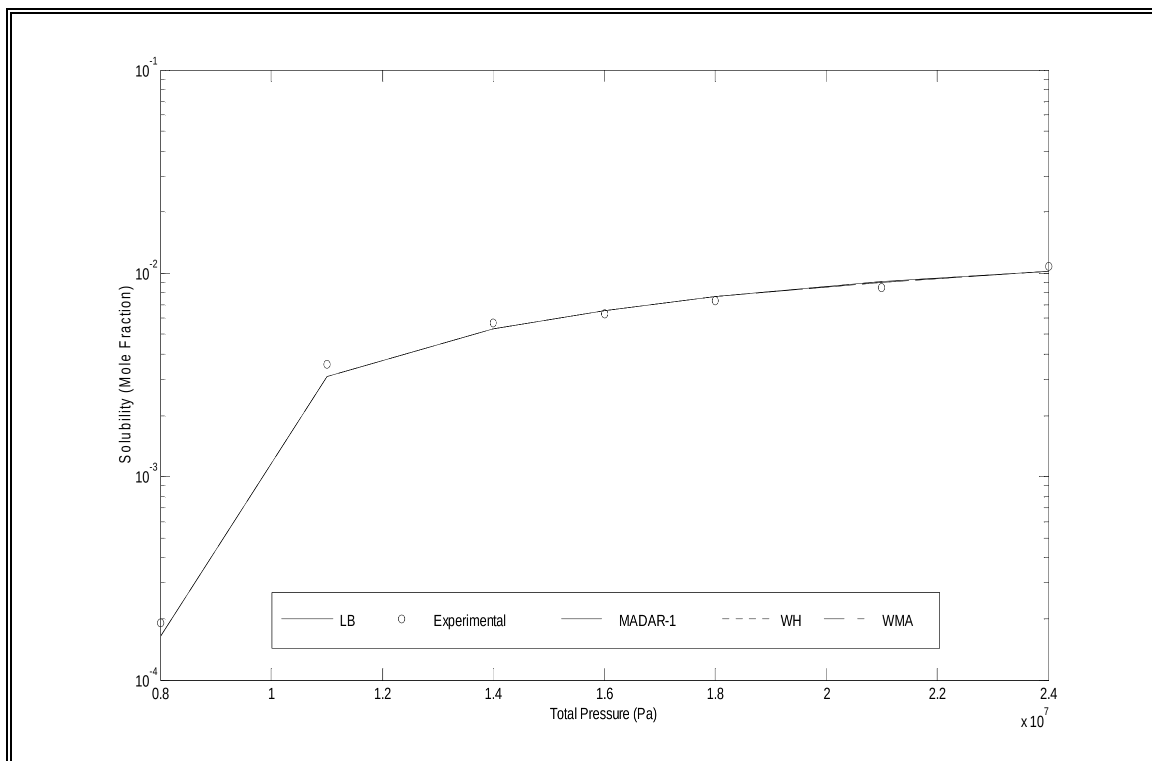

Figure A.1.5.3: Solubility of Xanthene in SC – CO_2 at 308.15 K with (a) & (b) parameters

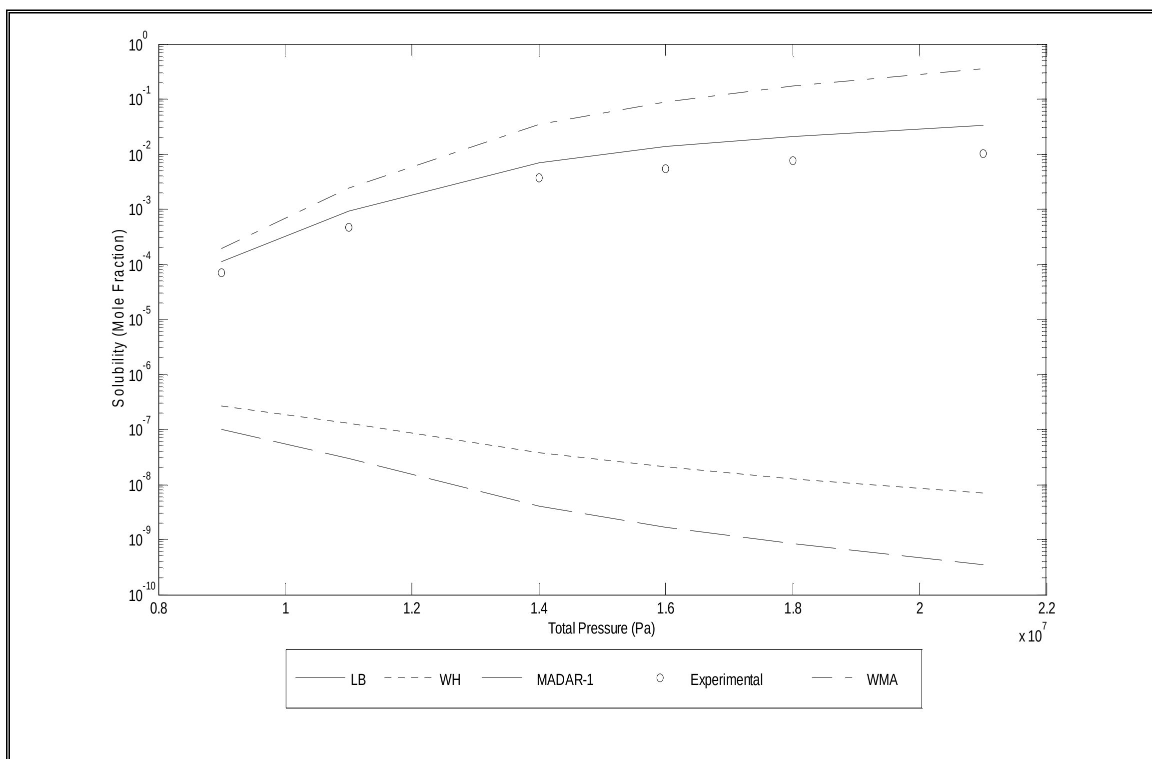

Figure A.1.5.4: Solubility of Xanthene in SC – CO_2 at 328.15 K (Pure Predictive)

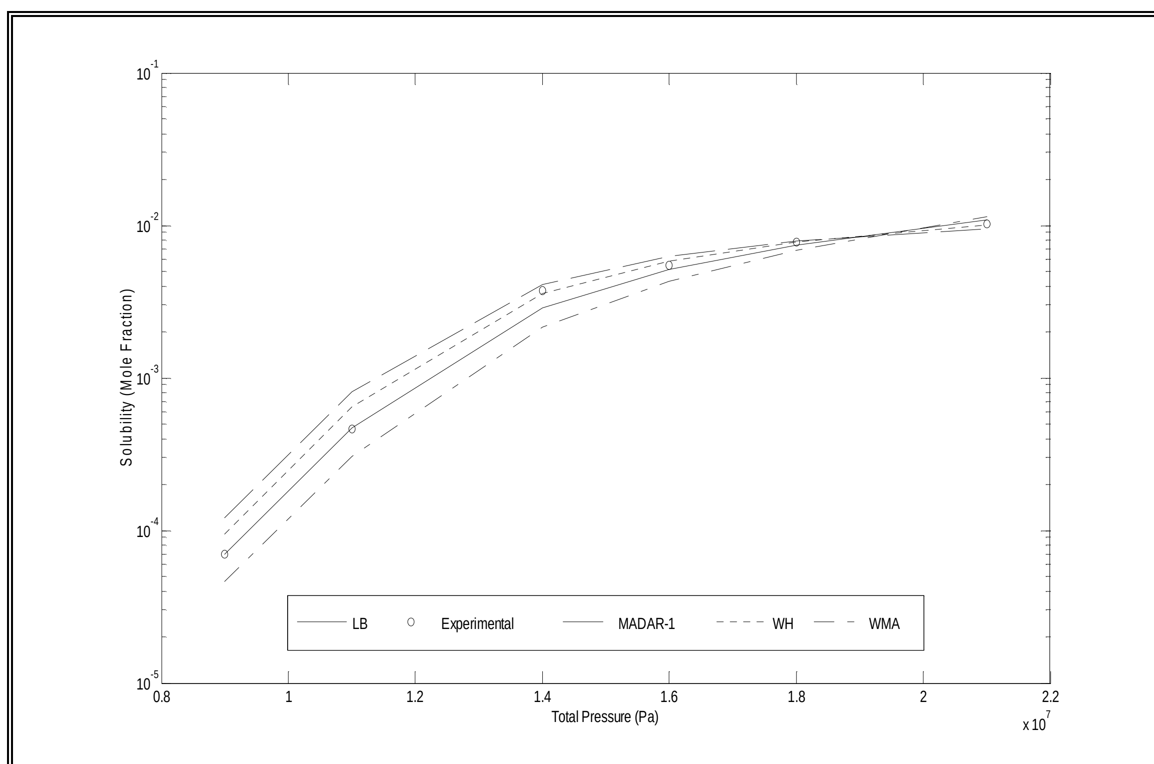

Figure A.1.5.5: Solubility of Xanthene in SC – CO_2 at 328.15 K with (a) parameters only

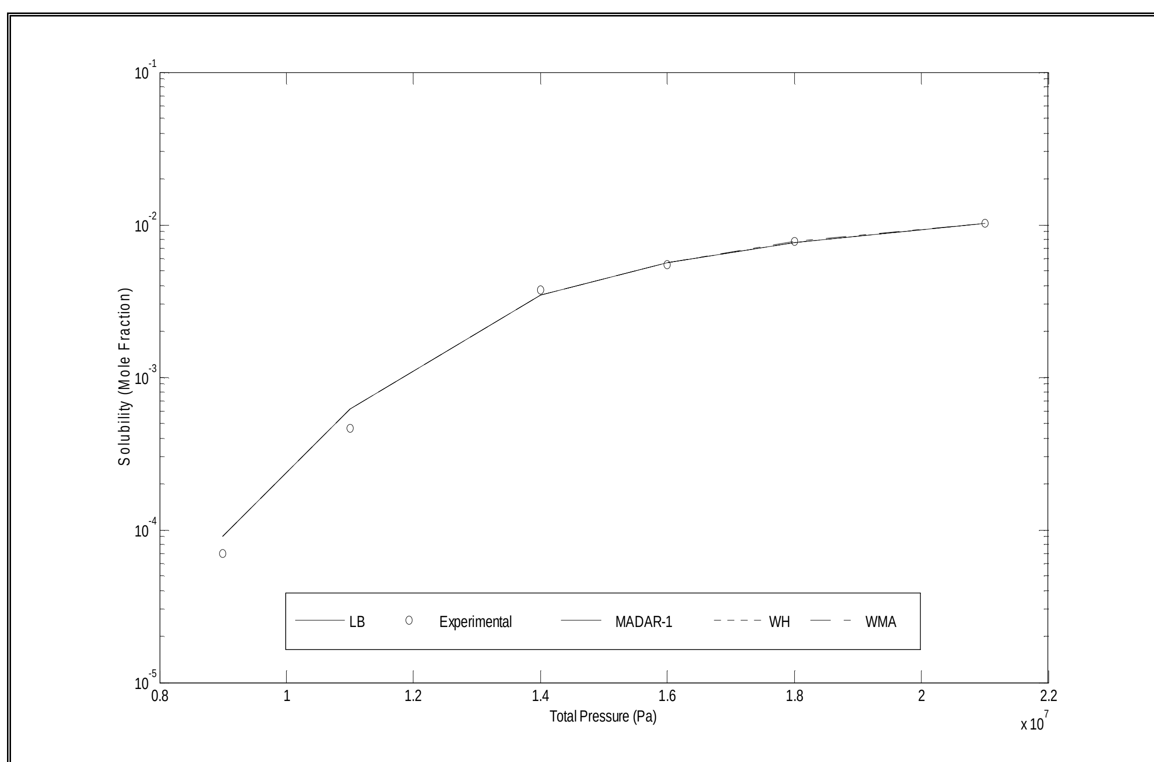

Figure A.1.5.6: Solubility of Xanthene in SC – CO_2 at 328.15 K with (a) & (b) parameters

A.1.6 Solubility of Xanthone Using Combining Rules and Weighting Matrix Approach

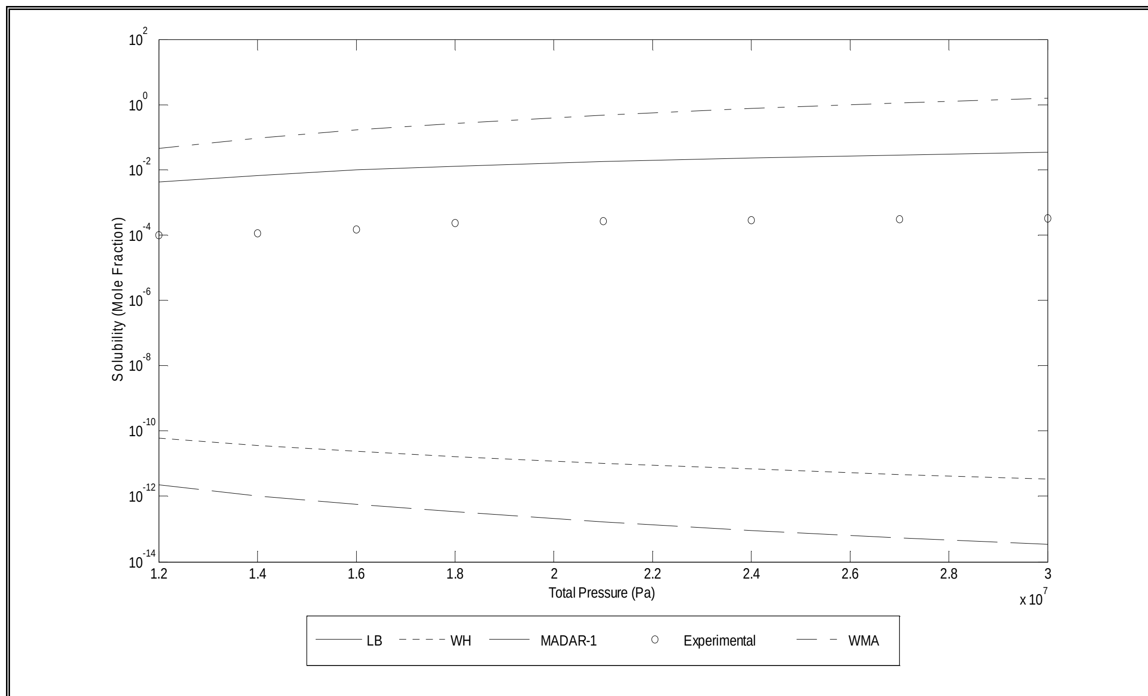

Figure A.1.6.1: Solubility of Xanthone in SC – CO_2 at 308.15 K (Pure Predictive)

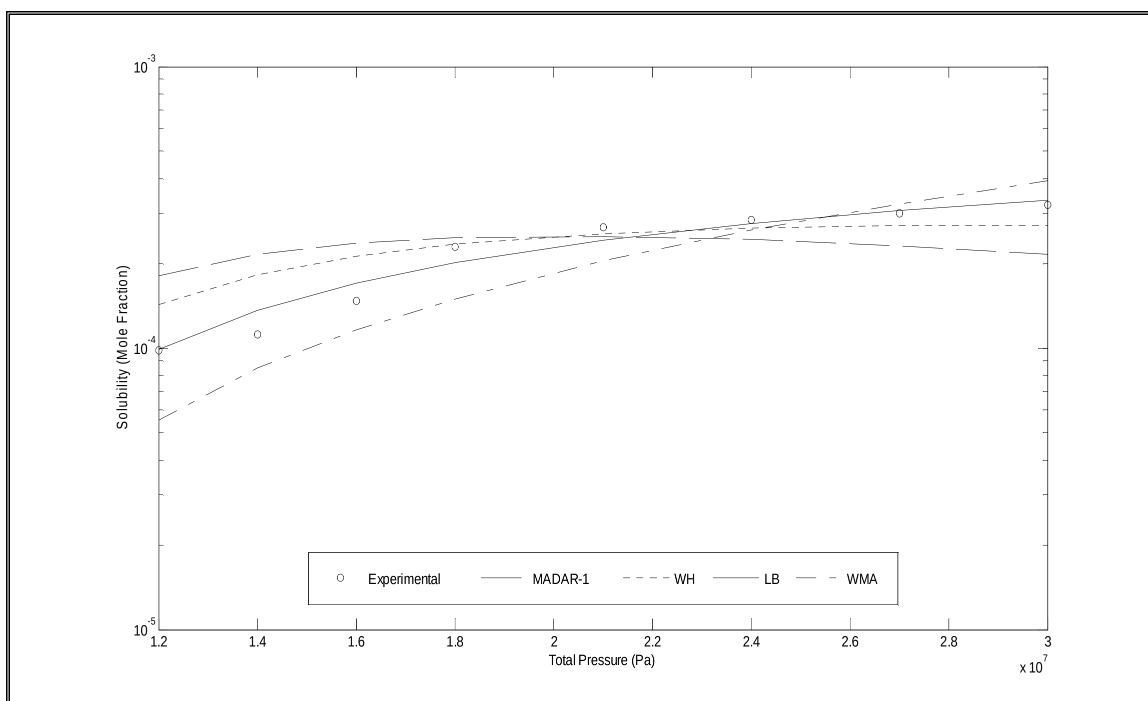

Figure A.1.6.2: Solubility of Xanthone in SC – CO_2 at 308.15 K with (a) parameters only

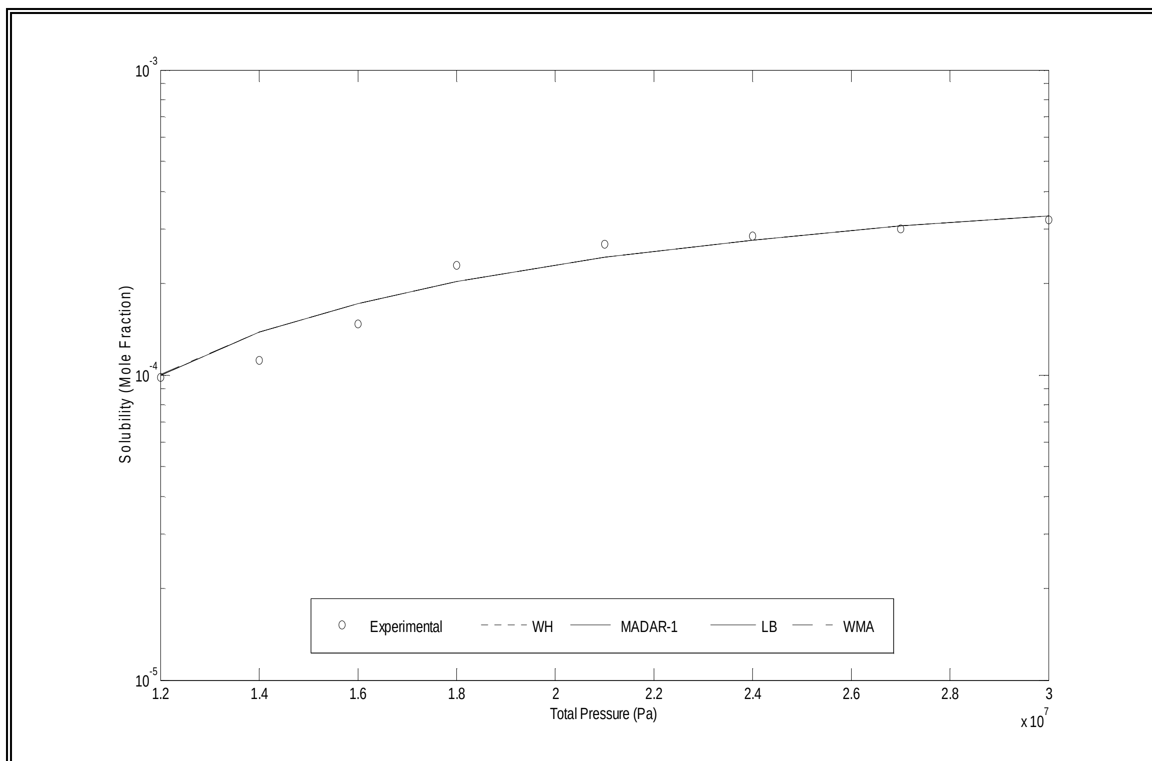

Figure A.1.6.3: Solubility of Xanthone in SC – CO_2 at 308.15 K with (a) & (b) parameters

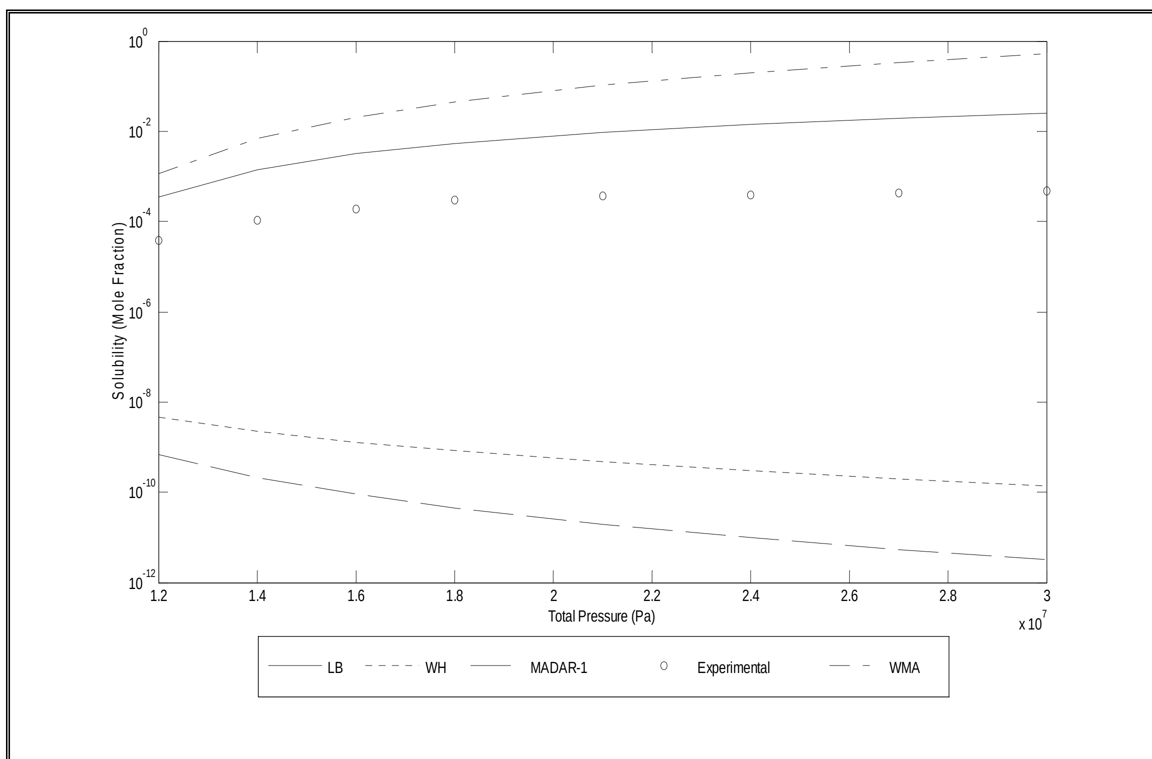

Figure A.1.6.4: Solubility of Xanthone in SC – CO_2 at 328.15 K (Pure Predictive)

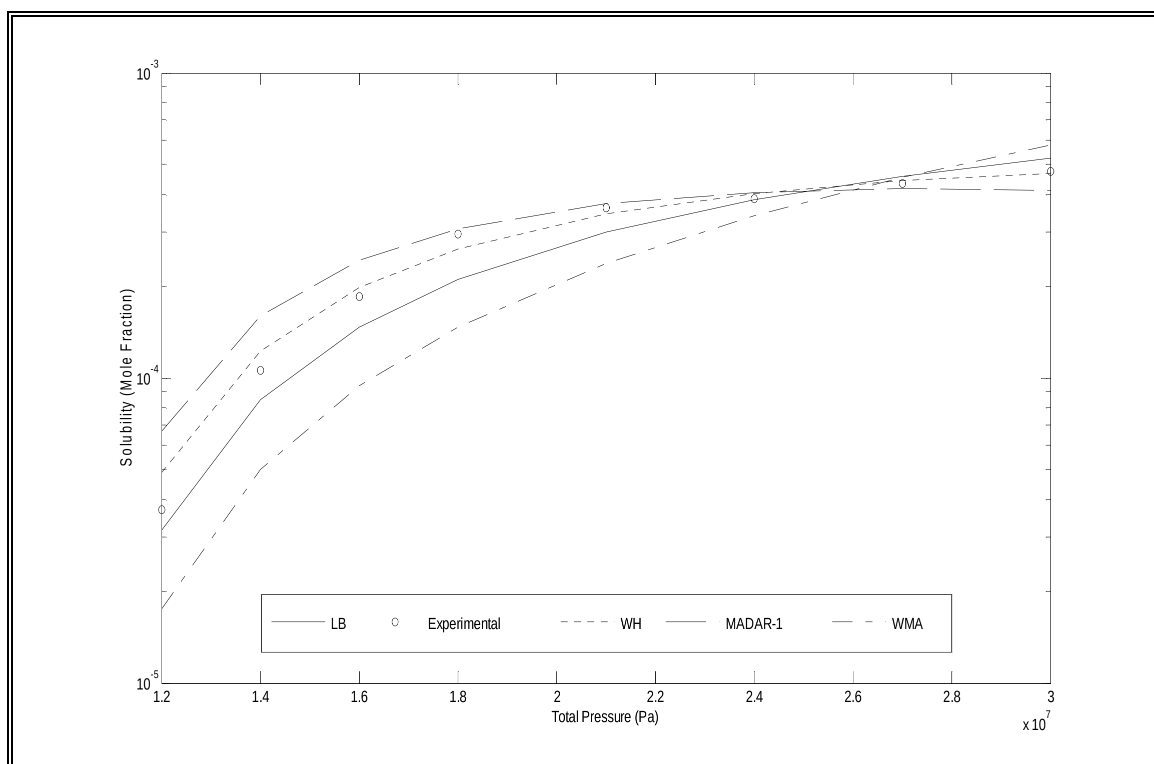

Figure A.1.6.5: Solubility of Xanthone in SC – CO_2 at 328.15 K with (a) parameters only

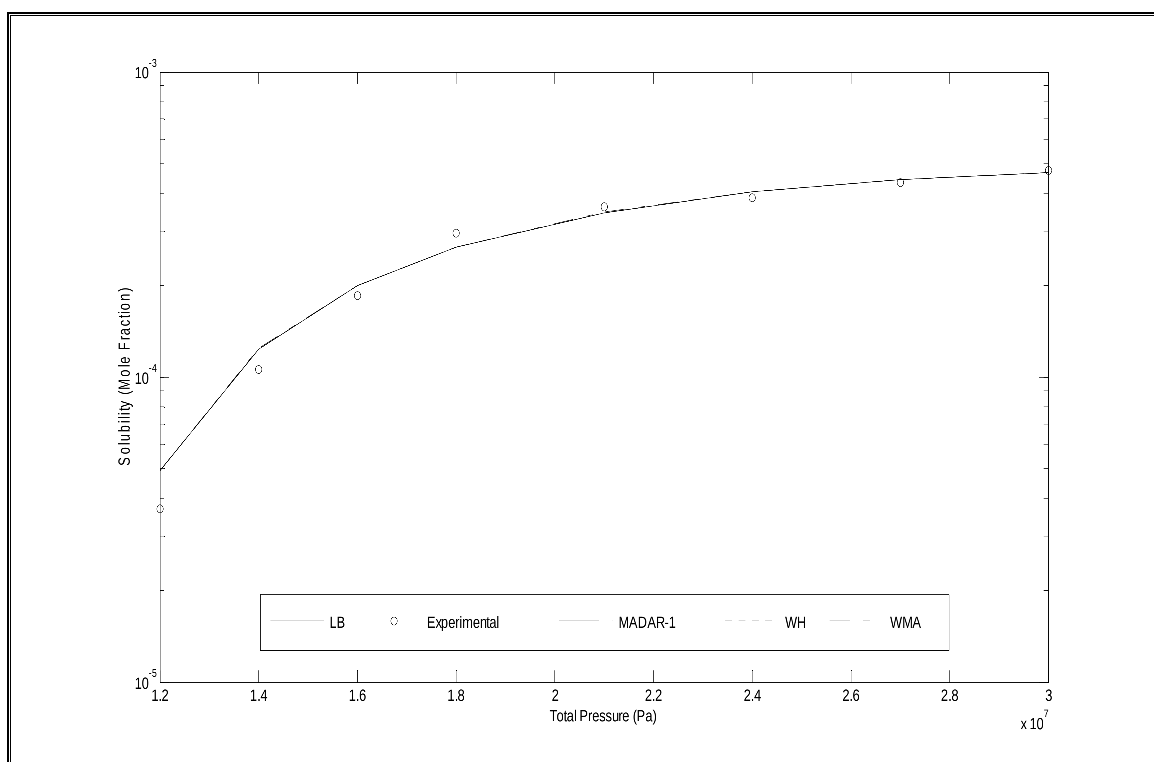

Figure A.1.6.6: Solubility of Xanthone in SC – CO_2 at 328.15 K with (a) & (b) parameters

Appendix B

`Matlab`© Codes for Aspirin (as an example)

```
% Prediction of solubility of Aspirin in supercritical CO2 using three mixing rules

clc
clear
format long e
sprintf('Executing ... Please be patient')

% Universal gas constant
   R = 8.3143;

% Number of components in the system
   ncomps = 2;

% The mole fractions of each component in the gas phase
   yinitial = [0 1]';

% Binary interaction coefficients
   kijSparse = [0]; % Get this value from corresponding excel sheet
   lijSparse = [0]; % Get this value from corresponding excel sheet
   [kij] = BinaryInteraction(ncomps, kijSparse);
   [lij] = BinaryInteraction(ncomps, lijSparse);

% Get critical constants and acentric factors, change according to solute
   Pc = [3.28e6 7.376e6]';
   Tc = [762.9 304.2]';
   w = [0.817 0.225]';

% Span the temperature range
   T = [308.15 318.15 328.15];

% Setting the pressure range
   [P Solub] = Experimental(T(1));

% Solid sublimation pressure and molar volume
   Psub = 0.09021;
   v = 1.2964e-4;

% Binary parameters of the PR EOS for pure components
   [bii aii] = PRaijbij(ncomps, R, Tc, Pc, w, T(1));

% Definition of several variables used throughout
   zz = [ ];
   rho = [ ];
   sol = [ ];
   PRhoSol = [ ];
   pressure = [ ];
   solT = [ ];

% Using mixing rules to calculate binary parameters for the mixture
   for s = 1:3
     [bij aij] = MixingRules(s,ncomps, bii, aii, kij, lij);

% Estimating the fugacity coefficient of the solid for increased accuracy
     A2s = aij(1,1)*Psub/(R*T(1))^2;
```

```
        B2s = bij(1,1)*Psub/(R*T(1));
        Z2s =  PRRoots(A2s, B2s);
        Phi2s = PRPhiPure(A2s, B2s, Z2s, R, T(1));

% Commencing the calculation of the solubility
        for i = 1: length(P);

         % Poynting correction factor
         Poynting(i) = exp(v/(R*T(1)) * (P(i) - Psub));

         % Calculation of solubility and density for corresponding temperature, pressure and mixing rule
         x = Phi2s * Psub * Poynting(i)/ P(i);
         [solubility(i) Z(i)] = SCFFugacity(x, ncomps, R, T(1), P(i), Poynting(i), Psub, Phi2s, aij, bij, yinitial);
         [y] = NormMoleFraction(ncomps, yinitial, solubility(i));
         Rho(i) = P(i)/(Z(i)*R*T(1));
        end

         % Saving the data in corresponding matrices.
         rho = [rho Rho'];
         sol=[sol solubility'];
         pressure = [pressure P'];
         zz = [zz Z'];
    end

    figure
    % Plotting the calculated data.
    set(0,'DefaultAxesColorOrder',[0 0 0],'DefaultAxesLineStyleOrder','-|:|--|-.')
    semilogy(pressure,sol,'k')
    title(['Solubility of Aspirin at a temperature of ',num2str(T(1)),' K']);
    xlabel('Total Pressure (Pa)');
    ylabel('Solubility (Mole Fraction)');
    solT = [solT sol];

    % Plotting the experimental data
    [P Solub] = Experimental(T(1));
    semilogy(P,Solub,'o')
    l = legend('Classical','WH','MADAR-1','Experimental',4);

    sprintf('DONE')

% Binary Interaction Coefficients Calculation
function [kij] = BinaryInteraction(ncomps, kijSparse)

    elements = nchoosek(ncomps,2);
    if (length(kijSparse) ~= elements)
    end;
    idx = 0;
    for i = 1 : ncomps;
       for j = i : ncomps;
          if( i == j)
             kij(i,j) = 0;
          else
             idx = idx + 1;
             kij(i,j) = kijSparse(idx);
```

```
            kij(j,i) = kij(i,j);
         end
      end
   end
end

% Parameters of the PR EOS
function [bii aii] = PRaijbij(ncomps, R, Tc, Pc, w, T)

   for i = 1: ncomps
      kappa(i) = .37464+(1.5422*w(i))-(.26992*(w(i)^2));
      alpha(i) = (1+kappa(i)*(1-sqrt((T/Tc(i)))))^2;
   end
   for i = 1: ncomps
      bii(i) = 0.077796074*R*Tc(i)/Pc(i);
      aii(i) = 0.457235529*(R*Tc(i))^2*alpha(i)/Pc(i);
   end
end

% Which mixing rule to use
function [bij aij] = MixingRules(WhichRule, ncomps, bii, aii, kij, lij)

   switch WhichRule
      case (1)
% Classical mixing rules (Lorentz-Berthelot)
         for i = 1: ncomps;
            for j = 1: ncomps;
               bij(i,j) = 0.5*(bii(i)+bii(j))*(1 - lij(i,j));
               aij(i,j) = sqrt(aii(i)*aii(j))*(1 - kij(i,j));
            end
         end

% Ali Al-Matar  WHAK rules derived based on Waldman-Hagler
      case (2)
         for i = 1: ncomps;
            for j = 1: ncomps;
               bij(i,j) = sqrt(0.5*(bii(i)^2 + bii(j)^2))*(1 - lij(i,j));
               aij(i,j) = sqrt(aii(i)*aii(j)) * (bii(i)* bii(j)/bij(i,j)^2) * (1 - kij(i,j));
            end
         end

% Ali Al-Matar  MADAR-1 rules derived based on Molecular based MADAR-1 rules
      case (3)
         for i = 1: ncomps;
            for j = 1: ncomps;
               for k = 0: 2;
                  apwr = 1.0/(2.0 - 2.0*k/3.0);
                  num1 = 0.25*(bii(i) + bii(j))^2;
                  denum1 = (bii(i) * bii(j))^(k/3.0);
                  numTot(k+1) = (num1/denum1)^apwr;
               end
               bij(i,j) = (sum(numTot)/3.0) * (1-lij(i,j));
               aij(i,j) = sqrt(aii(i)*aii(j)) * (bii(i)* bii(j)/bij(i,j)^2) * (1 - kij(i,j));
            end
         end
```

```
    end
end
% Returns the maximum real root from the PR EOS
function Z = PRRoots(A, B)

    alpha = -1 + B;
    beta = A - 3*B^2 - 2*B;
    gamma= -A*B + B^2 + B^3;
    coeff = [1 alpha beta gamma];
    compr = roots(coeff);
    RealRoot = [];
    for i = 1:3
        if (isreal(compr(i))==1)
            RealRoot = [RealRoot compr(i)];
        end
    end
    Z = max(RealRoot);
end

% Returns the fugacity coefficient from the PR-EOS for a pure component
function PRPhiPure = PRPhiPure(A, B, Z, R, T)

    sqrt2 = 1.41421356237310;
    sqrt8 = 2.828427124746190;
    term1 = (Z + (1 + sqrt2)*B)/(Z + (1 - sqrt2)*B);
    term2 = (Z - 1) - log(Z - B)  - A/(sqrt8*B) * log(term1);
    PRPhiPure=exp(term2);
end

% Calculation of fugacity for corresponding temperature, pressure and mixing rule
function [SCFRoot Z] = SCFFugacity(x, ncomps, R, T, P, Poynting, Psub, Phi2s, aij, bij, yinitial)

    % Re-normalization of mole fractions after estimation of initial guess
    [y] = NormMoleFraction(ncomps, yinitial, x);

    % Estimation of mixture parameters used in PR EOS
    [amix bmix Amix Bmix] = AmixBmix(ncomps, y, aij, bij, P, R, T);

    [Ai Bi] = AiBi(ncomps, 1, y, aij, bij, R, T, P, Bmix);

    % Corrected compressibility factor of the supercritical mixture
    Z = PRRoots(Amix, Bmix);

    % Corrected fugacity coefficient of the supercritical mixture
    phi = PRPhi(Amix, Bmix, Ai, Bi, Z, R, T);

    % Calculation of solubility using the minimization technique
    x = fminbnd(@SCFPhi,1e-50,1,optimset('TolX',1e-15,'TolFun',1e-15));
    [y] = NormMoleFraction(ncomps, yinitial, x);
    SCFRoot = x;

    function y2 = SCFPhi(x) % Computes the solubility/ fugacity
        y2 = (x  - Psub/P * Poynting * Phi2s/phi)^2;
    end
```

```
end

% Normalizes mole fractions for components other than the solid (1)
function [y] = NormMoleFraction(ncomps, yinitial, x1)
  y(1) = x1;
  if (ncomps == 2)
    y(2) = 1 - x1;
  else
    ytot = 1 - x1;
    for i = 2: ncomps
      y(i) = ytot * yinitial(i);
    end
  end
end

% Finds the mixture properties from composition and respective mixing rule i.e. amix, bmix
function [amix bmix Amix Bmix] = AmixBmix(ncomps, y, aij, bij, P, R, T)

  amix = y*aij*y';
  bmix = y*bij*y';
  Bmix = bmix * P/(R * T);
  Amix = amix * P/(R * T)^2;
end

% Finds the component idx properties from composition and respective mixing rule i.e. Ai and Bi
function [Ai Bi] = AiBi(ncomps, idx, y, aij, bij, R, T, P, Bmix)

  Bi = sum(y .* bij(idx,:));
  Ai = sum(y .* aij(idx,:));
  Bi = 2 * Bi * P/(R * T) - Bmix;
  Ai = Ai * P/(R * T)^2;
end

% Returns the fugacity coefficient from the PR-EOS
function PRPhi = PRPhi(A, B, Ai, Bi, Z, R, T)

% Notice that phi is defined from the general mixing rules (Bi different than pure component Bi)
  sqrt2 = 1.41421356237310;
  sqrt8 = 2.828427124746190;
  term1 = (Z + (1 + sqrt2)*B)/(Z + (1 - sqrt2)*B);
  term2 = 2*Ai/A - Bi/B;
  term3 = -log(Z - B) + (Bi/B) * (Z-1) - A/(sqrt8*B) * term2 * log(term1);
  PRPhi=exp(term3);
end

% Experimental Data for Aspirin (Pressure and Solubility)

function [p solub] = Experimental(T)
hold on
switch T

  case(308.15)
    p = [12.0e6 15.0e6 17.2e6 18.5e6 20.0e6 21.5e6 23.0e6 25.0e6];
    solub = [0.89e-4 1.12e-4 1.22e-4 1.29e-4 1.33e-4 1.42e-4 1.45e-4 1.51e-4];
```

```
    case(318.15)
        p = [12.0e6 15.0e6 17.2e6 18.5e6 20.0e6 21.5e6 23.0e6 25.0e6];
        solub = [0.72e-4 1.39e-4 1.75e-4 1.95e-4 2.12e-4 2.28e-4 2.34e-4 2.58e-4];
    case(328.15)
        p = [12.0e6 15.0e6 17.2e6 18.5e6 20.0e6 21.5e6 23.0e6 25.0e6];
        solub = [0.63e-4 1.37e-4 1.82e-4 2.34e-4 2.77e-4 2.86e-4 3.03e-4 3.47e-4];
end
end
```

الديناميكا الحرارية لاستخلاص المواد المذابة الصلبة باستخدام الموائع فوق الحرجة بطريقة مصفوفة الأوزان

إعداد
باسل نبيل عبد الكريم عبد الرازق

المشرف
الدكتور أحمد حلمي الطوبجي

المشرف المشارك
الدكتور علي خلف المطر

مـــــلـــــخـــــص

تعتبر معادلات الحالة (EOS) أداة مهمة للتنبؤ بالخصائص الحرارية وسلوك الحالة للمواد النقية والمخاليط ، لذا فإنها تستخدم على نطاق واسع في التصميم والمحاكاة والاستفادة المثلى من العمليات الكيميائية مثل الاستخلاص باستخدام الموائع فوق الحرجة (SFE). تستخدم معادلات الحالة تكعيبية الشكل مقرونة مع قواعد الخلط بشكل روتيني في الصناعات الكيميائية والبتروكيميائية لحساب الخصائص الثيرموفيزيائية وتوازنات الحالة ، وتعتبر معادلة بنغ - روبنسون (PR - EOS) من المعادلات الأكثر استعمالا في العمليات الحسابية للاستخلاص باستخدام الموائع فوق الحرجة.

لقد تم اقتراح عدة قواعد خلط لتوسيع مجالات استخدام معادلات الحالة تكعيبية الشكل وجعلها أكثر فائدة لنمذجة المخاليط المعقدة. ولكن نظرا للقصور الموجود في قواعد الخلط أو معادلات الحالة أو كلاهما معا ، فقد أدخلت معاملات التداخل الثنائية من أجل تحسين دقة هذه النماذج. يقترح هذا البحث طريقة مصفوفة الأوزان كبديل عن نموذج معاملات التداخل الثنائية. وقد تبين أنه يمكن تحويل الكثير من قواعد الخلط الموجودة مسبقا إلى النموذج المقترح مع الاختيار الصحيح لمعاملات مصفوفة الأوزان.

تم حساب معاملات الذوبان لكل من الأسبرين والصبغة المتفرقة حمراء اللون رقم-1(C.I. Disperse Red 1) و الصبغة المتفرقة حمراء اللون رقم-13 (C.I. Disperse Red 13) والنفثالين والزانثين (Xanthene) والزانثون (Xanthone) في ثاني أكسيد الكربون فوق الحرج عند قيم مختلفة من درجات الحرارة والضغوط عن طريق معادلة بنغ – روبنسون (PR – EOS) باستخدام طريقتين مختلفتين للنمذجة هما طريقة معاملات التداخل الثنائية وطريقة مصفوفة الأوزان المقترح ، وقد كان التوافق جيدا جدا بين نتائج كلا الطريقتين والقراءات المخبرية الموجودة مسبقا. ويجدر الإشارة إلى أنه قد تم احتساب معاملات الذوبان للمواد الصلبة التي تمت دراستها في هذا البحث باستخدام برنامجي (MatLab) و (Excel).

لقد تم حساب القيم المثلى لكل من معاملات التداخل الثنائية ومعاملات مصفوفات الأوزان للمواد التي تمت دراستها في هذا البحث عن طريق تقليل متوسط الانحرافات النسبية المطلقة (AARD) بين معاملات الذوبان التجريبية المتوقعة. وتمت مقارنة الـ (AARD) لنتائج كلا الطريقتين مع نتائج التنبؤ النقية (بدون استخدام معاملات التداخل) وكانت نتائج كلا الطريقتين جيدة جدا.

لقد تم إيجاد علاقات مناسبة تربط بين درجة حرارة الخليط وكل من معاملات التداخل الثنائية ومعاملات مصفوفات الأوزان لكل من الأسبرين والصبغة المتفرقة حمراء اللون رقم-1(C.I. Disperse Red 1) و الصبغة المتفرقة حمراء اللون رقم-13 (C.I. Disperse Red 13) والنفثالين والزانثين (Xanthene) والزانثون (Xanthone) في ثاني أكسيد الكربون فوق الحرج ، كما تم مقارنة مدى تأثير درجة حرارة الخليط على معاملات التداخل الثنائية ومعاملات مصفوفات الأوزان للمواد التي تم دراستها في هذا البحث. لقد وجد أن معاملات التداخل الثنائية أكثر اعتمادا على درجة حرارة الخليط من معاملات مصفوفات الأوزان.